THE SEPARATION AND DETERMINATION OF RARE EARTHS IN PHOSPHATE DEPOSITS FROM THE NORTH OF THE KINGDOM OF SAUDI ARABIA.

by

ASAAD M.B. MOUFTI, B.Sc, M.Sc.

A thesis submitted in part fulfilment of the requirements in the Department of Pure and Applied Chemistry, University of Strathclyde, Glasgow, for the degree of Doctor of Philosophy.

December 1987

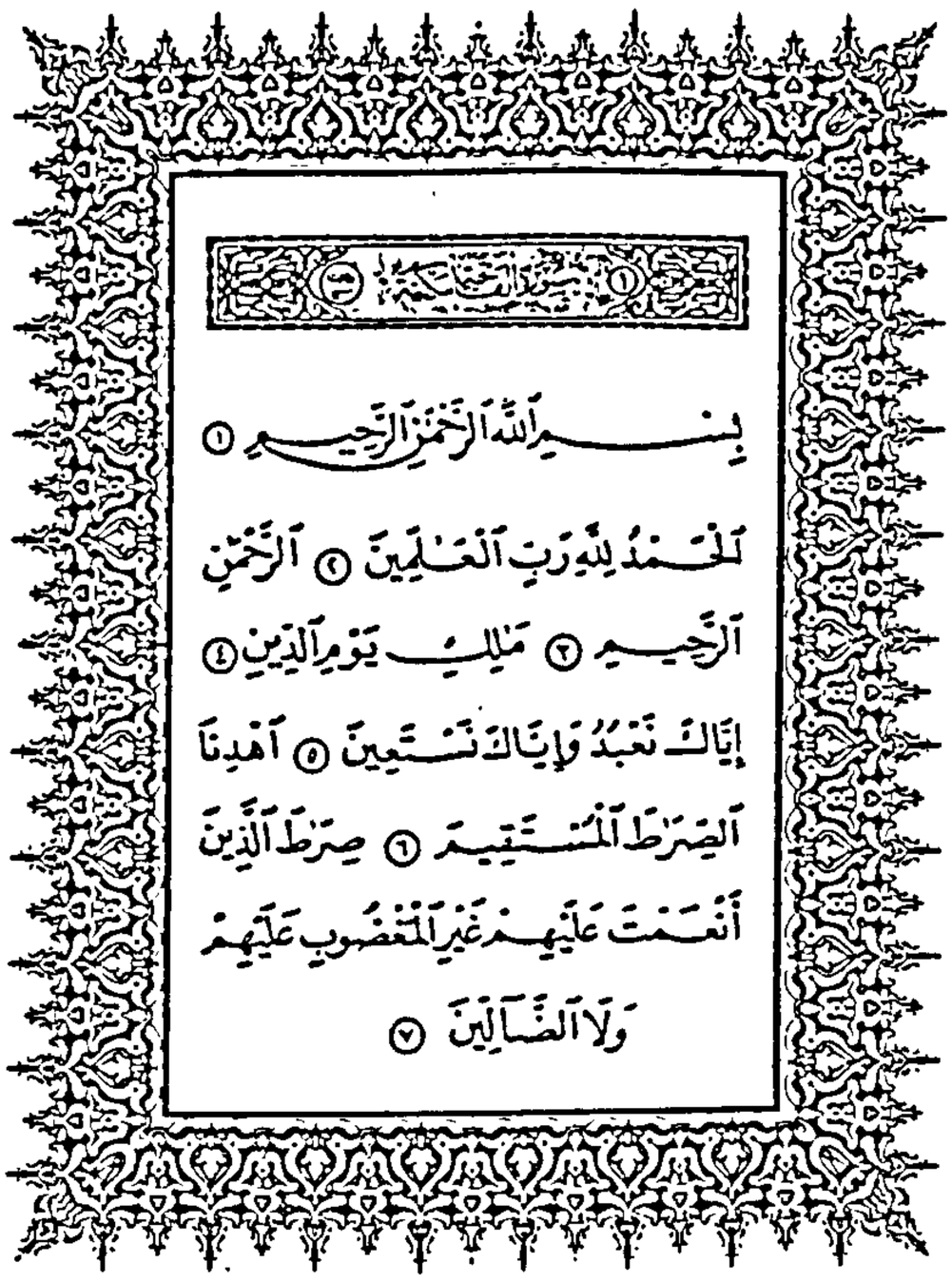

1- In the Name of ALLAH, the Most Beneficent, Most Merciful.

2- Praise be to ALLAH the Lord of the worlds .

3- The Most Beneficent, the Most Merciful.

4- Owner of the Day of Recompense.

5- You (alone) we worship and You (alone) we ask for help.

6- Guide us to the Straight way.

7- The way of those on whom You have bestowed Your Grace, not (the way) of those who earn Your anger nor of those who go astray.

To my parents and Amal

with love

ACKNOWLEDGEMENTS.

I wish to express my gratitude to the late Professor J.M. Ottaway for providing the facilities for this project and for his support and help.

I wish to express my thanks to Dr. B.G. Cooksey, my supervisor, for his much appreciated guidance and contribution to the development of the project.

My thanks also go to Dr. A. Bakur and Dr. M.A. Gazzaz and all the academic staff, from the Faculty of Earth Science in King Abdul-Aziz University in the Kingdom of Saudi Arabia, for their encouragement during the progress of this work.

Samples were collected from the north of Saudi Arabia, and I wish to thank the Deputy Ministry of Mineral Resources and Riofinix Mission Limited for valuable information and for the use of facilities at Turayf camp.

Major and trace element analysis of the samples was performed at the Directorate General of Mineral Resources, French Geological Survey (B.R.G.M.) and the Faculty of Earth Science chemical laboratories in the Kingdom of Saudi Arabia. I therefore express my thanks to the staff of all these laboratories for assisting in

the analysis.

Neutron activation analysis was performed in the Scottish Universities Research and Reactor Center in East Kilbride. I therefore express my thanks to Dr. J.E. Whitley for his help.

I thank Dr. B. Bell of the Department of Applied Geology, the University of Strathclyde for his assistance in the geochemical study and help.

My thanks to Dr. D. Littlejohn in the Department of Pure and Applied Chemistry, University of Strathclyde for his help and guidance during the progress of this project.

To my parents, brothers, family and friends, I give my sincere thanks for their support and encouragement during my study.

Last but not least, I owe my wife, my deepest thanks for her positive and stimulating attitude towards this work.

Asaad M.B. Moufti.

TABLE OF CONTENTS.

ABSTRACT.

The use of an ion and cation exchange for the separation of rare earth elements from phosphate rocks were investigated. The cation exchange method was found to be most suitable. Rare earth elements separated in this way were analysed by atomic emission using an inductively coupled plasma. Compromise optimum conditions were found and the combined procedure used for thirty nine phosphate rock samples from Saudi Arabia. . The results obtained were confirmed by internal checks on some samples using standard addition. In general, the recovery of individual rare earth elements is high but these vary from sample to sample depending on the sample composition.

CHAPTER ONE: - INTRODUCTION.

1.1 Phosphate Rocks.

Phosphate rocks are the major source of phosphate fertilizers. Phosphorus is a vital component of every living cell. Along with nitrogen and potassium it is a major and essential nutrient for agricultural crops. Phosphorous can be added to deficient soils in the form of natural or artificial fertilizers, and for sustained good yields it must be added to all soils when they are cropped heavily for a long time.

The rare earths can be obtained as a by product in the process of manufacturing phosphorus fertilizers from phosphate rocks. The concentration of rare earths in phosphate rocks vary considerably from place to place: 590 mg kg^{-3} in Florida deposits (109), 128-691 mg kg^{-3} in the Egyptian deposits in the Nile valley (107) and 1% in the Soviet deposit of Maikop and Mangyshlak (110).

There is growing interest in rare earth geochemistry, separation, analysis and industrial application. The growth in interest in the geochemistry of the rare earths has come about because of the realization that the pattern of concentration in the rock or a mineral can be used to study the genesis of

the rock or the mineral. Much of the new development of rare earth mining procedures is due to the growth of new uses of the pure elements. Such demands are illustrated by the new market for cracking catalysts using samarium and praesodymium, the use of europium in colour television and home lighting phosphors and the use of neodymium as an activator in laser materials. The versatility in fundamental properties of the rare earths makes them especially valuable in reactor and medical technology. Those with low-neutron cross section (Y, Ce and La) are ideal diluents for reactor fuels. Those with high-neutron cross section (Gd, Dy, Sm and Eu) are useful in shielding alloys and control rods. A number of short lived radio-active isotopes (^{153}Gd, ^{170}Tm, ^{171}Tm and ^{177}Lu) are of possible interest as sources of radio-activity, thermal energy and power. Thulium is remarkable, as its radio-active isotopes are sufficiently long-lived for such critical uses as heart machines and space exploration, and ^{170}Tm has low volatility and lacks alpha activity, and is thus free of obvious biological hazard (137).

The marine phosphorites are particularly attractive raw materials for the new technology. Compared to conventional rare earth sources, they are unusually enriched with these elements. Rare earths can be recovered as a byproduct during the production of wet process phosphoric acid from the phosphate rocks.

Approximately 21 tons of europium, 74 tons of gadolinium and 11 tons of thulium were recovered during the production of phosphoric acid from Florida phosphate rocks in 1964 (137).

1.1.1 Occurrence of Phosphate Rocks.

Phosphate rock is an imprecise term used by the mineral industry for any naturally-occurring raw material that contains one or more phosphate minerals, and after appropriate treatment produces phosphoric acid for commercial use. Geologically, therefore the term is used for a very wide variety of rock types of different origin, character and mode of occurrence. There are three main types of phosphate deposits of different origins. The first, are the sedimentary deposits which are the most important both in number and volume. The concentration of phosphate (% P_2O_5) in these deposits often exceeds 20 or even 30%. The second type of deposit is that of igneous origin; this type is less common, not so rich in phosphate (average phosphate concentration is 18%) and small. These deposits are associated with intrusive alkaline complexes in which the most abundant rocks are nepheline syenites, carbonatites, ijolites and pyroxenites. Finally, the last type are the guanos, which are formed by the reaction between the sea-bird droppings (containing about 4% of phosphate) and the underlying calcareous bedrock, forming calcium phosphate. These deposits are

small, but could contain up to 39% of phosphate. Similarly, the droppings of bats may also be a source of phosphate accumulation, with high grades found in caves. A detailed account of their geology, chemistry, mineralogy and occurrence is presented elsewhere (9-12).

There are over 200 minerals containing phosphate (12), but the most common mineral in the sedimentary phosphates is a member of the apatite family. The structure of sedimentary apatite allows a number of substitutions. The most common substitution is that of PO_3^{-3} by CO_3^{-2} maintaining electrical neutrality by the introduction of F^-. Another frequent substitution is that of Ca^{+2} by Na^+ and Mg^{+2}. The partial replacement of F^- by OH^- is also fairly frequent. The general structural formula of sedimentary apatite suggested by Lehr et al. (13) is:

$$(Ca,Na,Mg)_{10}\ (PO_4)_{6-x}\ (CO2)_x\ F_y\ (F,OH)_2$$

in which y varies between 0.33 and 0.5 x and x lies between 0 and 1.5.

The structure of sedimentary apatite allows a number of other substitutions but not generally to the same extent as those discussed before. Potassium, strontium, uranium, thorium, aluminium and the rare earths can partially replace calcium, while

AsO_4^{-3}, VO_4^{-3}, SiO_4^{-4} and AlO_4^{-5} substitute for PO_4^{-3} (10).

1.1.2 Geology of Phosphate Rocks in Saudi Arabia.

The first discovery of phosphate sedimentary rocks of the Kingdom of Saudi Arabia was in the northern province at Turayf by Sheldon in 1965 (1). Later, the phosphorite at West Thaniyat Turayf (subsequently referred to as West Thaniyat) was discovered by Mytton (2) and Meissner (3) in 1967. These areas are located between lat. 29° 15′ and 32° 00′ N. and long. 37° 00′ and 40° 00′ E., as can be seen in Figure 1.1. The geology of the area, texture and other characteristics had been discussed in detail elsewhere (4-8). There are now considered to be four phosphate levels in the Cretaceous and Eocene in the Turayf group (4), instead of the five levels previously identified (6), when the carbonate deposition cycles were used. The report by Meissner and Ankary (6) estimated a 722 million tons of sedimentary phosphate rocks, grading 18% P_2O_5 with a thickness of 4 metres, for the Turayf area. The report also estimated 190 million tons of phosphate rocks, grading 23% P_2O_5 over a thickness of 1.64 metres, for the Thaniyat area. These figures were calculated assuming no changes in the phosphate facies throughout the deposits.

The Turayf group is sub-divided into three

Figure (1.1)

Map of the Kingdom of Saudi Arabia showing Turayf phosphate and Thaniyat - Turayf phosphate .

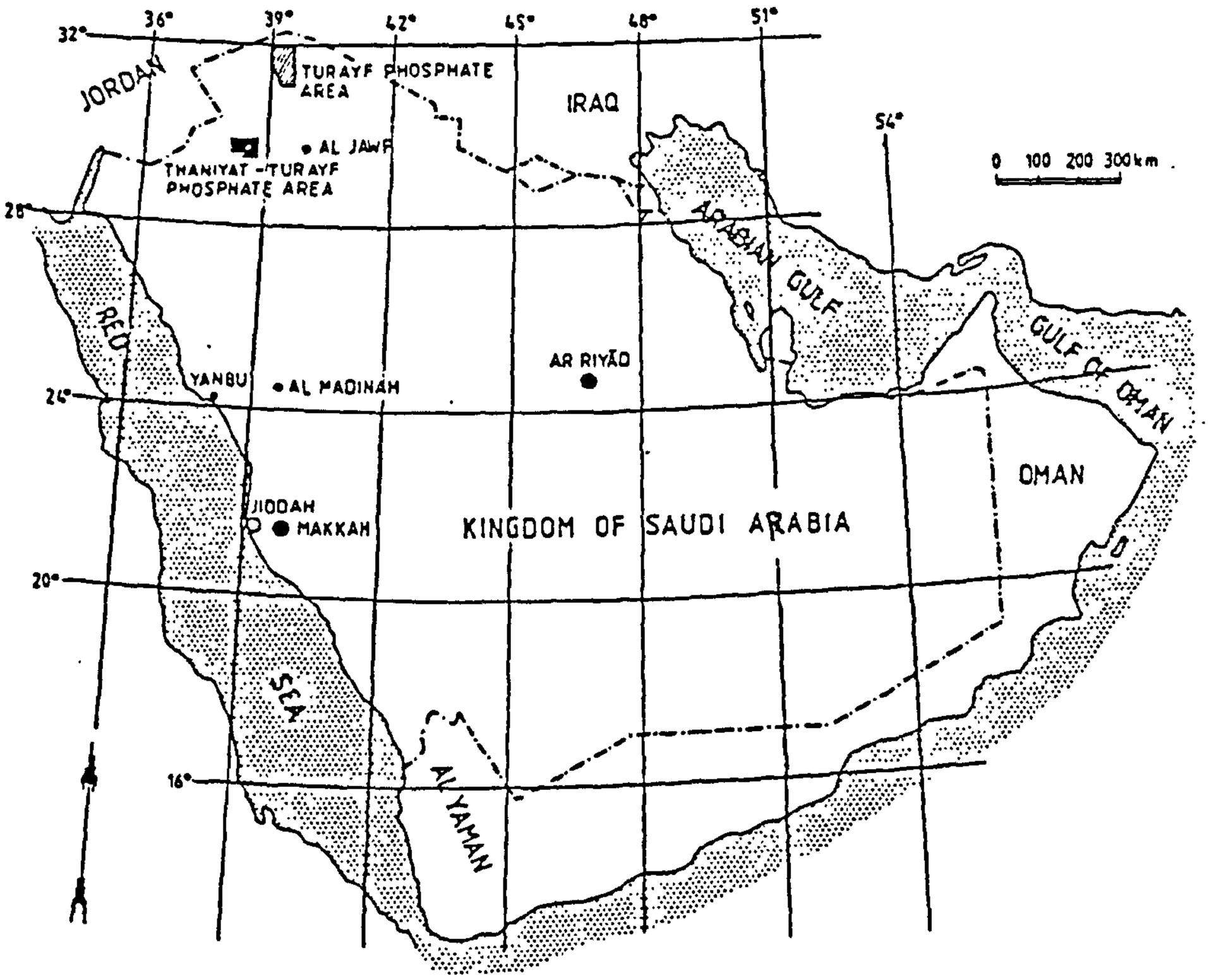

formations, the Jalamid, the Mira and the Umm Wu al; general lithologies and approximate ages of the Sirhan-Turayf region (7) is shown in Figure 1.2. The four phosphate levels which have been sampled are:

1 - Arqah Phosphorite

2 - Sib Phosphorite

3 - Ghinah Phosphorite

4 - Thaniyat Phosphorite

1.1.3 Trace Elements in Phosphate Rocks.

The chemistry of the enrichment of phosphate rock was the subject of many studies (14, 15, 16). These studies show that a group of elements, Ag, Cd, Mo, Sn, Sr, U, Y, Ni and REE (excluding Ce), were enriched in phosphate rocks regardless of the way the average was compared to their concentration in the crust or the average shale or sea water, as can be seen in Table 1.1. These studies also show that there is no correlation between the enrichments and the concentration of phosphate. Also they conclude that enrichment depends on the marine origin of the phosphate rock, the paragenetic association with organic matter and the crystallochemical properties of the apatite. Each deposit has a slightly different pattern probably characteristic of its geological history. The uranium concentration of some deposits reaches a very high value (1%) and this enrichment is believed to be due to

Figure (1.2)

General lithologies and approximate ages of the Sirhan - Turayf region (7)

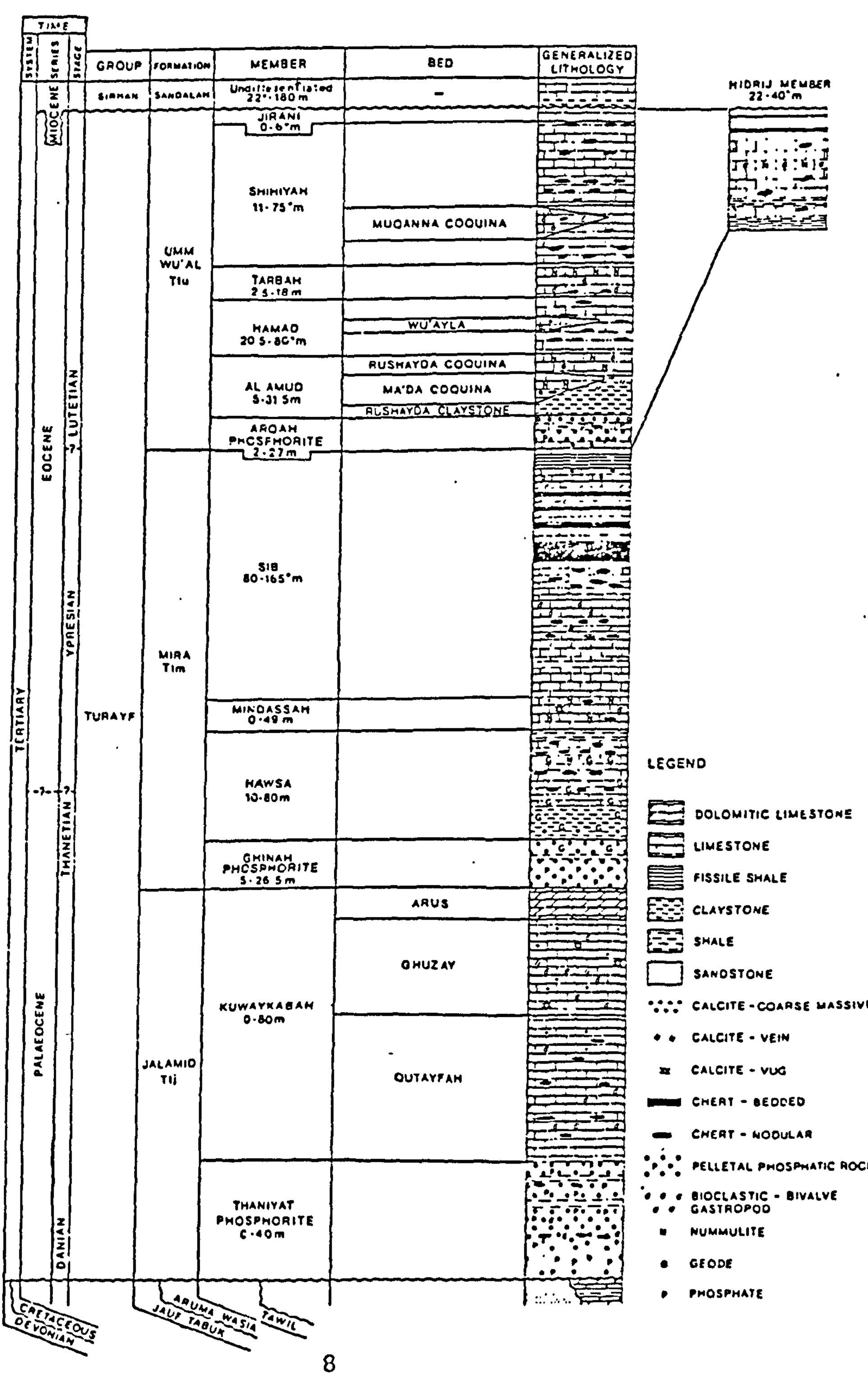

Table 1.1.

Trace elements abundance data in seawater, earth's crust, average shale and average phosphorites. All values in (mg kg^{-1}) except seawater, which is (ng dm^{-3}). (12)

Element	Sea water	Earth Crust	Average Shale	Average Phosphorite
Ag	0.07	0.28	0.07	2
As	1.8	2.6	13	23
B	10	4.45	100	16
Ba	425	21	580	350
Be	0.0006	2.8	3	2.6
Cd	0.11	0.2	0.3	18
Ce	0.0012	60	91	104
Co	0.39	25	19	7
Cr	0.2	100	90	125
Cu	0.9	55	45	75
Gd	0.03	15	19	4
La	0.0034	80	400	55
Li	170	30	40	147
Mn	0.04	20	66	5
Mo	10	950	850	1230
Ni	6.6	1.5	2.6	9
Pb	0.03	75	68	53
Sc	0.004	13	20	50
Se	0.09	22	13	11
Sn	0.81	0.05	0.06	4.6
Sr	8100	375	300	750
Ti	1	4400	4600	640
U	3.3	1.8	3.7	120
V	1.9	135	130	100
Y	0.013	33	26	260
Yb	0.00082	3	2.6	14
Zn	5	70	95	70

a secondary enrichment (17), uranium entering the apatite crystal by replacing calcium.

1.2 Aim of the research.

Uranium, thorium and the rare earths are a group of elements which have been enriched in the sedimentary phosphate rocks. In the north of Saudi Arabia, large deposits of the phosphate rocks were discovered. Most of the studies carried out on these deposits were geological studies and very limited chemical studies involving the determination of phosphate, calcium and field determinations of uranium by Gieger counter.

This investigation was intended to provide a complete analysis, major and trace elements, of all the phosphate levels identified in the studied areas and to apply various preconcentration techniques to the rare earth elements prior to their estimation by ICP. The procedure which gave the best recovery was chosen to determine the concentration of the rare earth elements in the samples collected. It was intended to separate uranium and thorium in addition to the rare earths, but as the preliminary results were not encouraging this was abandoned.

1.3 Ion Exchange Separation.

Ion exchange chromatography is a useful method of separation and concentration of trace elements from a large volume of sample solution which eliminates matrix interference in the analysis of these elements and improves the determination. This procedure is widely used in inorganic, organic and biochemical analysis.

Every ion exchanger is made up of a skeleton and fixed ionic groups carried by the skeleton. At present the skeleton of a modern synthetic organic ion exchanger consists of a copolymer of styrene with divinylbenzene (DVB) which gives a controlled amount of cross-linking (an important factor in chromatography). The degree of cross-linking affects the degree of swelling, selectivity and the rate of equilibration. A small degree of cross-linking leads to high swelling (ie. absorbing more liquid) and decreases the differences between the ion exchange constants of various ions thus making separation more difficult. On the other hand, a high degree of cross-linking leads to a reduction in the swelling as well as to an increase in selectivity due to small volume changes. The disadvantages of the highly cross-linked resins are their lower exchange capacity and a restriction of ionic diffusion inside the resin which results in slow

exchange kinetics. Details of the composition, structure, properties and use in inorganic and geological analysis can be found elsewhere (18-21).

The two fundamental types of ion exchange material are cation and anion exchangers, which in turn are sub-divided according to their strength into a strong, medium and weak, as can be seen in Table 1.2. The cation exchangers are cross-linked hydrocarbon chains carrying ionic groups such as sulphonate $-SO_3^-$, carboxylate $-COO^-$ and phosphonate $-PO(OH)_2^-$. They are attached to the polymer molecule in a regular way and are accessible to the solution containing the ions to be separated. The polar groups in anion exchange resins are tertiary amines ($-N(CH_3)_2$) or a mixture of tertiary and quarternary ammonium groups ($-\overset{+}{N}(CH_3)_3$) or polyamines.

The use of a column packed with a resin is the most frequent technique used in ion exchange separation procedures. Sample solution is passed through the column, the resin collecting either the matrix or the analyte elements, and after washing the column the absorbed elements are eluted, as shown in Figure 1.3. In the column during the separation procedure an equilibrium occurs between the ion exchanger and the ions in the solution. The equilibrium depends on the relative concentration of the ions in solution and on

Table 1.2

Basic classification of ion exchangers.

Ion Exchanger	Type	Usual inorganic groups
Cation Exchanger	Strongly acidic	Sulphonic ($-SO_3H$)
	Medium Acidic	Phosphoric($-PO(OH)_2$)
	Weakly acidic	Carboxylic (-COOH)
Anion Exchange	Strongly basic	Quarternary Ammonium group
	Medium basic	Mixture of tertiary amines and quarternary ammonium groups
	Weakly basic	amines, polyamines.

Figure (1.3)

Theoretical separation peaks of an element (2) from the matrix (1) .

C_{pl} = the maximum concentration of the matrix .

V_{pl} = the effluent volume corresponding to the peak concentration of the matrix .

σ_1 = the zone spreading constant for the matrix .

C_{p2} = The maximum concentration of the analyte .

V_{p2} = the effluent volume corresponding to the peak concentration of the analyte .

σ_2 = the zone spreading constant for the analyte .

the resin, the chemical nature of the ions in both phases, the resin used and the matrix elements in the analyte solution.

Plate theory (22) was first suggested for liquid-liquid partition chromatography. Later on, it was adapted to ion exchange chromatography (23). The column is treated as a series of theoretical stages (plates). The theoretical plate is defined as a height of packed bed within which the average concentration of the stationary phase is in equilibrium with the solution leaving it. Thus local equilibrium is assumed to exist between the mobile phase and the stationary phase at each plate (138). The faster the ion-exchanger solution equilibrium is established, the smaller is the height of the theoretical plate and the more efficient is the column. In general, the number of theoretical plates increase with a decrease of the particle size of stationary phase, decrease of flow rate or viscosity of the mobile phase and an increase in the temperature. The shape of the elution curve can be calculated from the following equation.

$$C = C_p \exp\left(- \frac{(V - V_p)^2}{2\sigma^2} \right)$$

Where V is the effluent volume, V_p is the retention volume (effluent volume corresponding to the peak concentration of the ion in the effluent), C is the

concentration of the ion in the emerging solution, C_p is the maximum concentration of the ion and σ is the zone spreading constant.

The volume of effluent passed when the maximum concentration of solute emerges is related to the distribution ratio (the ratio of the quantities of the ion present in the ion exchanger and in the solution $-D_x$), the weight of the solid stationary phase (g) in the column and the interstitial volume (the volume occupied by the mobile phase in the column - V_i), with the equation.

$$V_p = V_i + g * D_x$$

The distribution ratio (D_x) can also be calculated using the batch procedure. A known weight of the resin (W) is equilibrated with a known volume of the mobile phase (V) containing a known amount of the ion being studied, the amount of ion left after equilibrium (A_f) is measured and the amount of ions in the initial volume (A_i) is known. The distribution coefficient is calculated from the equation:

$$D_x = \frac{V}{W}\left(\frac{A_i}{A_f} - 1\right)$$

The maximum concentration of solute (C_p) is

related to the total weight of the solute chromatographed (W_t) and the zone spreading constant (σ) with the formula:

$$C_p = 0.4 * W_t / \sigma$$

The zone spreading constant (σ) is related to the number of theoretical plates (N) in the column and the volume of effuent passed when the maximum concentration of solute emerges by the following law:

$$\sigma^2 = V_p^2 / N$$

1.4 Inductively Coupled Plasma (ICP).

The first report on the use of the ICP as an exitation source for trace element analysis were published by Greenfield et al. (24) and Wendt and Fassel (25). There are a large number of publications dealing with exitation mechanism (26, 38), detection limit calculations (27-30), wavelength selection (31), elemental emission wavelengths (32, 33, 34), excitation and ionization temperature (35, 36, 37), analytical application to the analysis of geological samples (39), developments (40) and instrumentation (41, 42, 43).

The advantages of using the ICP in the determination of elements in geological samples are :

1) The high temperature of the plasma

   a) dissociate molecular species, even of refractory compounds, thus eliminating chemical interferences

   b) provides low detection limits.

2) The calibration graph is linear over 4 to 5 orders of magnitude; thus elements can be determined both at low (less that 1 mg dm^{-3}) and high levels (hundreds of mg dm^{-3}). This is very useful in multi-element analysis as major, trace and ultra-trace elements can be measured in the same solution without the need for dilution.

3) The use of a solution to introduce the sample into the plasma gives a great flexibility in the choice of sample weight and fasilitates standardisation.

4) The multi-element capability of the ICP technique provides a convenient method for the automation of geochemical survey analysis.

In spite of the advantages, the ICP technique suffers from the following:

1) The complex line-rich spectra produced by high temperature of the plasma, are likely to exhibit spectral interferences. The use of a high resolution monochromator reduces this type

of limitation.

2) Volatile elements may be lost during the dissolution of the sample.

3) Clogging of the nebulizer system can occur with sample solution of high salt content. It can be overcome by diluting the solution, but this may reduce the concentration of some trace elements below their detection limits.

4) Emission by major components present in the sample may cause "stray light" which will affect the background level in the sample but not in the standards, unless the latter are matrix matched to the sample.

1.4.1 Interferences in the Inductively Coupled Plasma.

Because of the high temperature of the plasma chemical and ionization interferences are rare in ICP analysis; the most significant interferences are spectral overlap, stray light and matrix effects. Spectral interference is classified into three types, as shown in Figure 1.4.

a) Direct spectral overlap, where a spectral line of another element underlies the analyte line. The problems created by spectral overlap are emphasized

Figure (1.4)

Schematic representation of different types of spectral overlap found in ICP spectrometry :- (a) direct overlap of analyte and interfering line , (b) partial overlap of analyte and interfering line and (c) continuum or background overlap , shown in three levels corresponding to an increase in the background .

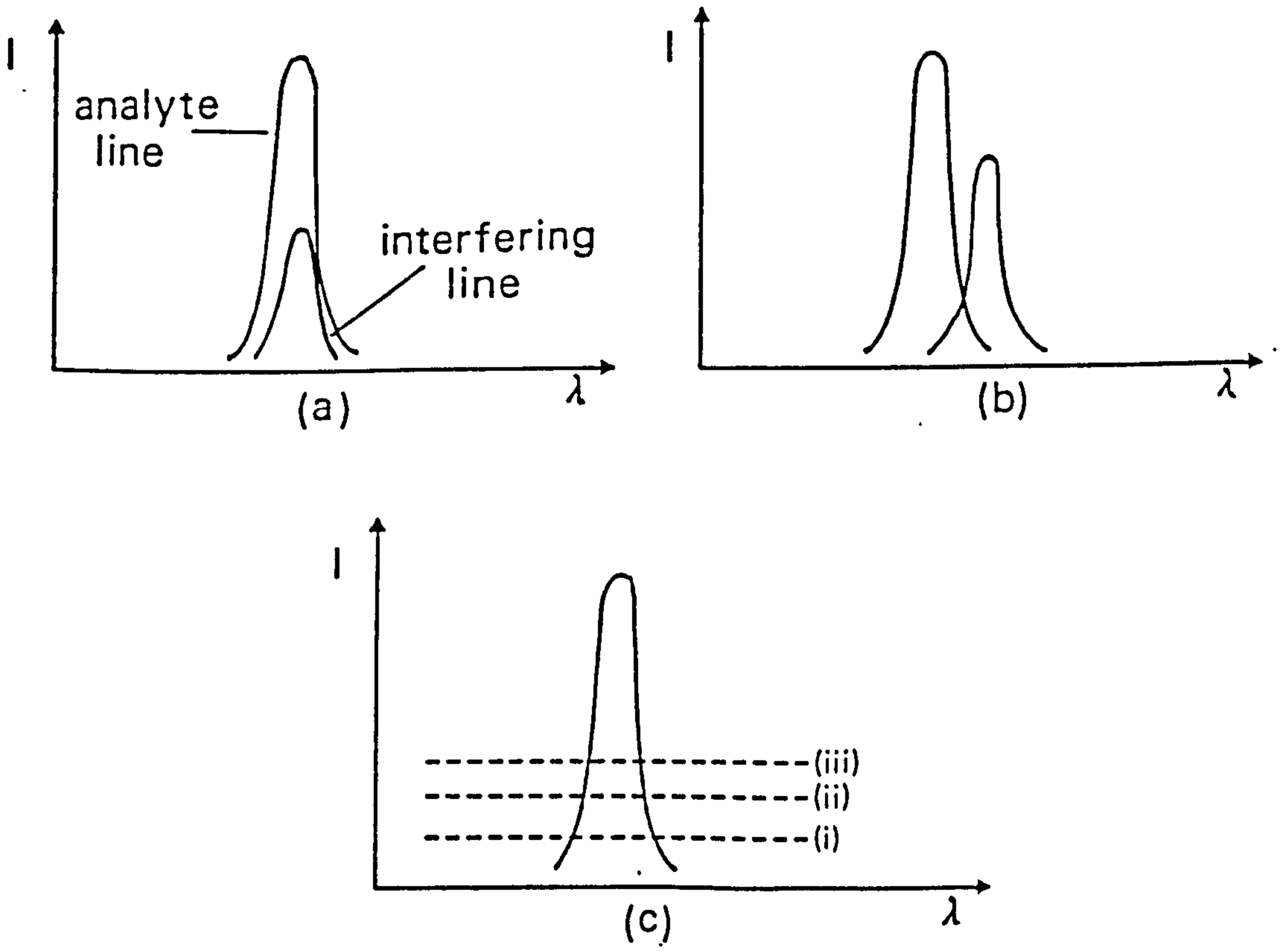

in the study of Mermet and Trassy (44), who drew attention to the large number of lines that are excited in the ICP, in addition to those listed in the classical tables (eg. MIT tables (45)) for arcs and sparks. The most satisfactory way to avoid this type of interference is the use of an alternative line free from interferences from the other elements. Another approach is to correct for direct line overlap by using an inter-element correction factor (46).

b) Partial spectral overlap, where part of the interferant line partially overlaps the analyte line. This type of interference is more difficult to correct because small changes in the slit width, grating resolution etc, will have a great effect on the magnitude of the correction factor by causing more or less overlap. This type of interference can be reduced by selecting another wavelength free from overlap.

c) Background continuum interference is caused by recombination radiation emitted when the free electrons in the plasma which have a continuous energy distribution are captured by the ions. As a result a radiation continuum is emitted. Stray light interference (47) is caused by the radiation scattered inside the monochromator; it can be

overcome by using holographic gratings. The introduction of a quartz refractor plate behind the entrance slit of the monochromator can be used to eliminate the effect of the continuum and stray light interferences by allowing the use of background correction (48).

1.5 Determination and Separation of Rare Earth Elements from Geological Samples.

Recently rare earth elements have received much attention in the field of geochemistry and industry (49, 50, 51). Rapid and accurate determination of them is increasingly required as industrial demand increases. A review of different analytical procedures used to measure these groups of elements is published elsewhere (50-53). However, the determination of the rare earths at the trace level is still very difficult because of interelement interferences or lack of sensitivity when instrumental techniques are used directly for analysis without a preconcentration step.

Neutron activation (54-57) is commonly used for the determination of rare earths. This technique suffers from many disadvantages such as high running cost, slow analysis times, poor precision and inter-element interferences. A separation procedure is

useful to overcome interferences of other elements present in the sample. Another technique commonly used is isotope dilution mass spectrometry (58,59). This technique is very sensitive for rare earth determinations. However, because of the presence in complex samples of isobars the selectivity of the mass spectrometer is not sufficient to analyse the sample directly, therefore some kind of separation is required. Also the isotope dilution cannot be applied to some rare earths (Pr, Tb, Ho and Tm) since they are monoisotopic. Spark source mass spectrometry (SSMS) can determine all the rare earth elements in soils and geological materials with detection limits of about 10 ug kg^{-1} nd a precision of $\pm$ 15% (148, 149, 119). X-ray fluorecence (XRF), which is available in many analytical laboratories, has been used for rare earth determinations in different geological samples (60-64). Matrix and line interferences are two of the major limitations of this technique. In addition the detection limits for the rare earths with XRF are sufficently low for the determination of light rare earths but, are often inadequate for the heavy rare earths which usually occur at very low concentrations in the normal samples. Many procedures have been used to eliminate matrix interferences; including matrix matching of standard and sample, the use of a thin film, a fused bead or a prior separation of the rare earths from the matrix. Atomic absorption spectrometry (AAS)

using a nitrous oxide-acetylene flame has been used for the analysis of rare earths (65-68), as well as other atom cells such as the carbon furnace (69-72) and tantalum ribbon electrothermal atomizer (70). These techniques have the advantages of having very low detection limits and being simple to operate but suffer from a small dynamic range, so that correct dilution is essential. In normal samples a preconcentration procedure is usually advisable to eliminate matrix interferences and increase sensitivity. Different atomic emission techniques such as flame (73), direct current plasma (74, 75), d.c. arc (76, 77) have been used. Recently inductively coupled plasma atomic emission spectrometry has been extensively used in the determination of rare earths in geological materials (76-89).

Many methods have been suggested to separate the rare earths from one another, such as liquid-liquid extraction with bis-(2-ethylhexyl)phosphoric acid (HDEHP)-cyclohexane-perchloric acid (102), precipitation of the rare earths as oxalates (69) or hydroxides (65, 103) and high performance liquid chromatography (HPLC) (76, 104) and gas liquid chromatography (105). The most common method used to separate individual rare earths is the ion exchange. Absorption of the rare earths using a strong base resin from aqueous solution containing citric acid (93), lactic acid (94) and

ethylendiaminetetraacetic acid (EDTA) (95) have been used for this purpose.

In many of the published methods for the determination of rare earth elements reviewed above, preconcentration and separation played an important role in removal of interfering elements prior to the analytical measurements. Other advantages of a preconcentration procedure are to enhance sensitivity and accuracy. The main procedures applied to rare earths separation from geological materials are cation and anion exchange procedures. Cation exchange involves the use of a strongly acidic resin and the rare earths are eluted by strong mineral acids, such as hydrochloric acid (60, 63, 64, 66, 71, 74, 77, 81, 86, 87, 90, 91). A recent study by Crock et al. (92) compares the elution of different elements present in geological materials. This study shows that the rare earth elution curves with nitric acid are sharper than those obtained with hydrochloric acid, when calcium and magnesium are the dominant interferents. However hydrochloric acid is superior when iron and aluminium are the dominant interferents. Nitric acid elution was chosen for the work reported in this thesis (see Chapter 5) because it is more suitable for the phosphate samples analysed (which contain high concentration of calcium and low concentration of iron). An anion exchange procedure has been used in the separation of rare earths from

geological materials (54, 56, 61, 99, 100, 101). These procedures involve the separation of the rare earths from organic solvent acid mixture such as methanol with nitric acid using strong base anion exchange (see Figure 1.5). In pure aqueous nitric acid solution, there is not significant absorption of the rare earths on strongly basic anion exchange resin at any acid concentration (96, 97). The absorption increases when the aqueous component is replaced by miscible organic solvents, such as methanol, ethanol, n-propanol or isopropanol (98).

The choice of the separation procedure depends on the composition of the sample. Most of the above procedures, separate rare earths from geological materials by precipitation as oxalate, hydroxide and sulphate or the use of anion exchange separation and sulphate solution as eluant. These procedures are unsuitable for phosphate samples because of the high concentration of calcium in such samples. Only those procedures which used nitric or hydrochloric acid solutions could be used for phosphate samples. Very little published materials on the separation of rare earths from the whole phosphate rocks is available (107, 108), some of the published material deals with the separation of rare earths from apatite minerals and monazite (100, 61, 106).

Figure 1.5.

The Chemistry of the Anion Exchange Process.

(1) The aqueous solution contains the rare earth metal (M) as nitrate which is completely ionized.

$$M(NO_3)_3 \text{ ------> } M^{3+} + 3NO_3^-$$

(2) The addition of methanol and nitric acid converts the Lanthanide ion to the nitrate complex.

$$M^{3+} + 6NO_3^- \text{ ------> } M(NO_3)_6^{3-}$$

nitrate complex

The methanol lowers the dielectric constant and ensures complete conversion to the complex.

(3) The phosphate from the sample is converted by the acid to undissociated phosphoric acid.

$$3H^+ + PO_4^{3-} \text{ ------> } H_3PO_4$$

(4) The complex anion is absorbed by the resin but the phosphoric acid is easily washed off.

$$M(NO_3)_6^{3-} + 3RNO_3 \text{ ------> } R_3M(NO_3)_6 + 3NO_3^-$$

resin in

nitrate form

CHAPTER TWO:- EXPERIMENTAL.

2.1 Preparation of sample for analysis.

A stratified sampling method was used, where only phosphate rocks had been sampled, other rocks (limestone, sandstone and claystone) found in the locations studied were not investigated. The samples collected from the locations described in Chapter 1 were split into two halves, one half was kept as a reference and the other half was used for analysis. In the field at the time of sample collection all weathered surfaces were rejected and only fresh material representative of the rock was collected.

The collected samples cannot be used in the form they were submitted to the laboratory, since a very fine powder is essential for all the methods of analysis used. The hard samples were crushed into small chips using a jaw crusher. The crushed or friable samples were split into four parts. Three parts were kept as a reference, and only one part was ground into a very fine powder using a Tema mill, in which the sample was ground for fifteen minutes. After each sample the mill was washed with hot water and dried before introducing a new sample. Cross contamination from sample to sample was avoided by grinding a small portion of the new sample for four minutes and rejecting the resulting powder.

2.2 Stock Solutions.

A 100 cm^3 stock solution of each analyte containing 1000 mg dm^{-3}, was prepared using analytical reagent grade chemicals. The weight of each compound used is shown in Table 2.1. Each compound was dissolved in the minimum amount of concentrated nitric acid and the solution was transferred to a 100 cm volumetric flask and diluted to the mark with water. This procedure was applied to prepare the stock solutions for the studied elements, except for cerium. For cerium, the oxide was dissolved first in the minimum amount of hot sulphuric acid, then the solution was evaporated twice to the dryness with nitric acid. The final residue was dissolved in the minimum amount of warm nitric acid, after cooling the solution was transferred to 100cm volumetric flask and water was added to the mark. The stock solutions were stored in clean polythene bottles.

2.3 Reagents.

All reagents were prepared from high quality salts dissolved in distilled water.

Table 2.1

Weight of compounds used to prepare 1000 mg cm^{-3} of the analytes.

Analyte	Compound used.	Weight (g)
Y	Yttrium Nitrate Hexahydrate	0.4308
La	Lanthanum Nitrate Hexahydrate	0.3095
Ce	Cerium (IV) Oxide	0.1228
Pr	Praseodymium Nitrate Pentahydrate	0.2959
Nd	Neodymium Oxide	0.1166
Sm	Samarium Oxide	0.1159
Eu	Europium Nitrate Pentahydrate	0.2817
Gd	Gadolinium Nitrate Pentahydrate	0.2756
Tb	Terbium Chloride Hexahydrate	0.2349
Dy	Dysprosium Oxide	0.1148
Ho	Holmium Oxide	0.1146
Er	Erbium Oxide	0.1144
Tm	Thulium Oxide	0.1142
Yb	Ytterbium Oxide	0.1139
Lu	Lutetium Oxide	0.1137
Th	Thorium Nitrate Pentahydrate	0.2457
U	Uranium (VI) Nitrate Hexahydrate	0.2110

2.3.1 Molybdovanadate Solution.

Sodium metavanadate (1.25 g) was dissolved in 100 cm^3 of nitric acid (50% v/v), this solution was called solution. Sodium molybdate dihydrate (18.75 g) was dissolved in 100 cm^3 of water - solution. The two solutions were mixed and diluted to 500 cm^3 with water.

2.3.2 Hexamine Solution.

Hexamine (3.5311 g) was dissolved in 250 cm^3 of water.

2.3.2 Hexamine Nitrate Solution.

Hexamine (3.5311 g) was dissolved in the minimum amount of water, then 1.6 cm^3 of concentrated nitric acid was added very carefully and the mixture was diluted to 250 cm^3 with water.

2.3.4 Lanthanum Solution (10% w/v).

Lanthanum nitrate (10 g) was dissolved in 100 cm^3 of water.

2.3.5 Arsenazo (III) Reagent (0.1% w/v).

Arsenazo (III) reagent (0.1 g) was dissolved in 100 cm^3 of water, a few drops of sodium hydroxide solution was added to assist solution (111).

2.3.6 Xylenol Orange Reagent (0.001 M).

Xylenol orange reagent (0.1892 g) was dissolved in 250 cm^3 of water.

2.3.7 Sulphuric Acid Solution (1 + 7).

Concentrated sulphuric acid (31.3 cm^3) was added very carefully to 150 cm of cold water, if the solution became warm, the beaker was cooled until the solution was at room temperature. The solution was transferred to a 250 cm^3 volumetric flask and diluted to the mark with water.

2.3.8. Citrate Buffer Solution.

Sodium citrate (147 g) and citric acid (96.5 g) were dissolved in 500 cm^3 of water.

2.3.9 Total Ionic Strength Adjustment Buffer (TISAB)

Sodium chloride (29 g), glacial acetic acid (28.5 cm^3) and sodium citrate (0.15 g) were dissolved in 250 cm^3 of water. The pH of the solution was adjusted to 5.5 using dilute sodium hydroxide solution, it was transferred to a 500 cm^3 volumetric flask and diluted to the mark with water, and stored in plastic bottles.

2.4 Sample Preparation.

Different decomposition procedures were used to

prepare the samples for analysis depending on the analytical method used. A survey of different decomposition procedures applicable to rocks and minerals is given by Bock (112) and Fletcher (113). Mixed acid attack (HF - $HClO_4$) was used to prepare samples for major oxide and trace element determinations with the ICP. Also mixed acid (HF - $HClO_4$) decomposition was used to prepare samples for anion and cation exchange separation of the rare earth elements. The fusion decomposition was used to prepare samples for XRF analysis, and fluoride determination.

2.4.1 Preparation of Samples for Major and Trace Elements by ICP Spectrometer.

The following procedure was used to decompose phosphate rock samples for the measurements of major oxides and trace elements using the ICP spectrometer. In a Teflon beaker 0.5 g of the very fine (less than 100 mesh) powdered rock sample (was weighed out accurately), then 4 cm^3 of concentrated perchloric acid (60% v/v) and 15 cm^3 of hydrofluoric acid (40%) v/v) was added. The mixture was heated overnight to complete dryness. After cooling 20 cm^3 of diluted hydrochloric acid (25% v/v) was added and the solution was gently warmed until all salts dissolved. The solution was cooled and transferred to a 50 cm^3 volumetric flask and diluted to the mark with hydrochloric acid (25% v/v).

2.4.2 Sample Preparation for the Separation of Rare Earths by Ion Exchange.

In the ion exchange procedure a large sample, 100 g for the anion exchange and 10 g for the cation exchange, was used to insure a sufficient concentration of the rare earth elements being separated for the ICP. Mixed acid, nitric, perchloric and hydrofluoric acids, were used. This mixture can not be added to the phosphate rock samples directly because the sample contain a large concentration of calcium (about 50% as CaO) and a large precipitate of calcium fluoride ($K_{so}=5 \times 10^{-11}$) would form. The sample was first wetted with water and then concentrated nitric acid (70% w/v) was added until no gases were evolved. The solution was warmed on a hot plate to assist the reaction. After cooling, the undissolved residue (sand, clay and refractory minerals) was separated from the solution by filtration using a Whatman No. 42 filter paper. The filter paper was washed several times with water. The filter paper with the residue was transferred to a Teflon beaker and 15 cm^3 of nitric and perchloric acids mixture (4 + 1) was added to decompose the filter paper (114). The mixture was heated to dryness, then another 15 cm^3 of the acid mixture (4+1, HNO_3 + $HClO_4$) was added. When this was hot, 25 cm^3 of hydrofluoric acid (48% v/v) was added in small quantities (0.5 cm^3) and the mixture was heated overnight to complete dryness. After

cooling the residue was evaporated twice to dryness with concentrated nitric acid. The final residue was dissolved in diluted nitric acid (40% v/v) then transferred to the beaker which contained the filtrate collected before, and the solution was evaporated to a stage near dryness where it becomes very viscous. This was used to prepare solutions for the anion and cation exchange procedures.

2.4.2.1 Anion Exchange.

The viscous residue obtained was diluted with 56 cm^3 of water and the mixture warmed. After cooling, 44 cm^3 of concentrated nitric acid followed by 500 cm^3 of methanol was added. The precipitate formed when methanol was added was removed by filteration through a Whatman No. 41 filter paper. The analysis of this precipitate by XRD show that it was silicon dioxide and/or hydrated calcium sulphate sometimes contaminated with iron nickel sulphide (Pentlandite). The filter paper was washed with methanol and the filterate was diluted to 2 dm^3 with methanol. This solution was later pumped through the anion exchange column to separate the rare earth elements.

2.4.2.2 Cation Exchange.

The thick solution obtained in section 2.4.2 was diluted with 20 cm^3 of water, then the mixture was warmed to assist dissolution. After cooling a volume of 6.3 cm^3

of concentrated nitric acid was added. The solution was then transferred to a 100 cm^3 volumetric flask and diluted to the mark with water. This solution was later passed through the cation exchange column to separate the rare earth elements.

2.4.3 Preparation of Fused Glass Discs for Major Oxides Analysis by XRF.

The following procedure was used to prepare the fused glass disc which was used in the XRF determination of major oxides. An accurate weight (0.3 g) of the very fine powdered phosphate sample was mixed with 3.0 g of lithium metaborate flux (MERCK - SPECTROMELT - A 10) on a paraffin paper by stirring with a Pt-wire (5% gold). Particular attention was paid in order to avoid loss or contamination of the mixture. The mixture was placed in a Pt-crucible (5% gold). The crucible was placed in position in the bead machine - Philips P W 1234/20, and the recommended procedure from the manual was used to operate the machine. The prefusion step was extended to one minute and the heat increased more slowly as recommended for phosphate samples to allow all the gases to be evolved and to prevent the loss of sample by spitting. After the sample was cooled, the necessary information (sample number, date and geologist name) was marked on the top of the glass disc, the bottom surface was used for the x-ray analysis.

2.4.4 Preparation for Fluoride Determination.

An alkaline fusion has been used in many schemes (115, 116) to decompose rock samples for fluoride determination. The procedure used in this work is as follows. In a nickel crucible 0.25 g of the sample and 1.25 g of the fusion flux (2 parts of sodium carbonate + 1 part of potassium nitrate) were weighted accurately and mixed well with a small plastic rod. Particular attention was taken to avoid loss or contamination of the mixture. The crucible was heated using a Meker burner, using initially a gentle heat until the gases are all evolved then full heating was applied until the sample was completely decomposed. The melt was gently swirled around the crucible to incorporate into the the melt any powder or droplets of the melt on the sides of the crucible, The cool crucible was placed into a beaker with 10 cm^3 of water and allowed to stand overnight. This solution was used for the fluoride determination.

2.5 Cleaning.

Before starting any experiment all vessels were cleaned and dried to be ready for a new run. The vessels used were glass-ware, platinum crucibles, nickel crucibles, porcelain boats and polythene bottles. Different procedures were used to clean each type and these are discussed below. After the vessels were

cleaned they were washed thoroughly with water then dried in an oven at 100 C before use, except for the glass-ware and polythene bottles which were left to dry on the bench.

The platinum crucibles and the porcelain boats were cleaned by boiling them in diluted nitric acid (10% v/v) until they were visually clean. While nickel crucibles were boiled in distilled water. The glass-ware and the polythene bottles were soaked overnight in diluted nitric acid (20% v/v).

2.6 Spectrophotometric Analysis.

These methods depend on a reaction between the analyte element and a reagent to form a coloured species which absorbs light of a wavelength different from that of the original reagent. Some of these reagents are specific for one element only, others are not. The spectrophotometric procedure was used in the determination of phosphate ions, thorium, uranium and individual rare earth elements, and are discussed in detail below.

2.6.1 The Determination of Phosphate Ions.

The yellow molybdovanadophosphoric acid complex is the basis of the method considered to be the most specific for phosphorus (117). The procedure used was the

recommended procedure for the determination of phosphate (expressed as P_2O_5) in phosphate rocks (118). To an aliquot of the solution which contain phosphate ions, 5 cm^3 of sulphuric acid solution (1+7) was added followed by 25 cm^3 of the molybdovanadate reagent. The mixture was diluted to 100 cm^3 with water, mixed thoroughly, and then allowed to stand at room temperature for 30 minutes. The absorbance of the yellow complex was measured at 420 nm, in a 1 cm cell against a blank containing the reagents, using the Pye Unicam - SP 1800 spectrophotometer.

2.6.2 The Determination of Uranium.

Numerous reagents have been used for spectrophotometric determination of uranium, but Arsenazo III is the most widespread reagent. The procedure used is a modification of that suggested by Kadam et al. (111), where the diethylen-triaminepentaacetic acid (DTPA), used as a masking agent, was omitted since only pure uranium solutions were being tested. The procedure used was as follows. A volume of 1 cm^3 of the reagent was added to an aliquot of the solution. The pH of the solution was adjusted to a value around 5.5 using (10% w/v) hexamine solution. The mixture was diluted to a 100 cm3 with water. The absorbance of the solution was measured at 635 nm, in a 1 cm cell against a blank containing the reagents, using the Pye Unicam - SP 1800

spectrophotometer.

2.6.3 The Determination of Thorium (120).

The pH of an aliquot was adjusted to a value of 7 using dilute sodium hydroxide and dilute hydrochloric acid, followed by the addition of 42 cm^3 of concentrated hydrocholric acid. Then 1 cm^3 of arsenazo III reagent was added and the solution was diluted to 100 cm^3 with water. The absorbance of the solution was measured at 630 nm, in a 1 cm cell against a blank containing the reagents, using the Pye Unicam - SP 1800 spectrophotometer

2.6.4 The Determination of Rare Earth Elements.

The method chosen for the determination of rare earth elements was that using xylenol orange as suggested by Serdyuk and Smirnaya (121). The reaction between the indicator and the elements is not selective, hence each element must be present alone in the solution. The procedure followed was used to determine a rare earth element in the solution obtained when optimising the anion exchange procedure. To an aliquot sample, 2 cm^3 of the xylenol orange reagent was added and the solution was neutralized using dilute sodium hydroxide, until the colour just changed from yellow to purple. Then 2 cm^3 of hexamine solution and 2 cm^3 of hexamine nitrate solution were added (ie. hexamine buffer used to adjust the pH of the solution to a value

of 5-6). The solution was diluted to 100 cm^3 with water. The absorbance of the solution was measured at 575 nm, in a 1 cm cell against a blank containing the reagent, with a Pye Unicam - SP 1800 spectrophotometer.

2.7 Determination of Fluoride.

The measurement of fluoride concentration with a fluoride electrode was chosen because of the good selectivity of the electrode, which allowed the measurement of fluoride without separation from the bulk of the sample (122). The procedure used was suggested by Crenshaw and Ward (116). The solution obtained after sample decomposition, see section 2.4.4, was stirred with small stirring rod and transferred to a 100 cm^3 volumetric flask, the nickel crucible being washed first with 20 cm^3 of water followed by 10cm^3 of citrate buffer (to adjust the pH of the solution to a value of about 4.3)and finally with 10 cm^3 of water. The flask was swirled to liberate the carbon dioxide formed by the reaction of acid with carbonate and diluted to the mark with water. The contents of the flask were transferred to a polypropylene beaker immediately and allowed to stand for an hour. an aliquot of 50 cm^3 was transferred to a clean polypropylene beaker and mixed with 50 cm^3 of TISAB solution. The reference electrode (single junction reference electrode - ORION model 90-01), and the fluoride electrode (ORION - model 96-09) were immersed into the solution. The solution

was stirred with a magnetic stirrer for one minute, then the concentration of fluoride in the solution was measured using a potentiometer (ORION microprocessor ionalyzer - model 901) which had been adjusted to read concentration. The concentration of fluoride in the sample is calculated using the equation.

$$F_{SM} = \frac{F_S * R_{SM}}{R_S}$$

F_{SM} = concentration of fluoride in the sample (mg kg^{-1})

F_S = concentration of fluoride in the standard reference rock (mg kg^{-1})

R_S = concentration of fluoride in aliquot (50 cm^3) of the standard rock (mg kg^{-1})

R_{SM} = concentration of fluoride in aliquot (50 cm^3) of the sample (mg kg^{-1})

2.8 The Determination of Carbon Dioxide.

Carbon dioxide was measured using a coulometric method (123). The coulometric process unlike other processes (infra-red absorption, thermal conductivity, electrical conductivity and detection with a flame ionization detector) gives results in fundamental theoretical units. Therefore, chemical or sample calibration is not required. The procedure used for the

measurements is based on the recommended procedure in the manufacturers instruction manual. The porcelain boat containing 0.2 g of the sample was dropped into the sample tube in the apparatus (Coulometric Inc. - model 5030). Then 2 cm^3 of 2 N perchloric acid was added. The evolved gases were carried with air from which carbon dioxide was removed by passing it through an air scrubber solution (45% KOH w/v). The evolved gases were passed to a carbon dioxide coulometric measurement unit (Coulometric Inc. - model 5010). Only carbon dioxide was allowed to pass to the measurement unit, other gases, H_2S, SO_2, HCl, Cl_2 and NO_2, were absorbed by passing the evolved gases through a solution of KI (50% w/v) at a pH = 3. These gases interfere with carbon dioxide measurements. The evolved carbon dioxide was introduced to the coulometer cell which was filled with a partially aqueous medium containing ethanolamine and a colorimetric indicator. When the gases were passed through the solution, carbon dioxide was quantitatively absorbed and was converted to a strong titratable acid by the ethanolamine. The solution turned to deep blue as the end point is reached, and titration end point was detected by a photometer set at 612nm. Electronic scaling within the coulometer convert the number of coulombs to a digital readout of micrograms of carbon. The concentration of carbon dioxide in the sample was calculated from the equation.

$$\% \text{ carbonate carbon} = \frac{(\text{micrograms C} - \text{blank}) * 100}{\text{micrograms sample}}$$

$$\% CO_2 = \% \text{ carbonate carbon} * 3.664$$

2.9 The Determination of Calcium.

The concentration of calcium in the eluant obtained in the optimisation of the separation procedure was measured by using flame atomic absorption spectrophotmetry. Lanthanum was added (final concentration 0.5%) to eliminate phosphate ion interference (124). The flame (air-acetylene), hollow cathode lamp current and wavelength (422.7nm) used were as recommended in the instrument (Instrumentation Laboratory Incorporated - model IL 251) manual.

2.10 The Determination of Major Oxides and Trace Elements Using ICP.

The concentration of major oxides and trace elements in the sample solution obtained from the acid decomposition (see section 2.4.1) were measured using ICP spectrometer (IRL 34000).

Lack of time did not allow the optimisation of the spectrometer parameters (carrier gas, auxiliary gas, plasma gas and position of measurements above the coil)

and measurement of inter-element interferences and correction factors for the present sample - phosphate rock. These interferences were corrected by using the existing computer program. The plasma conditions used are shown in Table 2.2, the wavelengths in Table 2.3.

2.11 Determination of Major Oxides Using XRF.

The fused glass discs (see section 2.4.3) were used to measure major oxides in the phosphate samples. However manganese oxide, magnesium oxide and sodium oxide were not estimated by XRF. The procedure used was the procedure recommended in the manual of the instrument (Philips - model PW 1410/10). The operating conditions of power, current, anode targe, crystal, collimator, 2 and counting time are shown in Table 2.4. A standard reference phosphate rock, such as NBS-120b, was used to prepare the calibration graph. The use of a fused glass sample and a matching standard eliminate matrix interferences. The concentration of each analyte was calculated from the equation.

$$C_u = \frac{C_s * I_u}{I_s}$$

Where C_u = concentration of analyte in the sample (%).

C_s = recommended concentration of the analyte

Table 2.2

Instrumental conditions used with IRL 34000 ICP spectrometer.

Parameters	Conditions Used
Frequency (MHz)	50
Power of the plasma (kW)	1.25
Sample uptake rate (cm^3 min^{-1})	0.23
Carrier gas flow rate (dm^3 min^{-1})	0.8
Auxiliary gas flow rate (dm^3 min^{-1})	1.0
Plasma gas flow rate (dm^3 min^{-1})	10
Observation height above the coil (mm)	18

Table 2.3

Wavelength used in the determination of major oxides and trace elements.

Analyte	Wavelength (nm)
As	193.72
Mo	202.03
Sb	206.83
Zn	213.85
Pb	220.35
Ni	231.60
W	239.71
B	249.67
Mn	257.61
Cr	267.72
Fe	275.57
Mg	279.08
Sn	303.40
Nb	309.42
Ca	315.89
Cu	324.75
Ag	329.07
Zr	343.82
Ti	368.51
Al	396.15
Ba	455.40
Na	588.99
K	766.49

TABLE 2.4

INSTRUMENTAL CONDITIONS FOR PHILIPS, PW 1410/10 SPECTROMETER.

ANALYTE		Fe_2O_3	TiO_2	CaO	K_2O	Al_2O_3	SiO_2	P_2O_5
PARAMETER								
	ANODE	Cr	Cr	Cr	Cr	Cr	Cr	Cr
X-RAY	kV	40	40	30	30	30	30	30
TUBE	mA	50	50	10	20	80	80	80
COLLIMATOR		FINE	FINE	FINE	COARSE	COARSE	COARSE	COARSE
CRYSTAL		LIF (200)	LIF (200)	LIF (200)	LIF (200)	PE	PE	PE
2θ		57°54	86°18	113°13	136°71	144°78	109°05	89°57
COUNTING TIME (SEC)		10	40	10	10	40	40	40

in the standard rock (%).

I_u = XRF intensity for the sample (counts sec^{-1})

I_s = XRF intensity for the standard rock (counts sec^{-1}).

2.12 Neutron Activation Analysis of Phosphate Rock for Rare Earth Elements.

The procedure used to prepare the samples for irradiation and measurement of rare earth elements was that used in the Scottish Universities Research and Reactor Center in East Kilbride. Eight elements, lanthanum, cerium, neodymium, samarium, europium, terbium, holmium, ytterbium and lutetium were measured. The procedure was as follows. An accurate weight of the sample, 0.2g, was placed inside a small polythene tube and the tube then sealed. The tube and 0.098g of iron wire (99.5% pure), used as a flux monitor, were wrapped in aluminium foil. The samples were irradiated in the central stringer (CVS) for 6 hours in a flux of 3.6×10^{-12} n cm^{-2} sec^{-1} and the time of termination of irradiation (t_o) was noted. After 3-4 days decay, the flux monitors were separated and external contamination was removed from the sample containers. Gamma ray energies for rare earth isotopes are shown in Table 2.5 Gamma emitters with energies

Table 2.5.

Rare earth element isotopes, half lives and gamma ray energies.

Isotope	Half Life	Photopeak KeV
^{140}La	40.2 h	328.7 487 816 1596
^{131}Ce	33 d	145.5
^{147}Nd	11.1 d	91.1 531
^{153}Sm	47 h	70 103.2
^{152}Eu	12 y	122 779 1409.9
^{166}Ho	26.9 h	80.6
^{175}Yb	4.21 d	63 177 198 396
^{177}Lu	6.7 d	208.4

below 140 KeV were counted with an 0.5cm planar Ge(Li) detector with a resolution of 623 eV at 122 KeV and gamma emitters with energies above 150 KeV were counted with an 80cm coaxial Ge(Li) detector with a resolution of 2.2 KeV at 1.33 Mev. Both detectors were controlled by an EGG-ORTEC Data Acquisition and Analysis System which processed the resulting spectra to provide net photopeak areas for isotopes of interest. Results were calculated by comparing the activities of the sample with that of a standard reference rock (BCR-1) which was irradiated with the samples. The concentration of analyte elements were calculated from the following equations.

$$A_o = A_t * e^{\lambda t}$$

Where A_o = activity at time zero.

A_t = activity at measurements time.

λ = decay constant = $(\ln 2)/t_{1/2}$.

$t_{1/2}$ = isotope half life.

t = time passed after irradiation (hours).

The concentration of analyte in the sample (expressed as mg kg^{-1}) is calculated from the equation.

$$C_u = \frac{A_{uo} * W_s * C_s}{A_{so} * W_u}$$

Where C_u = concentration of analyte in the sample.

C_s = concentration of analyte in the standard rock.

A_{uo}= corrected activity of analyte in the sample (counts sec^{-1}) at time zero.

A_{so}= corrected activity of analyte in the standard rock (counts sec^{-1}) at time zero.

W_u = weight of the sample (g).

W_s = weight of the standard rock (g).

2.13 Determination of Rare Earth Elements with the ICP.

The rare earths were measured using the ICP spectrometer constructed at the University of Strathclyde which is described in detail below. The plasma parameters (carried gas flow rate, auxiliary gas flow rate, power, plasma gas flow rate and observation height above the coil) used were those obtained after optimisation, see Table 6.1 (for the anion exchange) and Table 6.3 (for the cation exchange) in chapter six. The monochromator has a single PMT, so each element was measured separately at the most sensitive ionic line, see Table 2.6 (33). In the anion exchange analysis, the background intensity was measured by aspirating a blank solution, while in the cation exchange analysis it was possible to measure the background intensities at both sides of the analyte wavelength due to the introduction

Table 2.6

Wavelengths used in determination of analytes of interest.

Analyte	Wavelength (nm)
Y	371.030
La	408.672
Ce	413.765
Pr	390.844
Nd	401.225
Sm	359.260
Eu	381.967
Gd	342.247
Tb	350.917
Dy	353.170
Ho	345.600
Er	337.271
Tm	313.126
Yb	328.937
Lu	261.542
Th	283.730

of a background correction system.

2.14 Instrumentation

The apparatus used in this work is described in detail below. The system consists of a plasma source unit, and Echelle monochromator and a signal processing unit as shown in Figure 2.1.

2.14.1 Plasma Source Unit.

The main components of the unit are:

- Plasma source (Philips PV 8490)
- standard torch
- Babington type nebuliser
- spray chamber with flow spoiler
- peristaltic pump

The plasma source consists of a radio frequency generator operating at a nominal free running frequency of 50 MHz and capable of delivering a continuously variable power between 0.7 and 2.0 kW into the plasma. The current induces a magnetic field by means of a two-turn water-cooled load coil. The plasma is started by means of a Tesla discharge which causes primary ionisation of the argon atoms, thus enabling coupling to the radio frequency power via the magnetic field.

The torch is of quartz "organic 36" type. The torch assembly consists of three welded quartz tubes, as shown in Figure 2.2. The three gas flows have ranges as follows:

Figure (2.1)
Schematic diagram of the main components of the ICP system

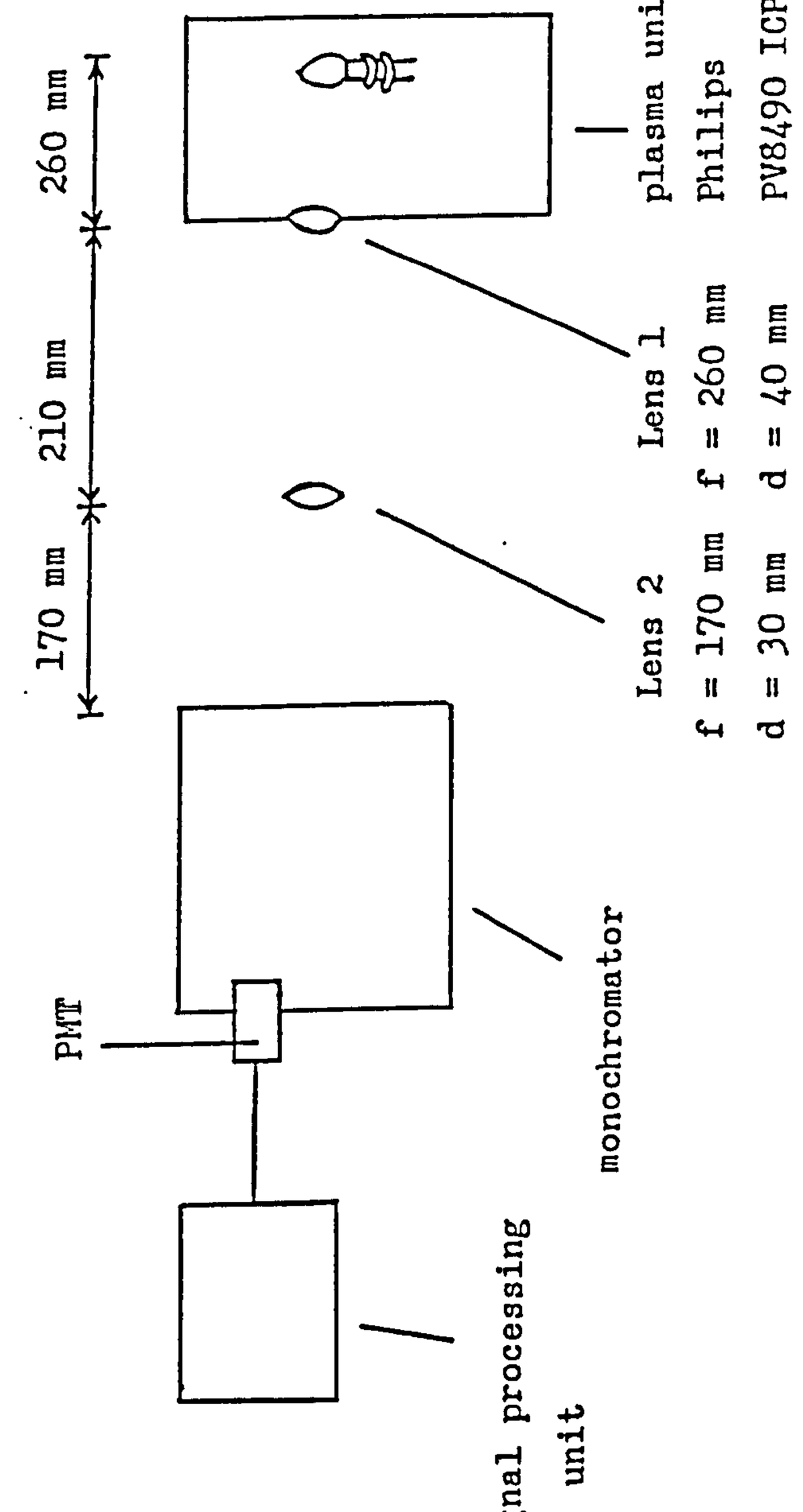

Figure (2.2)

Schematic drawing of the torch assembly

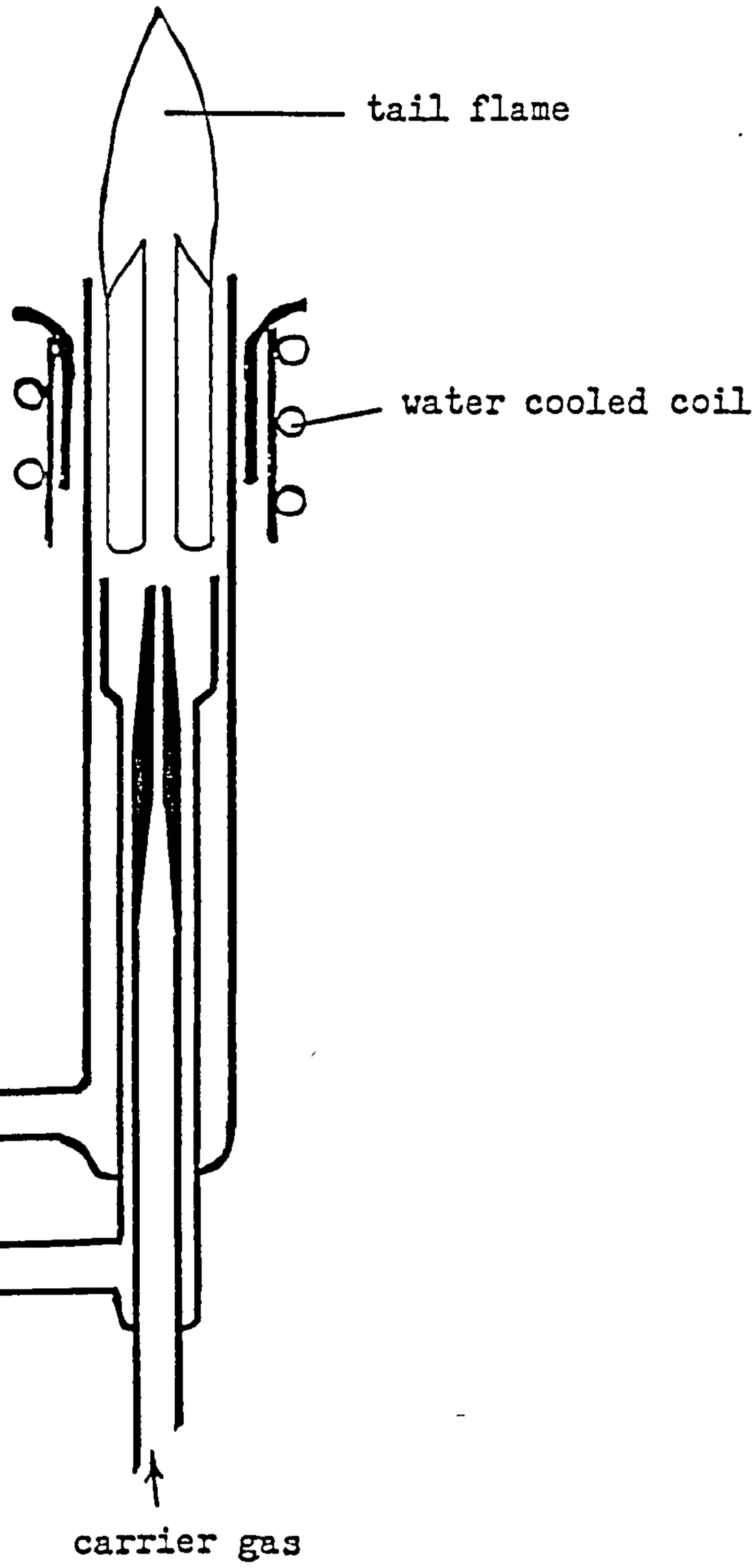

carrier gas flow 0 to 0.75 dm^3 min^{-1}

auxiliary gas flow 0 to 6 dm3 min^{-1}

plasma gas flow 0 to 25 dm^3 min^{-1}

Argon gas of at least 99.5% purity was used for all experiments. The use of three separately controlled gas flows insures a high temperature plasma; prevents the quartz tubes of the torch from melting and positions the plasma inside the coil in such a manner as to form the plasma into a toroidal shape through which a sample aerosol can be transported by the carrier gas.

The glass nebuliser used was an 0.2 mm Babington-type, in which the solution is fed on to a V-cut on the tip of the horizontal gas capillary. The spray chamber was connected to the nebuliser by a hollow Teflon tube, had a flow spoiler and, at the far end of the chamber, an uptake pipe and a drain, as seen in Figure 2.3. The sample solution was pumped to the nebuliser by a peristaltic pump at 1.5 cm^3 min^{-1}. The nebulizer produces an aerosol of the sample in argon gas, this aerosol carrier gas flows through the spray chamber to separate the coarse droplets from the fine ones, these later are injected through the central tube of the torch into the plasma.

2.14.2 The Monochomator.

The radiation from the plasma was focussed on

Figure (2.3)

Schematic drawing of the complete nebulizer system :- nebulizer , spray chamber and drain " U " tube .

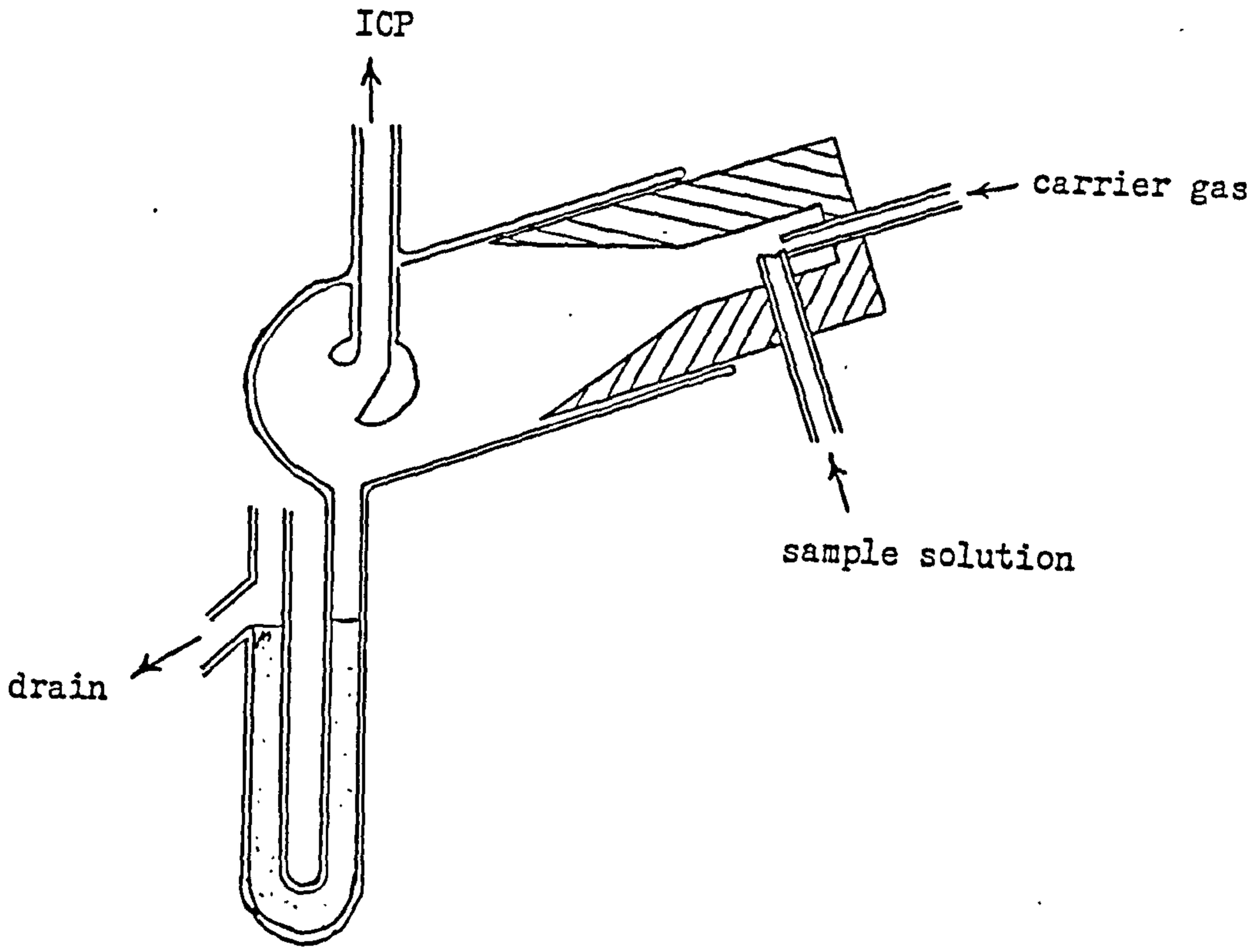

the entrance slit of the monochromator using two long-focus lenses, as can be seen in Figure 2.1. The monochromator used was a Spectrametrices Inc. SMI III echelle monochromator. The optical characteristics of the monochromator are given in Table 2.7. The input radiation was refracted twice by a prism located in front of the echelle grating. The prism serves to separate the spectral orders from the grating while the echelle grating separates wavelength within the orders. The correlative linear dispersion varies from 0.062 nm mm^{-1} at 200 nm to 0.25 nm mm^{-1} at 800 nm. The two dispersing elements (the prism and the grating) are independently moved and have distinct manual wavelength controls. The two dimensional spectrum is presented at the exit slit. In this work the system was used in a single channel mode. However, a multichannel option is available using a multichannel cassette which has a number of exit slits and an array honeycomb held in a "honeycomb" structure for simultaneous multi-wavelength work. A schematic diagram of the major optical components are given in Figure 2.4. Entrance and exit slits sizes are variable, and the sizes available are given in Table 2.8. Selection of slit width and height was achieved by the movement of two sliding orthogonal slit carriers. Throughout this work the slits were maintained at the maximum slit height of 0.5 mm and a width of 0.1 mm.

Figure (2.4)

Diagram of the Echelle III monochromator

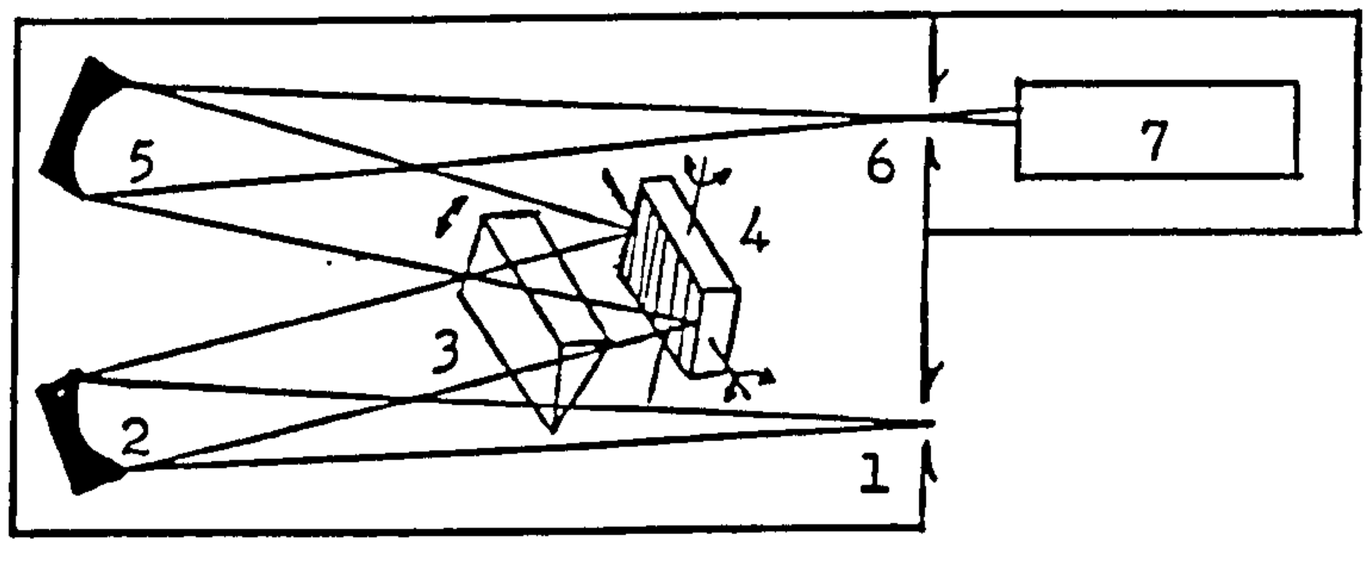

1. entrance slit 2. collimating mirror 3. prism
4. grating 5. focusing mirror 6. exit slit
7. photomultiplier tube (PMT)

Table 2.7

Optical characteristics of Spectraspan Echelle III B monochomator.

Grating	Echelle grating
Size	96 mm x 46 mm
Focal length	F = 750 mm
Aperture	Effective diameter of the optics F/13
Diffraction angle	63^{o} 26'
Groove spacing	79 grooves mm^{-1}
Order disperser	30^{o} prism (Suprasil-W1)
Spectral order used	28 th - 118 th

Table 2.8.

Entrance and exit slit dimensions.

Vertical slit		Horizontal slit	
Position	Height (mm)	Position	Width (mm)
1	0.1	1	0.025
2	0.2	2	0.05
3	0.3	3	0.1
4	0.5	4	0.2
		5	0.5

The detector used was a Hamamatsu R292 photomultiplier tube (PMT) which exhibits a spectral response in the range 160-650nm. The PMT anode voltage is varied from 550 V to 1000 V in ten preset positions.

2.14.3 Signal Processing.

Throughout the progress of the work, the whole signal processing system was continually being modified because of a second project running at the same time (48).

At the beginning, the plasma intensity was modulated with a sectored disk chopper at 175 Hz. The modulation facilitated the use of a lock-in amplifier (Ortec Brookdeal 9501 E) for amplification and readout of the PMT signal. The output of the lock-in amplifier was displayed on a Servoscribe R E 541.20 chart recorder. The major components of this system are presented in Figure 2.5. This arrangement was used in the optimisation of plasma parameters for methanolic solution.

A lock-in amplifier has a phase sensitive detector and as such will provide a d.c. output which is proportional to the amplitude of an a.c. input locked to the phase of the reference. In this case the a.c. input is the plasma intensity modulated by the chopper and the reference is derived from the same chopper. The two

Figure (2.5)

Schematic diagram of the original signal processing unit

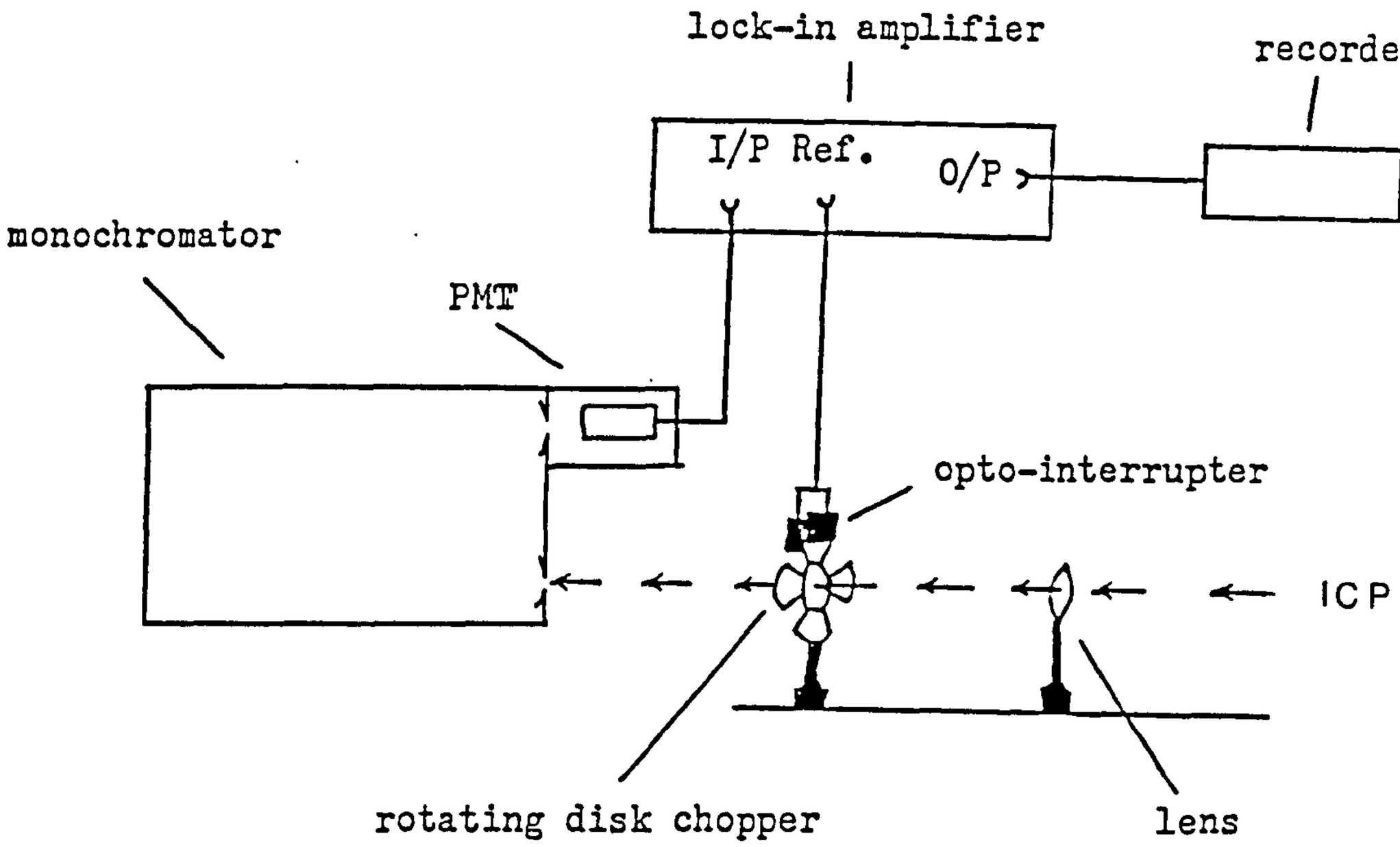

signals are phased manually using a ten-turn potentiometer on the lock-in amplifier, which gives a phase shift of up to 90°. The resulting signal is displayed on the chart recorder. The height of the background (in mm) was measured from the base line when aspirating the blank solution, while the height of the analyte intensity (in mm) was measured from the base line when aspirating the analyte solution.

The system was modified (48) by removing the lock-in amplifier and the rotating chopper. The PMT anode current was delivered to an amplifier constructed at Strathclyde University. The fist stage is a current-to-voltage amplifier. The analogue output voltage is then digitised by an Interactive Structures AI-13 12-bit analogue to digital converter (ADC) connected to an Apple IIe 64K microcomputer. With the software developed at Strathclyde University, it was possible to control the ADC sensitivity ranges, number of measurements and time of measurement. A schematic diagram of this modification is shown in Figure 2.6. This arrangement was used in the study of the rare earths spectral interferences and in the analysis of eluante solution from the anion exchange procedure.

The final modification (48) was the introduction of a computer-controlled torque motor/quartz plate combination into the previous

Figure (2.6)

Schematic diagram of the first modification in the signal processing unit

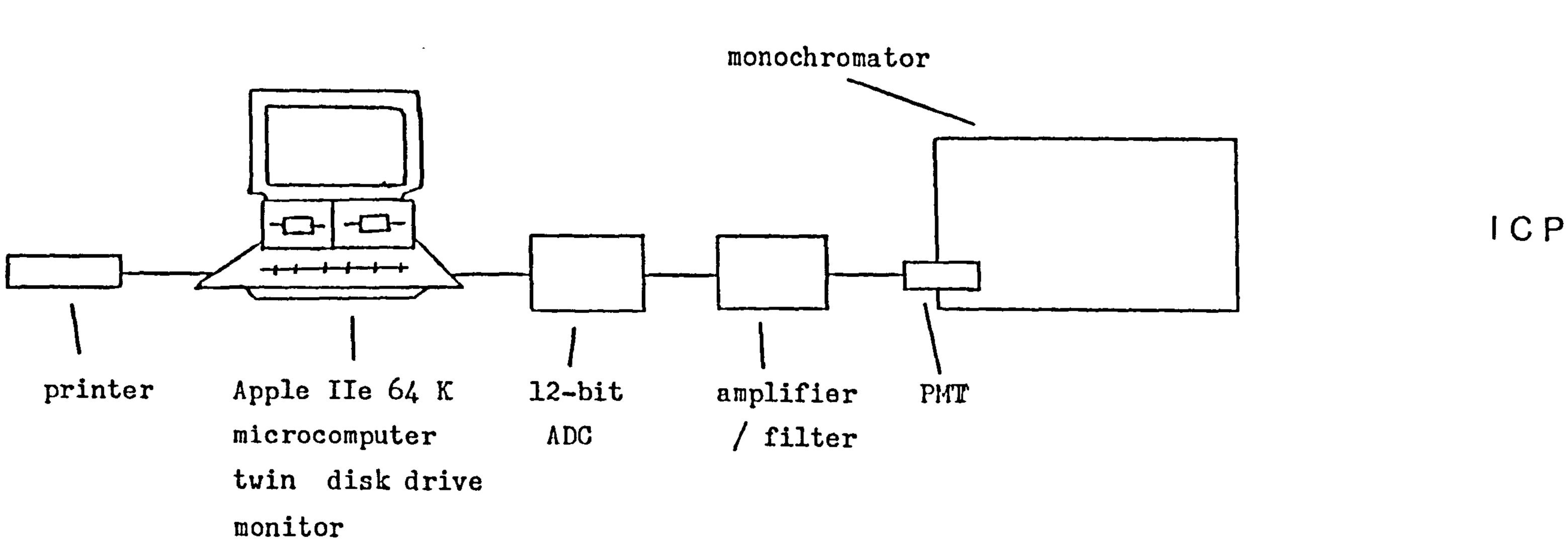

arrangement after the entrance slit. This allowed automatic background correction to be made. A schematic diagram of the components is shown in Figure 2.7. The additional hardware consists of a General Scanning G300PD torque motor with a compatible scanner controller, a "Suprasil" quartz plate (20x20x5mm) and an Interactive Structure AO 03 8-bit digital to analoge converter (DAC). This new system was used in the study of interferences and the analysis of solutions eluted from the cation exchange procedure.

2.15 Separation Columns.

2.15.1 Anion Exchange.

The anion exchange procedure used to separate the rare earth elements from the phosphate samples was similar to that recommended by Roelandts et al (100). The only difference was the use of a different strongly basic anion exchange resin, ie. the commercially available AMBERLIT IRA-401 resin in the chloride form. Before using the resin in any separation experiments it had to be transformed to the nitrate form. Five hundred grams of the AMBERLIT IRA-401 resin were suspended in 3 dm^3 of water, the mixture was stirred. Broken and fine particles were removed by decantation. The resin was transferred to a large column and converted to the nitrate form by elution with diluted nitric acid (in the range 1 to 7 M) until no chloride was detectable in the

Figure (2.7)

Schematic diagram of the computer controlled system for background correction

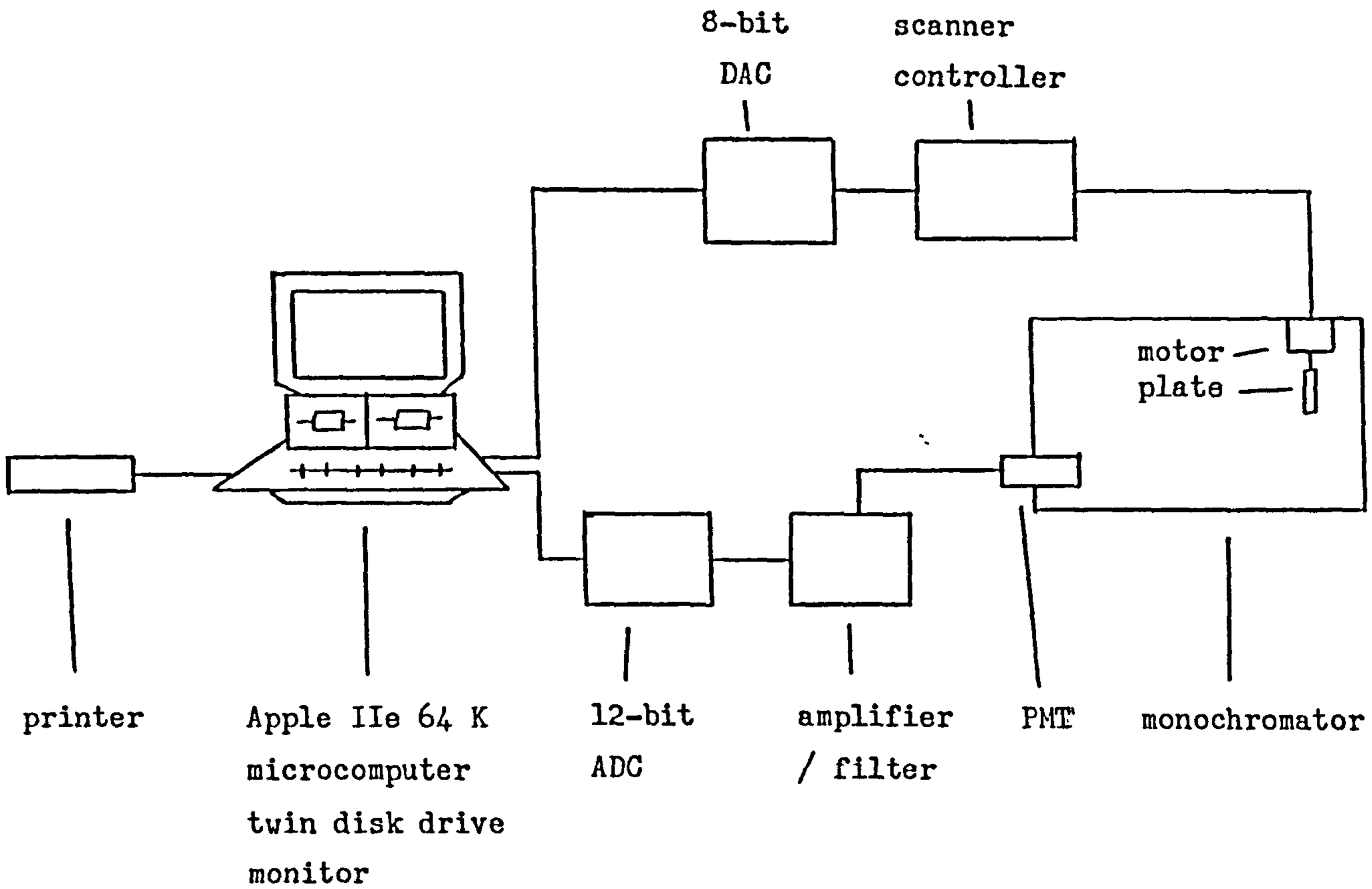

effluent using diluted silver nitrate solution. The free nitric acid was removed by passing water through the column until the effluent was neutral, methyl orange indicator was used to detect the acidity change. The resin was placed in an oven at 70 C until it was completely dry, then it was cooled to room temperature and stored in a screw-cap bottle for further use.

The equipment used in the ion-exchange separation was constructed at Strathclyde university. It consisted of a separation column, solvent premix column and a peristaltic pump. This system is schematically illustrated in Figure 2.8. The separation column was made of borosilicate glass with an internal diameter of 2 cm. The length of the column was varied, either 30 cm (small column) or 110 cm (large column). A glass wool plug was placed at the bottom of the column to support the resin bed. In order to pack the column with a water-swollen resin, the column was filled with water to a certain level and the water-suspended resin was introduced in small quantities and allowed to settle freely to form the bed and to prevent the presence of air bubbles. The resin was added until the recommended height was reached, 20 cm for the small column and 100 cm for the large column.

The rare earth elements are absorbed by the resin when these elements are in methanolic solution,

Figure (2.8)

Schematic diagram of the column configuration for the anion exchange separation :- separation column , premix column , three way tap and peristaltic pump .

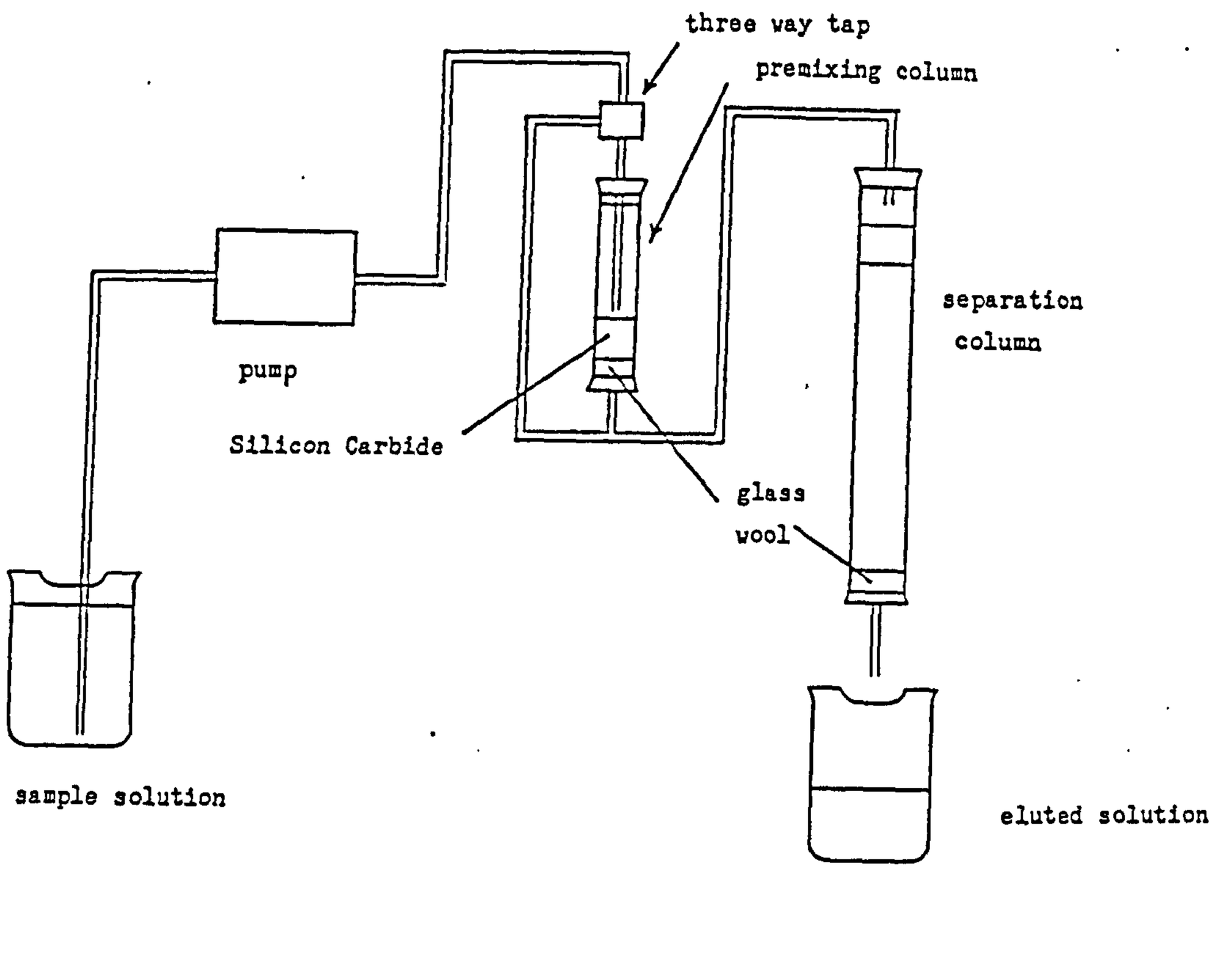

but they are released by elution with water. The introduction of an aqueous eluant to the column which already contains an organic phase (or vice versa), causes the formation of air bubbles in the column. This is true even when the two phases were mixed in a test tube. So a gradual mixing in a premix column is essential, any bubbles being formed and evolved before the solution enters the separating column. This was achieved by the use of a layer of coarse crystals of Carborundum (silicon carbide) in the premix column. This column is a 150 cm^3 cylindrical funnel containing a 2 cm layer of silicon carbide supported by a glass wool plug. When the system was in the aqueous phase and was to be transformed to the organic phase a small glass tube reaching a position near the surface of the carbide layer was fitted to the input, so the methanolic solution flows upwards through the aqueous solution and is gradually mixed into the aqueous phase. This tube was removed when it was necessary to change the phase from organic to aqueous, the aqueous solution will sink through the methanolic solution and so will change gradually. As soon as the eluant in the separation column had been altered to organic phase, the sample and washing solutions were pumped directly into the analytical column bypassing the premix column using a three way tap.

The flow rate of the phosphate solution (see

section 2.4.2.1) was maintained constant at 1.8 cm^3 min^{-1} using a peristaltic pump (Technicon - Auto Analyzer). acid and organic solvent resistant pump tubes (Sterilin Instruments) were used. The system was sealed to prevent any leaks and to maintain a constant pressure throughout the operation.

Several ion exchange columns were prepared to run a batch of samples at the same time. The columns were equilibrated before introducing any sample by passing alternately methanolic solution then water. This procedure was repeated twice.

2.15.2 Cation Exchange.

The cation exchange procedure used to separate rare earth elements from the phosphate solution is similar to that used by Crock et al. (126). The available commercial cation exchange resins (AMBERLIT IR-120, DOWEX 50W X8 and BIO RAD AG50W X8) were dried in an oven at 70C until the resins were completely dry. The dry resin was kept in a screw-top bottle for further use.

The column configuration is shown in Figure 2.9. It consists of a borosilicate glass column, either 30 cm for the small column or 110 cm for the large column. The weight of the dry resin used in the column was 25 g for the small column or 50 g for the large

Figure (2.9)

Schematic diagram of the column configuration for the cation exchange separation :- separation column and peristaltic pump .

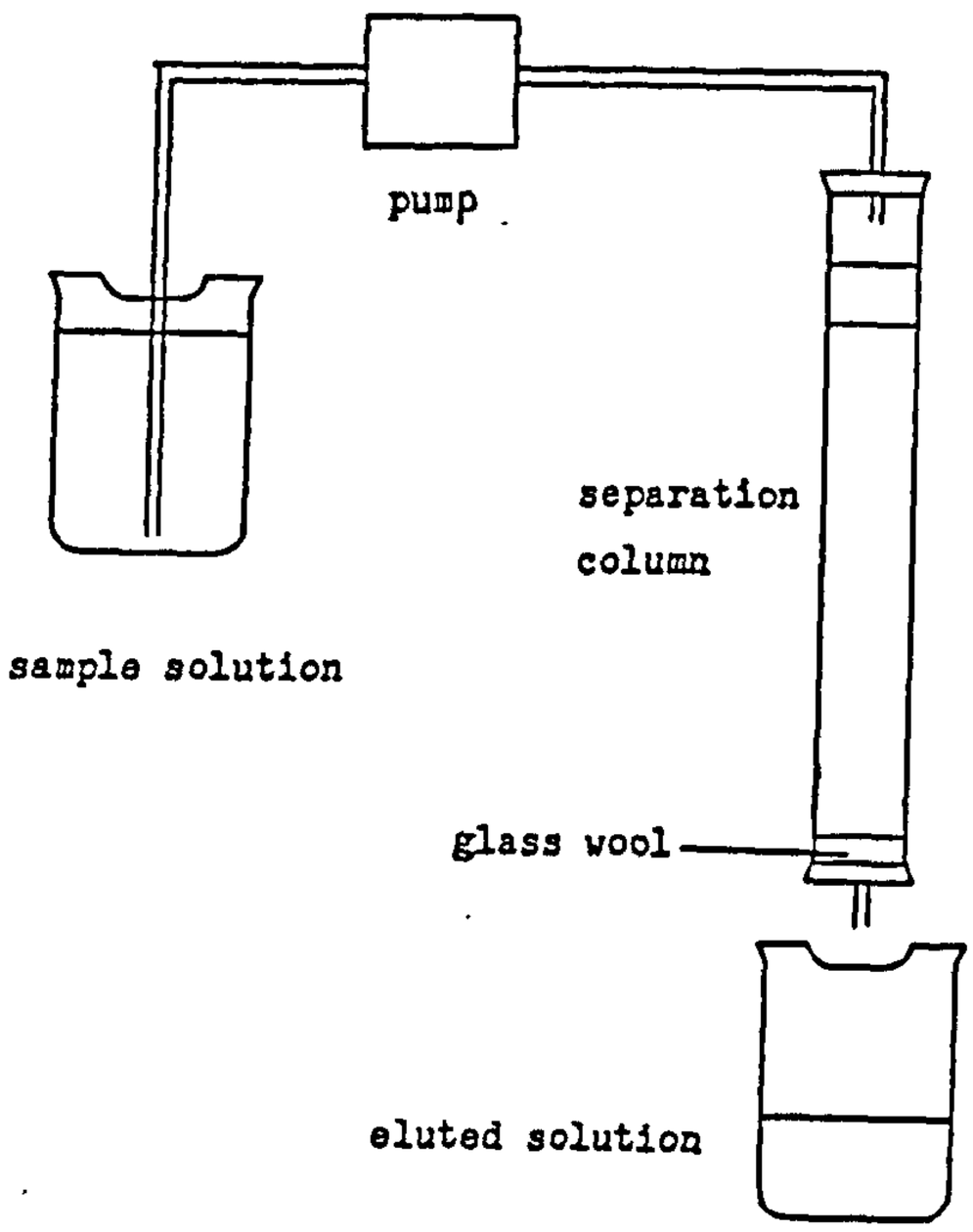

column. A glass wool plug was placed at the bottom of the column to support the resin bed. In order to pack the column with a water-swollen resin, the column was filled with water to a certain level and the resin, suspended in water, was introduced in small quantities and allowed to settle freely to form a bed and to prevent the presence of air bubbles. The column was sealed and connected to a peristaltic pump (Technicon - Auto Analyzer). Acid resistant pump tubes (Sterilin Instruments) were used to pump the sample solution (see Section 2.4.2.2) at a flow rate of 1.8 cm^3 min^{-1}.

Several cation exchange columns were prepared so as to run a batch of samples at the same time. The columns were equilibrated before introducing any samples by passing 1 M nitric acid solution followed by a solution of nitric acid (6M). This procedure was repeated twice.

2.16 Rare Earth Elements Separation Procedure.

2.16.1 Anion Exchange Separation Procedure.

The following procedure was used for the separation of rare earths from the solution. First, the column was transferred from the aqueous phase to the organic phase. This was achieved by passing a blank methanolic solution (5% 7M nitric acid + 95% methanol). A volume of 150 cm^3 for the small column and 400 cm^3 for the large column were sufficient to completely

change the eluant from aqueous to organic. The three-way tap located before the premix column was opened so that the blank solution was passing through the premix column. A glass tube was fitted to the input just reaching the surface of the silicon carbide layer, this arrangement allows the methanolic solution to float through the aqueous solution and gradually mix into the aqueous phase.

As soon as the transformation was completed, the sample solution was pumped directly into the separation column bypassing the premix column, this was possible by changing the flow in the three way tap. After the sample was successfully passed through, the analytical column was washed free from sample matrix (ie. phosphate) with a methanolic washing solution (5% 7M nitric acid + 95% methanol). The washing solution was pumped directly into the separation column bypassing the premix column.

The rare earths absorbed by the resin were released by changing the phases from organic to aqueous. The three-way tap was changed over so that elution solution (distilled water) was pumped into the separation column via the premix column. The glass tube, which was used in the transformation of the column from aqueous phase to organic phase, was removed so that water will sink through the methanolic solution and give

a gradual change. The rare earths were collected at the separation column output. The composition of the collected solution was not suitable for rare-earths analysis with the ICP spectrometer because the volume was large (500 cm^3 for the small column and 1 dm^3 for the large column) and contained organics. So this solution was evaporated to the dryness then redissolved in 100 cm^3 of diluted methanolic nitric acid (5% CH_3OH + 0.3% HNO_3) before analysing with the ICP.

2.16.2 Cation Exchange Separation Procedure.

The following procedure was used for the separation of rare earths using the cation exchange separation column. First the column was transformed to a phase of suitable nitric acid concentration (ie. 1M), this was achieved by passing 150 cm^3 for the small column or 300 cm^3 for the large column.

Next sample solution was pumped into the analyte column. After the sample was successfully passed through, sample matrix was washed from the column using diluted nitric acid washing solution (2M). Finally the absorbed rare earths were eluted with 6M nitric acid solution. The volume and the acid concentration of the final solution was not suitable for ICP analysis, so the solution was heated to the dryness and the residue was redissolved in a suitable volume of diluted nitric acid (0.5% v/v) before the analysis.

Chapter Three - Total Rock Analysis.

The chemical components of geological materials (rocks, minerals and soils) can be divided into two main groups, major elements and trace elements. The reporting of major elements as oxide is very useful because oxygen is the commonest element in most rocks and this procedure allows an assessment of the completeness of the analysis. The sum of these oxides should be close to 100%. There are 13 to 18 elements, which are usually listed in a standard order suggested by Washington (127). In this way the general chemical character and the importance of various elements is immediately apparent. The choice of elements for analysis is governed by the particular petrographical, minerological or geochemical investigation for which the analysis is made.

In recent years there have been increasing demands for the trace element analysis of geological materials. The term trace element is used for any elements with an average concentration of less than 0.1% (1000 mg kg^{-1}). The growth of this field owes a great deal to the development of improved analytical techniques and instrumentation. For many purposes the study of trace elements is more rewarding than that of major oxides, because their concentration can range over several orders of magnitude. These concentrations give

a good idea of the nature of the physical and chemical process's which have affected the rock throughout its geological history. Also the presence of an element can be used to indicate the location of a potential ore deposit of economic value.

The chemical analysis of geological materials was a favourite subject of the chemist during the earlier half of the nineteenth century. This resulted in the continuous development of analytical schemes and new and improved laboratory facilities. We owe the classical methods of rock and mineral analysis that are still used to Washington (128), Hillebrand et al. (129) and Groves (130). But these classical methods are time consuming. Starting about 1947, various rapid analytical schemes were proposed as alternatives. These in turn are now being replaced by instrumental techniques. These instrumental methods include X-ray fluorescence (XRF), atomic absorption spectrometry (AAS), optical emission spectroscopy, using sources such as DC - arc and spark and inductively coupled plasma (ICP), as well as electron beam micro-techniques. Electrochemical methods have not been used as widely in the analysis of geological materials as in some other fields, but the use of an ion - selective electrode for the potentiometric estimation of fluoride is now common. All the techniques used in the chemical analysis of rocks and geological materials are discussed

in detail elsewhere (Johnson and Maxwell (131-136). The selection of an analytical method is dictated by many factors; sensitivity, specificity, precision, accuracy, ease of operation, speed, cost and the nature of the sample. All techniques have their own strengths and weaknesses, and none is capable of being used for the whole range of geological samples. It is necessary that the analyst be familiar with each technique in order to choose the best technique for a particular application.

In our analysis, all major oxides (except F, M_gO, CO_2, Na_2O and Mn O) have been estimated by XRF using a PHILIPS PW 1410/10 semi-automatic X-ray spectrometer. Magnesium, Manganese and sodium were not analysed by this technique because for manganese the anode in the X-ray tube used (Cr) was unsuitable for this determination, and for magnesium and sodium the available crystals were unsuitable. For XRF analysis each sample was fused with lithium metaborate using a fusion bead machine (PHILIPS PW 1234/20). The same samples were then re-analysed for the major oxides by emission spectrometry using the ARL 34000 ICP instrument. Silicon was not estimated by ICP because hydrofluoric acid was used in the sample dissolution. Also the ICP instrument used was unsuitable for phosphorous analysis. Fluoride and carbon dioxide require a special analytical technique. Fluoride was measured using fluoride ion selective electrode, while

carbon dioxide was measured using a coulometer. Trace elements (15 elements) in the phosphate rock samples were analysed using ARL 34000 ICP spectrometer. All the experimental conditions and sample treatments used are discussed in detail in chapter 2.

Several samples were collected from each sedimentary phosphate layer, and duplicate analysis were carried out on each sample. The average result is given in Tables 3.2 to 3.16. The XRF results for titanium, aluminium, iron and potassium tend to be higher than the results obtained by ICP, as can be seen in the analysis of the standard NBS-120 b (Table 3.1), this is probably due to the phosphate interference as it was not possible to optimise the multi-element ICP instrument for this particular circumstance. Calcium results with both techniques agreed very well. The results obtained by XRF were used to calculate the sum of all the major oxides in the sample. The results obtained by ICP were used for those oxides which were not determined by XRF. The sum is close to 100%, except for the samples C-TH-1, SEMI-S-TH-1, SAND-TH-SC-1 and S-A-12. The low results for these samples could be due to the presence of other components (sulphate for example). From the tables we can see that the composition of the phosphate rocks are variable. Phosphate content varies from 11 to 37%, calcium from 20 to 51%, carbon dioxide from 1 to 21%, silicon from 1 to 43%, fluoride from 1 to 4%. The rest

of all oxides form less than 4% of the rock.

Table 3.1

Concentration of major oxides and trace elements in the standard (NBS-120b).

1. Major oxides (%)				2. Trace Elements (mg kg^{-1})	
Analyte	XRF	ICP	Certificate	Analyte	Conc.
SiO_2	4.68	---	4.68	Cu	13
TiO_2	0.15	0.13	0.15	Pb	L11
Al_2O_3	1.06	1.04	1.06	Zn	102
Fe_2O_3	1.09	0.98	1.1	As	L10
MnO	----	0.04	0.03	Ni	12
MgO	----	0.38	0.28	Cr	128
CaO	49.77	50.21	49.4	Mo	11
Na_2O	----	0.21	0.35	B	L4
K_2O	0.11	0.08	0.12	Sn	L40
P_2O_5	34.64	----	34.57	Ag	3
				Ba	58
F	3.85		3.84	Zr	66
CO_2	2.75		2.79	Sb	L40
				Nb	L20
Total	98.72		98.37	W	L40

N.B. The National Bureau of Standards has not published a trace elements analysis certificate for this standard.

L = L e s s t h a n .

Table 3.2.

Concentration of major oxides and trace elements in the sample (C-A-1).

1. Major oxides (%)

Analyte	XRF	ICP
SiO_2	3.77	---
TiO_2	0.05	0.02
Al_2O_3	0.86	0.33
Fe_2O_3	0.27	0.15
MnO	----	0.03
MgO	----	0.21
CaO	49.1	49.97
Na_2O	----	0.53
K_2O	0.06	0.04
P_2O_5	30.96	----
F	3.83	
CO_2	8.43	
Total	98.1	

2. Trace Elements (mg kg^{-1})

Analyte	Concent.
Cu	20
Pb	L11
Zn	74
As	L10
Ni	22
Cr	173
Mo	7
B	L4
Sn	L40
Ag	2
Ba	33
Zr	24
Sb	L40
Nb	L20
W	L40

L = Less than

Table 3.3

Concentration of major oxides and trace elements in the sample (S-A-12).

1. Major oxides (%)

Analyte	XRF	ICP
SiO_2	43.87	---
TiO_2	0.03	0.01
Al_2O_3	0.57	0.15
Fe_2O_3	0.22	0.09
MnO	----	0.02
MgO	----	1.03
CaO	19.81	18.73
Na_2O	----	0.17
K_2O	0.06	0.02
P_2O_5	10.69	----
F	1.02	
CO_2	1.37	
Total	78.86	

2. Trace Elements (mg kg^{-1})

Analyte	Concent.
Cu	9
Pb	L11
Zn	33
As	L10
Ni	13
Cr	106
Mo	6
B	L4
Sn	L40
Ag	2
Ba	55
Zr	L20
Sb	L40
Nb	L20
W	L40

L =Less than

Table 3.4

Concentration of major oxides and trace elements in the sample (S-S-2).

1. Major oxides (%)

Analyte	XRF	ICP
SiO_2	5.3	---
TiO_2	0.03	0.02
Al_2O_3	0.96	0.18
Fe_2O_3	0.24	0.12
MnO	----	0.02
MgO	----	0.24
CaO	50.56	49.91
Na_2O	----	0.21
K_2O	0.06	0.04
P_2O_5	24.4	----
F	2.52	
CO_2	15.81	
Total	100.35	

2. Trace Elements (mg kg^{-1})

Analyte	Conc.
Cu	20
Pb	L11
Zn	140
As	L10
Ni	17
Cr	138
Mo	6
B	L4
Sn	L40
Ag	L1
Ba	209
Zr	42
Sb	L40
Nb	L20
W	53

L = Less than

Table 3.5.

Concentration of major oxides and trace elements in the sample (S-G-1).

1. Major oxides (%)

Analyte	XRF	ICP
SiO_2	1.87	---
TiO_2	0.03	0.02
Al_2O_3	0.63	0.3
Fe_2O_3	0.2	0.1
MnO	----	0.02
MgO	----	1.25
CaO	51.87	52.74
Na_2O	----	0.43
K_2O	0.06	0.04
P_2O_5	21.27	----
F	2.43	
CO_2	21.69	
Total	101.75	

2. Trace Elements (mg kg^{-1})

Analyte	Conc.
Cu	33
Pb	L11
Zn	68
As	L10
Ni	19
Cr	227
Mo	9
B	L4
Sn	L40
Ag	5
Ba	38
Zr	42
Sb	L40
Nb	L20
W	L40

L = Less than

Table 3.6.

Concentration of major oxides and trace elements in the sample (CONG-G-1).

1. Major oxides (%)

Analyte	XRF	ICP
SiO_2	2.55	---
TiO_2	0.04	0.02
Al_2O_3	0.8	0.75
Fe_2O_3	0.35	0.28
MnO	----	0.02
MgO	----	0.61
CaO	50.13	51.09
Na_2O	----	0.69
K_2O	0.06	0.04
P_2O_5	26.78	----
F	2.28	
CO_2	16.5	
Total	100.81	

2. Trace Elements (mg kg^{-1})

Analyte	Conc.
Cu	35
Pb	L11
Zn	108
As	L10
Ni	51
Cr	370
Mo	9
B	L4
Sn	L40
Ag	5
Ba	41
Zr	20
Sb	L40
Nb	L20
W	L40

L = Less than

Table 3.7.

Concentration of major oxides and trace elements in the sample (F-TH-SC-1).

1. Major oxides (%)

Analyte	XRF	ICP
SiO_2	4.69	---
TiO_2	0.04	0.02
Al_2O_3	1.13	0.7
Fe_2O_3	0.43	0.27
MnO	----	0.05
MgO	----	0.29
CaO	50.67	51.64
Na_2O	----	0.19
K_2O	0.05	0.04
P_2O_5	35.2	----
F	3.12	
CO_2	2.53	
Total	98.39	

2. Trace Elements (mg kg^{-1})

Analyte	Conc.
Cu	13
Pb	L11
Zn	90
As	L10
Ni	17
Cr	292
Mo	7
B	L4
Sn	L40
Ag	2
Ba	153
Zr	L20
Sb	L40
Nb	L20
W	L40

L = Less than

Table 3.8.

Concentration of major oxides and trace elements in the sample (C-TH-SC-1A).

1. Major oxides (%)

Analyte	XRF	ICP
SiO_2	15.53	---
TiO_2	0.05	0.02
Al_2O_3	0.95	0.75
Fe_2O_3	0.37	0.23
MnO	----	0.05
MgO	----	0.34
CaO	46.68	47.38
Na_2O	----	0.18
K_2O	0.08	0.04
P_2O_5	31.23	----
F	2.53	
CO_2	2.83	
Total	100.82	

2. Trace Elements (mg kg^{-1})

Analyte	Conc.
Cu	12
Pb	L11
Zn	86
As	L10
Ni	19
Cr	203
Mo	7
B	L4
Sn	L40
Ag	3
Ba	137
Zr	L20
Sb	L40
Nb	L20
W	L40

L = Less than

Table 3.9.

Concentration of major oxides and trace elements in the sample (SAND-TH-SC-1).

1. Major oxides (%)

Analyte	XRF	ICP
SiO_2	26.27	---
TiO_2	0.07	0.03
Al_2O_3	1.24	0.77
Fe_2O_3	1.16	0.75
MnO	----	0.08
MgO	----	0.24
CaO	32.36	30.77
Na_2O	----	0.12
K_2O	0.07	0.03
P_2O_5	19.89	----
F	2.04	
CO_2	1.89	
Total	85.43	

2. Trace Elements ($mg\ kg^{-1}$)

Analyte	Conc.
Cu	15
Pb	15
Zn	92
As	L10
Ni	14
Cr	100
Mo	4
B	L4
Sn	L40
Ag	1
Ba	175
Zr	L20
Sb	L40
Nb	L20
W	58

L = Less than

Table 3.10.

Concentration of major oxides and trace elements in the sample (C-TH-SC-1).

1. Major oxides (%)

Analyte	XRF	ICP
SiO_2	8.88	---
TiO_2	0.06	0.04
Al_2O_3	1.09	1.25
Fe_2O_3	0.42	0.29
MnO	----	0.02
MgO	----	0.46
CaO	43.82	42.98
Na_2O	----	0.19
K_2O	0.07	0.05
P_2O_5	26.23	----
F	2.95	
CO_2	2.21	
Total	86.4	

2. Trace Elements (mg kg^{-1})

Analyte	Conc.
Cu	11
Pb	L11
Zn	62
As	L10
Ni	14
Cr	200
Mo	9
B	L4
Sn	L40
Ag	2
Ba	70
Zr	L20
Sb	L40
Nb	L20
W	L40

L = Less than

Table 3.11.

Concentration of major oxides and trace elements in the sample (CHALK-TH-SC-1).

1. Major oxides (%)

Analyte	XRF	ICP
SiO_2	15.33	---
TiO_2	0.05	0.03
Al_2O_3	1.21	0.92
Fe_2O_3	0.26	0.13
MnO	----	0.02
MgO	----	1.14
CaO	45.21	45.75
Na_2O	----	0.18
K_2O	0.06	0.04
P_2O_5	31.02	----
F	3.53	
CO_2	2.43	
Total	100.44	

2. Trace Elements (mg kg^{-1})

Analyte	Conc.
Cu	10
Pb	L11
Zn	65
As	L10
Ni	14
Cr	167
Mo	11
B	L4
Sn	L40
Ag	3
Ba	69
Zr	L20
Sb	L40
Nb	L20
W	L40

L = Less than

Table 3.12.

Concentration of major oxides and trace elements in the sample (F-TH-SC-2).

1. Major oxides (%)

Analyte	XRF	ICP
SiO_2	3.78	---
TiO_2	0.06	0.03
Al_2O_3	0.83	0.73
Fe_2O_3	0.52	0.35
MnO	----	0.03
MgO	----	0.35
CaO	51.29	50.8
Na_2O	----	0.13
K_2O	0.07	0.06
P_2O_5	37.14	----
F	2.21	
CO_2	2.58	
Total	98.99	

2. Trace Elements (mg kg^{-1})

Analyte	Conc.
Cu	15
Pb	L11
Zn	116
As	L10
Ni	25
Cr	388
Mo	8
B	L4
Sn	L40
Ag	2
Ba	77
Zr	40
Sb	L40
Nb	L20
W	L40

L = Less than

Table 3.13.

Concentration of major oxides and trace elements in the sample (SEMI-S-TH-1).

1. Major oxides (%)

Analyte	XRF	ICP
SiO_2	30.35	---
TiO_2	0.04	0.02
Al_2O_3	0.63	0.42
Fe_2O_3	0.45	0.28
MnO	----	0.01
MgO	----	0.85
CaO	29.67	28.5
Na_2O	----	0.27
K_2O	0.06	0.03
P_2O_5	17.83	----
F	1.86	
CO_2	5.14	
Total	86.71	

2. Trace Elements (mg kg^{-1})

Analyte	Conc.
Cu	13
Pb	L11
Zn	65
As	L10
Ni	16
Cr	157
Mo	12
B	L4
Sn	L40
Ag	1
Ba	35
Zr	L20
Sb	L40
Nb	L20
W	L40

L = Less than

Table 3.14.

Concentration of major oxides and trace elements in the sample (C-TH-2).

1. Major oxides (%)

Analyte	XRF	ICP
SiO_2	20.74	---
TiO_2	0.04	0.02
Al_2O_3	0.63	0.33
Fe_2O_3	0.43	0.23
MnO	----	0.02
MgO	----	0.35
CaO	41.2	40.04
Na_2O	----	0.12
K_2O	0.07	0.04
P_2O_5	14.84	----
F	1.13	
CO_2	18.9	
Total	98.47	

2. Trace Elements (mg kg^{-1})

Analyte	Conc.
Cu	11
Pb	L11
Zn	66
As	L10
Ni	24
Cr	114
Mo	14
B	L4
Sn	L40
Ag	2
Ba	75
Zr	L20
Sb	L40
Nb	L20
W	L40

L = Less than

Table 3.15.

Concentration of major oxides and trace elements in the sample (C-TH-1).

1. Major oxides (%)

Analyte	XRF	ICP
SiO_2	17.72	---
TiO_2	0.05	0.03
Al_2O_3	0.81	0.62
Fe_2O_3	0.38	0.31
MnO	----	0.02
MgO	----	0.64
CaO	40.32	39.9
Na_2O	----	0.42
K_2O	0.06	0.04
P_2O_5	25.46	----
F	2.51	
CO_2	2.33	
Total	90.72	

2. Trace Elements (mg kg^{-1})

Analyte	Conc.
Cu	8
Pb	L11
Zn	67
As	L10
Ni	12
Cr	211
Mo	12
B	L4
Sn	L40
Ag	L1
Ba	32
Zr	L20
Sb	L40
Nb	L20
W	L40

L = Less than

Table 3.16.

Concentration of major oxides and trace elements in the sample (F-TH-1).

1. Major oxides (%)

Analyte	XRF	ICP
SiO_2	12.07	---
TiO_2	0.03	0.02
Al_2O_3	0.57	0.3
Fe_2O_3	0.43	0.28
MnO	----	0.02
MgO	----	0.33
CaO	45.75	44.95
Na_2O	----	0.18
K_2O	0.06	0.04
P_2O_5	19.9	----
F	2.49	
CO_2	15.18	
Total	97.01	

2. Trace Elements (mg kg^{-1})

Analyte	Conc.
Cu	12
Pb	L11
Zn	88
As	L10
Ni	17
Cr	167
Mo	9
B	L4
Sn	L40
Ag	L1
Ba	23
Zr	23
Sb	L40
Nb	L20
W	L40

L = Less than

CHAPTER FOUR: ANION EXCHANGE

In this chapter an investigation is described which was carried out to calculate the distribution coefficient for different ions, lanthanum, thorium, uranium and phosphate, which are likely to be present in the phosphate rock samples, using the batch method (see section 4.1).

To set the experimental conditions for the separation, these ions individually were passed through the column and the pattern of the separation was followed (see section 4.2). Then different mixtures of these elements plus some other rare earth elements, samarium, holmium, lutetium and cerium, were used to calculate the recovery from the column (see section 4.3).

Next six phosphate rock samples were analysed using the procedure developed. The results were compared with those obtained by neutron activation analysis (see section 4.4).

An attempt was made to modify the composition of the sample solution to improve the distribution ratio. The modification was carried out by varying the concentration of methanol, water and nitric acid (see

section 4.5). Finally the effect of an increasing weight of calcium phosphate on the recovery of a mixture of all the rare earths, was investigated (see section 4.6).

4.1 Distribution Coefficient.

The equilibrium state in the ion exchange system is very often expressed in term of the distribution coefficient. This quantity is the ratio of the equilibrium concentration of the same ion in the exchanger phase and in solution. The greater the ratio, the better the separation. The distribution coefficient can be measured by batch or the column methods. Rare earth element distribution coefficients were measured using the batch method. A known amount of the ion exchanger in a known ionic form, is added to a solution of a known volume and quantitative composition. After equilibration (mechanical shaking for two hours was sufficient for equilibrium, as shown for lanthanum in Figure 4.1) the resin was removed by filtration and the concentration of the ions in the filtrate were measured using spectrophotometric methods (see section 2.6). The distribution coefficient D_x, was calculated using the following equation:

$$D_x = \frac{v}{w}\left(\frac{A_i}{A_f} - 1\right)$$

Figure (4.1)

Optimization of shaking time

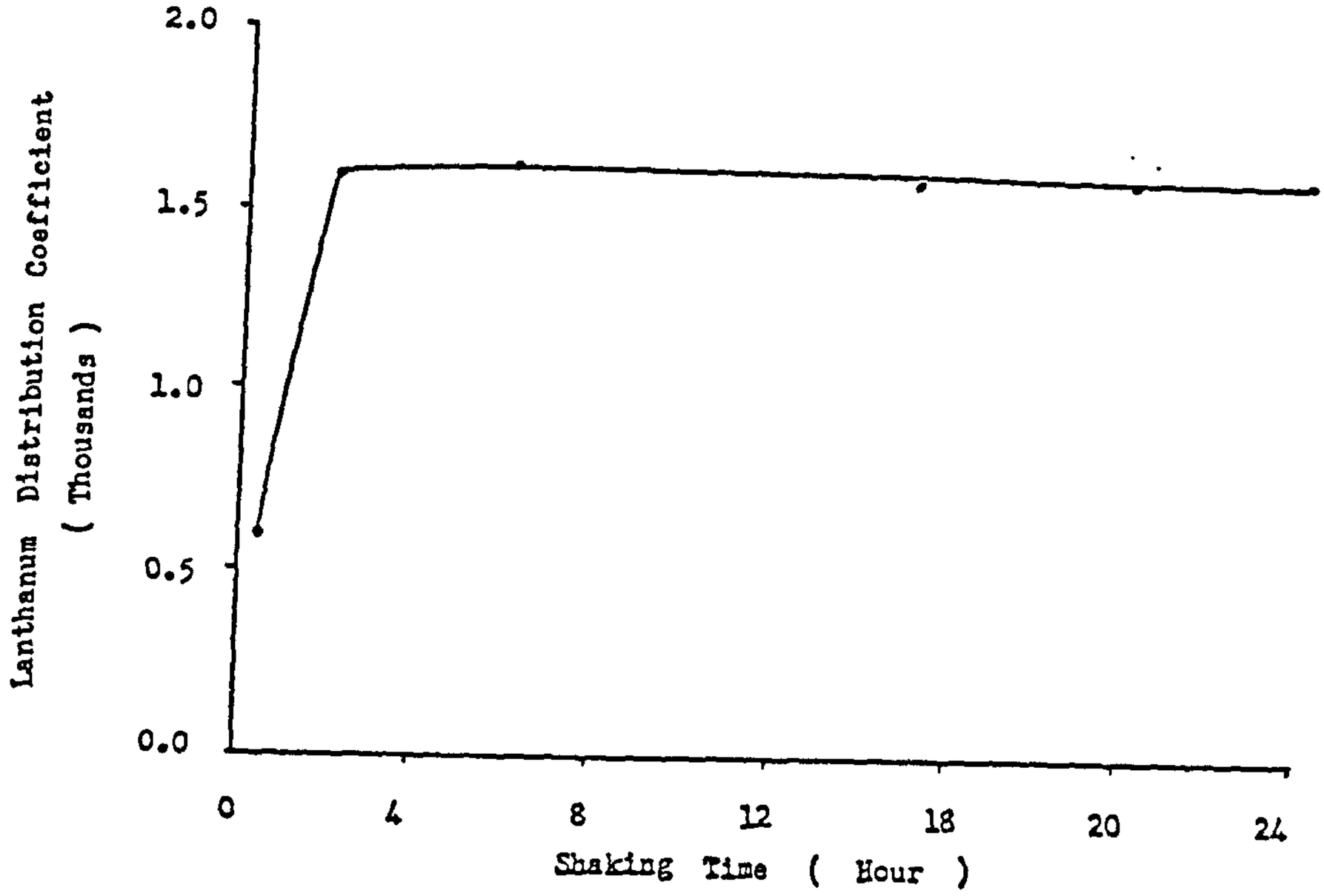

where V = volume of methanolic phase.

W = weight of the dry resin.

A_f = absorbance equivalent to the concentration in the filtrate of the ion being tested.

A_i = absorbance equivalent to the concentration in the initial solution before equilibrium of the ion being tested.

The distribution coefficient for the ions of interest (ie. lanthanum, thorium, uranium and holmium) were studied using a strongly basic anion exchanger, AMBERLITE IRA - 401 in the nitrate form. The results show that uranium does not absorb on the resin over the range of ratios of 7M nitric acid to methanol investigated (from 5/95% to 50/50% by volume - see Figure 4.2). The variations observed are due to experimental error (ca 3%). Lanthanum, thorium and holmium all behave in the same way. The D_x values fall as the ratio of 7M nitric acid to methanol change from 5/95% to 50/50%, as shown in Figure 4.3. Thorium is absorbed very strongly by the resin since it had the highest D_x value (D_x = 5700). The distribution coefficient for lanthanum is much smaller than that for thorium (D_x = 1600) indicating less absorption. A much poorer result was obtained for holmium (D_x = 40).

Figure (4.2)

Distribution coefficient of uranium

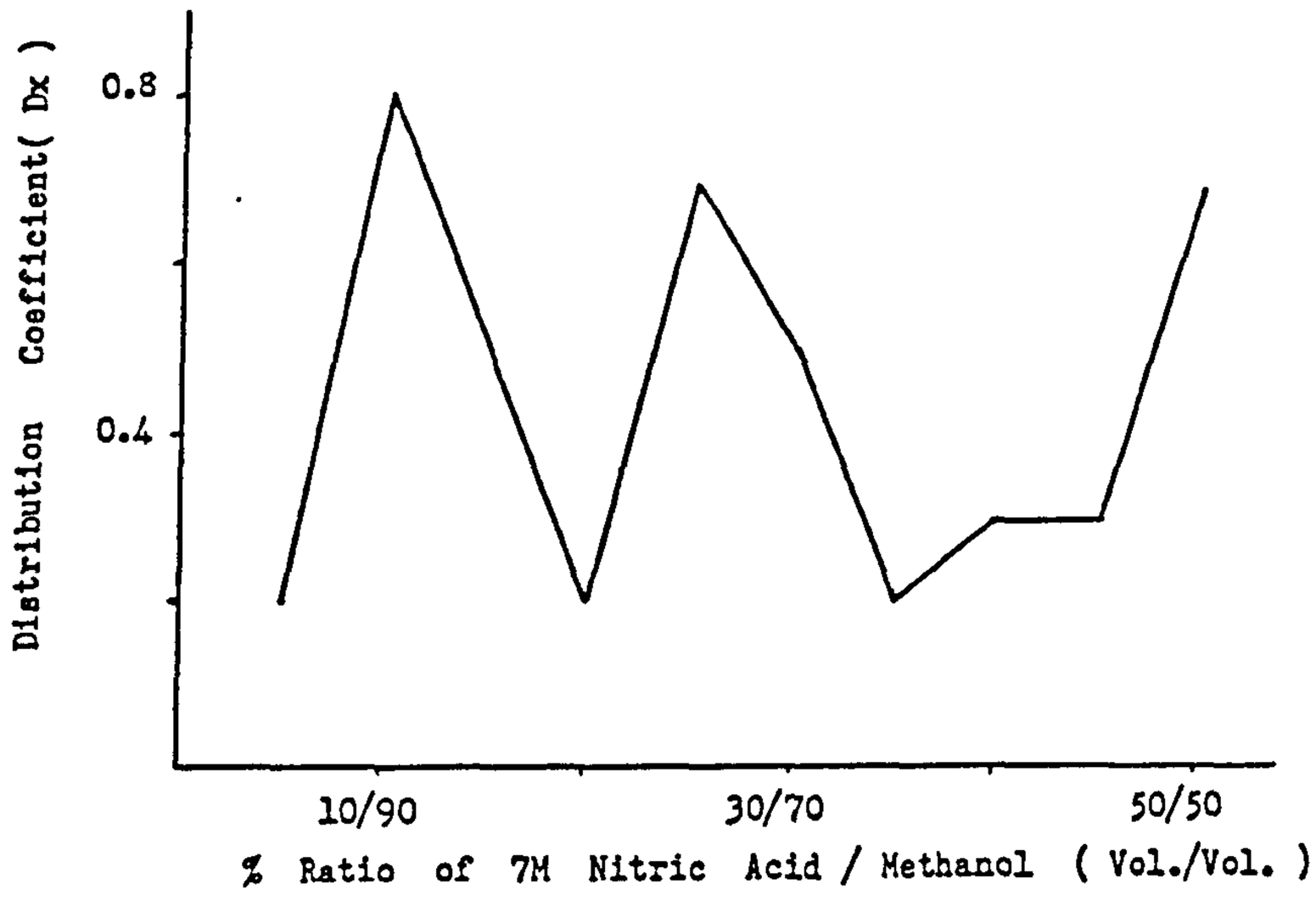

Figure (4.3)

Distribution coefficient of lanthanum , holmium and thorium

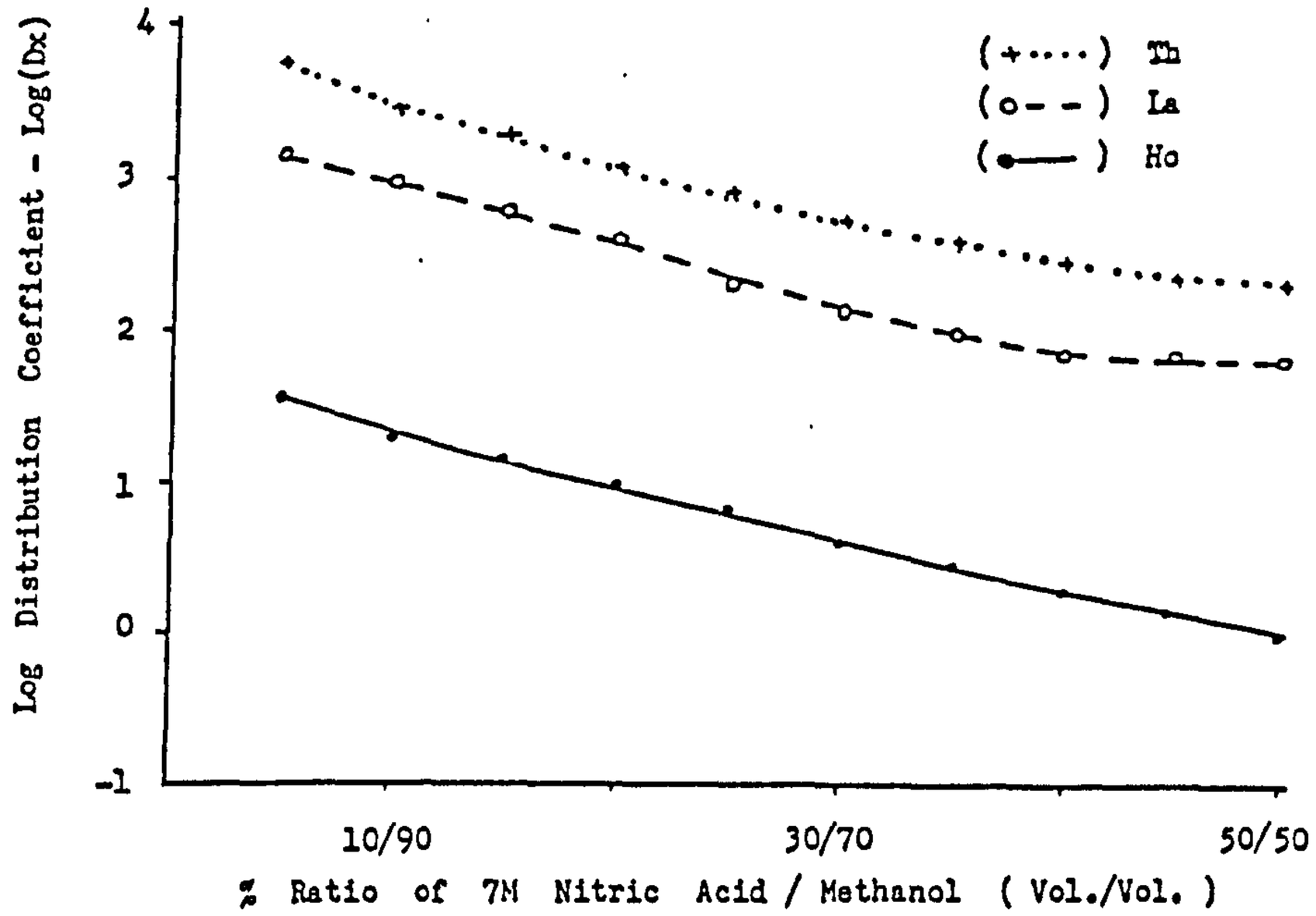

4.1.1 Conclusion.

The results clearly show that rare earths absorption on the resin from these mixed solvent solutions is much higher at higher methanol concentrations, and is reduced with an increase in the aqueous nitric acid concentration. The lighter rare earth elements are more strongly retained by the anionic resin than the heavier ones.

4.2 Separation of Rare Earths from Calcium Phosphate.

The method of separation being tested consisted of passing the test solution (containing both calcium phosphate and the rare earth element) through the column. Washing with a wash solution (5% 7M nitric acid + 95% methanol) to remove the calcium and phosphorous and discarding these washings. The rare earth was then eluted with water and the collected eluant analysed. In order to set up the experimental conditions for the separation of rare earths from phosphate rock using this procedure - anion exchange, the elution of lanthanum, thorium, uranium and phosphate ions were studied using a small column (20cm x 2cm). Calcium was not considered because it was not retained by the anionic resin (100). Each ion was measured spectrophotometrically (see section 2.6) in sequentially collected 10 cm^3 fractions.

The phosphate ion, as expected, was washed out

of the column without retention. A volume of 200 cm^4 of the washing solution (5% of 7M HNO_3 + 95% CH_3OH) was sufficient to remove all phosphate ions (2 grams of calcium phosphate in 50 cm^3 solution) as can be seen in Figure 4.4. Uranium also was not absorbed by the resin and was washed out by the washing solution, but there are two peaks, Figure 4.5. The initial peak corresponds to uranium (VI). Some of this ion may have been reduced possibly to uranium (IV). A volume of 200 cm^3 of washing solution was sufficient to wash all uranium ions from the column.

The absorbed elements (lanthanum and thorium) were eluted by passing water through the column. A volume of 150 cm^3 was sufficient to elute these elements, as can be seen in Figure 4.6 and 4.7.

As it was intended to use a large sample (100 grams) a larger column (1 metre x 2cm) was needed. Another reason for using a large column was because of a small break through of heavy rare earths during the washing stage (holmium was used as an example of the heavy rare earths), as shown in Figure 4.8. Holmium was detected after passing 45 cm^3 of a solution containing 3 mg dm^{-3} through the small column. While with the large column, a volume of 1300 cm^3 of a solution containing 5 mg dm^{-3} of holmium had to be passed through before holmium could be detected.

Figure (4.4) - Washing of phosphate ions

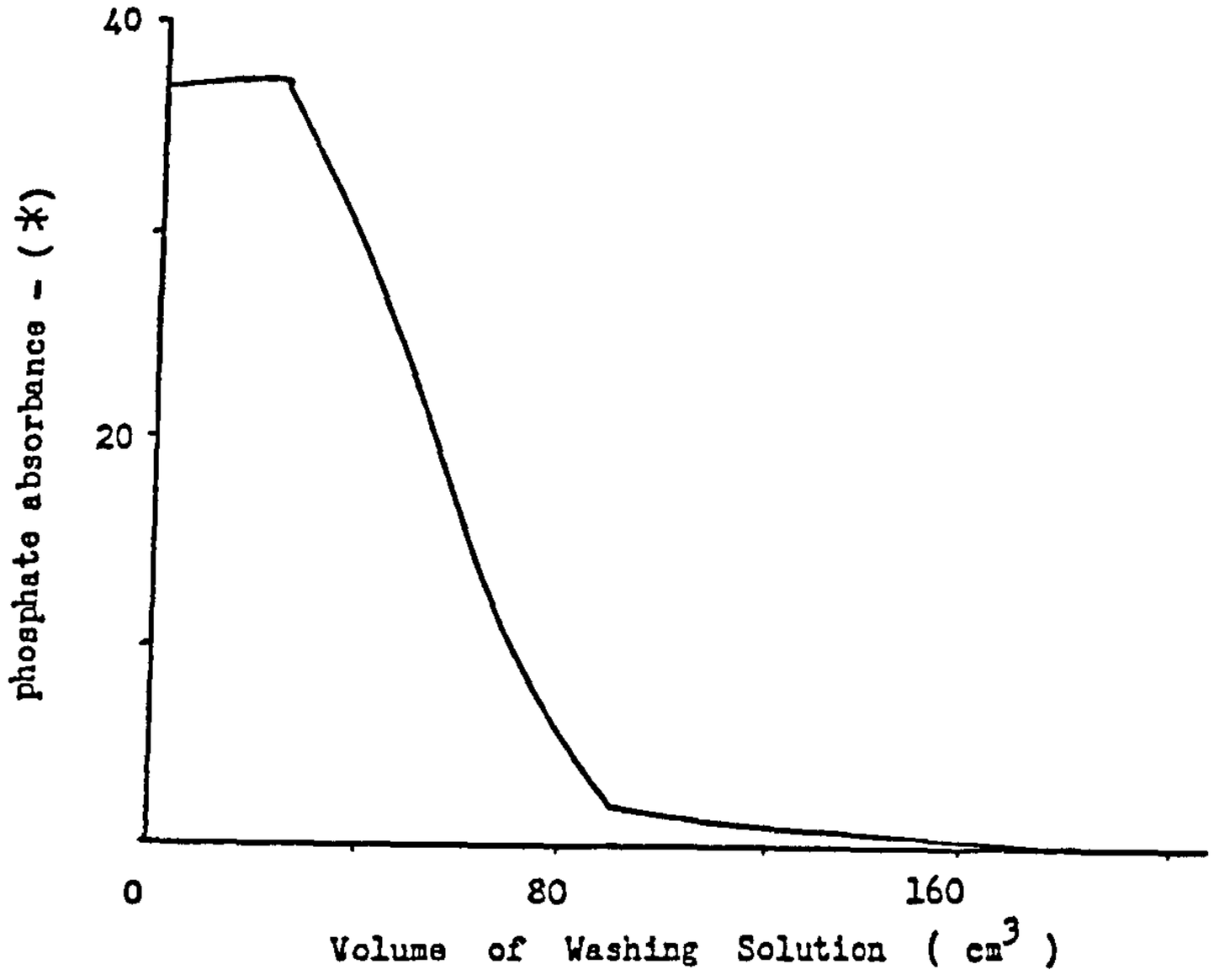

(*) - The Y axis has been corrected for the dilution used in order to obtained a measurable absorbance,(i.e. between 0.1 and 1)

Figure (4.5) - Washing of uraium

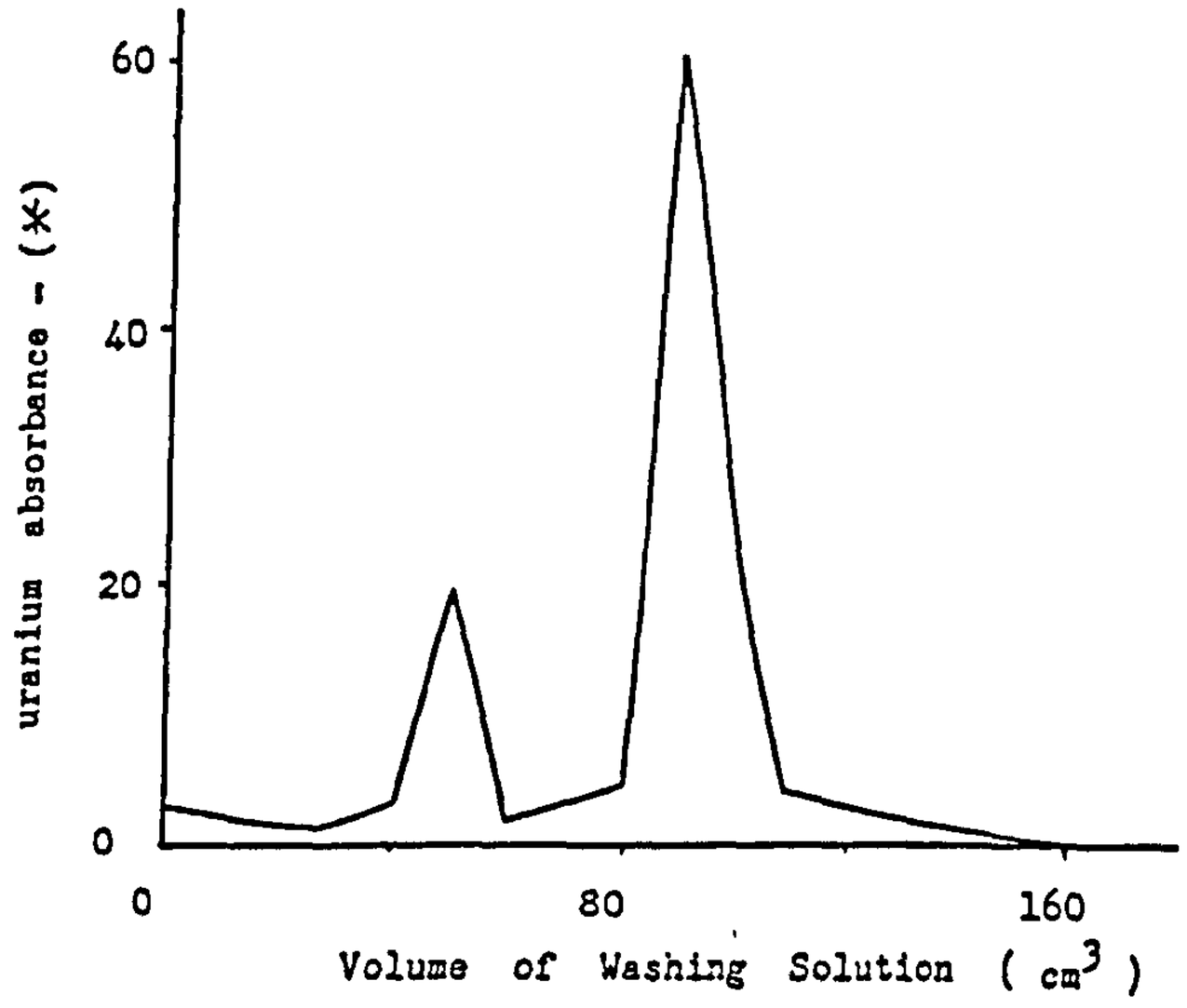

(*) - The Y axis has been corrected for the dilution used in order to obtain a measurable absorbance,(i.e. between 0.1 and 1)

Figure (4.6) - Elution of thorium

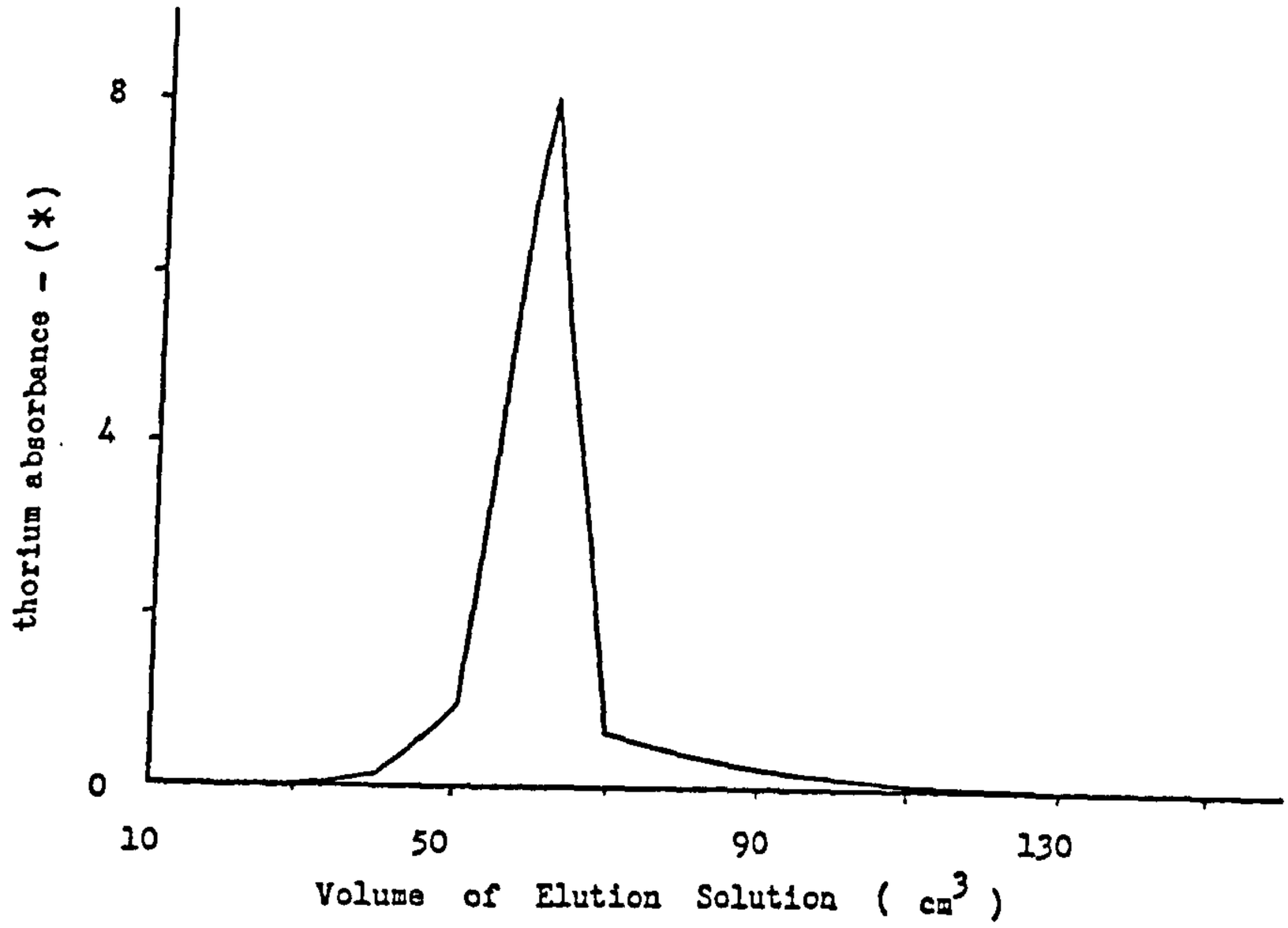

(*) - The Y axis has been corrected for the dilution used in order to obtain a measurable absorbance,(i.e. between 0.1 and 1)

Figure (4.7) - Elution of lanthanum

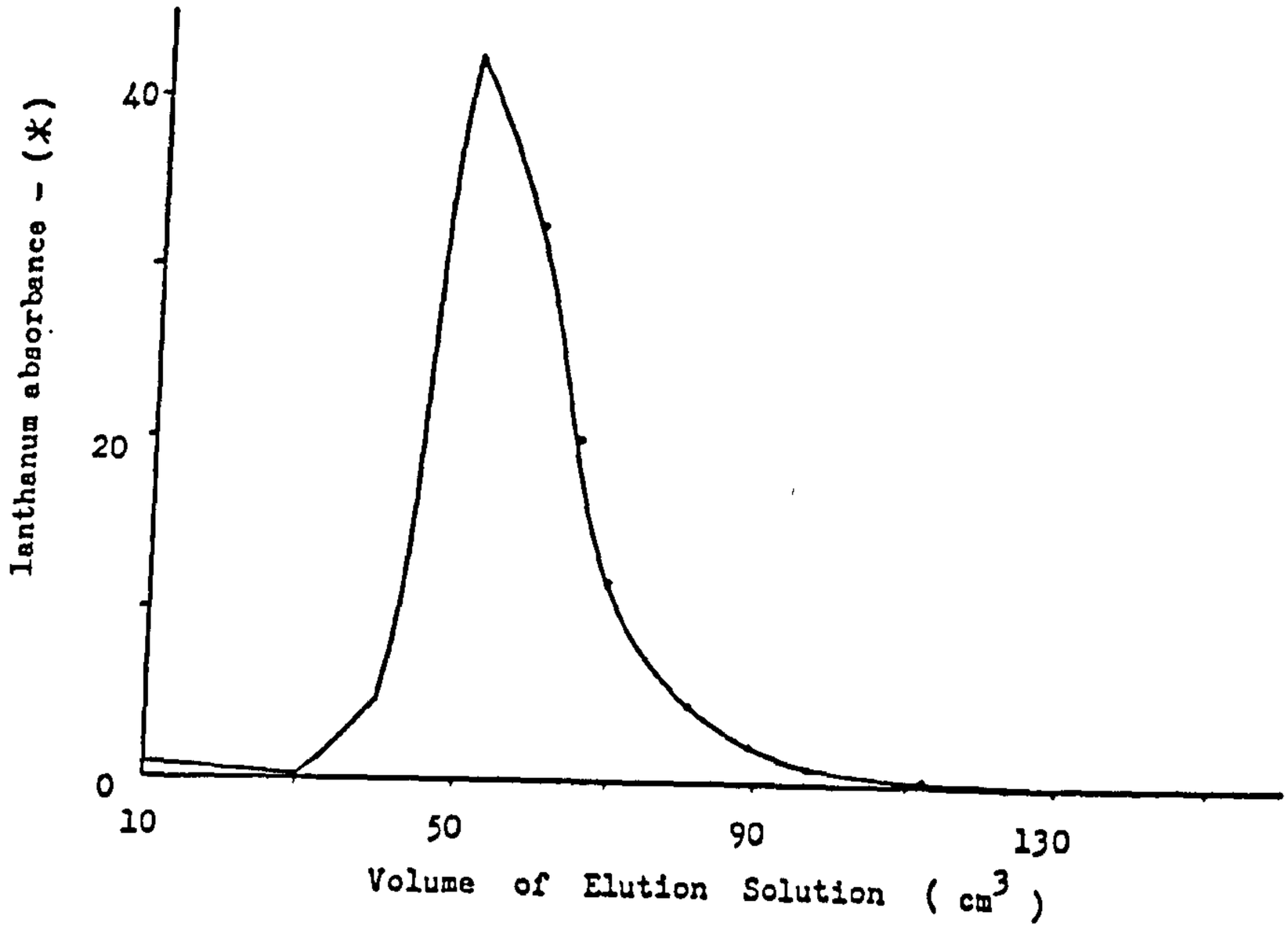

(*) - The Y axis has been corrected for the dilution used in order to obtain a measurable absorbance, (i.e. between 0.1 and 1)

Figure (4.8)

Break through of holmium from a large and a small column

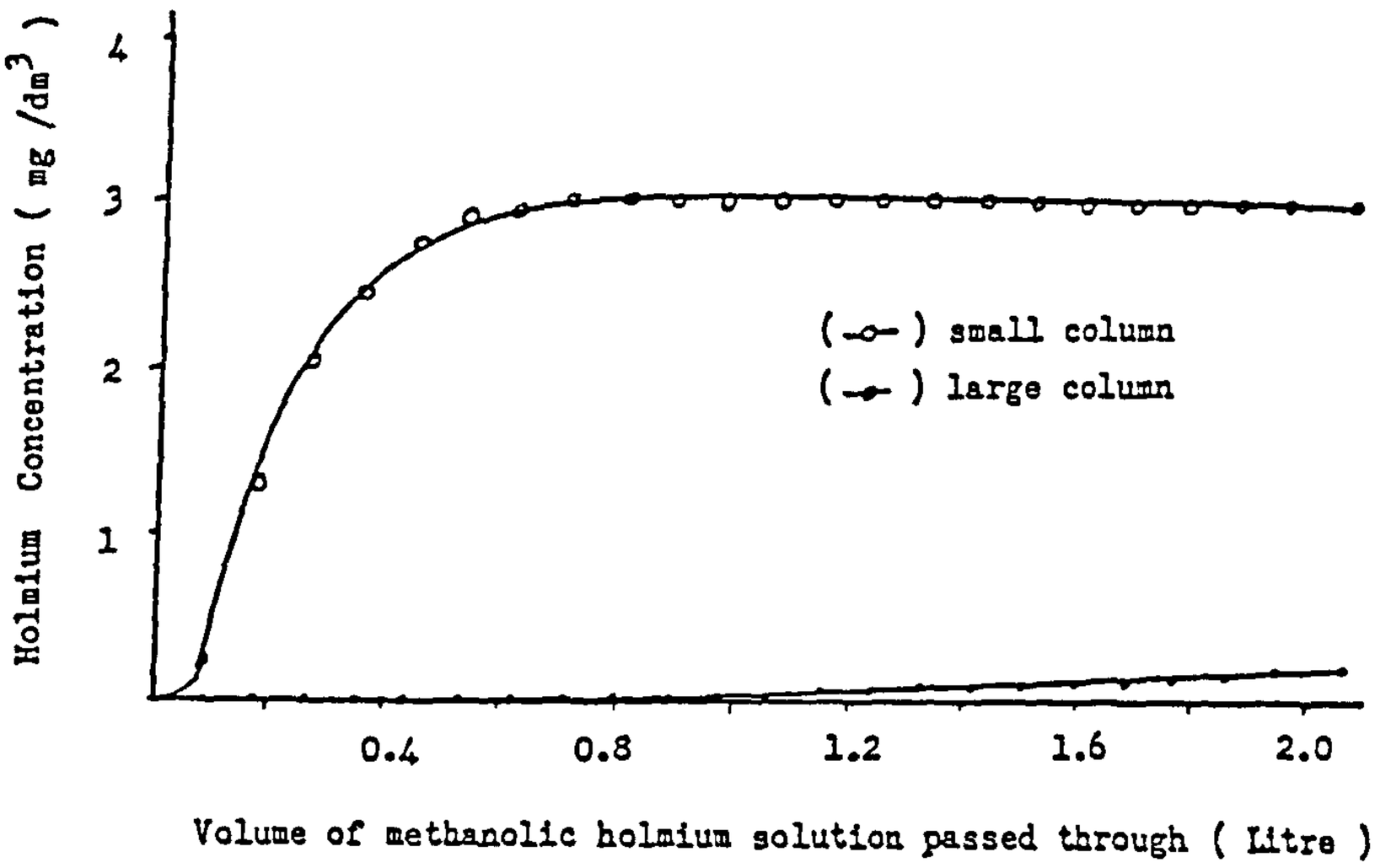

The washing and eluting stages now needed to be re-investigated. A volume of 400 cm^3 of the washing solution was sufficient to wash all the phosphate (50 g of calcium phosphate in 2 dm^3 methanolic solution - equivalent to 100 g of phosphate rock sample) from the large column, as shown in Figure 4.9. Three solutions each containing one of the following elements, lanthanum, samarium and holmium, were passed through the column and eluted with water. These elements had been chosen to represent light, medium and heavy rare earths, and the concentrations used were proportional to the concentrations present in the real phosphate rock samples. The elution curves for the three elements are shown in Figures 4.10 and 4.11. The concentration of methanol and nitric acid in the first fractions eluted is high. This fraction gave a cloudy solution when reagent solutions for the spectrophotometric analysis were added. The turbidity reduced until the eluted solutions were clear after passing about 120 cm^3 of water. After that the absorbance measured is due to the presence of the rare earths, but the first points are an overestimate of the rare earths concentration. For the three elements a volume of 500 cm^3 of the elutant (water) ensures that all the rare earths are successfully eluted.

4.2.1 Conclusion.

The large column was used in all subsequent

Figure (4.10) - Elution of lanthanum from the large column

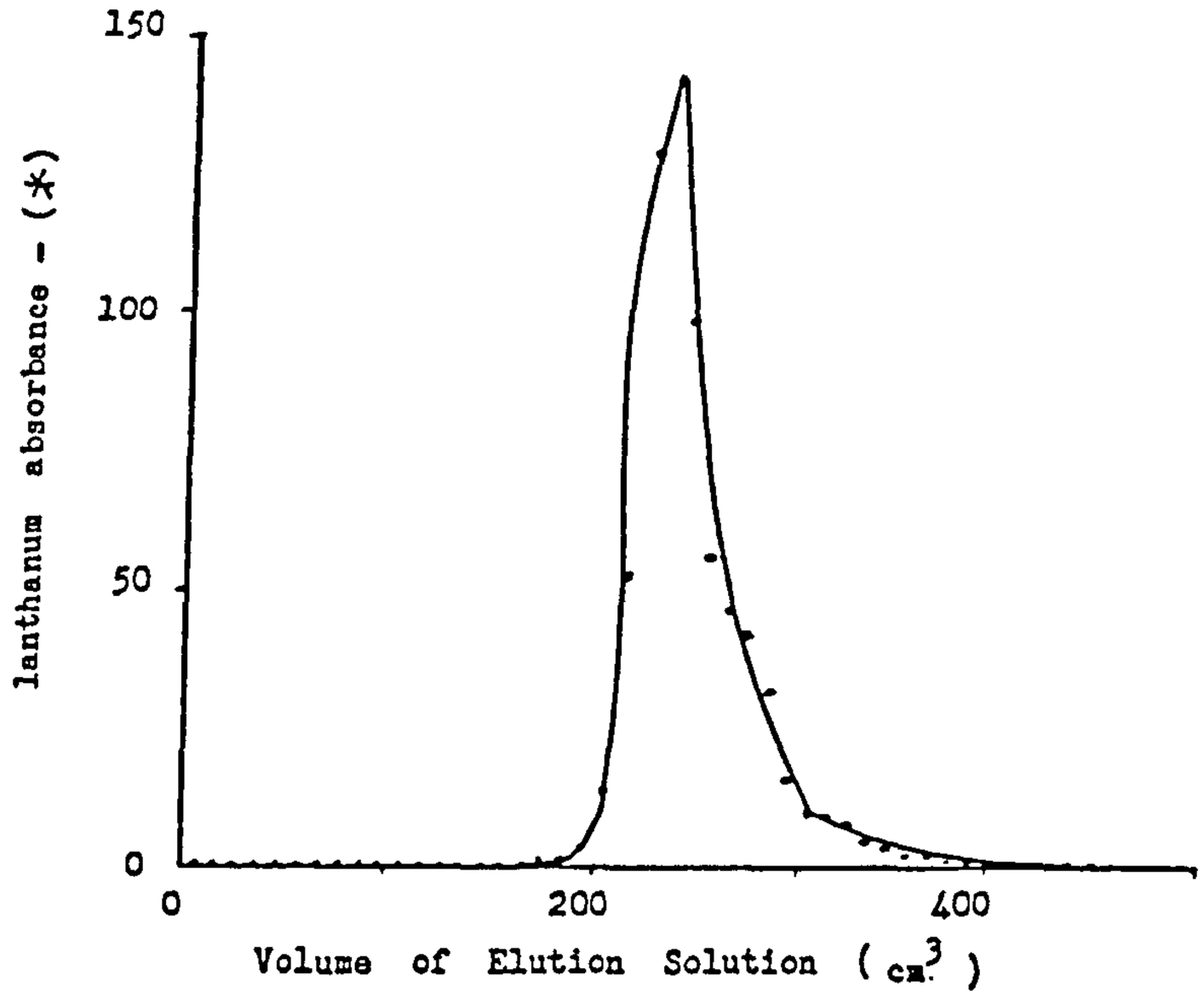

(*) - The Y axis has been corrected for the dilution used in order to obtain a measurable absorbance,(i.e. between 0.1 and 1)

Figure (4.11) - Elution of samarium ánd holmium from the large column

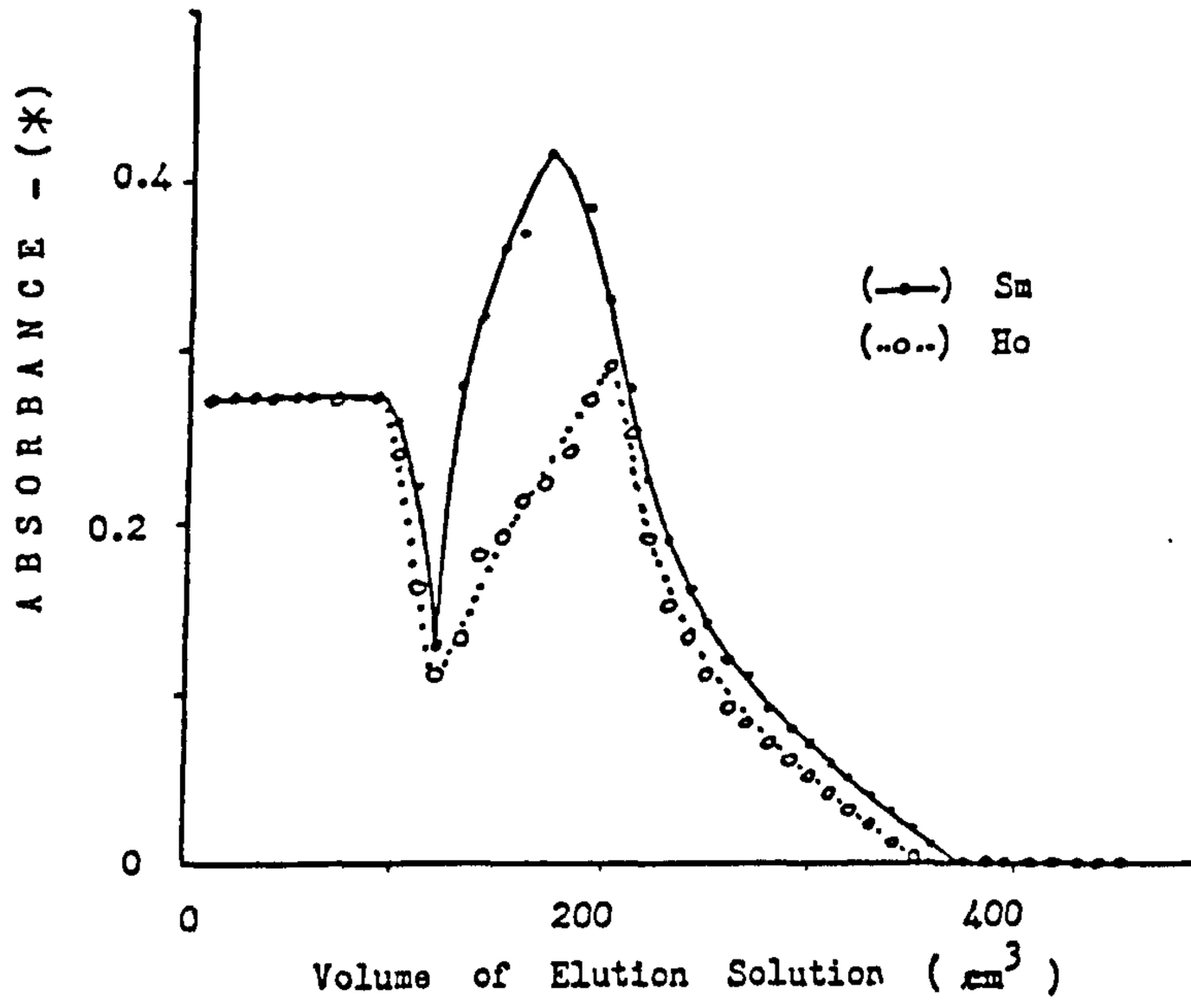

(*) - The Y axis has been corrected for the dilution used in order to obtain a measurable absorbance,(i.e. between 0.1 and 1)

separations. A volume of 400 cm^3 of washing solution was chosen to remove all the calcium and phosphate. To elute the rare earths, a volume of 500 cm^3 of water was used.

4.3 Recovery.

In order to justify the anion exchange procedure, a single element (either thorium or a lanthanide) was mixed with one of the interferences (calcium phosphate or uranyl nitrate) and the separation procedure developed in (section 4.2) using the large column was applied. A single element separation was used because the ICP apparatus was not available and the spectrophotometric method is not selective and only measures total rare earths. The results show a high recovery ranging from 96% to 99.9% for the elements and the interferent, as shown in Table 4.1.

4.3.1 Conclusion.

The separation procedure developed (in section 4.2) looks a very promising method for separating rare earths from phosphate rock.

Table 4.1

Recovery rare earths and matrix for,

the large anion exchange column.

Analyte	A	B	C	D
La	89	99.9	Calcium Phos.	99.6
Ce	20	98.1	" "	96.9
Sm	12	99.1	" "	99.7
Ho	8	97.0	" "	96.0
Lu	4	98.5	" "	99.1
Th	119	99.0	Uranyl nitrate	97.3
La	90	95.9	" "	96.4

A = Concentration of analyte mg dm^{-3}

B = Recovery of analyte R%

C = Interferent

D = Recovery of interfernt R%

* The sample solution also contains 40 g of calcium phosphate per 1 dm^3 or 1.14 g of uranyl nitrate per 1 dm^3.

4.4 Sample Analysis.

In order to check the anion exchange procedure, six phosphate rock samples (F-TH-SC-1, S-G-1, C-TH-SC-1A, SAND-TH-SC-1, S-S-2 and CHALK-TH-SC-1) were analysed by both the anion exchange procedure and neutron activation analysis. A large sample (100 g) was used with the anion exchange procedure to ensure adequate sensitivity, while a much smaller sample (0.2 g) was used with the other procedure. In the anion exchange procedure, the samples were decomposed using the decomposition procedure (see section 2.4). The final residue after the dissolution procedure was redissolved in the organic mixture, 95% methanol + 5% 7M nitric acid. As a large sample was used, 2 dm^3 of this solution was required. Calcium phosphate was separated and rare earths were eluted using the recommended volume (see section 4.2). The eluted rare earths were measured using an inductively coupled plasma (ICP) technique (see section 6.1). The final concentration of the rare earths were calculated after correction for interelement interferences (see section 6.3). These results were compared with the results obtained by neutron activation analysis at the Scottish Reactor Centre (see section 7.1). The results, Table 4.2, show a great difference between the two techniques, the neutron activation results being higher than those obtained by the anion exchange procedure. Also neutron activation analysis failed to detect cerium in two

TABLE 4.2

A COMPARISON OF THE CONCENTRATION (in mg kg^{-1}) OF THE RARE EARTH ELEMENTS IN SIX PHOSPHATE ROCK SAMPLES - RESULTS OBTAINED BY ANION EXCHANGE AND NEUTRON ACTIVATION ANALYSIS.

SAMPLE	C-TH-SC-1A		SAND-TH-SC-1		S-S-2		CHALK-TH-SC-1		F-TH-SC-1		S-G-1	
ANALYTE	A.E	N.A.A.	A.E	N.A.A.	A.E	N.A.A.	A.E	N.A.A.	A.E	N.A.A.	A.E	N.A.A.
La	37.2	40.8	32.8	44.3	5.47	20.8	7.35	28.5	23.5	33.8	87.4	102.8
Ce	41.7	79.4	42.3	107.0	9.62	57.3	16.0	57.3	27.7	N.D.	42.7	N.D.
Nd	34.1	15.0	20.4	18.9	6.38	7.8	11.2	7.4	17.0	11.3	56.4	39.7
Sm	3.21	38.6	3.01	18.2	0.56	10.7	0.82	17.6	1.89	24.4	9.9	26.4
Eu	0.72	1.23	0.18	1.6	0.17	0.6	0.44	0.9	0.16	1.2	0.54	3.3
Ho	0.08	3.5	0.07	3.5	0.12	3.5	0.05	3.5	0.13	3.5	0.68	4.33
Yb	0.22	3.8	0.35	4.7	0.36	2.0	0.22	3.0	0.31	3.7	1.48	9.8
Lu	0.06	3.3	0.04	1.8	0.05	1.1	0.06	1.6	0.04	2.3	0.22	3.2

A.E. - ANION EXCHANGE

N.A.A. - NEUTRON ACTIVATION ANALYSIS

N.D. - NOT DETECTED

samples, F-TH-SC-1 AND S-G-1, while the ion exchange procedure reveals a large concentration, 27.7 and 42.7 mg kg^{-1}.

The low results by the ion exchange method, results which become increasingly low as the atomic weight is increased, and which paralleled the low distribution ratio's for the heavy rare earths, were regarded as very suspicious and tests were initiated to check the recovery of the rare earths. To discover if rare earths were being lost from the column during the washing stage, the length of the column was doubled (two one metre columns one after the other were used instead of one). The rare earths were eluted from both columns separately to assess the proportion passing through the first column. Four samples were treated in this way and the results (see Table 4.3) show that the heavy rare earths were lost to a large extent and even the light rare earths were not recovered well.

The losses of rare earth elements into the second column could be due to competition with other rare earths (the original test which gave high recoveries having used solutions of single rare earths) or to some component in the sample (perhaps F^- or SO_4^{-2}) not present in the test solution used to measure the recovery. The solution which passes into the second column should be very similar to that passing

Table 4.3

Analysis of phosphate rock samples by anion exchange:- rare earth elements (in mg kg^{-1}) eluted from two columns.

Sample	C-TH-SC-1A		SAND-TH-SC-1		S-S-2		CHALK-TH-SC-1	
Analyte	1	2	1	2	1	2	1	2
Y	3.69	1.7	3.69	6.39	6.72	0.51	3.72	1.52
La	37. 2	8.09	32.8	0.55	5.47	0.46	7.35	1.13
Ce	41.7	12.2	42.3	3.7	9.62	2.61	16.0	4.39
Pr	1.56	1.21	1.54	0.76	1.34	0.56	0.66	0.78
Nd	34.1	12.9	20.4	5.2	6.38	1.95	11.2	5.07
Sm	3.21	1.8	3.01	2.7	0.56	0.48	0.82	1.0
Eu	0.72	0.5	0.18	1.13	0.17	0.22	0.44	0.33
Gd	1.33	0.74	0.88	1.83	0.36	0.28	0.52	0.52
Tb	0.66	0.41	0.17	0.56	0.2	0.31	0.4	0.42
Dy	0.86	0.54	0.59	1.33	0.48	0.18	0.38	0.38
Ho	0.08	0.16	0.07	0.26	0.12	0.06	0.05	0.09
Er	0.97	0.89	1.87	1.28	0.76	0.46	2.59	1.65
Tm	N.D.	0.12	0.07	0.23	0.12	0.14	0.08	0.18
Yb	0.22	0.19	0.35	0.47	0.36	0.11	0.22	0.19
Lu	0.06	0.06	0.04	0.1	0.05	0.05	0.06	0.07
Th	1.6	1.56	0.39	1.48	0.56	0.95	1.01	1.83

1 - Column 1 2 - Column 2

N.D. - Not Detected

into the first one, except for rare earths content and, assuming that competition between rare earths is unimportant, the proportion of metal absorbed in the two columns should be identical. If this assumption is made, it is possible to calculate the total amount of rare earths in the sample from the amounts recovered in each column separately.

let W = weight of rare earth in sample.

X_1 = weight of rare earth in column 1.

X_2 = weight of rare earth in column 2.

Y = weight of rare earth passing through both columns.

Thus

$$W = X_1 + X_2 + Y \qquad (1)$$

assuming that both columns behave in a similar fashion:-

$$\frac{Y + X_2}{X_1} = \frac{Y}{X_2} = \frac{\text{weight passing through}}{\text{weight retained}} \qquad (2)$$

hence

$$X_2 (Y + X_2) = X_1 * Y$$

$$(X_2)^2 = Y (X_1 - X_2)$$

$$Y = (X_2)^2 \ / \ (X_1 - X_2) \qquad (3)$$

giving

$$W = X_1 + X_2 + (X_2)^2 / (X_1 - X_2)$$

and the recovery from either single column is:

$$R = \frac{\text{(weight retained) * 100}}{\text{(weight entering))}}$$

$$R = \frac{X_1 * 100}{W} = \frac{X_2 * 100}{(X_2 + Y)}$$

These calculations were carried out for the four samples which had been passed through the two columns. The results, shown in Tables 4.4 to 4.7, show better, but still bad, agreement with the neutron activation results.

The results of applying the correction are in fact confusing. There are many cases for which $X_2 > X_1$ (that is more rare earths are absorbed on the second column than the first column). This is contrary to the assumption made in the calculations - that both columns recover the same proportion of metal entering the column. It suggests in fact that the first column is removing the interferant that is lowering the recovery. If this is in fact true. then:-

$$\frac{Y + X_2}{X_1} < \frac{Y}{X_2}$$

In the extreme case all metal passing column 1 will be trapped in column 2. The correction calculated above is now too great, and the true results should lie between W (the corrected result) and $X_1 + X_2$ (the

Table 4.4

Comparison of the concentration of rare earths (mg kg^{-1}) in the sample (C-TH-SC-1A) using anion exchange and neutron activation analysis.

Analyte	X1	X2	Y	W	X1+X2	R%	N.A.A.
La	37.2	8.09	2.25	47.5	45.3	78.2	40.8
Ce	41.7	12.2	5.08	58.9	53.9	70.7	79.4
Nd	34.1	12.9	7.84	54.8	47.0	62.2	15.0
Sm	3.21	1.8	2.3	7.31	5.01	43.9	38.6
Eu	0.72	0.5	1.14	2.36	1.22	30.5	1.23
Ho	0.08	0.16	∞	∞	0.24	0	3.5
Yb	0.22	0.19	1.2	1.61	0.41	13.7	3.8
Lu	0.06	0.06	∞	∞	0.12	0	3.3

X1 = concentration recovered in first column.

X2 = concentration recovered in second column.

Y = concentration passing through both columns.

W = total concentration in the sample.

R% = recovery.

N.A.A = neutron activation analysis.

Table 4.5

Comparison of the concentration of rare earths (mg kg^{-1}) in the sample (SAND-TH-SC-1) using anion exchange and neutron activation analysis.

Analyte	X1	X2	Y	W	X1+ X2	R%	N.A.A.
La	32.8	0.55	0.01	33.3	33.3	98.3	44.3
Ce	42.3	3.7	0.35	46.4	46.0	91.3	107.0
Nd	20.4	5.2	1.78	27.4	25.6	74.5	18.9
Sm	3.01	2.7	23.5	29.2	5.71	10.3	18.2
Eu	0.18	1.13	∞	∞	1.31	0	1.6
Ho	0.07	0.26	∞	∞	0.33	0	3.5
Yb	0.35	0.47	∞	∞	0.82	0	4.7
Lu	0.04	0.1	∞	∞	0.14	0	1.8

X1 = concentration recovered in first column.

X2 = concentration recovered in second column.

Y = concentration passing through both columns.

W = total concentration in the sample.

R% = recovery.

N.A.A.= neutron activation analysis.

Table 4.6

Comparison of the concentration of rare earths (mg kg^{-1}) in the sample (CHALK-TH-SC-1) using anion exchange and neutron activation analysis.

Analyte	X1	X2	Y	W	X1+ X2	R%	N.A.A.
La	7.35	1.13	0.21	8.69	8.48	84.6	28.5
Ce	16.0	4.39	1.66	22.1	20.4	72.6	57.2
Nd	11.2	5.07	4.21	20.5	16.3	54.6	7.4
Sm	0.82	1.0	∞	∞	1.82	0	17.6
Eu	0.44	0.33	0.99	1.76	0.77	25.0	0.9
Ho	0.05	0.9	∞	∞	0.14	0	3.5
Yb	0.22	0.19	1.2	1.61	0.41	13.7	3.0
Lu	0.06	0.07	∞	∞	0.13	0	1.6

X1 = concentration recovered in first column.

X2 = concentration recovered in second column.

Y = concentration passing through both columns.

W = total concentration in the sample.

R% = recovery.

N.A.A.= neutron activation analysis.

Table 4.7

Comparison of the concentration of rare earths (mg kg^{-1}) in the sample (S-S-2) using anion exchange and neutron activation analysis.

Analyte	X1	X2	Y	W	X1+ X2	R%	N.A.A.
La	5.47	0.51	0.05	5.98	5.93	91.5	20.8
Ce	9.62	2.61	0.97	13.2	12.2	72.9	57.3
Nd	6.38	1.95	0.86	9.19	8.33	69.4	7.8
Sm	0.56	0.48	2.88	3.92	1.04	14.3	10.7
Eu	0.17	0.22	∞	∞	0.39	0	0.6
Ho	0.12	0.06	0.06	0.24	0.18	50.0	3.5
Yb	0.36	0.11	0.05	0.52	0.47	69.2	2.0
Lu	0.05	0.05	∞	∞	0.1	0	1.1

X1 = concentration recovered in first column.

X2 = concentration recovered in second column.

Y = concentration passing through both columns.

W = total concentration in the sample.

R% = recovery.

N.A.A.= neutron activation analysis.

sum of the metal collected on the two columns).

In fact some of the neutron activation results do lie within this range, but mostly these are those cases where W is infinity because $X_2 > X_1$. In most other comparisons the neutron activation results are too high - or alternatively the above reasoning is incorrect. In a later chapter (chapter 6) it will be shown that the neutron activation results are higher than those obtained by cation exchange method and may well be wrong.

4.4.1 Conclusion.

The absorption of the mixed rare earths from the phosphate rock samples is not complete. The heavy rare earths are lost to a much greater extent than the light rare earths.

4.5 Procedure Modification.

Having discovered that the recovery of heavy rare earths was very low, an attempt was made to improve the recovery by altering the concentration of nitric acid and water independently, whereas, in the previous investigation (see section 4.1), the ratio of water to concentrated nitric acid was kept at 1: 1.27. The investigation was restricted to two elements, lanthanum (to represent the light rare earths) and holmium (to

represent the heavy rare earths). The batch procedure was used to estimate the distribution ratio as before (see section 4.1 - equation (1)).

In the first experiment the methanol concentration was fixed at 95%, while the concentration of nitric acid was changed from 0 to 5%, the water content varying in a complementary manner to the acid. The results for both elements show that the distribution coefficient increases as the concentration of nitric acid is increased. The increase in D_x values is more noticeable with lanthanum, Figure 4.12, where it increased from 250 to 1400. The results for holmium show a similar pattern but the variation of D_x values is much less, the lowest value is 28 and the highest is 40, as can be seen in Figure 4.13. For both elements, the maximum D_x value was when the concentration of nitric acid is 3.5%. This should be compared with the value used in the previous analysis of 2.2%.

In the second experiment the concentration of nitric acid was fixed at 1%, while water concentration was changed from 1 to 10%, the methanol varying from 98 to 89%. Both elements, lanthanum and holmium, show the same response, where the distribution ratio drops as the water concentration increases, as shown in Figure 4.14 and 4.15.

Figure (4.12)

The effect of changing nitric acid content on the distrbution coefficient of lanthanum

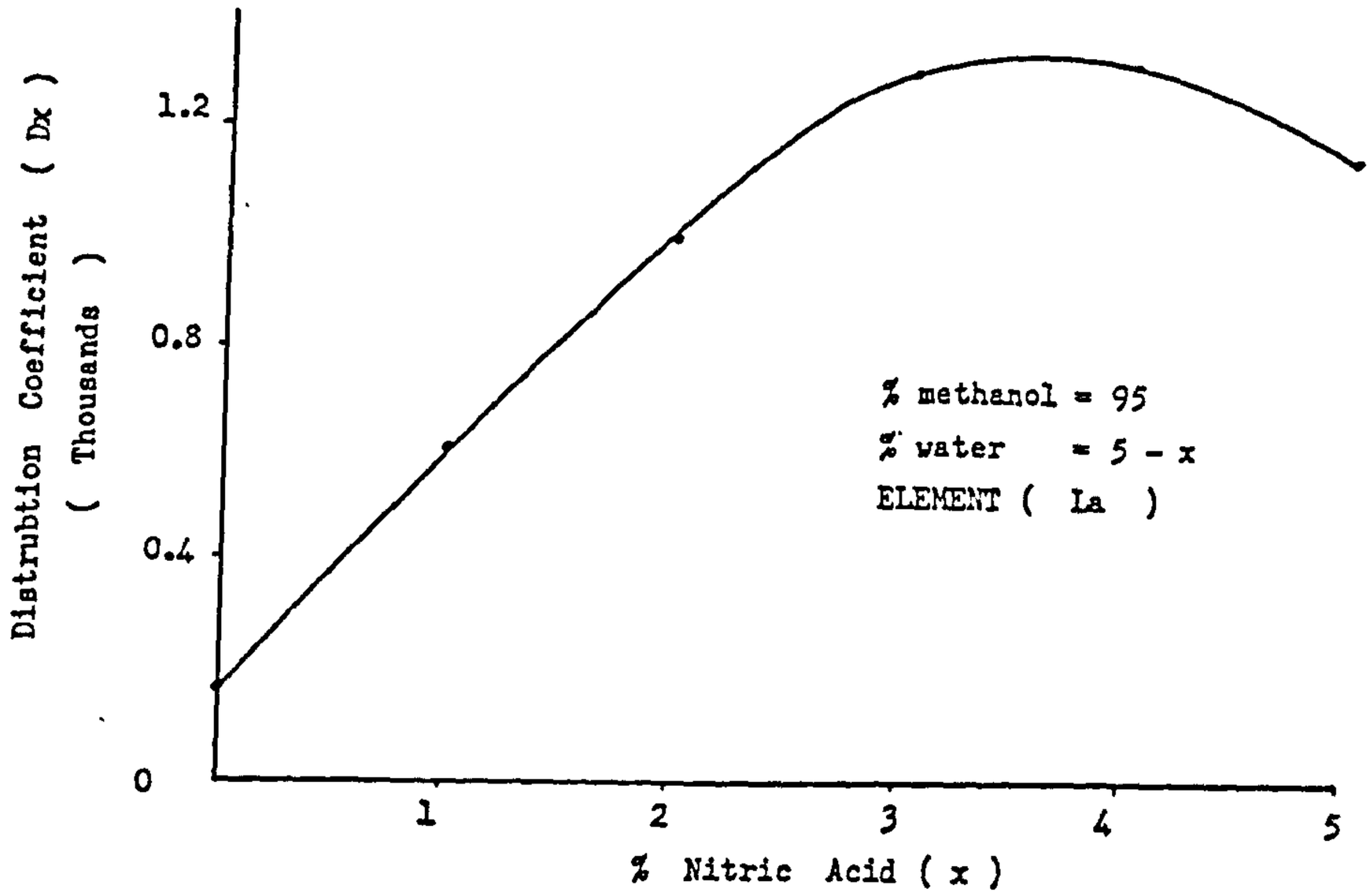

Figure (4.13)

The effect of changing nitric acid content on the distrbution coefficient of holmium

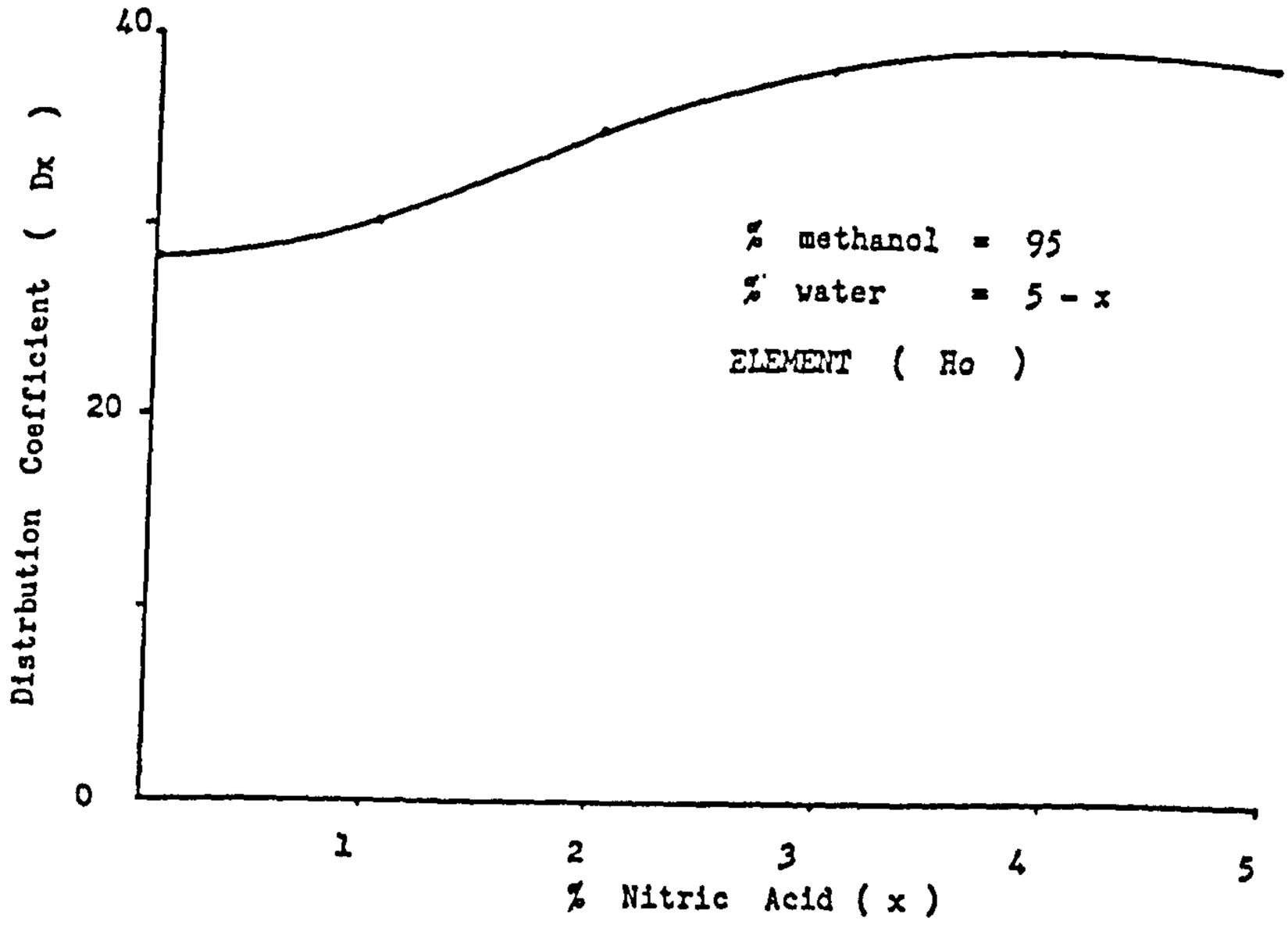

Figure (4.1 4)

The effect of changing water cocentration on distrbution ratio for lanthanum .

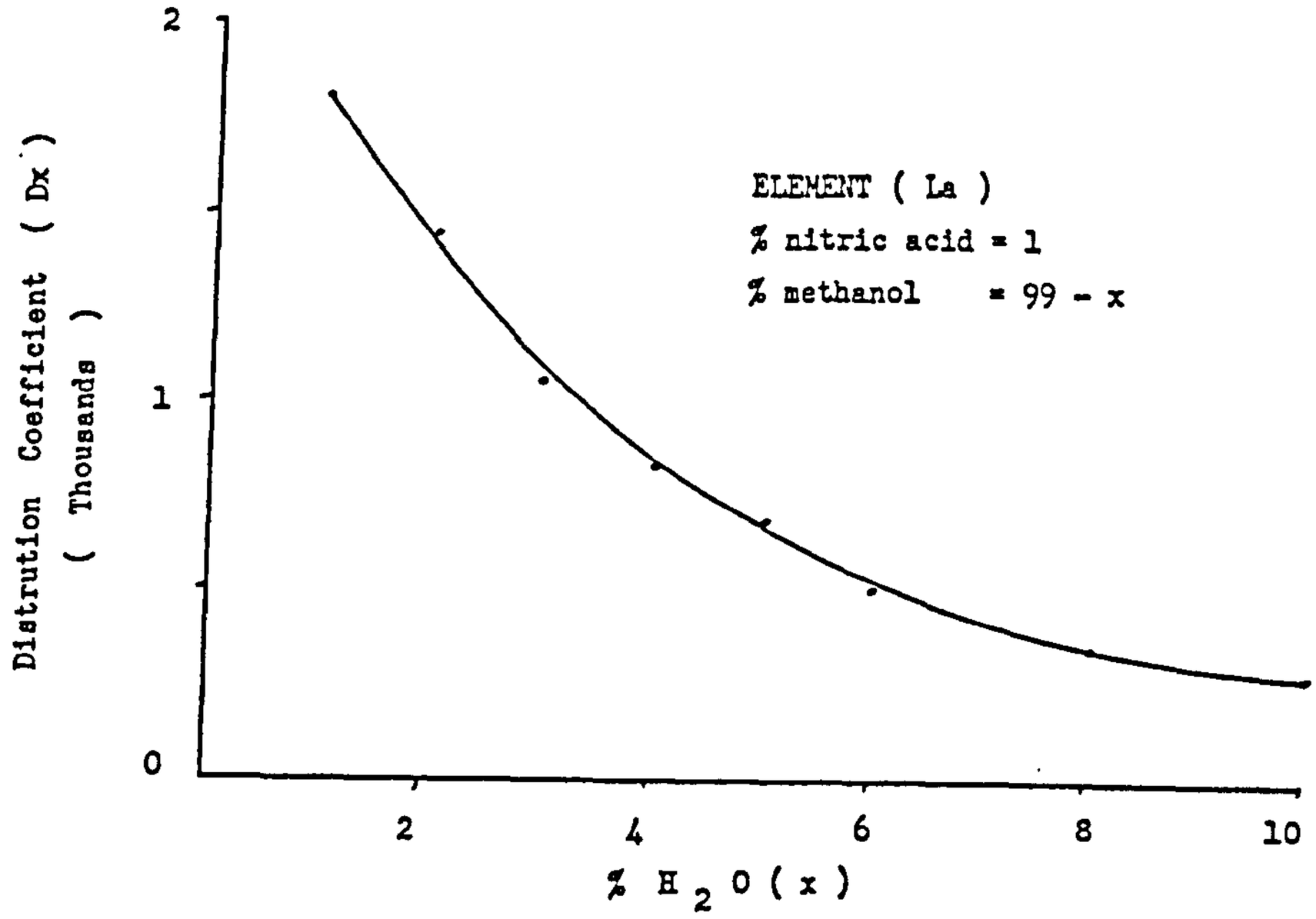

Figure (4.15)

The effect of changing water centent on the distrbution ratio for holmium

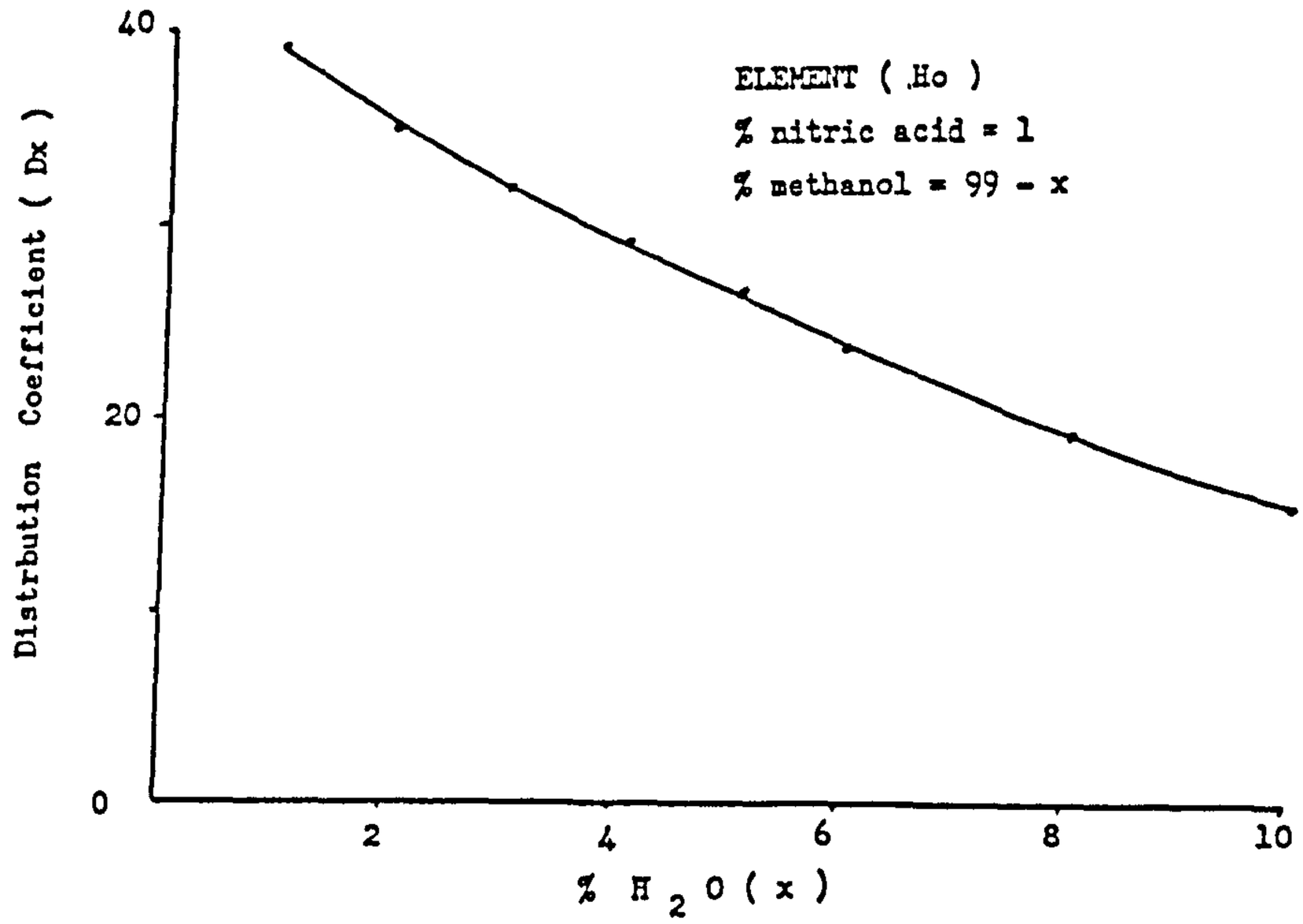

4.5.1 Conclusion.

Very little improvement was made on the distribution ratio by altering the composition of the sample solution. A solution containing, methanol 98%, water 1% and nitric acid 1%, gave better recoveries but was rejected because there was not sufficient water and nitric acid to dissolve the residue after dissolution and evaporation. The composition of the sample solution which can be used is, methanol 95%, water 1.5% and nitric acid 3.5%.

4.6 Interference of Calcium Phosphate.

The recovery of single rare earth elements is very high approaching 100%, as has been discussed earlier (see section 4.2). But recovery of the mixed rare earths in a real phosphate rock sample is not complete (see section 4.4). So it is important to investigate the effect of increasing concentration of calcium phosphate on a mixture of rare earths.

Several solutions of 2 litres of the organic solvent (see section 4.5) containing the same concentration (5 mg dm^{-3}) of each of all the rare earths, yttrium and thorium. The weight of calcium phosphate was varied from 0.0 to 50 g. Then each element in the eluted solution was measured using the ICP technique (see section 6.1).

The results show, see Figure 4.16, that when calcium phosphate was absent, the recovery of the light rare earths (lanthanum to samarium) is complete (95 to 100%). While the recovery of the heavy rare earths could be separated into three groups. The first group (for the elements from samarium to holmium), for which the recovery decreases with the increase in atomic weight. The second group is for the elements holmium to thulium, for which the recovery increases with the atomic weight. Finally the last group for the elements thulium to lutetium, in this group the recovery again falls as the atomic weight is increased. Yttrium and thorium show a low recovery, about 55%.

The presence of calcium phosphate causes a drop in the recovery of the rare earths from the mixture, as can be seen in Figure 4.16. For the elements samarium to lutetium, the same pattern of recovery was found, as that observed when calcium phosphate was absent. The recovery of the light rare earths, lanthanum to samarium, could be separated into two regions. The first, from lanthanum to praseodymium, where the recovery decreases with the increase in atomic weight. The second region, from praseodymium to samarium, where the recovery increases with the atomic weight.

For all rare earths, the pattern of recoveries does not change as the weight of calcium phosphate

Figure (4.16) - Recovery of REE , Y and Th from anion exchange column :- solution volume = 2 dm^3 , concentration of each element = 5 mg dm^{-3} - (●—) no calcium phosphate , (×····) 10 g calcium phosphate and (Δ·—) 50 g calcium phosphate , (○——) 30 g clacium phosphate .

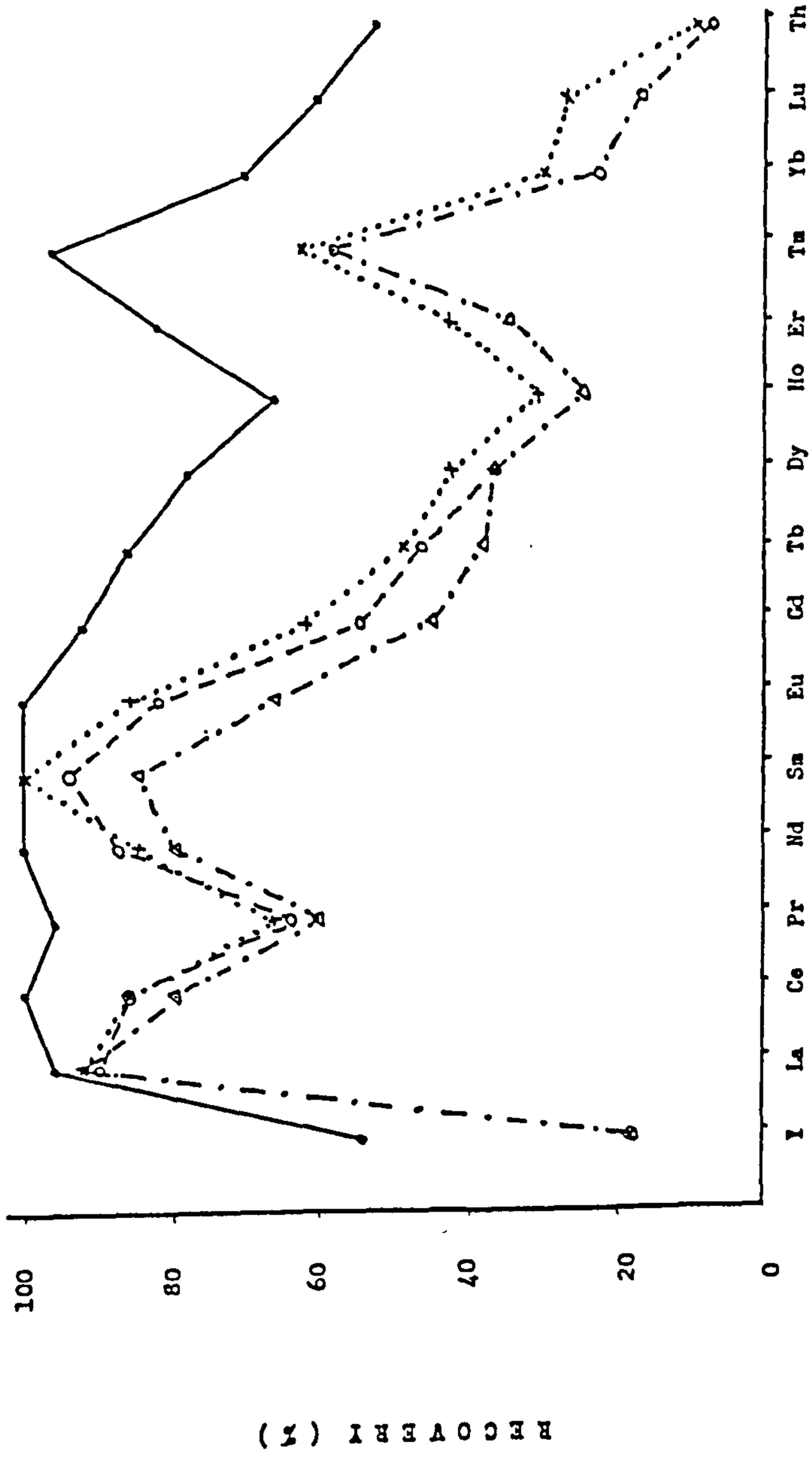

increases to 50 grams, however the recoveries are reduced particularly for the heavier rare earths. Thorium and yttrium recoveries drop to a very low level when calcium phosphate is introduced, a further increase in the calcium phosphate concentration did not reduce the recovery much more.

4.6.1 Conclusion.

The recovery of the light rare earths is tolerable when calcium phosphate was absent, but is lower for the heavier rare earths. The recovery decreases with an increase in the weight of calcium phosphate. The pattern of recovery remaining constant despite the increase in calcium phosphate. The anion exchange procedure was abandoned at this stage because there seemed no way of overcoming the interference of calcium phosphate.

CHAPTER FIVE: CATION EXCHANGE.

In this chapter an investigation was conducted to establish the volume of 2M nitric acid needed to wash the calcium and phosphate of the column prior to the recovery of rare earths and the volume of 6M nitric acid needed for complete elution of the rare earths (see section 5.1) .

As the investigated samples contain a high concentration of calcium phosphate. The effects of the presence and the absence of calcium phosphate on the recoveries of various concentrations of the rare earths, were studied (see section 5.2).

In order to achieve complete recoveries a large column was studied (see section 5.1). The final procedure using the larger column was tested on an artificial phosphate rock containing all the lanthanide elements and yttrium (see section 5.4).

5.1 Choice of Resin and Volume of Eluant.

In this section we are comparing the behavior of calcium, phosphate ions, rare earth elements and thorium in synthetic solutions containing all these species on three strongly acidic cation exchange resins (25 g),

i.e.

1 -	DOWEX 50WX8	16 - 60 mesh
2 -	BIO RAD AG 50WX8	50 - 100 mesh
3 -	AMBERLIT IR-120	14 - 52 mesh

The results show that phosphate ions are not retained on any of the three resins and are quickly removed by washing with 2M nitric acid, as shown in Figure 5.1. Calcium ions however, require a larger volume of 2M nitric acid to be washed from the resins than do the unretained phosphate ions, as shown in Figure 5.2. Thus calcium is weakly held by all three resins .

After washing the column with 2M nitric acid to remove the calcium and phosphate ions, the rare earths, yttrium,lanthanum, praseodymium, gadolinium, erbium and lutetium, were eluted with 6M nitric acid. The elution curves of the three resins are shown in Figures 5.3 to 5.8. The DOWEX resin released the absorbed rare earth ions more slowly than the other two resins and the elution curve is more drawn out with a long tail. The elution curves for the other two resins are sharper and recoveries are similar on both resins for all the rare earths except for the elements praseodymium and gadolinium. BIORAAD resin gave better recoveries of praseodymium, Figure 5.8, and poorer recoveries of gadolinium, Figure 5.6.

Figure (5.1)

Washing of phosphate ions from three cation exchange resins

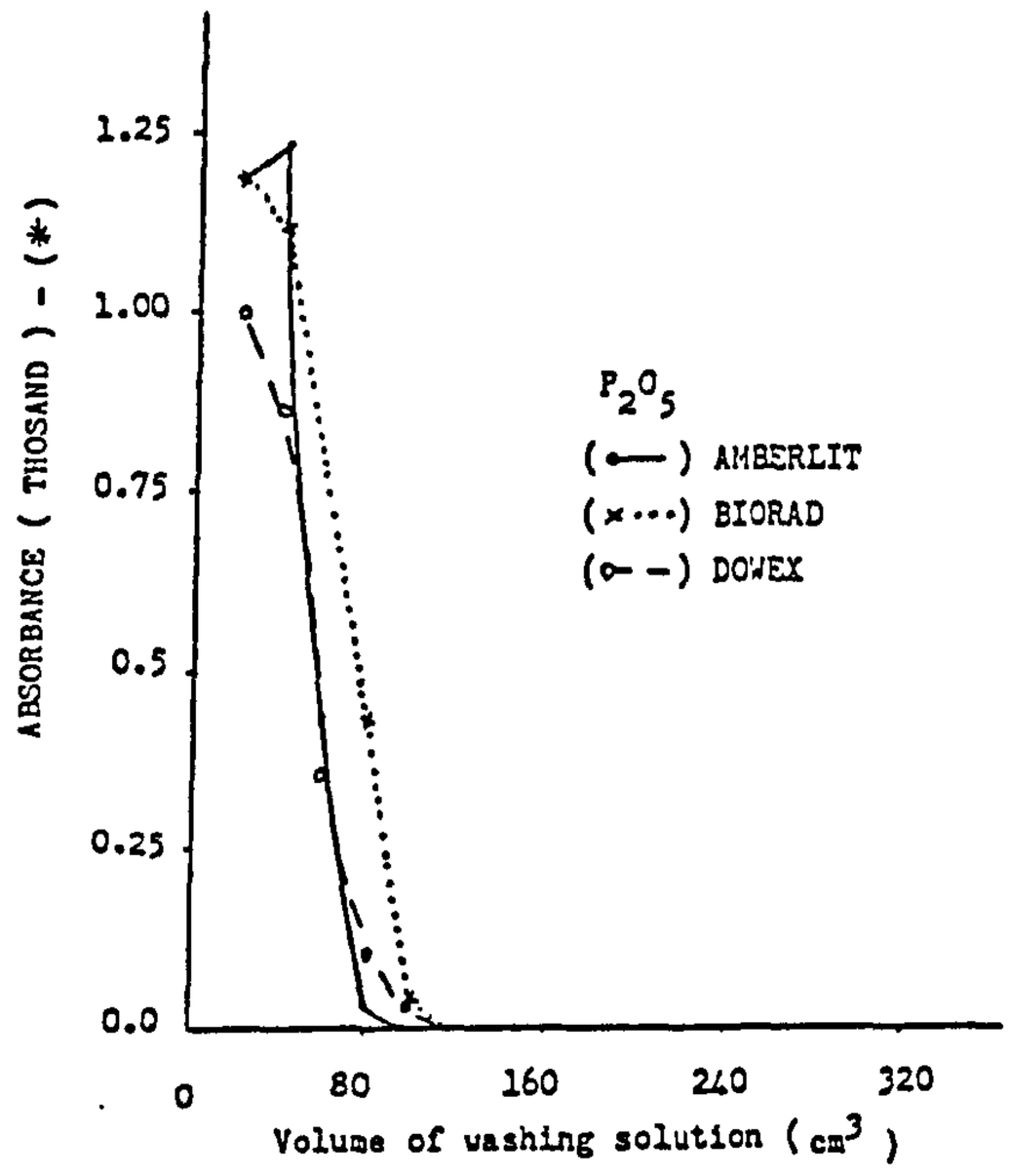

(*)- The Y axis has been corrected for the dilution used in order to obtain a measurable absorbance, (i.e. between 0.1 and 1)

Figure (5.2)

Washing of calcium from three cation exchange resins

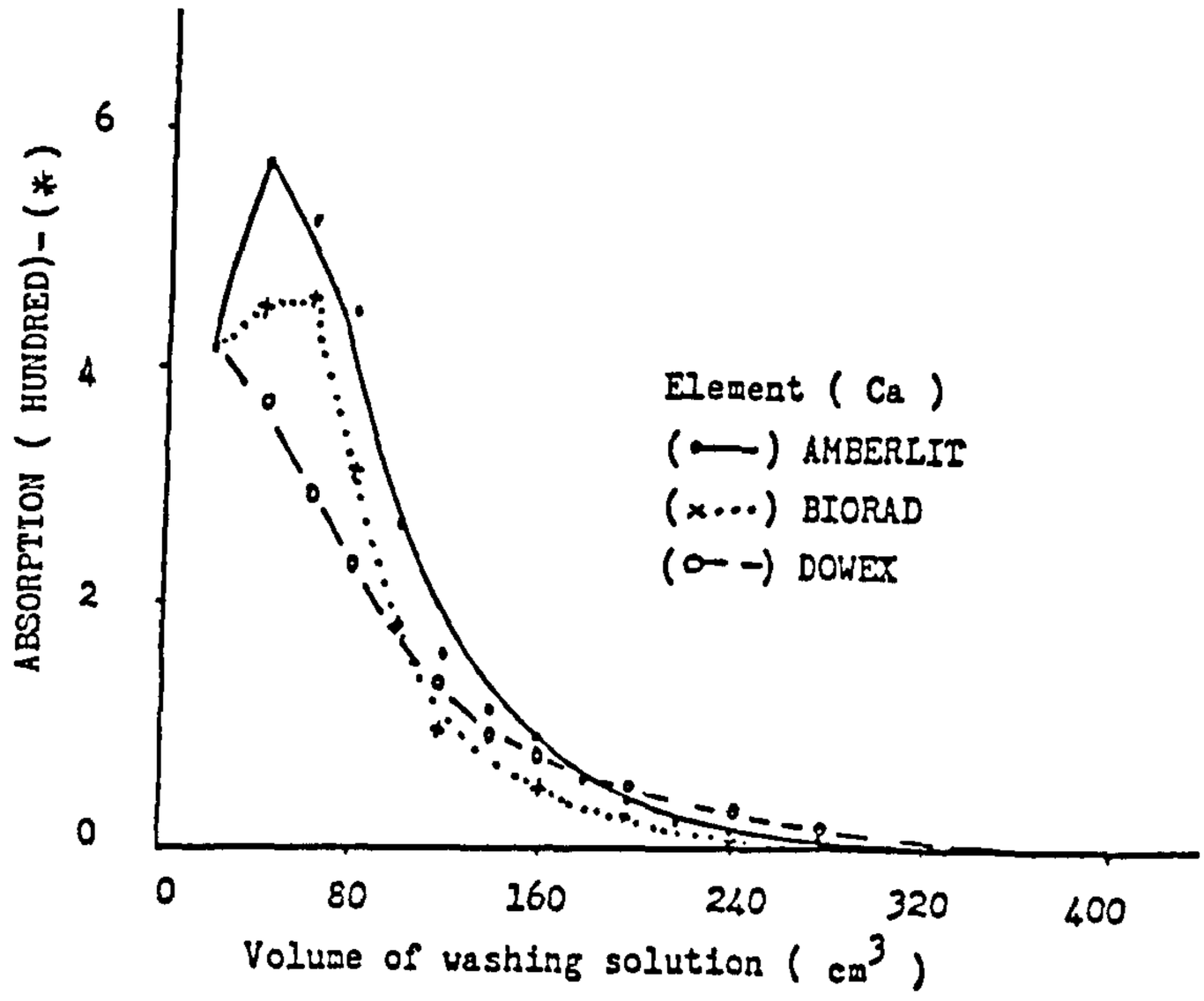

(*) - The Y axis has been corrected for the dilution used in order to obtain a measurable absorbance, (i.e. between 0.1 and 1)

Figure (5.3)

Elution of yttrium from three cation exchange resins

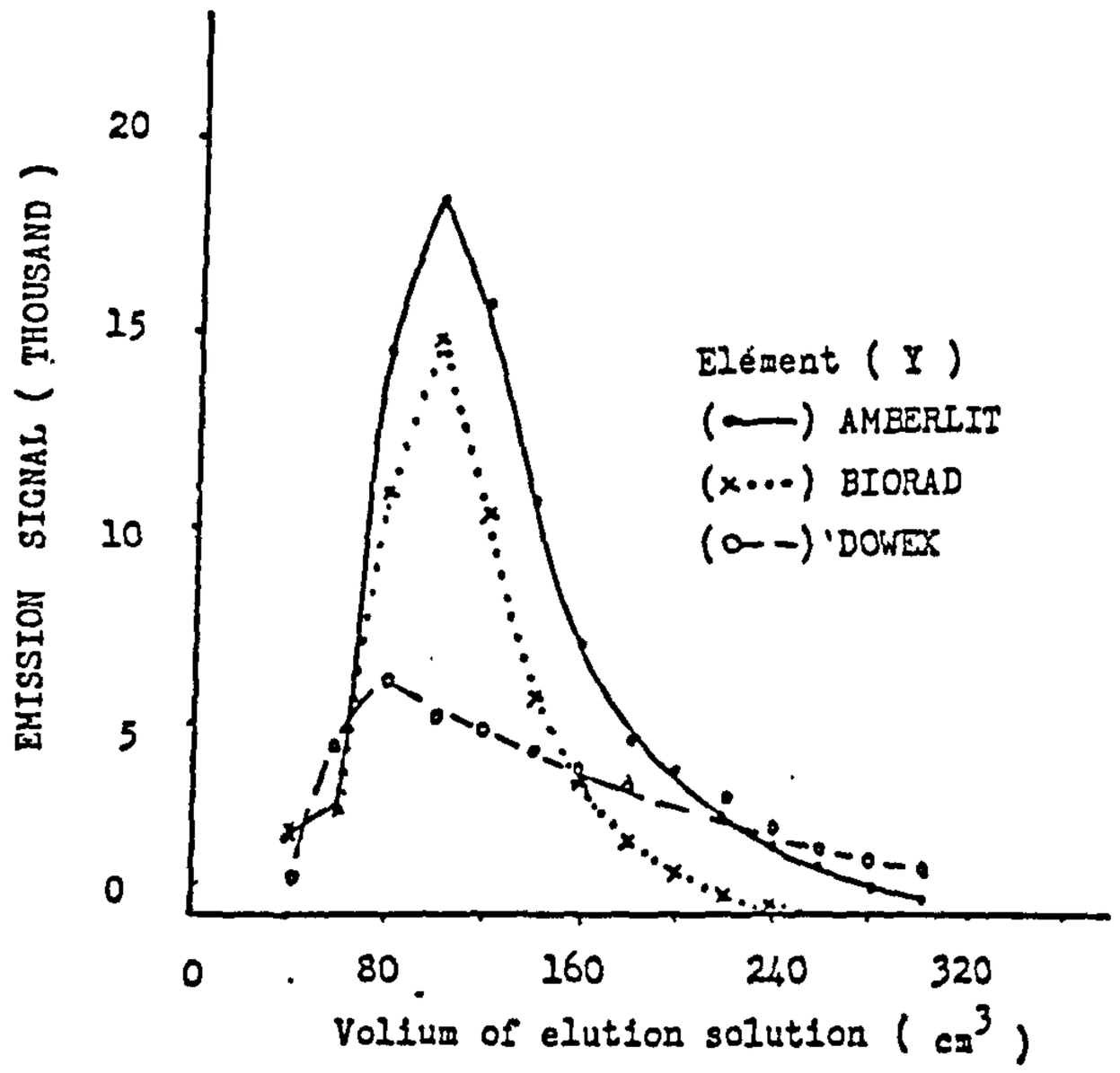

Figure (5.4)

Elution of lanthanum from three cation exchange resins

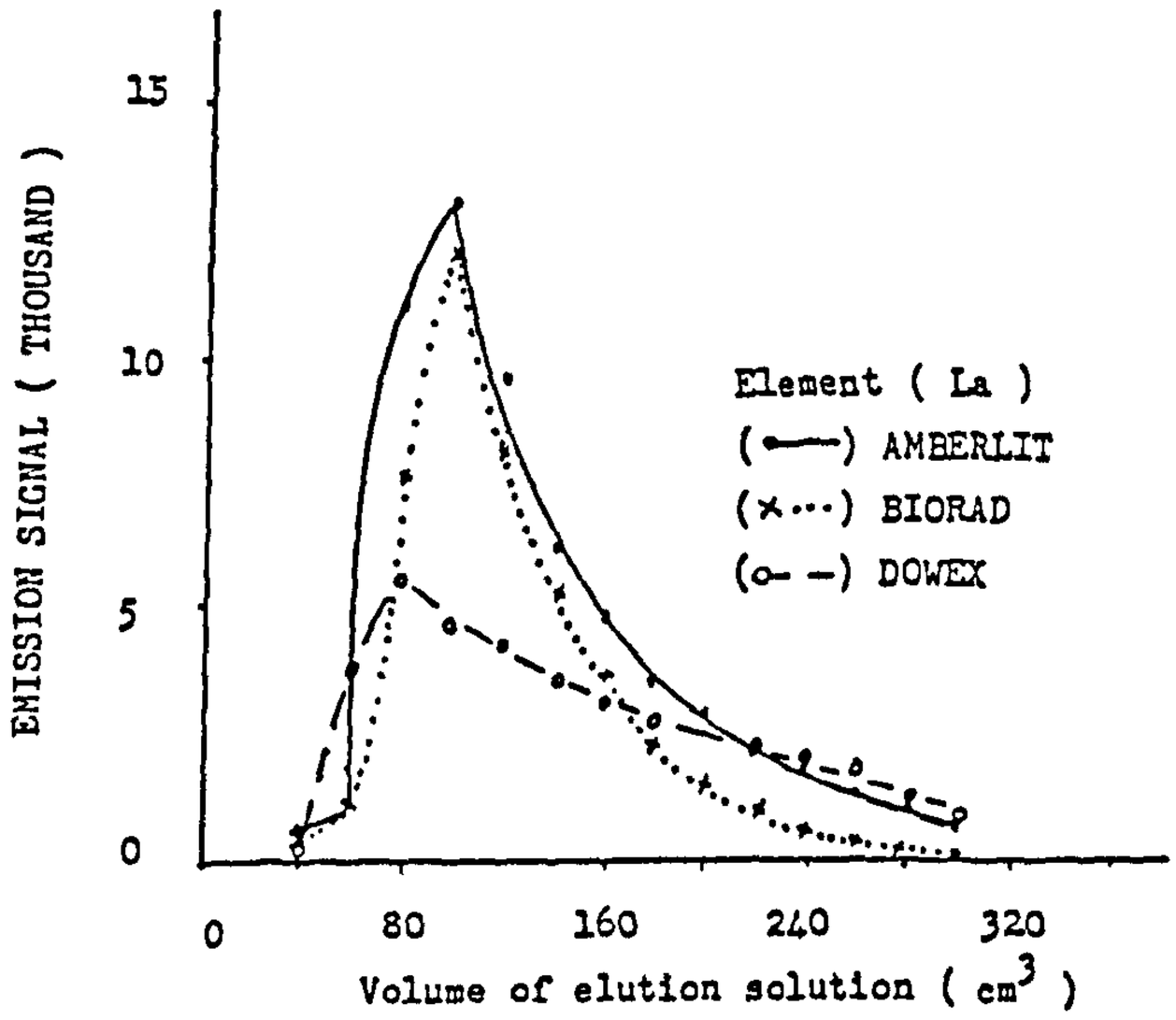

Figure (5.5)

Elution of praseodymium from three cation exchange resins

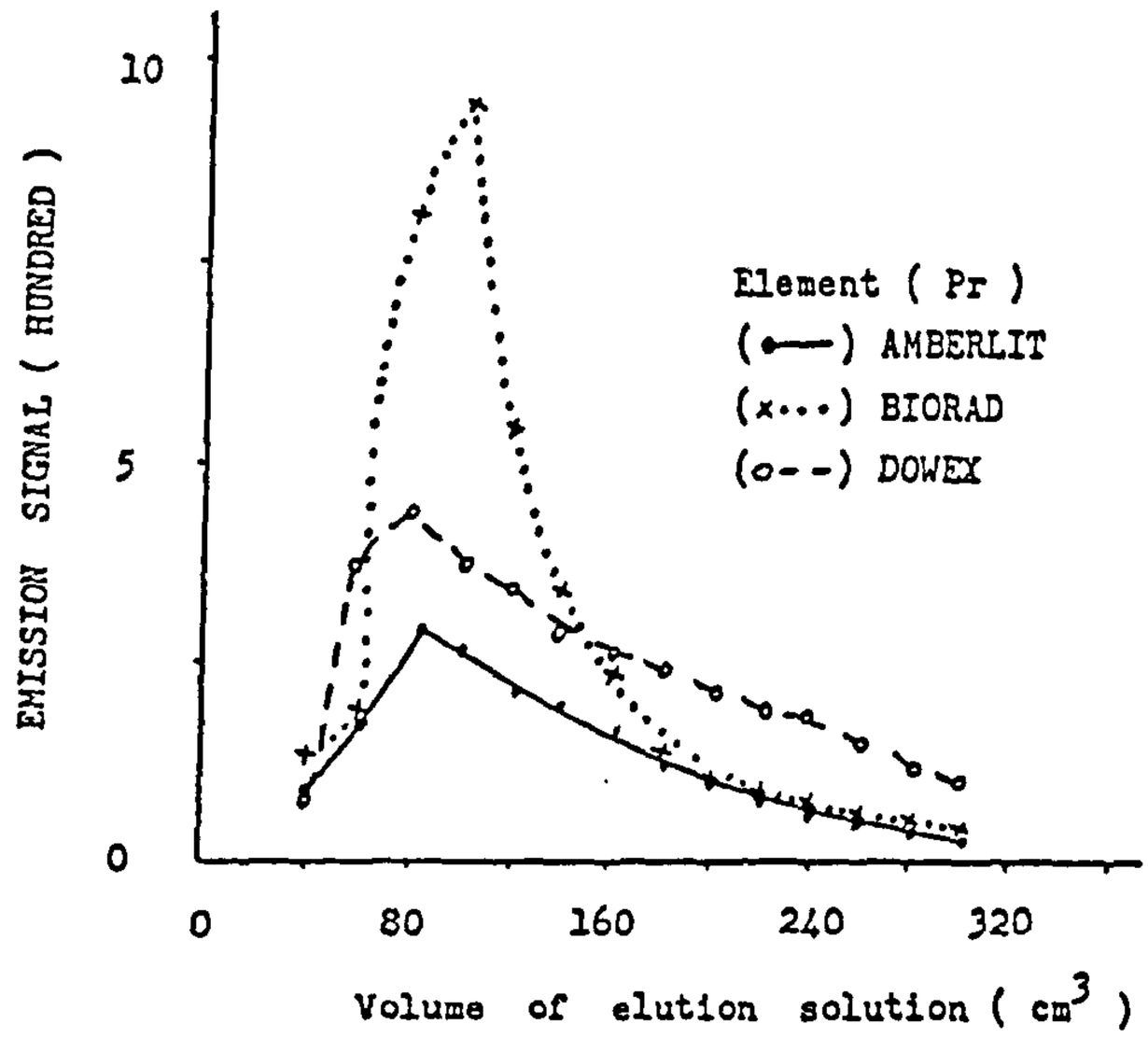

Figure (5.6)

Elution of gadolinium from three cation exchange resins

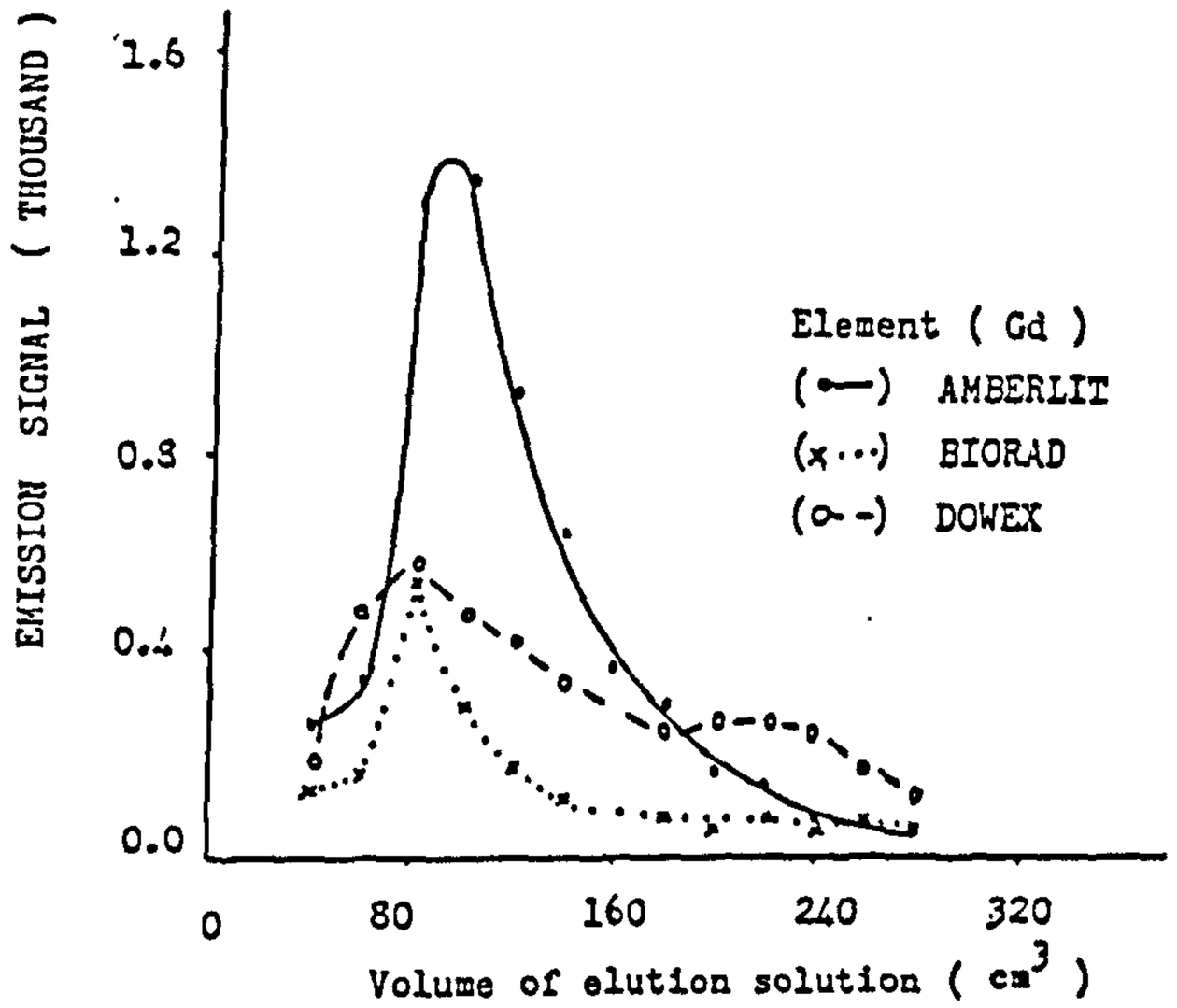

Figure (5.7)

Elution of erbium from three cation exchange resins

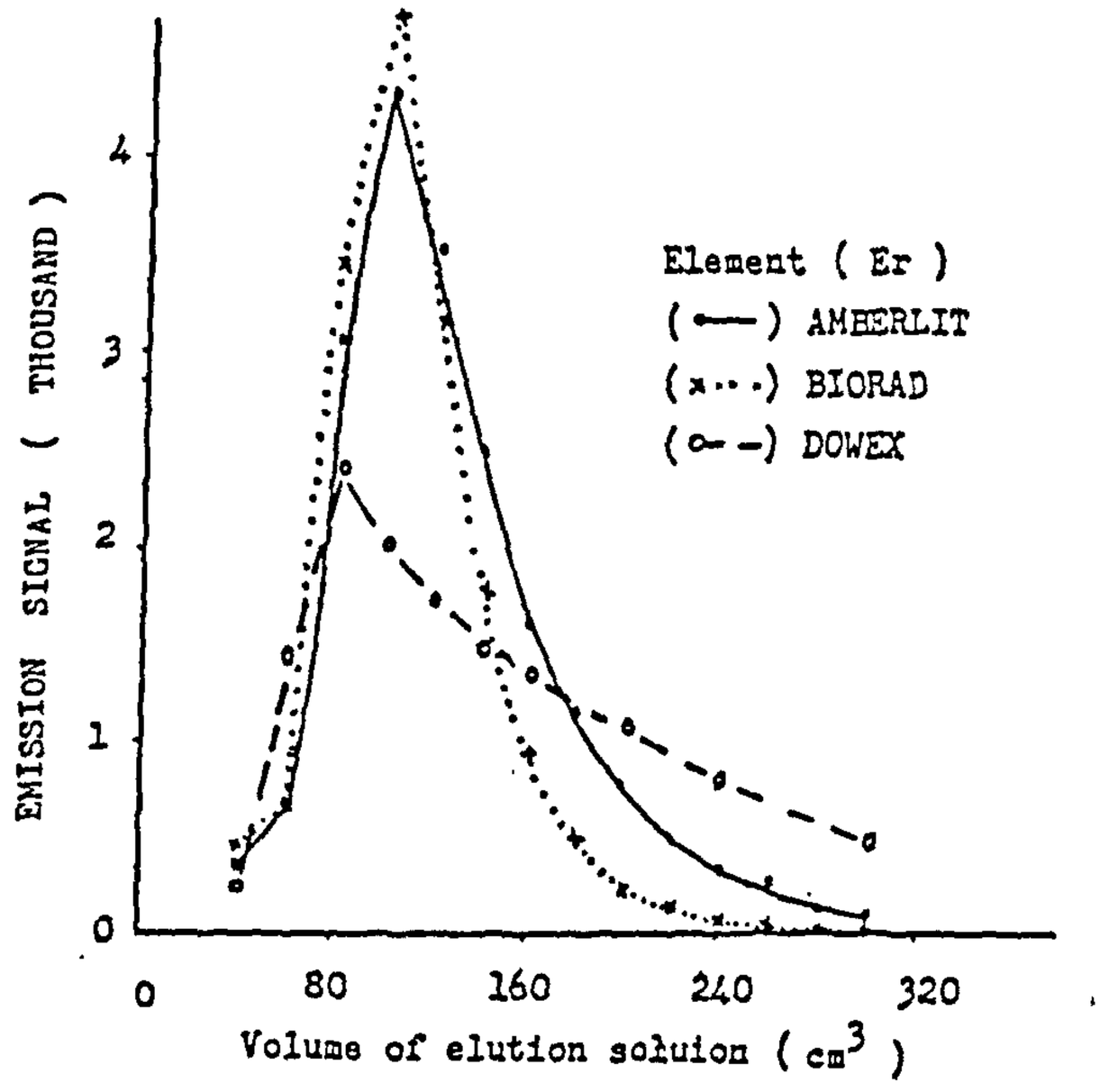

Figure (5.8)

Elution of lutetium from three cation exchange resins

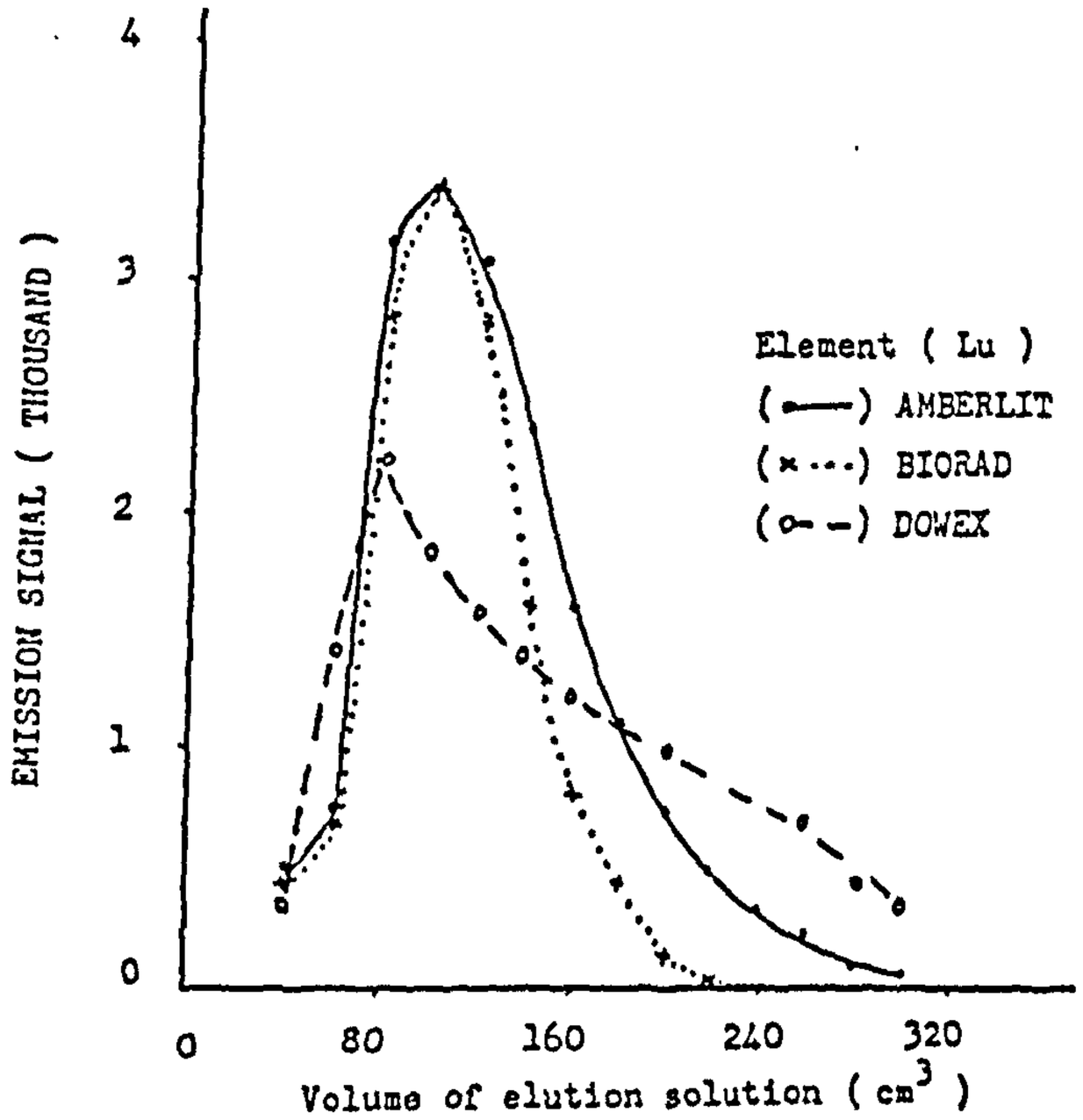

The recoveries of the various resins are compared in Table 5.1. The units are arbitrary but for any one element are the same for each resin. Thus for yttrium the DOWEX resin has a recovery of about half that of the AMBERLIT resin (47/78 = 0.53).

The analysis of the eluted solutions for all three resins show no traces of thorium, suggesting that it had been washed out during previous (2M nitric acid) stage. This element was not investigated further.

Table 5.1.

A comparison between the recoveries* of the three resins (mixed synthetic solutions).

ANALYTE	DOWEX	BIORAD	AMBERLIT
Y	47	53	88
LA	42	45	61
Pr	4	4	2
Gd	4	2	6
Er	17	16	19
Lu	16	13	18

* The emission signal for each rare earth was integrated by Simpsons rule to obtain the area under the elution curve which is proportional to the total amount of rare earth recovered.

5.1.1 Conclusion.

In general AMBERLIT resin is the best because it has a sharp elution curve, a higher recovery and a low price. All further experiments were conducted using this chosen resin. A volume of 350 cm^3 of 2M nitric acid was sufficient to wash all calcium and phosphate ions from the small column, followed by 500 cm^3 of 6M nitric acid to elute all the absorbed rare earths.

5.2 Variation of the Rare Earths Recoveries in the Presence and the Absence of Calcium Phosphate.

Calcium and phosphate ions constitute most of the phosphate rock and their effect on the recoveries of the rare earths were investigated. Three samples were prepared containing 2 mg dm^{-3} of each of the six rare earths, yttrium, lanthanum, praseodymium, gadolinium, erbium and lutetium, in 1M nitric acid with no calcium or phosphate (sample 1), with calcium only (sample 2) and with phosphate ions only (sample 3). A recovery of 89 - 99.9% for all these six elements was observed (Table 5.2) when the pure solution, sample 1, was investigated. Phosphate ions alone, sample 3, in a concentration similar to that of 10% (w/v) calcium phosphate (45.8 g dm^{-3} P_2O_5) gave similar results (Table 5.2 also). But calcium alone in a concentration similar to that of 10% (w/v) calcium phosphate

(i.e 54.2 g dm^{-3} CaO) cause a drop in the recovery to 38 - 88%, as shown in Table 5.2. The reduction of the recovery is even greater when both calcium and phosphate ions are present in the same solution, as will be discussed later.

After decomposition of the sample calcium and phosphate ions will be present together in the solution, so the effects of both ions were investigated when present at the same time. The recoveries of the rare earths were measured in presence of 10% (w/v) calcium phosphate [$Ca_3(PO_4)_2$]. The recoveries of each rare earths was almost constant (28 - 62%). When the concentration of each element was increased from 2 mg dm^{-3}, sample 4, to 5 mg dm^{-3}, sample 5, as shown in Table 5.3. Erbium however, is an exception, it gave worse recoveries when the concentration of the rare earths was increased, as can be seen in Table 5.3. All fifteen rare earth elements were next tested in the same solution (the concentration of the rare earths used was 1 mg dm^{-3} each in a solution of 10% (w/v) calcium phosphate). Almost the same recoveries were obtained, as can be seen in Table 5.4.

In the phosphate rock samples, the concentration of the light rare earths is much higher than that of the heavier rare earths. A similar pattern of the six rare earths previously chosen was next

Table 5.2.

A comparison of the recoveries of the rare earths, 2 mg dm^{-3} each, in the presence and the absence of calcium and phosphate ions.

ANALYTE	SAMPLE (1)	SAMPLE (2)	SAMPLE (3)
Y	99.7	99.9	86.1
La	99.8	99.9	88.3
Pr	99.5	99.6	54.3
Gd	89.5	98.3	36.6
Er	92.2	99.4	56.4
Lu	99.0	99.0	60.8

Sample (1) contains rare earths only

Sample (2) contains rare earths with phosphate ions only

Sample (3) contains rare earths with calcium only

Table 5.3.

The recovery of rare earths in the presence of 10% (w/v) calcium phosphate.

ANALYTE	SAMPLE (4)	SAMPLE (5)
Y	45.3	46.4
La	57.1	65.9
Pr	42.5	42.4
Gd	26.8	28.1
Ev	98.7	62.5
Lu	36.1	38.4

Sample (4) contain 2 mg dm^{-3} of each of the rare earths

Sample (5) contain 5 mg dm^{-3} of each of the rare earths

Table 5.4.

Calculated recoveries when all elements were present at concentration of 1 mg dm^{-3} each in a solution containing 10% (w/v) calcium phosphate.

ANALYTE	RECOVERY %
Y	48.6
La	64.6
Ce	64.4
Pr	45.2
Nd	78.8
Sm	27.9
Eu	24.2
Gd	25.5
Tb	39.6
Dy	38.8
Ho	34.8
Er	99.7
Tm	41.7
Yb	58.8
Lu	34.5

investigated in the present of 10% (w/v) calcium phosphate. The recoveries show a slight reduction in comparison to that obtained when all elements have the same concentration, as seen in Table 5.5. Except for erbium which maintains its high recovery (99 %).

The removal of calcium by precipitation as sulphate does not improve the recovery of 2 mg dm^{-3} of each of the rare earths, but it makes it worse (20-39%:- as shown in Table 5.6). This very low recovery indicated co-precipitation of rare earths with calcium sulphate.

Table 5.5.

Recovery of rare earths from a solution simulating the concentration distribution present in phosphate rock (*).

ANALYTE	INITIAL CONTENT mg dm^{-3}	RECOVERY R%	RECOVERY R%**
Y	10	36.7	45.8
La	10	54.5	61.6
Pr	6	38.7	42.4
Gd	3.5	24.7	27.5
Er	1.5	99.2	80.6
Lu	0.5	33.3	37.2

* In most samples the concentration of heavy rare earths is lower than the concentration of light rare earths.

** Average recovery from Table 5.3.

Table 5.6.

Recoveries of rare earths, 2 mg dm^{-3} each, after the separation of calcium as calcium sulphate from 10% (w/v) calcium phosphate.

ELEMENT	RECOVERY R%
Y	38.4
La	30.2
Nd	20.5
Gd	27.6
Ho	28.6
Lu	39.6

5.2.1 Conclusion.

The recovery of rare earths was independent of the concentration of the rare earth elements used as long as the concentration of calcium phosphate was maintained constant. A high recovery was obtained when phosphate ions were present alone, but the recovery reduced when calcium was present alone. A greater reduction in the recovery occurred when both calcium and phosphate ions were present in the same solution. When calcium is removed from the solution as sulphate, the recovery was very bad. Clearly in order to use this technique in samples, the recovery must be improved.

5.3 The Effect of Calcium Phosphate on the Recovery

The recovery of the rare earths (2 mg dm^{-3} each) from a small column, which contained 25 g of the resin (as used in the previous two sections, 5.1 and 5.2), were measured as the concentration of calcium phosphate was increased from 1 to 10% (w/v). The recoveries were maintained at high values (95 - 100%) up to 3% (w/v) calcium phosphate, as shown in Figures 5.9 and 5.10. This was true for all elements tested, yttrium, lanthanum, neodymium, gadolinium, holmium and lutetium. As the concentration of calcium phosphate increases the recoveries fall, reaching 76-85% when the calcium phosphate concentration was 5% (w/v), except for

Figure (5.9)

Interference of calcium phosphate on the recovery of rare ear

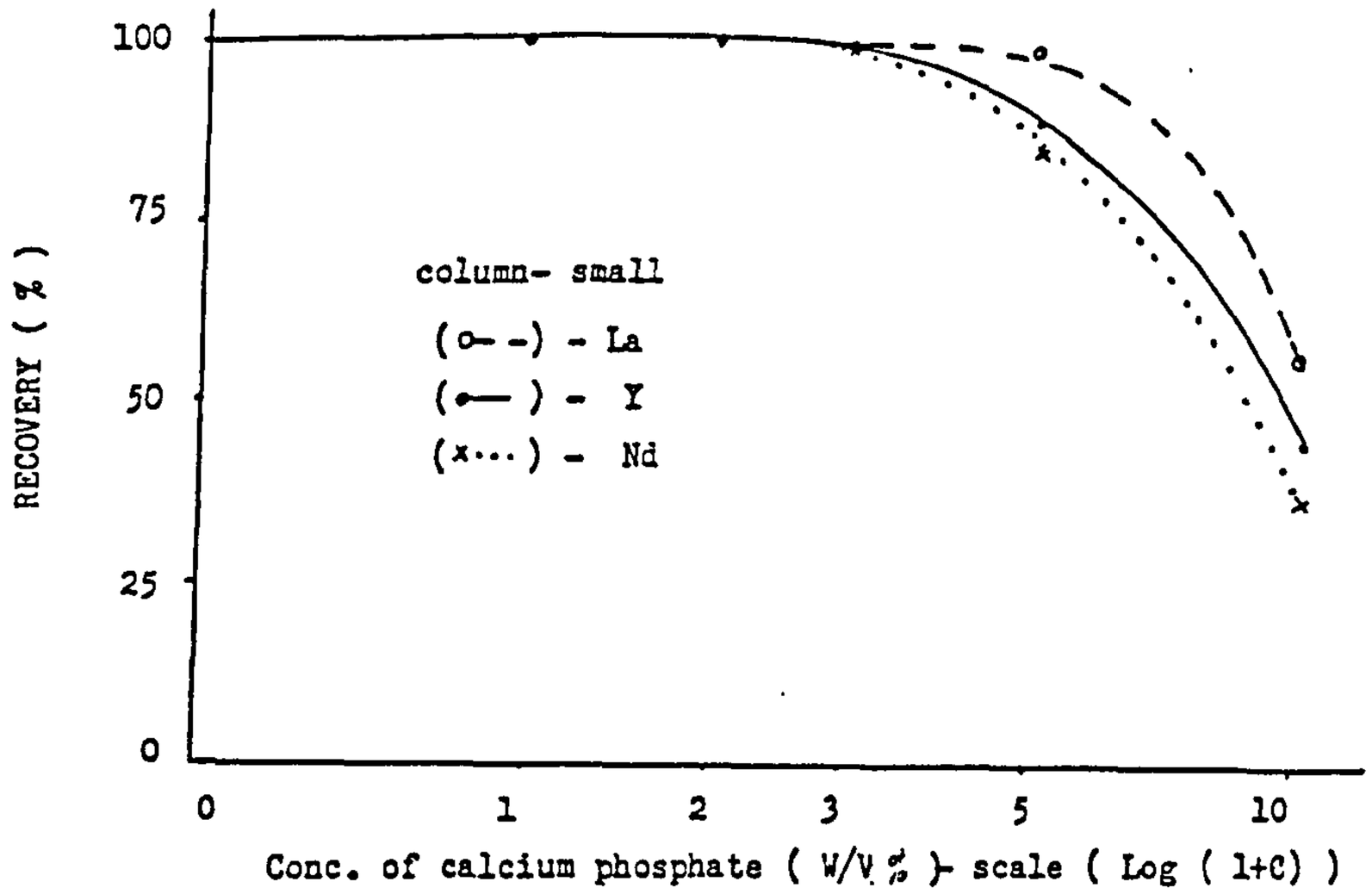

Figure (5.10)

Interference of calcium phosphate on the recovery of rare earths

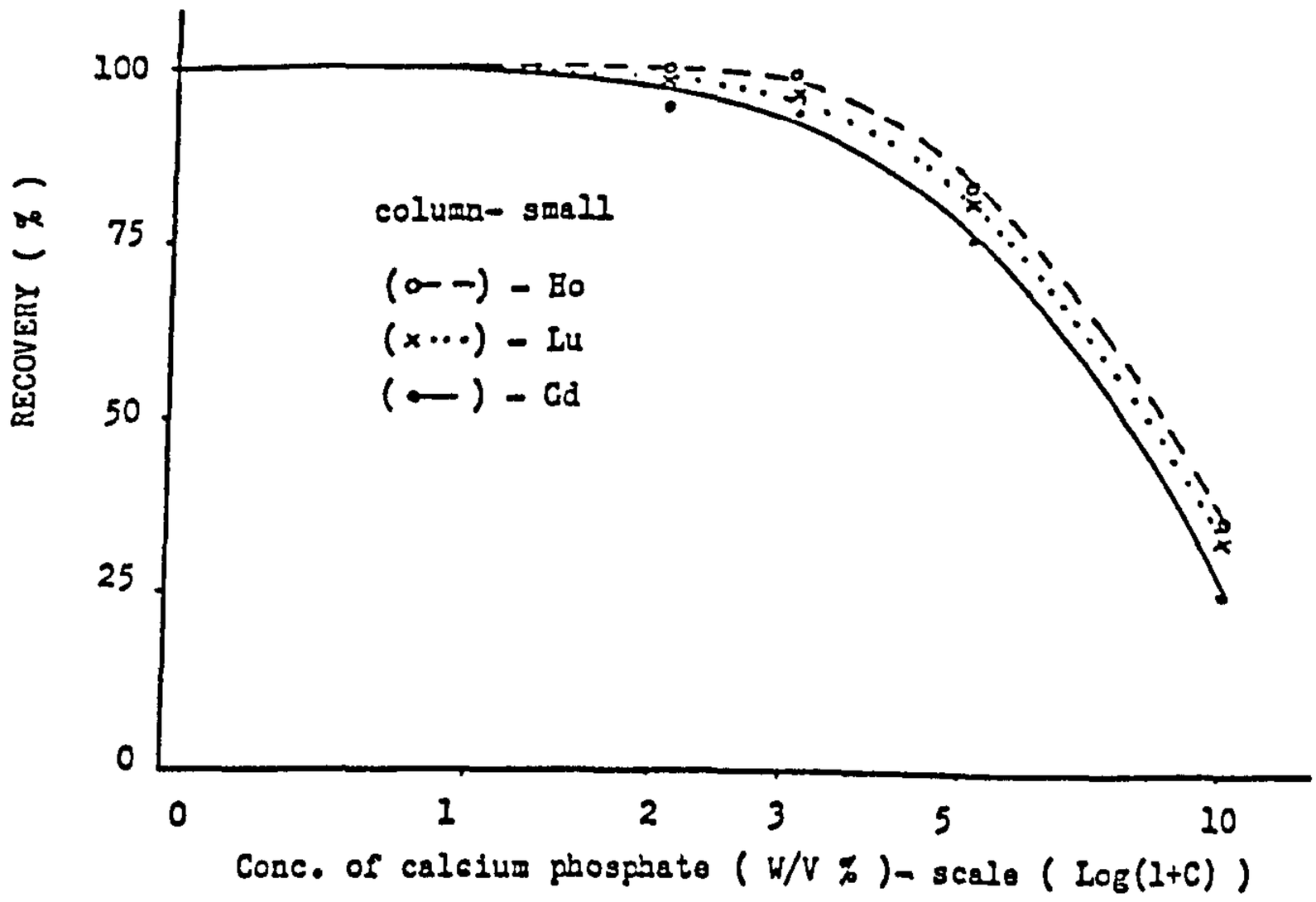

yttrium and lanthanum where their recoveries were still high, 90-100%. The fall in the recovery was greater, 26-57%, for all the elements when calcium phosphate concentration was 10% (w/v), as seen in Table 5.7.

The use of this small column allows the separation of rare earths from 6 g of phosphate rock, but for adequate sensitivity larger samples are needed, so a larger column was tested. When a larger column containing twice the weight of the resin (50 g) was used, twice the volume (700 cm^3) of 2M nitric acid washing solution was required, as well as twice the volume (1 dm^3) of 6M nitric acid to elute the absorbed rare earths. This column was tested in exactly the same way as the smaller column. The recoveries were maintained at high values, 90-100%, up to 5% (w/v) calcium phosphate, see Figures 5.11 and 5.12. This was true for all elements tested. The recoveries drop to a lower value, 55-77%, as the concentration of calcium phosphate was 10% (w/v). This was true for all elements, except for lanthanum where it maintained a high value, 95%, as seen in Table 5.8.

Table 5.7.

The recovery of 2 mg dm^{-3} of the rare earths from the small column which contain 25 g of the resin.

	CONCENTRATION OF CALCIUM PHOSPHATE (w/v) %				
ANALYTE	1	2	3	5	10
Y	100	100	100	90.9	45.3
La	100	100	100	100	57.2
Nd	100	100	99.0	85.1	37.5
Gd	100	95.6	95.0	76.9	26.8
Ho	100	100	100	84.3	36.5
Lu	100	98.5	97.2	83.2	36.1

Figure (5.11)

Interference of calcium phosphate on the recovery of rare earths

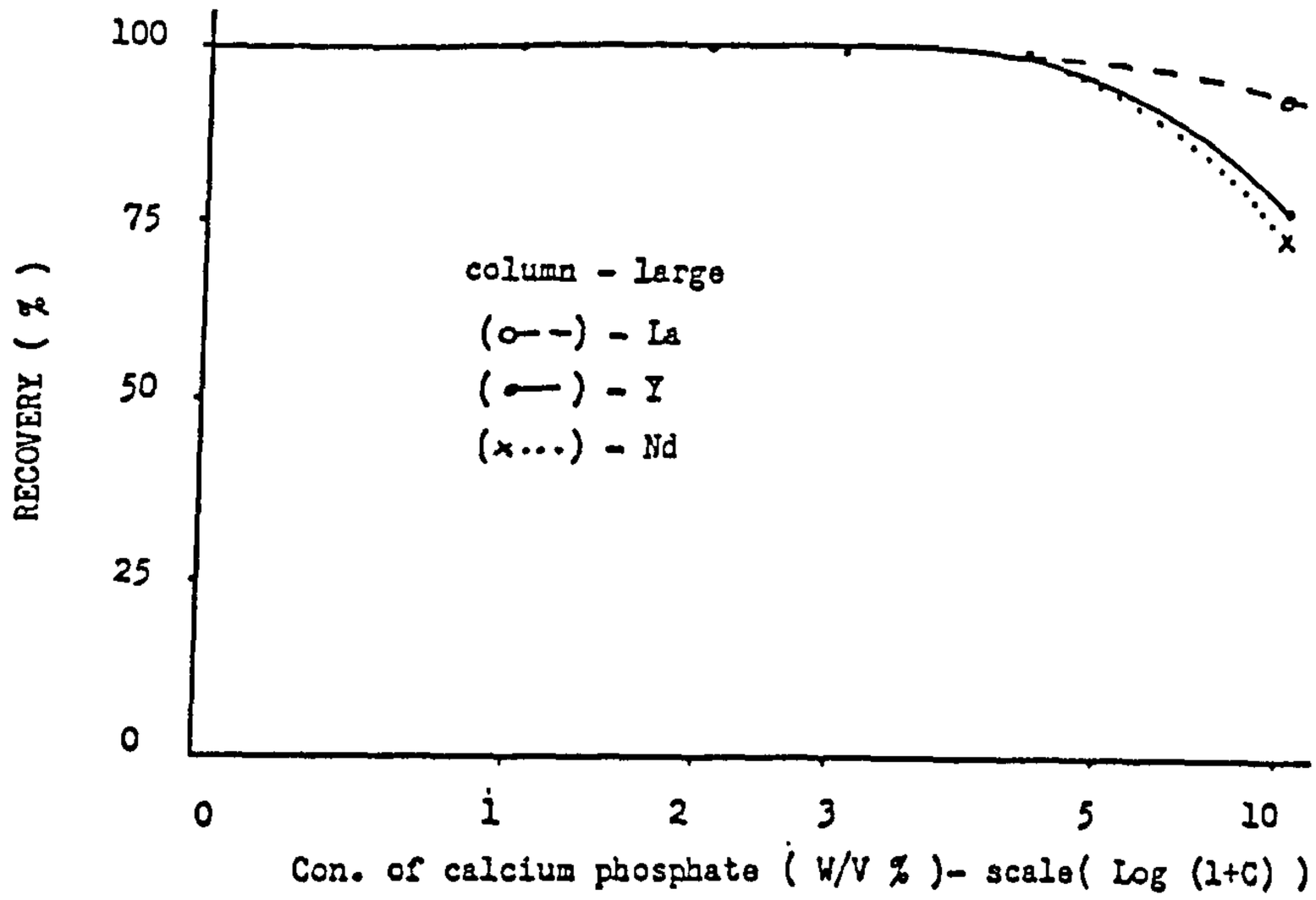

Figure (5.12)

Ineterference of calcium phosphate on the recovery of rare earths

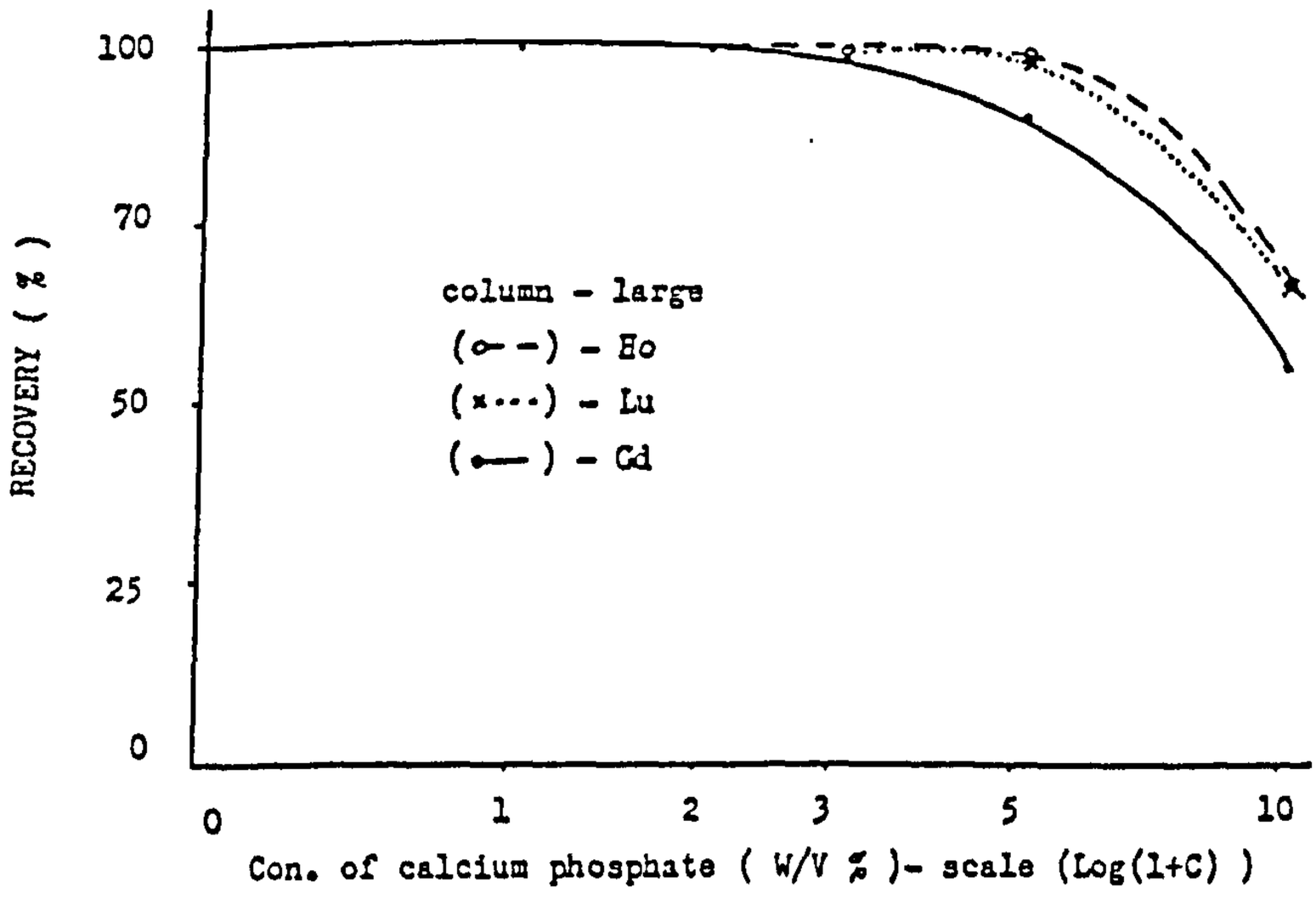

Table 5.8.

Measured recoveries of 2 mg dm^{-3} of each of the rare earths from the large column.

	CONCENTRATION OF CALCIUM PHOSPHATE (w/v) %.				
ANALYTE	1	2	3	5	10
Y	100	100	100	100	77.2
La	100	100	100	100	94.9
Nd	100	100	100	100	74.5
Gd	100	100	98.3	90.1	55.2
Ho	100	100	100	100	67.3
Lu	100	100	100	97.6	67.5

5.3.1 Conclusion.

A better recovery of the rare earths was observed when a large column was used, when even 5% (w/v) of calcium phosphate has no effect. The large column was chosen to be used in all future experiments and to separate the rare earths from 10 g phosphate rock samples, which contain approximately 50% of calcium phosphate. 700 cm^3 of 2M nitric acid was used to wash the column from sample matrix and 1 dm^3 of 6M nitric acid to elute the absorbed rare earths.

5.4 Analysis of an Artificial Phosphate Rock Sample.

An artificial phosphate rock sample, 10 g, containing all the major oxides found in the real samples, was used to justify the procedure recommended for the separation of the rare earths (see section 5.3). The rare earths were added to the sample first before any treatment. After this the sample was treated as a real sample and digested with nitric acid using the procedure developed for the real samples (see section 2.4.2). This artificial sample contained 50% of calcium phosphate, that is 5 g, which has been shown in the previous section (see section 5.3) to be the maximum if full recovery is to be maintained during the ion exchange separation. The artificial sample also contained 4% Fe_2O_3, 2.8% Al_2O_3, 22.9% P_2O_5, 27.1% CaO, 0.3% K_2O, 1%

MgO, 0.5% MnO and 4.4% Na_2O (the remaining 37% in real samples being CO_2, F, SiO_2 and H_2O). These ions were washed off the cation exchange column with 700 cm^3 of 2M nitric acid and the rare earths recovered from the column by elution with 1 dm^3 of 6M nitric acid. Recoveries obtained by this procedure are shown in Table 5.9. These recoveries are satisfactory (i.e. >88%), except for gadolinium which was slightly low (81%).

5.4.1 Conclusion.

The procedure yields high recovery values for the separation of the rare earths from the artificial phosphate rock, and it is recommended for the analysis of real phosphate rock samples.

Table 5.9.

Recovery of rare earths from 10 g of artificial phosphate rock sample.

ANALYTE	INITIAL CONC mg kg^{-1}	ELUTED CONC. mg kg^{-1}	RECOVERY R%
Y	200	186.6	93.2
La	100	100	100
Ce	100	98.5	98.5
Pr	50	49.9	99.9
Nd	60	60.0	100
Sm	10	10.0	100
Eu	2	1.95	97.4
Gd	20	16.2	80.9
Tb	2	1.98	99.0
Dy	20	18.1	90.4
Ho	5	4.99	100
Er	20	17.8	88.7
Tm	2	1.89	94.4
Yb	10	9.13	91.3
Lu	2	2.0	100

Chapter Six

Optimisation of Plasma Parameters and Assessment of Spectral Interference in the Determination of Rare Earth Elements by ICP-AES

In this project rare earths were extracted from the phosphate rock samples by two procedures using firstly anion exchange and secondly cation exchange. Before the analysis of the solutions obtained by either procedure, the ICP instrument parameters (carrier gas flow, auxiliary gas flow, power, plasma gas flow and the measurement height above the coil) need to be optimised. The optimisation gives slightly different results for the two separations and are discussed in section 6.1.1 (for anion exchange) and 6.2.1 (for cation exchange).

The final solution obtained by either method will contain the rare earths only, so that only rare earth spectral interelement interferences had to be carefully studied. This is described in section 6.2.1 for the anion exchange, and in section 6.2.2 for the cation exchange .

During the course of this project the ICP spectrometer was modified for wavelength modulation. The modification made it possible to obtain high resolution spectra over approximately 0.1 nm region around the analyte emission line. Such spectra are very

useful for interpreting spectral interferences and understanding the pattern of interference interaction between the rare earths. This work is described in section 6.2.3.

Finally the two optimisation conditions in the presence and the absence of methanol were compared, and the signal to background ratio for all the rare earth elements analysed with the two conditions shown to be similar (see section 6.3).

6.1 Anion Exchange.

6.1.1 Optimisation of ICP.

The object of this project is to separate all the rare earth elements from calcium phosphate, the major component of the phosphate rock and other minor matrix components. Anion exchange was one of the two procedures used. After the separation the main interferences will be the spectral interference between the rare earth elements. It is essential to optimise the ICP instrument parameters, carrier gas flow rate, auxiliary gas flow rate, applied power, plasma gas flow rate and the height of measurement above the coil. The elements measured were the fourteen rare earth elements together with yttrium and thorium. It was expected that the instrument conditions would differ from one element to another, and that compromise conditions would have to

be used either for simultaneous multi-element analysis or to simplify the operational procedure for sequential determination of the elements. Hence the optimisation of parameters for five representative elements were studied, cerium, samarium, holmium, lutetium and thorium. These gave such similar results that a full study was thought unnecessary.

An Echelle monochromator, as described in section 2.13.2, was attached to the plasma unit. The signal from the photomultiplier tube (PMT) in the monochromator was processed by a lock-in amplifier and displayed using a chart recorder. The height of the emission signal on the chart recorder (in mm) was used to estimate the intensity of the signal. Each one of the above elements was optimised separately because the monochromator had only a single channel. It was intended to analyse directly the solution containing the rare earths eluted from the small ion exchange column see section 4.2). The solution contained methanol (about 5% v/v) and so methanol was added in similar concentration to the solutions used in optimisations .

The optimisation was carried out by varying one parameter and fixing the other parameters. The optimum value of the parameter was chosen as that which give the highest signal to background ratio ((S-B)/B, where S is the total signal and B is the background signal

intensity). The parameters were each optimised consecutively, the carrier gas flow rate first and the height of measurement last in the order given in Table 6.1. Whilst optimising the carrier gas flow rate the other parameters were kept at the initial setting. When the optimum carrier gas flow rate had been found, this optimum value was used during the optimisation of the auxiliary gas flow rate, but the other parameters were still kept at their initial settings. In this way the final parameter, height of measurement was optimised at the optimum values of all the other parameters. It is fully realised that this procedure assumes that there is no interaction between the parameters - an assumption known to be false, in particular the gas flow rates all affect the power used. However, it is believed that this interaction has only a small effect when the initial setting are already close to the maximum as is the case here, see Table 6.1.

The Carrier gas flow rate was varied from 0.5 to 0.75 dm^3 min^{-1}. Below 0.5 dm^3 min^{-1} the plasma was unstable and collapsed due to the presence of methanol. With the nebuliser used in this work (see section 2.13.1) a maximum flow rate of 0.75 dm^3 min^{-1} was reached with the control valve wide open .The results for all elements studied showed a similar effect and holmium has been used to illustrate the influence of varying the carrier gas flow rate on the

Table 6.1.

Optimisation of ICP parameters for analysis of anion exchange eluate.

Parameters	Range of variation	Conditions Initial	Optimum
Carrier gas			
Flow rate $dm^3\ min^{-1}$	0.5 - 0.75	-	0.75
Auxiliary gas			
Flow rate $dm^3\ min^{-1}$	0.0 - 1.125	0.9	1.125
Anode Current (mA)	400 - 500	400	400
Plasma gas			
Flow rate $dm^3\ min^{-1}$	15.25 - 18.5	16.0	15.25
Measurement height above the coil (mm)	4 - 12	6	9

analyte signal intensity (Figure 6.1). The height of both the signal and the background dropped with an increase in the flow rate, but the drop in the background was greater than that of the signal so that the ratio was best at high flow rates. At the same time the anode current increased from 400 to 430 mA. This increase in the current implied an increase in the applied power in the presence of methanol. The signal to background ratio for all the elements, see Figure 6.2, were at the maximum value at the highest obtainable flow rate (0.75 dm^3 min^{-1}) even though the measured signal was lower. This is because of the even lower background intensities.

The auxiliary gas flow rate was optimised by varying the flow rate from 0.0 to 1.125 dm^3 min^{-1}. Above 1.125 dm^3 min^{-1}, the plasma was not stable and optimisation above this flow rate was abandoned. The results for holmium, Figure 6.3, show that the signal and the background were almost constant as the auxiliary gas was increased from 0.0 to 0.4 dm^3 min^{-1}. Then as the flow rate was further increased both the signal and the background decreased. The effect of the power applied to the plasma followed a similar pattern, the analyte intensity varying little initially, but decreasing more rapidly at high flow rates. The drop in the anode current below 400 mA accompanied by an increase in the auxiliary gas flow

Figure (6.1)

The effect of changing carrier gas flow rate on the intensity of holmium solution (o—) , background (•--) and anode current (x····) .

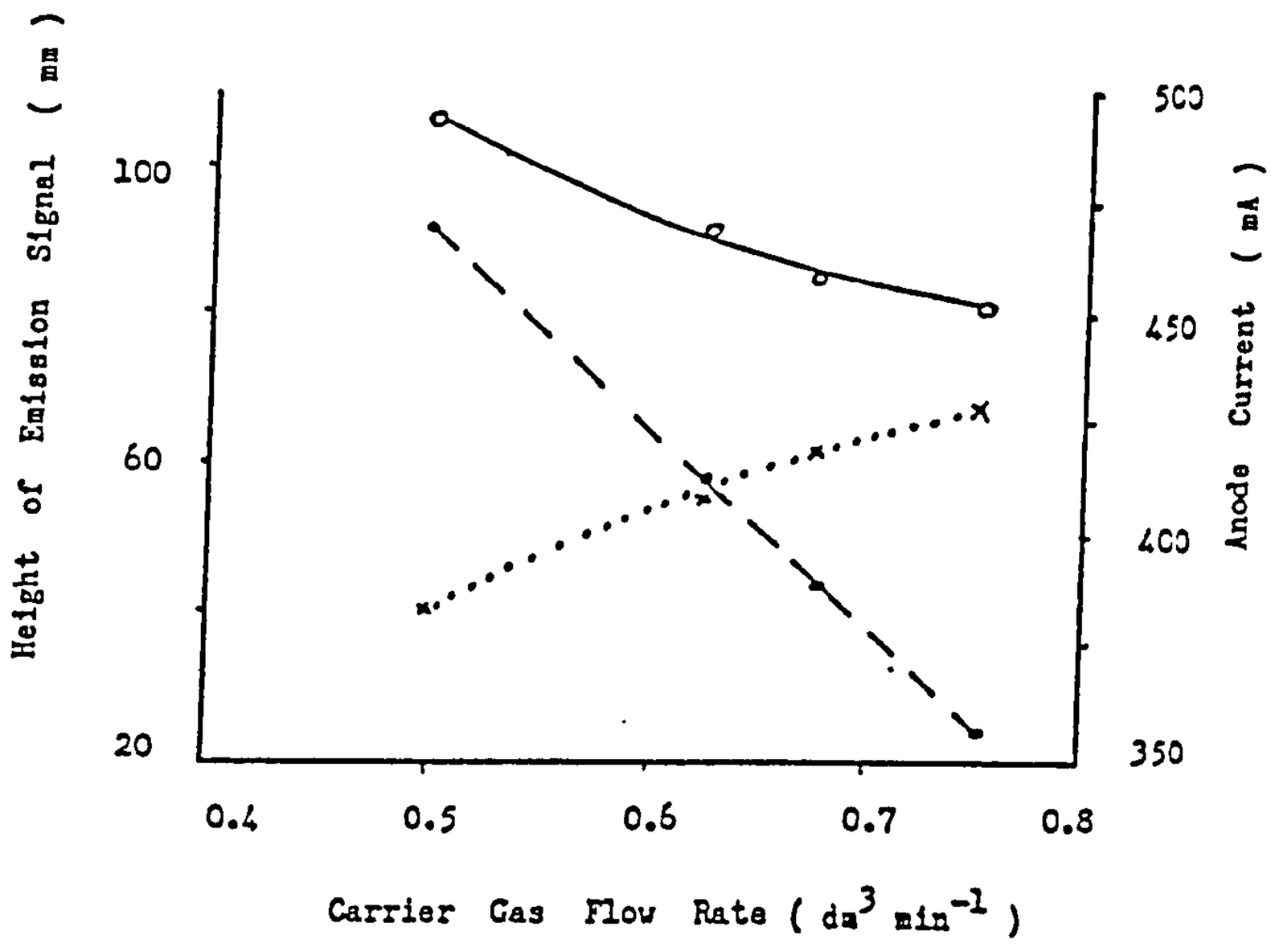

Figure (6.2)

The effect of changing carrier gas flow rate on signal to backgrond ratio of the elements :- Lu (□--) , Ho (•—) , Sm (x···) , Ce (o- —) and Th (Δ-··) .

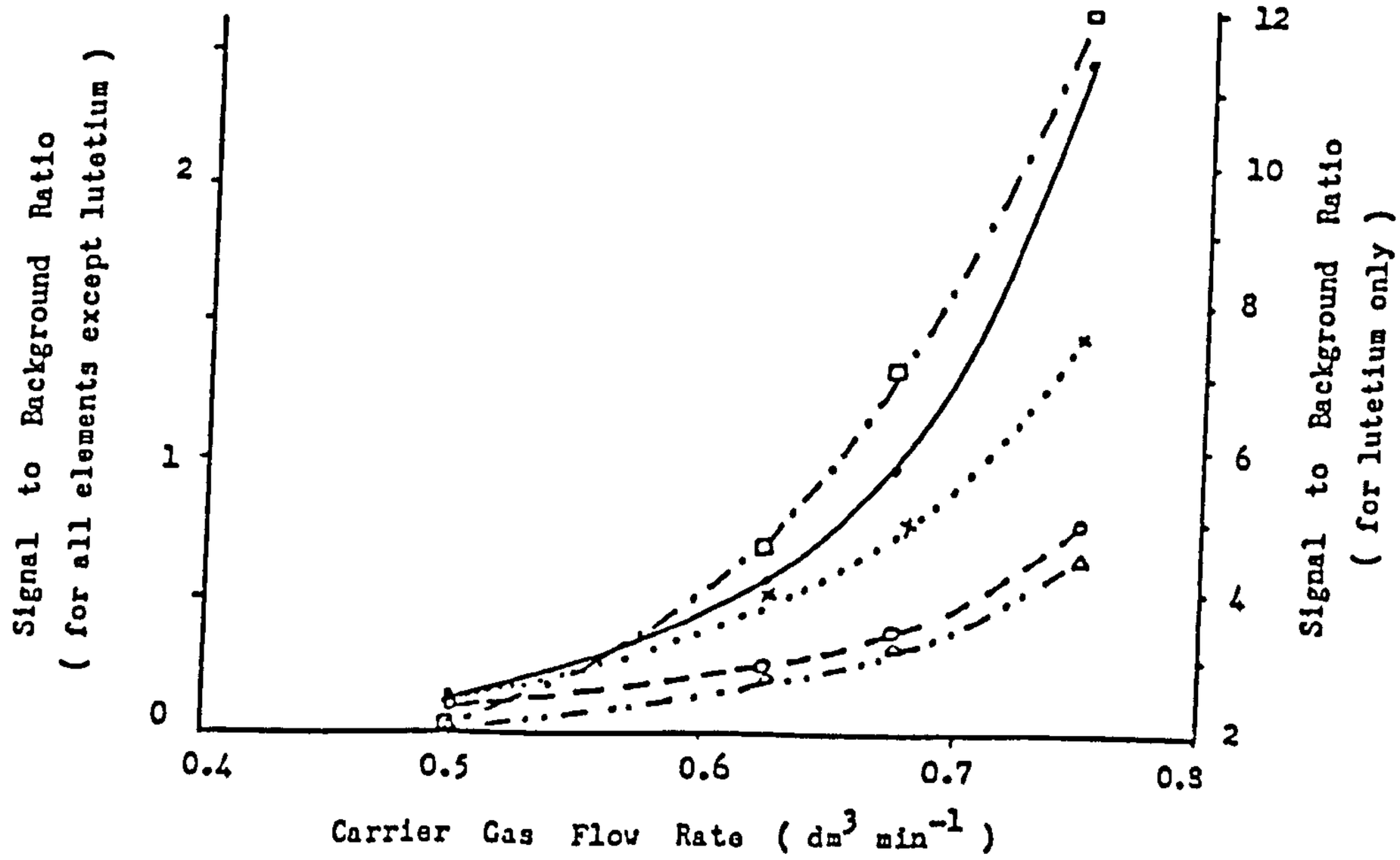

rate cause instability of the plasma and at a higher flow rate extinguish the plasma. The change in the signal to background ratio values with the increase in the auxiliary gas flow rate is shown in Figure 6.4 for all the test elements. The maximum value was obtained when the flow rate was at its maximum stable value -1.125 dm^3 min^{-1}, just prior extinction.

The power of the plasma was adjusted from 0.95 to 1.5 kW, the optimisation was carried out by increasing the anode current from 400 to 500 mA, it was not possible to go below 0.95 kW because the plasma became unstable and collapsed due to the presence of methanol in the aspirated solution. All the test elements studied showed a similar response to the changes in the power, and the results for holmium are given in Figure 6.5. The graph shows an increase in the signal and the background with an increase in the power. However, the signal to background ratio for all the test elements decreased as the power was increased, see Figure 6.6, and the maximum ratio values were obtained when the power was at the minimum value 0.95 kW (400 mA).

The plasma gas flow rate was optimised by varying the flow rate from 15.25 to 18.5 dm^3 min^{-1}. All the test elements exhibited similar effects with the signal and background ratio values showing a slight

Figure (6.3)

The effect of changing auxilary gas flow rate on the intensity of holmium solution (o—) , background (•– –) and anode current (×···) .

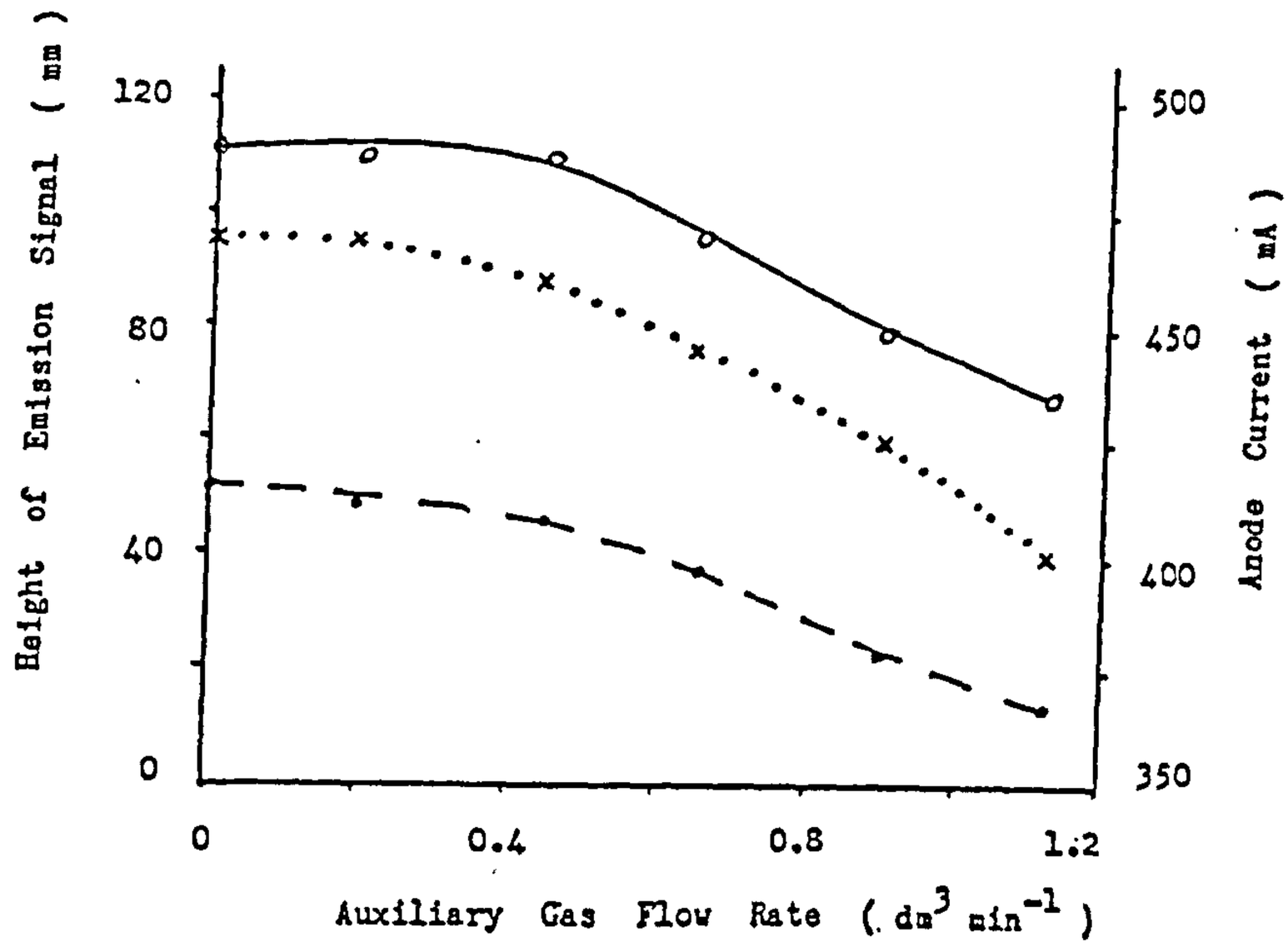

Figure (6.4)

The effect of changing auxilary gas flow rate on the signal to background ratio for the elements :- Lu (□–·) , Ho (•—) , Sm (×···) , Ce (o– –) and Th (△–··) .

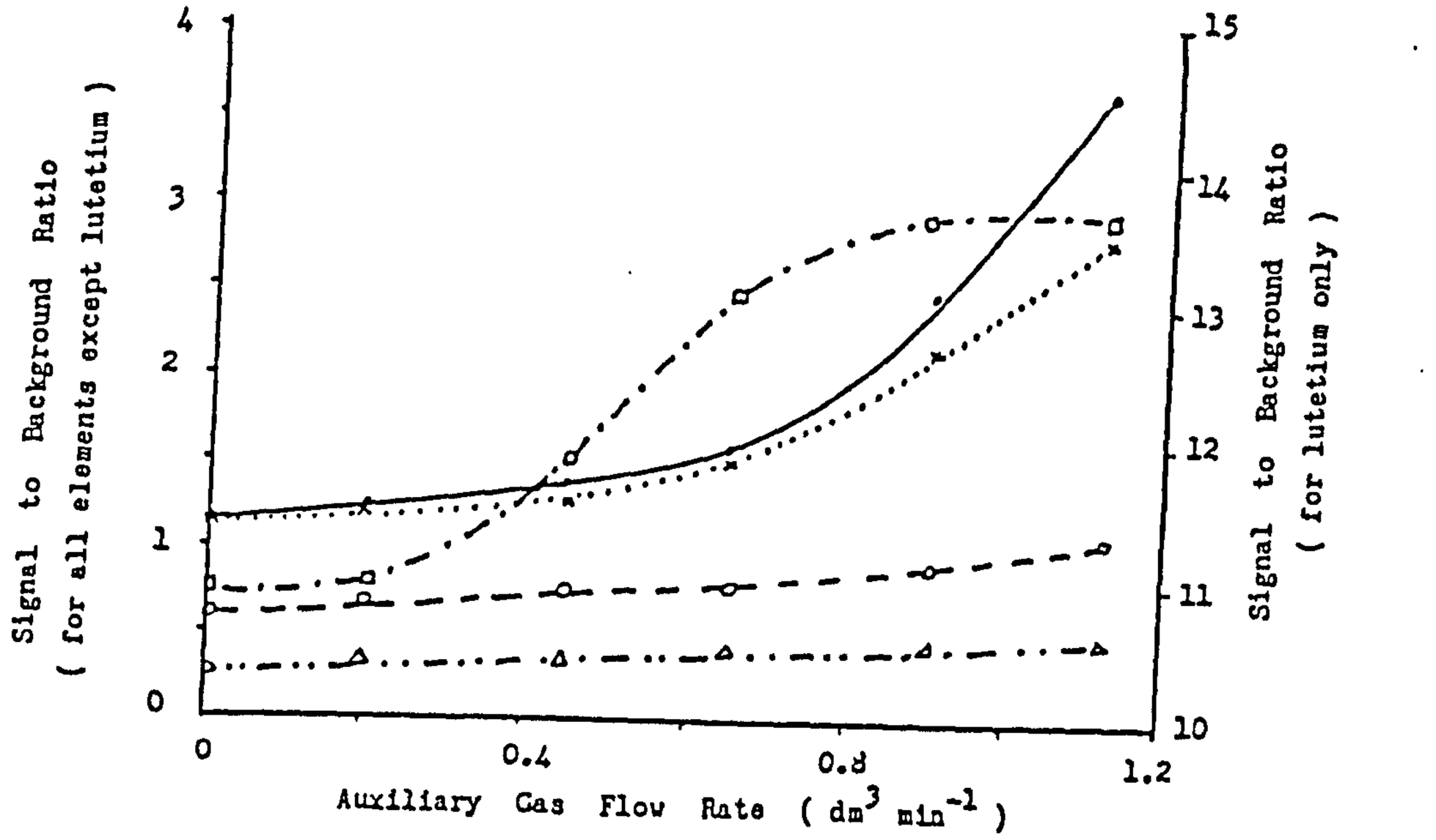

Figure (6.5)

The effect of changing anode current on the intensity of holmium solution (o—) and background (•- -) .

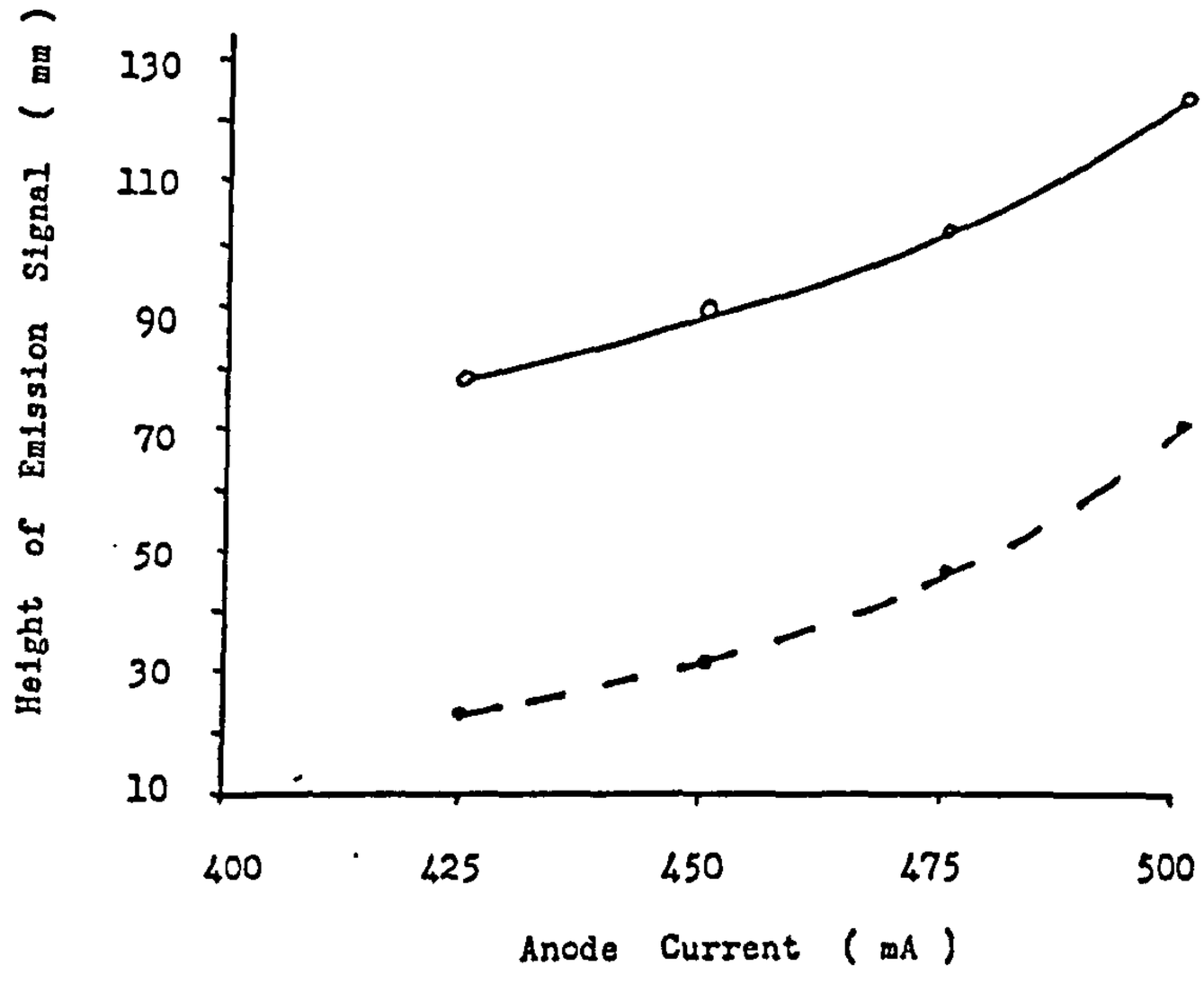

Figure (6.6)

The effect of changing anode current on the signal to background ratio for the elements :- Lu (□—·) , Ho (•—) , Sm (×···) , Ce (○- -) and Th (△—··) .

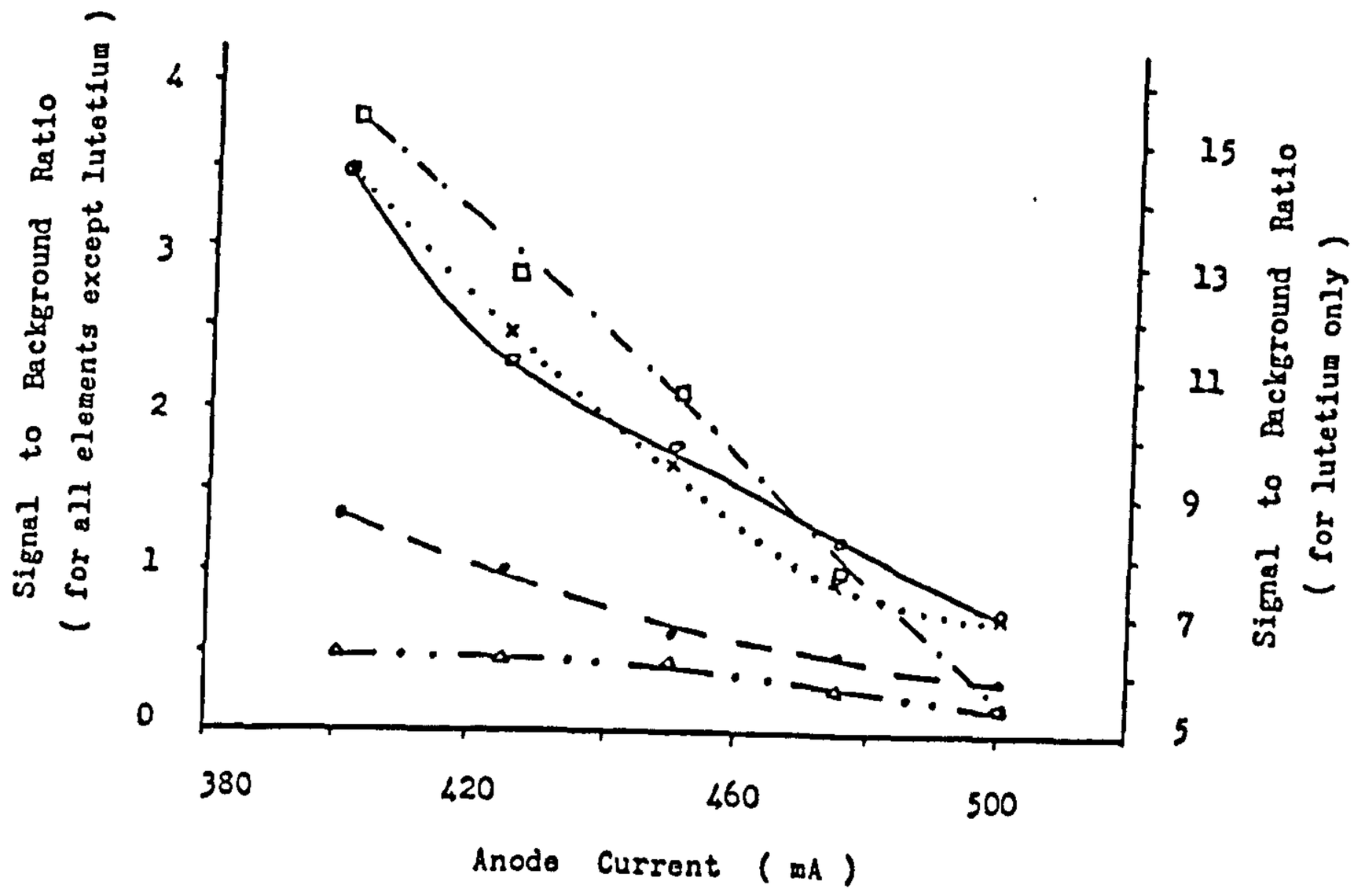

increase with increase in the plasma gas flow rate, and the results for holmium are given in Figure 6.7. The anode current was also observed to increase, from 400 to 450 mA, at the same time as the plasma gas flow rate was increased. Again the signal to background ratio was at the highest value when the plasma gas flow rate was at the minimum value applied, which was 15.25 dm^3 min^{-1} and the ratio decreased as the flow rate increased, as can be seen in Figure 6.8.

Finally, the height at which emission measurements were made by varying the height of the lens which was placed between the torch and the entrance slit of the monochromator. The true height was calculated using the equation suggested by Dr. D. Hall (48) and used in the optimisation. The true height was changed from 4 to 12mm above the coil. The results for all test elements showed a similar change in the signal and the background intensities as the measurement height was increased, (Figure 6.9, for holmium). For all test elements studied the highest signal to background ratio was obtained close to, but slightly higher than the position in the plasma where the highest ionic population was found. This point was slightly different from element to element, as can be seen in Figure 6.10. A compromise value of 9 mm was chosen for analytical use to simplify the selection of operating parameters.

Figure (6.7)

Optimisation of plasma gas flow rate using methanolic solution of holmium , signal (o—) , background (•–-) and anode current (×··) .

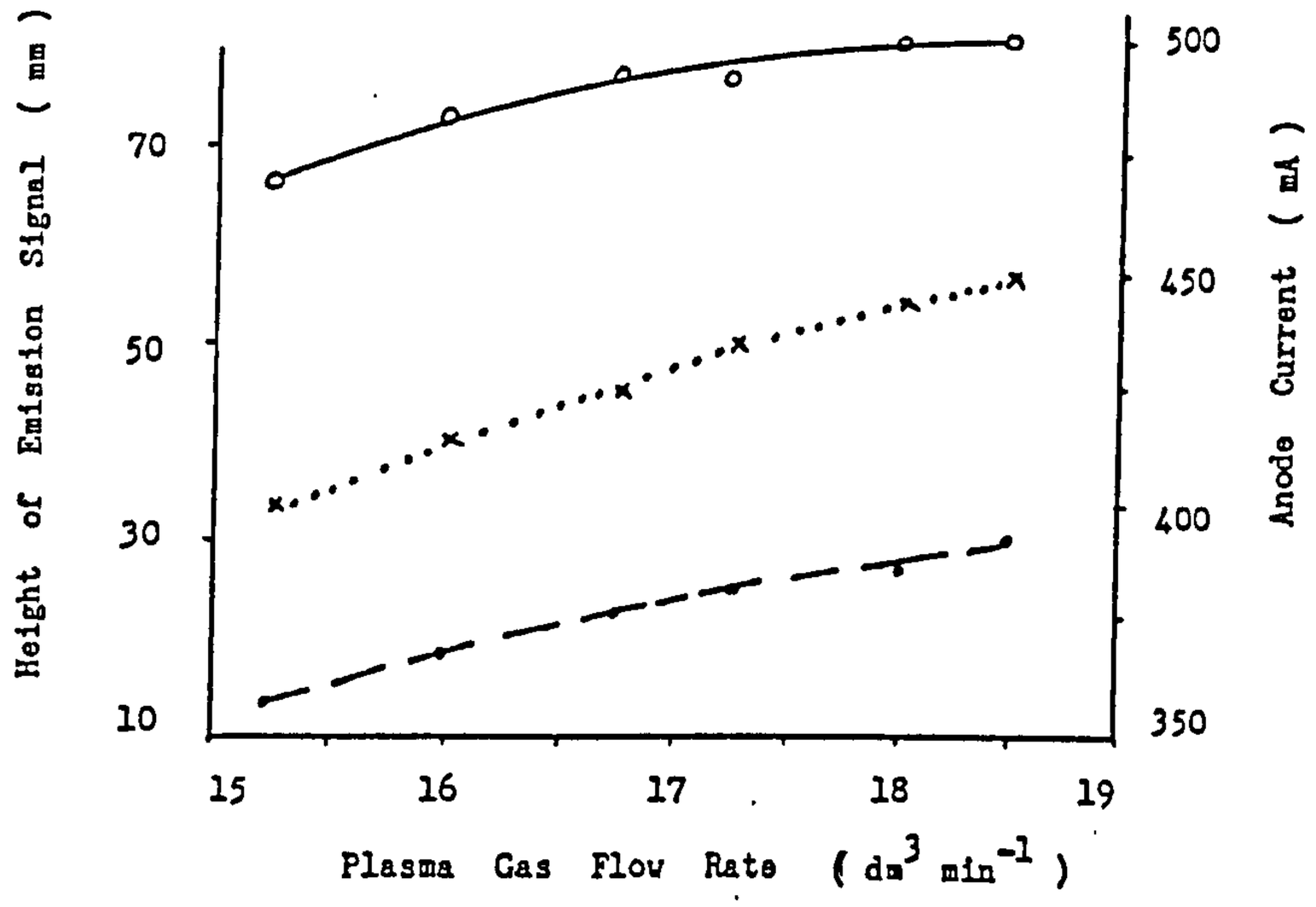

Figure (6.8)

The effect of changing plasma gas flow rate on the signal to background ratio for the elements :- Lu (□–·) , Ho (•—) , Sm (×··) , Ce (o– -) and Th (△–··) in methanolic solution .

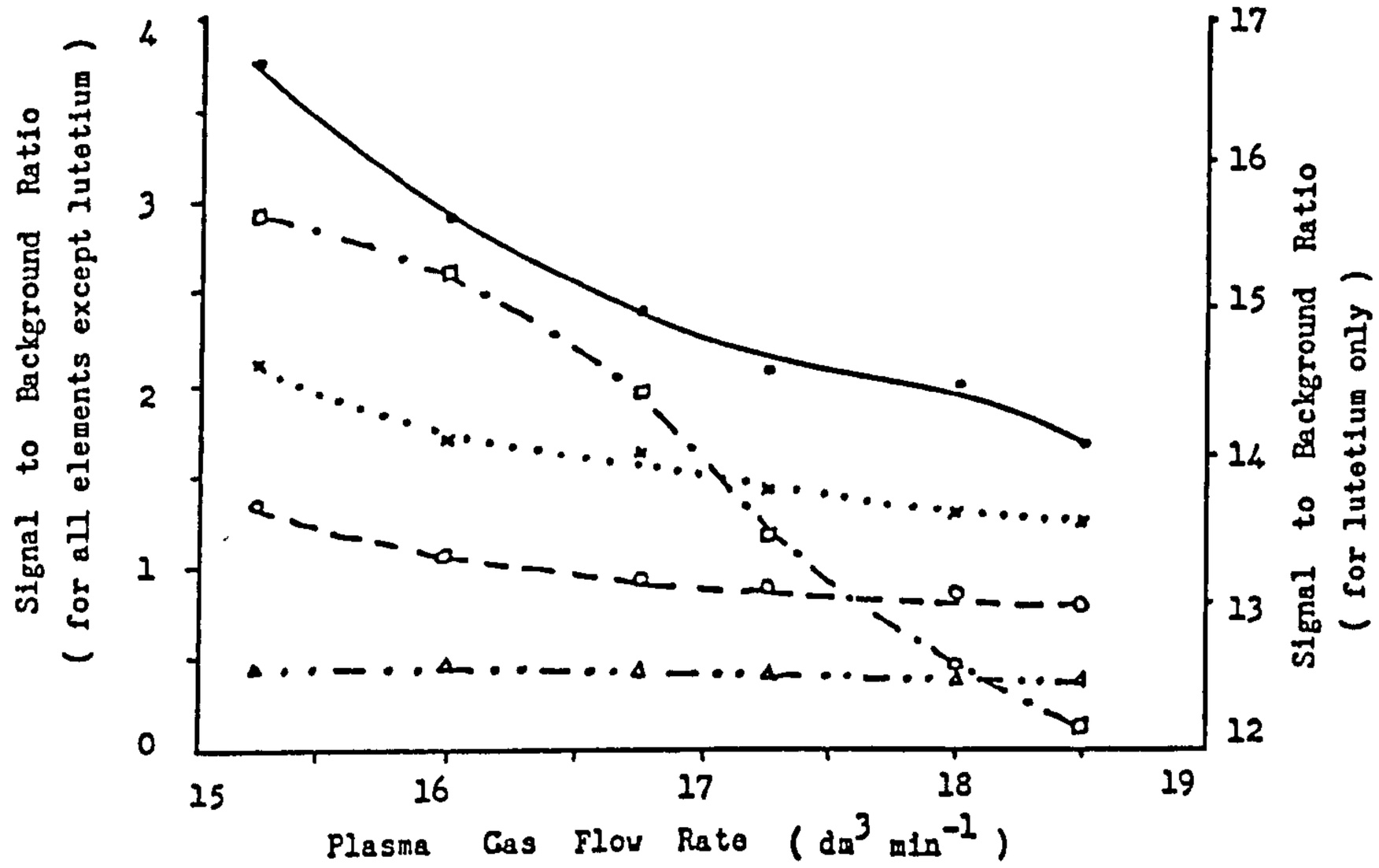

Figure (6.9)

Optimisation of the measurement height above the coil using a methanolic solution of holmium - signal (o—) , background (•--) .

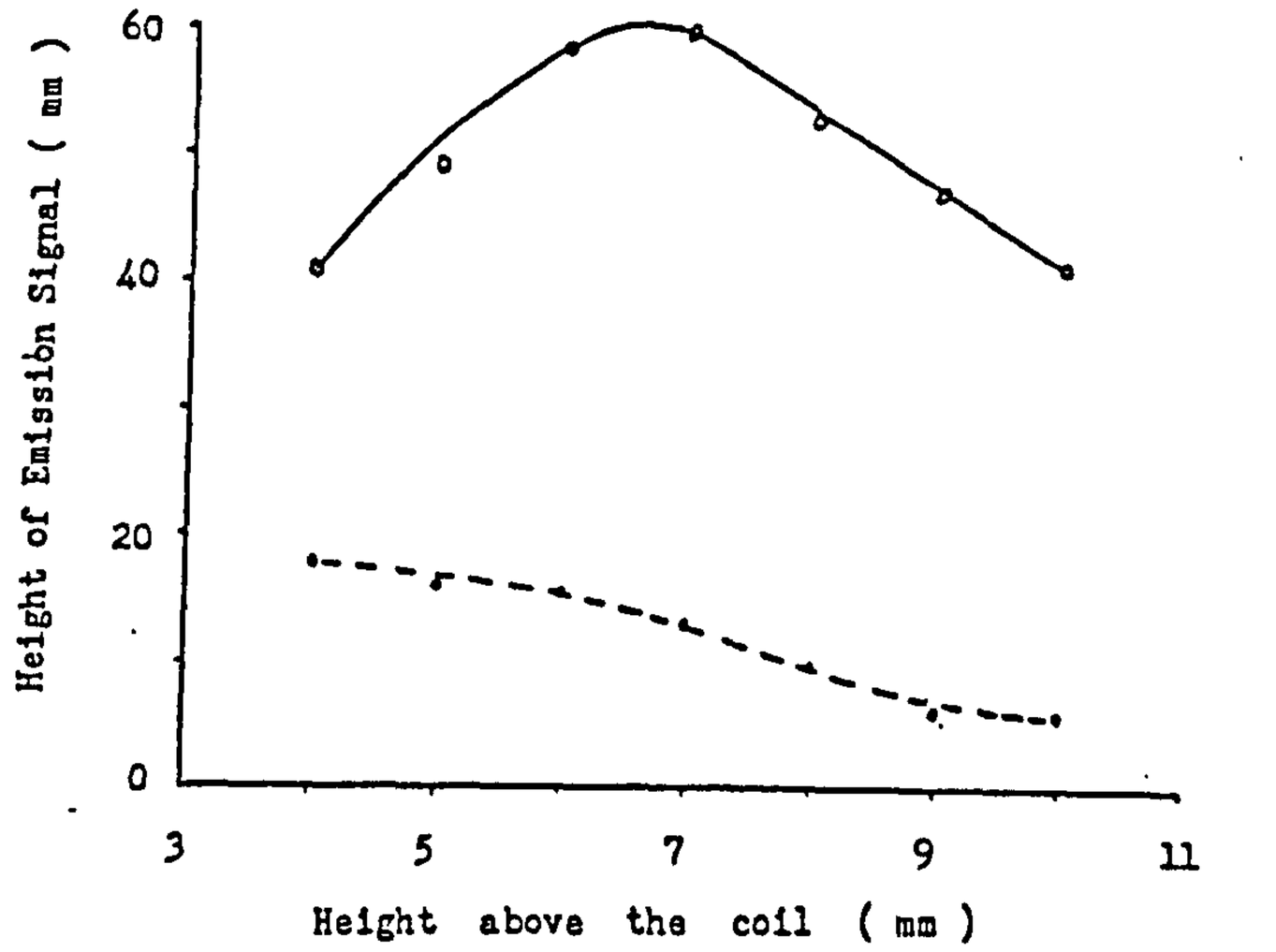

Figure (6.10)

The effect of changing the measurement height on the signal to background ratio for the elements :- Lu (□—·) , Ho (•—) , Sm (×··) , Ce (o--) and Th (△—··) in methanolic solution .

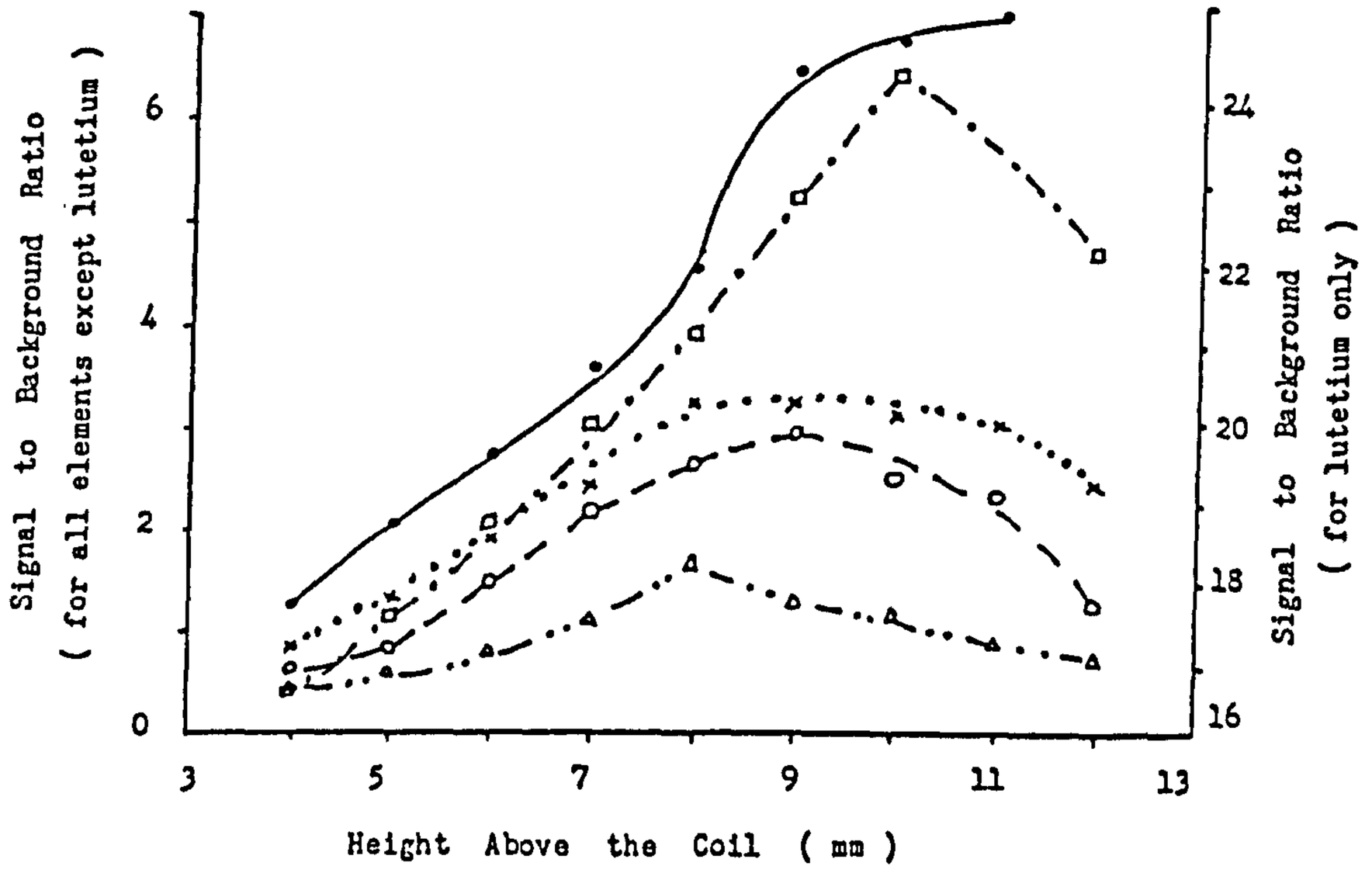

6.1.1.1 Conclusion.

The setting at which the highest signals were obtained was not used, instead the position was chosen which gave the highest signal to background ratio. Altering the flow rate of the different plasma gases changes the anode current, when it falls bellow 400 mA, the plasma collapses due to the presence of methanol in the sample solution, the optimum conditions for the plasma for all the studied elements are similar to each other, and the conditions for any element will be usable. The compromise conditions chosen for analysis of the effluents from the anion exchange separation are shown in Table 6.1.

6.1.2 Rare Earth Elements Spectral Interferences.

The use of an anion exchange procedure (see section 4.2) separates the rare earth elements from other elements found in the phosphate rock matrix. One of the advantages of the ICP is the reduced occurrence of chemical interferences, but spectral interferences need to be investigated.

After the optimisation experiments were completed, the ICP spectrometer was modified (48). The PMT output current was passed via an ADC to an APPLE IIe computer for data processing, in place of the lock-in amplifier previously used. Details are given in section 2.13.3. The signal at each element wavelength was

measured for 5 seconds and the average count rate was displayed. The measurement for each solution was repeated five times, and the average of all the measurements for each solution was used to calculate the signal.

A known concentration of the analyte was aspirated into the plasma and the signal is measured at the wavelength of the most sensitive line, see Table 2.6. Then a solution containing a high concentration of one interfering element (i.e 10 mg dm^{-3}) was aspirated into the plasma. The concentration of the analyte which gives a signal equal to the signal obtained from the interferrant was calculated and this was called the "equivalent concentration" of the interferent.

The results of this study for the 256 possible combinations of interferant and analyte are shown in Table 6.2. The worst interferences were shown by cerium on praseodymium and neodymium and by neodymium and gadolinium on samarium. The calculated equivalent concentration shown should be compared with the detection limits shown in Table 7.15.

6.1.3 Correction for Interferences.

The solution eluted from the anion exchange treatment of a phosphate rock sample solution, will contain all the rare earths, so multi-element correction is required

TABLE 6.2

EQUIVELANT CONCENTRATION (mg dm^{-3}) CORRESPONDS TO THE INTRODUCTION OF 10 mg dm^{-3} OF THE INTERFERRENT ELEMENT AT ANALYTE WAVELENGTH - NO BACKGROUND CORRECTION.

ANALYTE	Y	La	Ce	Pr	Nd	Sm	Eu	Gd	Tb	Dy	Ho	Er	Tm	Yb	Lu	Th
INTERFERENT																
Y	*	*	*	*	*	*	*	*	*	*	*	*	*	*	*	*
La	*	*	*	*	*	*	*	*	*	*	*	*	*	*	*	*
Ce	*	0.03	*	1.22	0.91	*	*	0.09	*	*	*	*	*	*	*	*
Pr	*	0.08	0.08	*	0.1	*	*	*	*	*	0.02	*	*	*	*	*
Nd	*	0.02	*	0.01	*	0.44	0.07	*	*	0.04	0.02	0.01	*	*	*	0.41
Sm	*	*	*	*	*	*	*	*	0.12	*	*	*	0.01	*	*	*
Eu	*	*	*	*	*	*	*	*	*	*	*	*	*	*	*	*
Gd	*	*	0.02	*	*	0.39	*	*	*	*	*	*	*	*	*	*
Tb	*	*	*	*	*	*	*	0.05	*	0.05	0.03	0.18	0.02	*	*	0.05
Dy	0.01	*	*	*	*	*	*	0.05	*	*	*	*	*	0.01	*	0.04
Ho	*	*	*	*	*	*	*	0.04	0.12	*	*	*	*	*	*	*
Er	0.01	*	*	0.16	*	*	*	*	*	*	0.01	*	0.02	*	*	0.07
Tm	*	*	*	*	*	*	*	*	*	*	*	*	*	0.01	*	
Yb	0.01	*	*	*	*	*	*	*	*	*	*	*	*	*	*	
Lu	*	*	*	*	*	*	*	*	*	*	*	*	*	*	*	
Th	*	*	*	*	*	*	*	*	*	*	*	*	*	*	*	

N.B.:- * MEANS THAT THERE IS NO INTERFERENCE OR THE INTERFERENCE IS TOO SMALL (0.01 mg dm^{-3}), AND MAY BE TAKEN AS HAVING ZERO EQUIVELANT CONCENTRATION.

for the spectral overlap interferences amongst the elements.

For the analyte

A = a subscript to identify the analyte

λ_A = analyte wavelength

S_A = analyte signal (counts sec^{-1})

For the interferent element

F = a subscript to identify the interferent

λ_F = interferent wavelength

S_F = interferent signal (counts sec^{-1})

We shall have two values for both S_A and S_F at λ_A and λ_F respectively.

S_{AA} = signal for analyte at λ_A

S_{AF} = signal for analyte at λ_F

S_{FA} = signal for interferent at λ_A

S_{FF} = signal for interferent at λ_F

The concentrations equivalent to these signals are

C_{AA} = concentration of analyte used at λ_A

C_{AF} = concentration of analyte used at λ_F

C_{FA} = concentration of interferent used at λ_A

C_{FF} = concentration of interferent used at λ_F

In general

$$S_{XY} = C_{XY} * K_{XY}$$

where K_{XY} = the slope of calibration graph for element X at wavelength of element Y.

So

$$S_{AA} = C_{AA} * K_{AA}$$
$$S_{AF} = C_{AF} * K_{AF}$$
$$S_{FA} = C_{FA} * K_{FA}$$
$$S_{FF} = C_{FF} * K_{FF}$$

So

$$K_{AA} = \frac{S_{AA}}{C_{AA}}$$

$$K_{AF} = \frac{S_{AF}}{C_{AF}}$$

$$K_{FA} = \frac{S_{FA}}{C_{FA}}$$

$$K_{FF} = \frac{S_{FF}}{C_{FF}}$$

However, we DO NOT know the concentration of the interferent in the eluted solution, so we must use the signal obtained at the interferent wavelength instead (S_{TF}).

In the samples, let

C_A = concentration of analyte in sample

C_F = concentration of interferent in sample

S_{TA} = total intensity at analyte wavelength λ_A

S_{TF} = total intensity at interferent wavelength λ_F

$$S_{TA} = K_{AA} * C_A + \sum K_{FA} * C_F$$

$$S_{TF} = K_{FF} * C_F + \sum K_{AF} * C_A$$

or

$$C_F = \frac{\left(S_{TF} - \sum K_{AF} * C_A \right)}{K_{FF}}$$

giving

$$S_{TA} = K_{AA} * C_A + \sum \frac{K_{FA}}{K_{FF}} \left(S_{TF} - \sum K_{AF} * C_A \right) \qquad (6.1)$$

However, K_{AF} is usually very small and can be assumed zero for the present case, hence

$$S_{TA} = K_{AA} * C_A + \sum \frac{K_{FA}}{K_{FF}} S_{TF}$$

or

$$S_{TA} = K_{AA} * C_A + \sum H_{FA} * S_{TF} \qquad (6.2)$$

Where

$$H_{FA} = \frac{K_{FA}}{K_{FF}} = \frac{S_{FA} * C_{FF}}{S_{FF} * C_{FA}}$$

A computer programme was written to correct all the interferences on the analyte using equation (6.2). The full programme is shown in appendix (1). This program does not assume that K_{AF} is zero. Every analyte signal (S_{TA}) is corrected for every other analyte signal (S_{TF}) and these corrected values are reused to calculate a new series of corrected signals (S_{TA}) for use in equation 6.2. This process is repeated until no further change in the corrected

signals occur.

In this way all the signals used in equation 6.2 have been completely corrected for the other analytes present by means of an equation similar to 6.1 - but generalised, to include corrections to the corrections (viz the $K_{AF} * C_A$ terms). Hence the final concentrations (C_A) should be completely corrected for spectral interference.

6.2 Cation Exchange.

6.2.1 Optimisation of ICP Operating Parameters

A new optimisation regime was needed for the analysis of the effluent from the cation exchange separation because these effluents did not contain methanol. The results of the previous section have shown that all the rare earths gave similar optimisation patterns and that optimisation for any one of them was sufficient to define the optimum parameters for all the analyte elements. Lanthanum was chosen for this purpose. In these experiments full wavelength modulation background correction was used by measuring the emission intensity at both sides of the analytical wavelength as well as at the analytical wavelength (48). A rotating quartz plate was placed behind the entrance slit, in the spectral path to the grating. The

refracting plate could be rotated slowly by means of a scanner controller and hence it was possible to scan a small wavelength region (see section 2.13.3).

The optimisation was carried out in a manner similar to that described in section 6.1.1, except for the use of a single element (lanthanum). The initial and final conditions are shown in Table 6.3 (compare with Table 6.1 for the anion exchange separation).

The carrier gas flow rate was varied from 0.05 to 0.75 dm^3 min^{-1}. As the flow rate increased both the intensity of the signal and the average intensity of the background increased to a maximum then, both decreased with a further increase in the flow rate, however, the rate of decrease was greater for the background, as can be seen in Figure 6.11. The anode current of the plasma changed very little with the increase in the flow rate. This is due to the absence of methanol and these results should be compared to those shown in Figure 6.1, which illustrate the observation of a similar investigation when methanol was present in the analyte solution. The best signal to background ratio was achieved when the flow rate was at the highest value (0.75 dm^3 min^{-1} - control valve wide open), as shown in Figure 6.12 .

The carrier gas flow rate was now set to the

Table 6.3.

Optimisation of ICP parameters for analysis of cation exchange eluate.

Parameters	Range of variation	Conditions Initial	Optimum
Carrier gas			
Flow rate $dm^3\ min^{-1}$	0.5 - 0.75	-	0.75
Auxiliary gas			
Flow rate $dm^3\ min^{-1}$	0.5 - 2.4	0.813	2.4
Anode Current (mA)	340 - 500	400	360
Plasma gas			
Flow rate $dm^3\ min^{-1}$	10.5 - 18.75	14.797	14.75
Measurement height above the coil (mm)	3 - 28	20	20

Figure (6.11)

Optimisation of carrier gas flow rate using an aqueous solution of lanthanum- signal (o—) , background (•--) and anode current (×···).

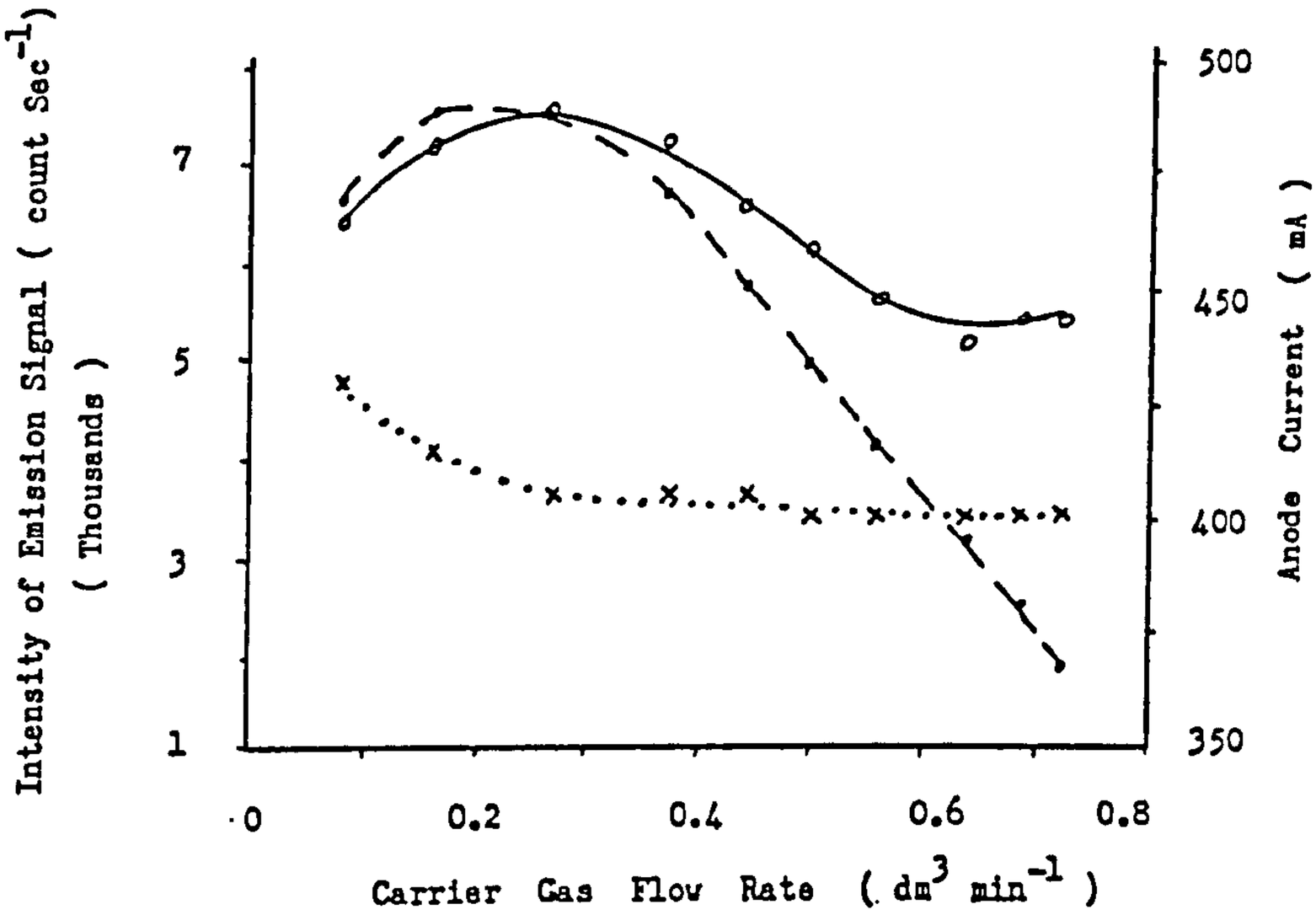

Figure (6.12)

The effect of changing carrier gas flow rate on the signal to background ratio of an aqueous solution of lanthanum .

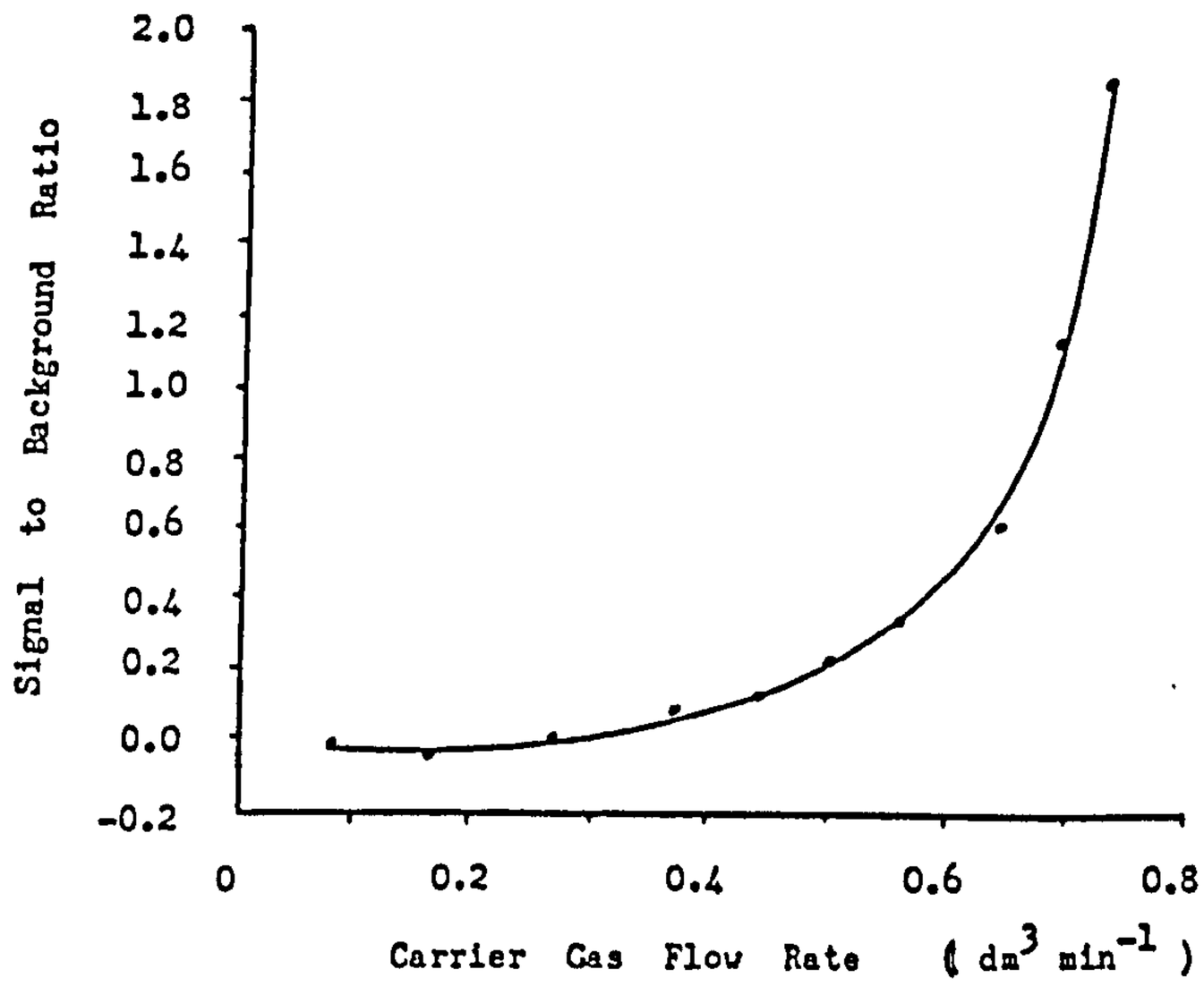

optimum (0.75 dm^3 min^{-1}) and the auxiliary gas flow rate optimised. This was varied from 0.5 to 2.4 dm^3 min^{-1}. At flow rate over 2.4 dm^3 min^{-1}, the plasma was unstable and no measurements were made. As the flow rate increased both the signal and the background were reduced, as can be seen in Figure 6.13. The anode current of the plasma dropped from 410 to 365 mA, as the flow rate was changed from 0.5 to 2.4 dm^3 min^{-1}. The signal to background ratio increased with increasing flow rate, as can be seen in Figure 6.14, and the optimum flow rate was also the maximum (i.e. 2.4 dm^3 min^{-1}).

Next, the power of the plasma was varied from 0.675 to 1.5 kW, by changing the anode current from 340 to 500 mA. This change varied the size of the plasma from very small to very large. Both the signal and the background increased with an increase in power but at a different rate, as shown in Figure 6.15. The signal to background ratio reached its maximum value when the power was 0.78 kW (360 mA). As the power increased further the ratio decreased, as can be seen in Figure 6.16.

Then the plasma gas flow rate was optimised by varying the flow rate from 10.5 to 18.75 dm^3 min^{-1}, beyond these limits the plasma became unstable. As the flow rate increased the signal and the background

Figure (6.13)

Optimisation of auxilary gas flow rate using an aqueous solution of lanthanum - signal (o—) , background (•--) and anode current (x···) .

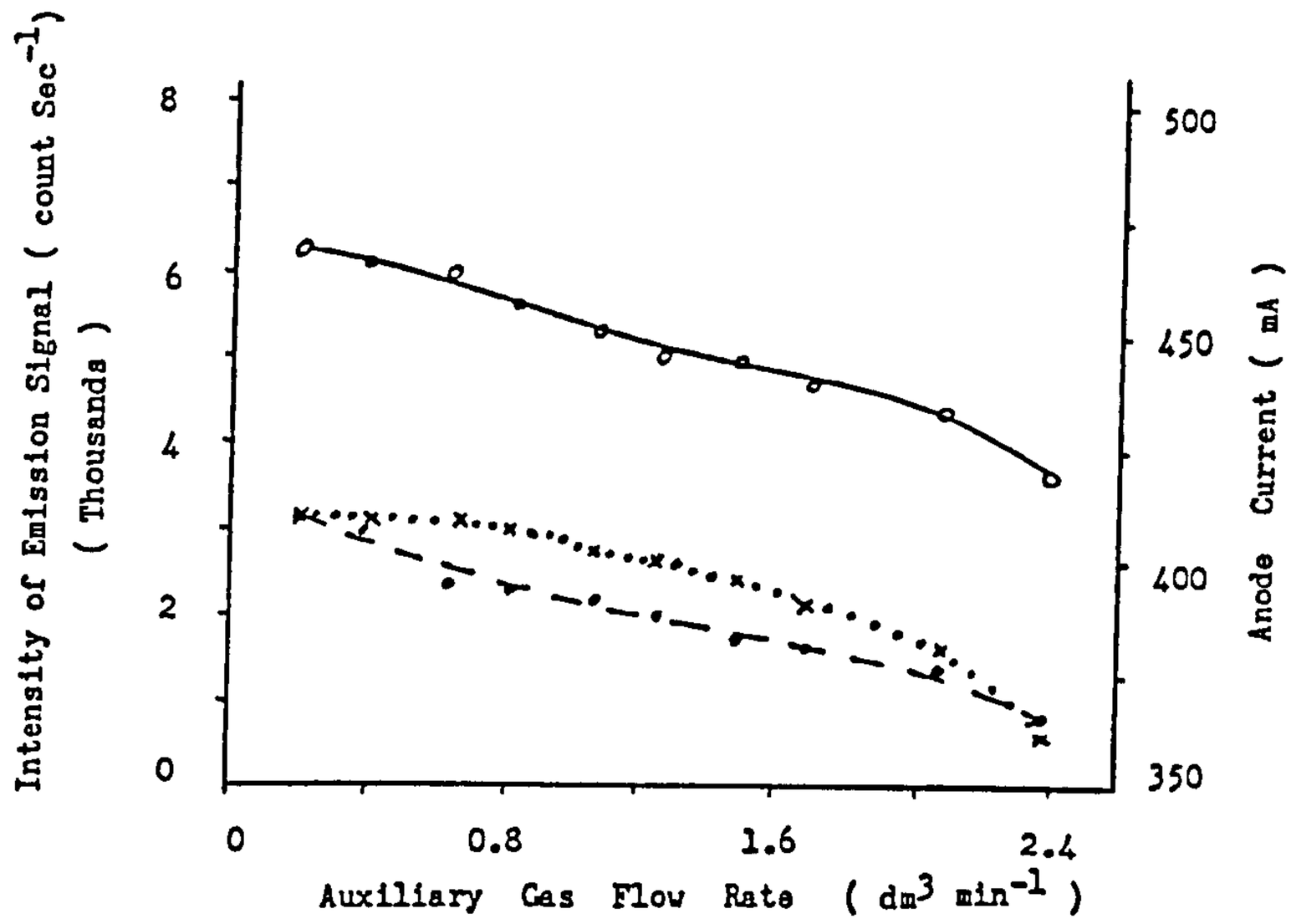

Figure (6.14)

The effect of changing auxilary gas flow rate on the signal to background ratio of an aqueous solution of lanthanum .

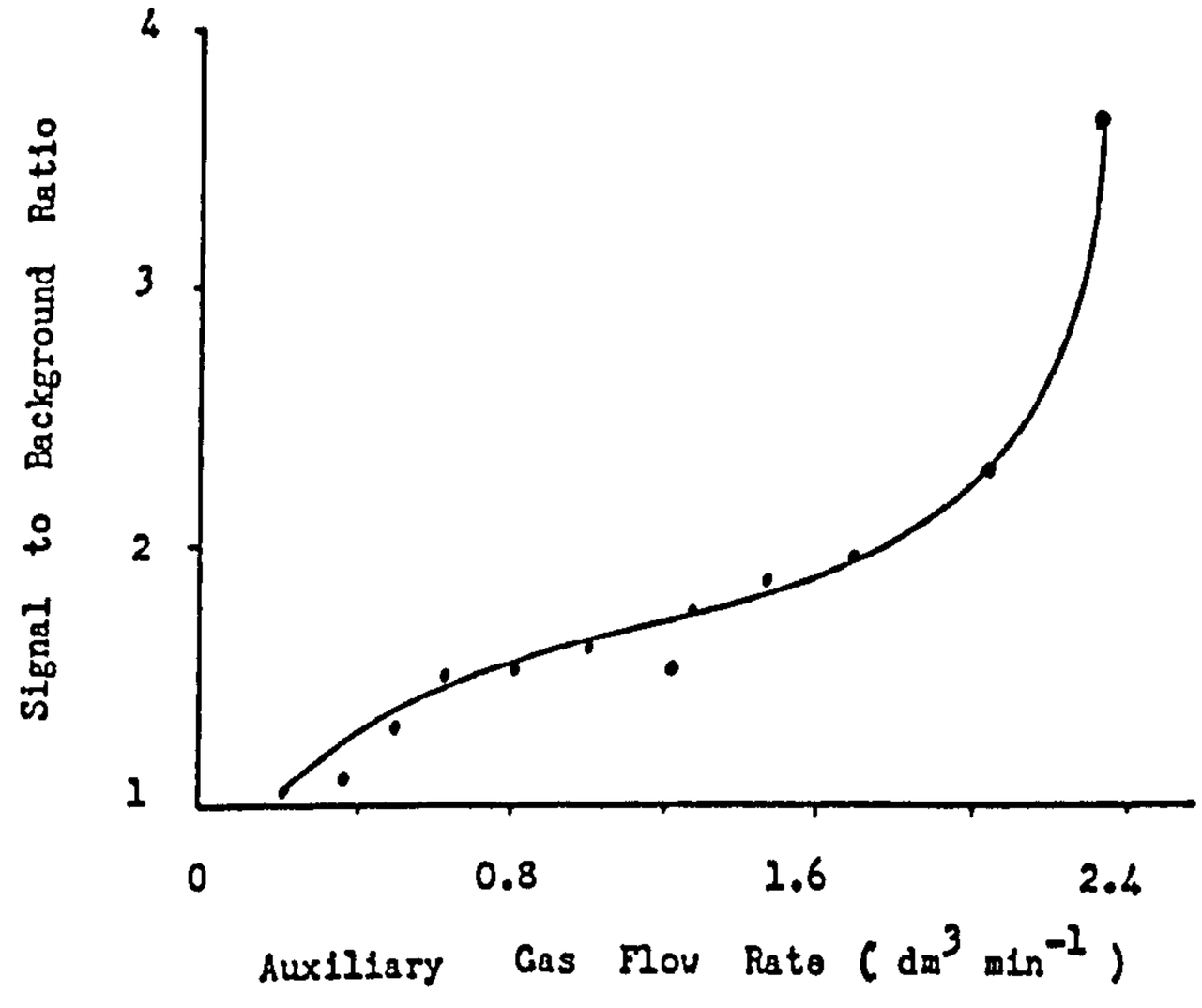

Figure (6.15)

Optimisation of anode current using an aqueous solution of lanthanum - signal (o—) and background (•--) .

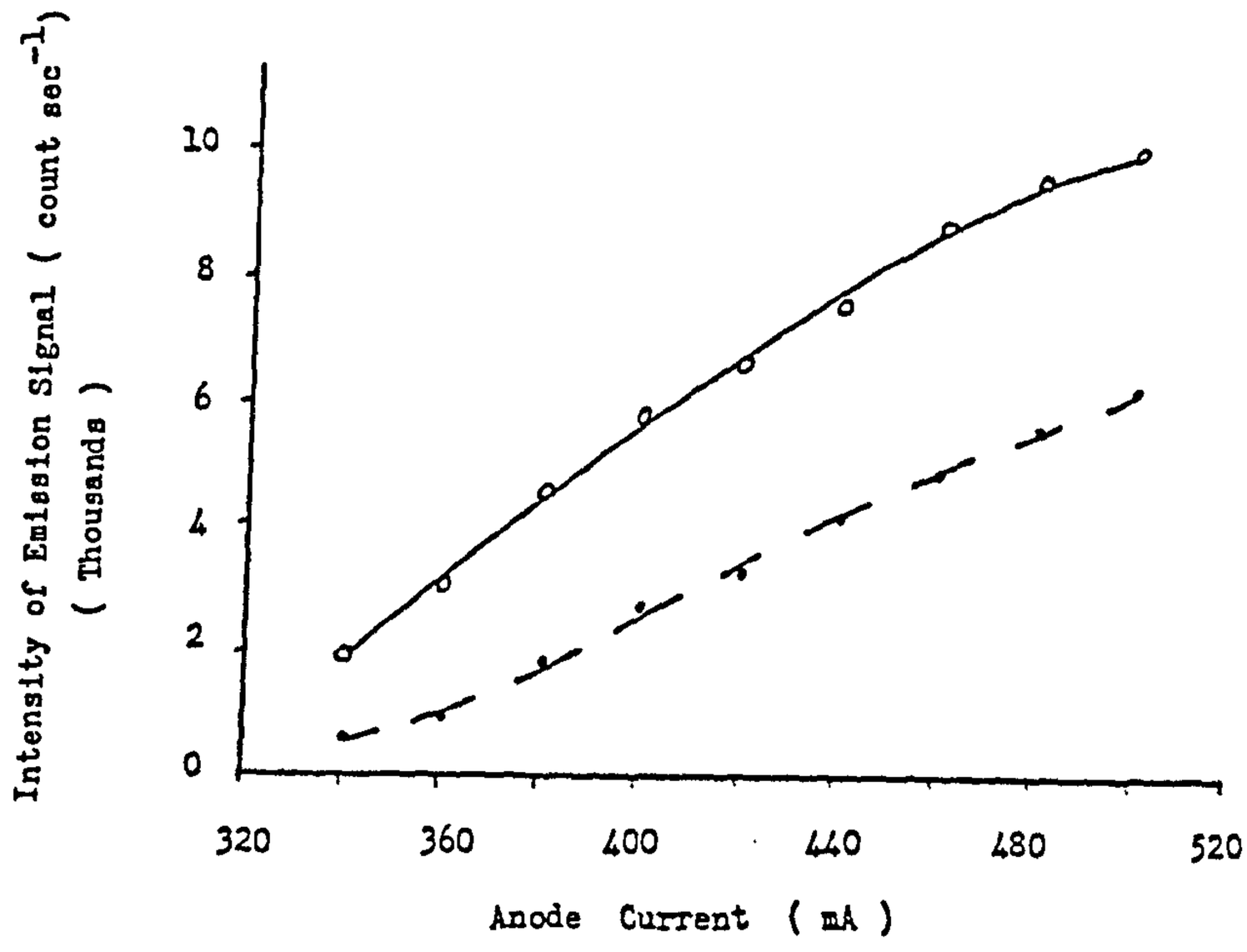

Figure (6.16)

The effect of changing anode current on the signal to background ratio of an aqueous solution of lanthanum .

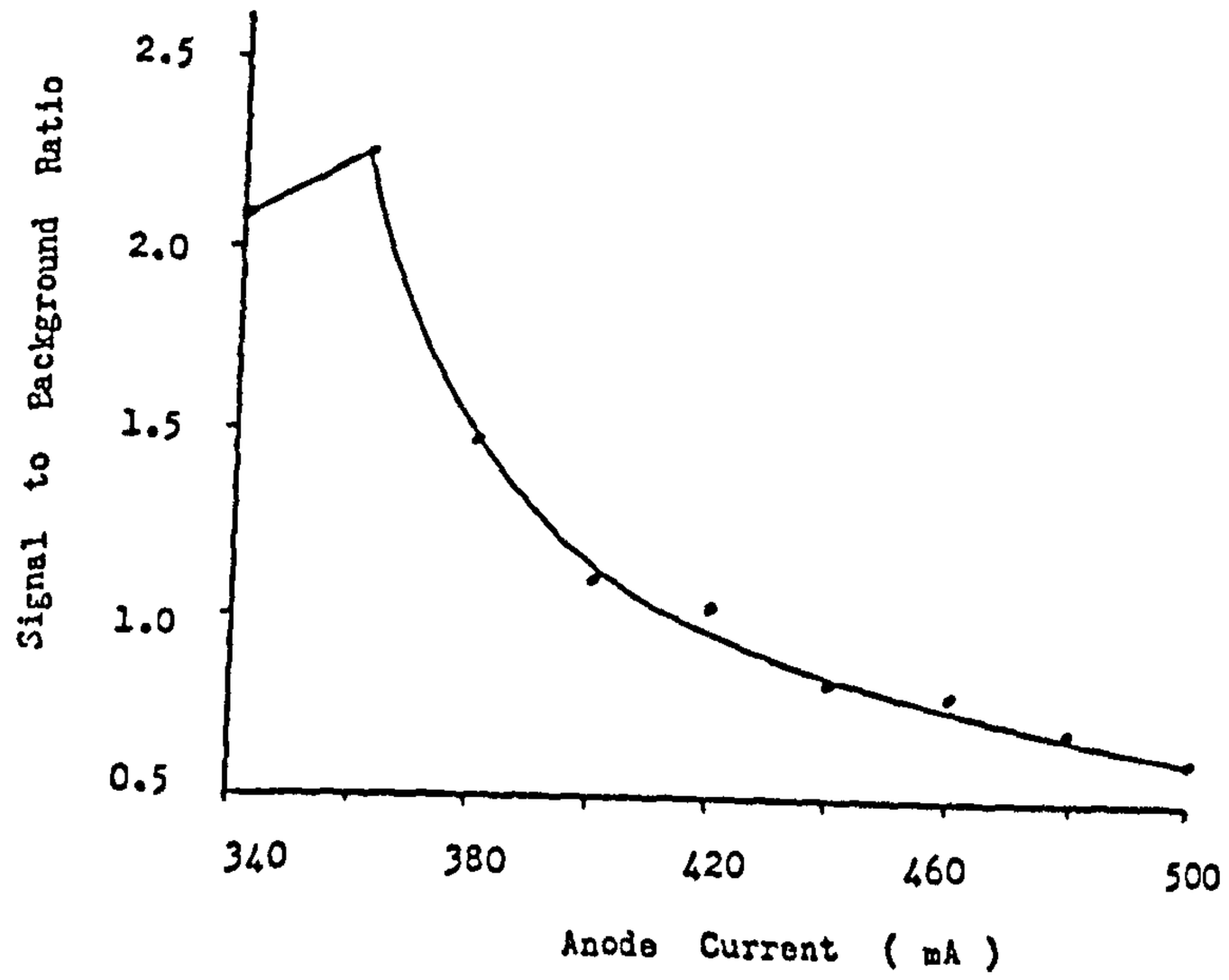

increased but the anode current was unchanged at 400 mA. The increase at higher flow rates was small, as can be seen in Figure 6.17. The signal to background ratio increased with an increase in the flow rate, reaching a maximum value at a flow rate of 14.75 dm^3 min^{-1}, after which it decreases with any further increase in the flow rate, as shown in Figure 6.18.

Finally the position of measurement in the plasma was optimised by varying the height of the lens. The intensity of the signal and background both reach maxima as the height increased, as can be seen in Figure 6.19. But each maxima occurred at a different height, the analyte intensity had a maximum intensity at a height of 14 mm above the coil where the background intensity maximised at 9 mm above the coil. The position of the highest signal to background ratio also different from the positions of both the signal and the background optima, and occurred at 20 mm above the coil, as shown in Figure 6.20.

6.2.1.1 Conclusion.

The settings giving the maximum signal or background differ from those chosen which are for the maximum signal to background ratio ((S-B)/ B), and were used for the analysis of the effluent from the cation exchange separation column. These instrumental conditions are shown in Table 6.3.

Figure (6.17)

Optimisation of plasma gas flow rate using an aqueous solution of lanthanum - signal (o—) , background (•--) and anode current (×···).

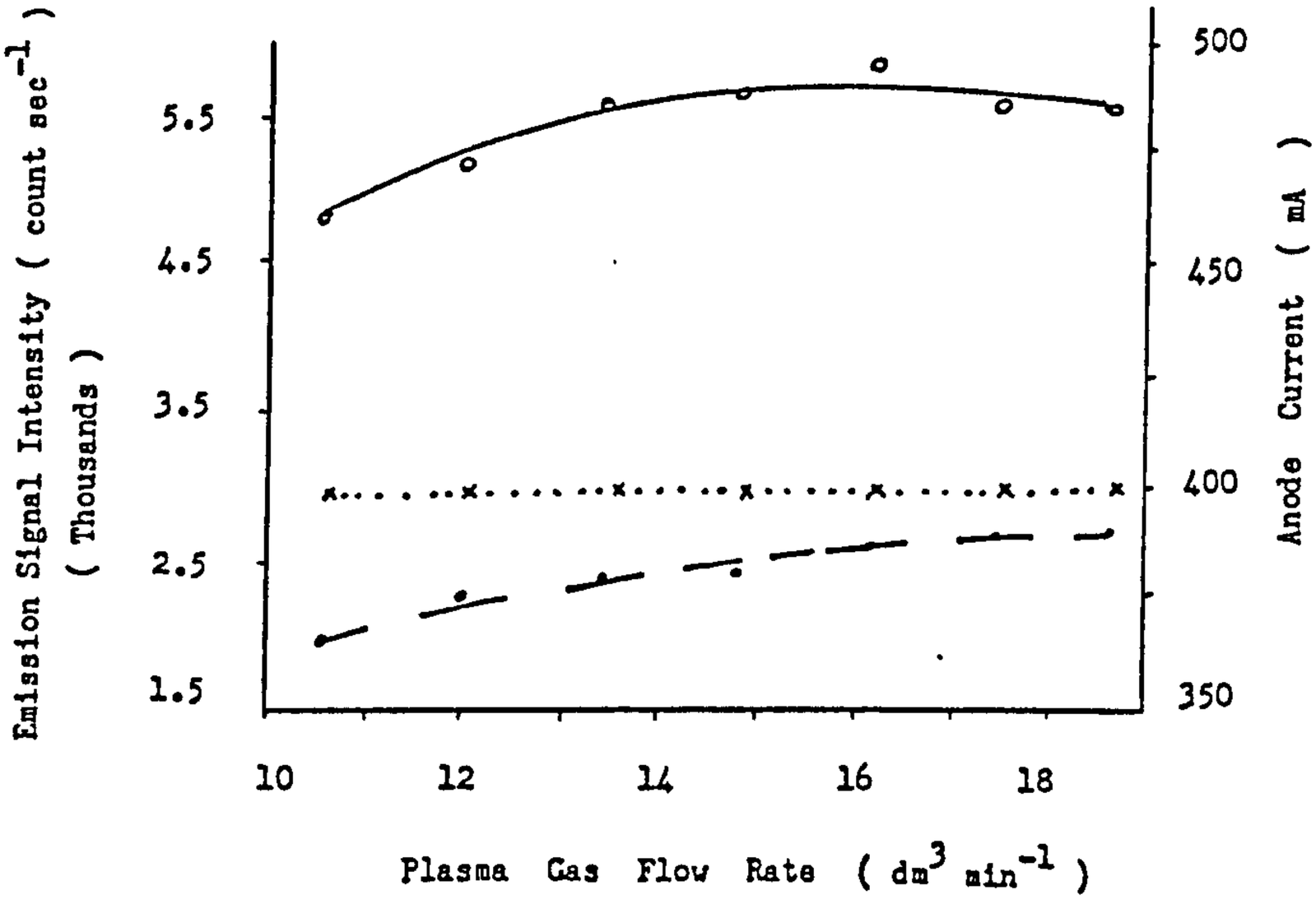

Figure (6.18)

The effect of changing plasma gas flow rate on the signal to background ratio using an aqueous solution of lanthanum .

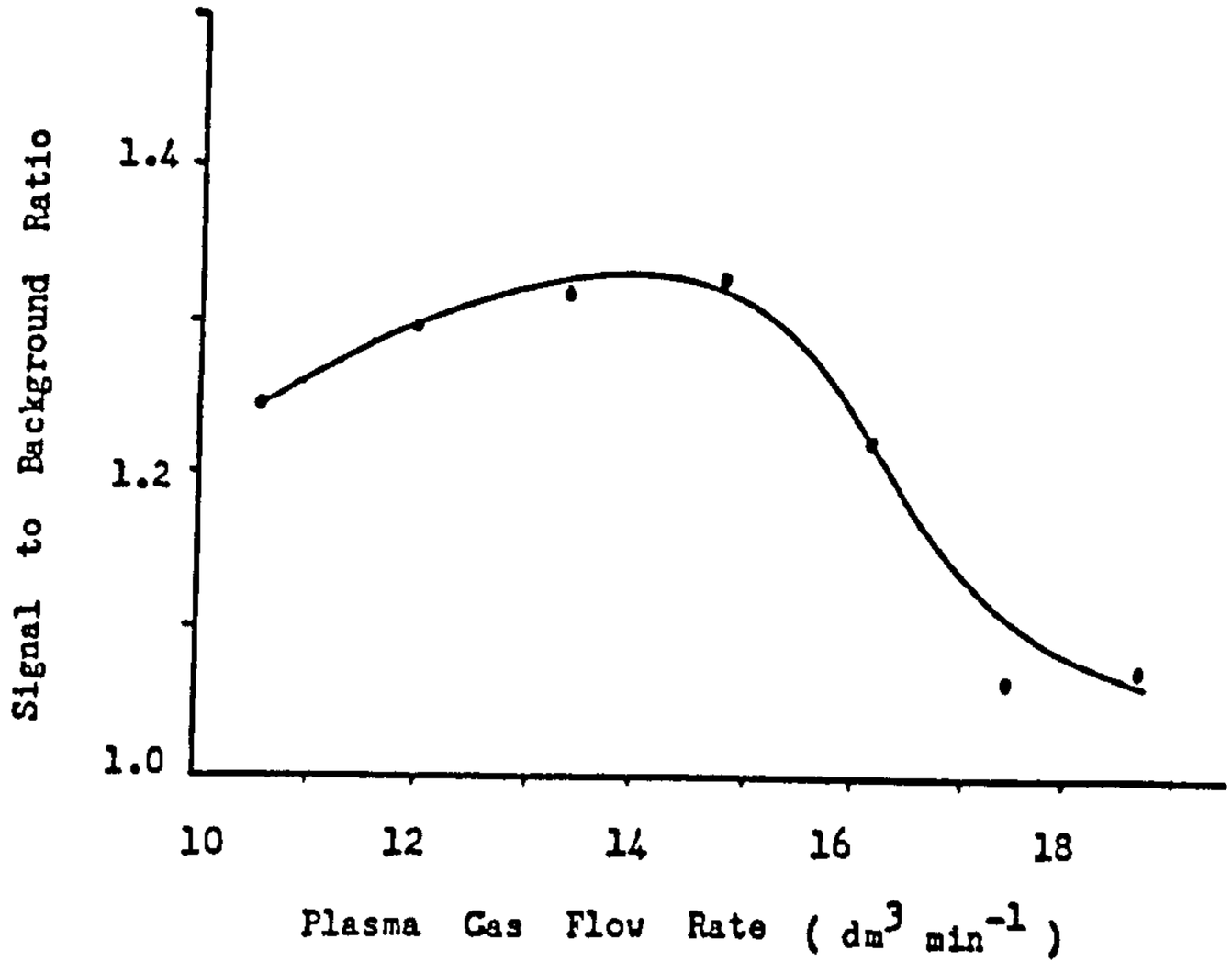

Figure (6.19)

Optimisation of measurement height above the coil using an aqueous solution of lanthanum - signal (•—) and background (o--) .

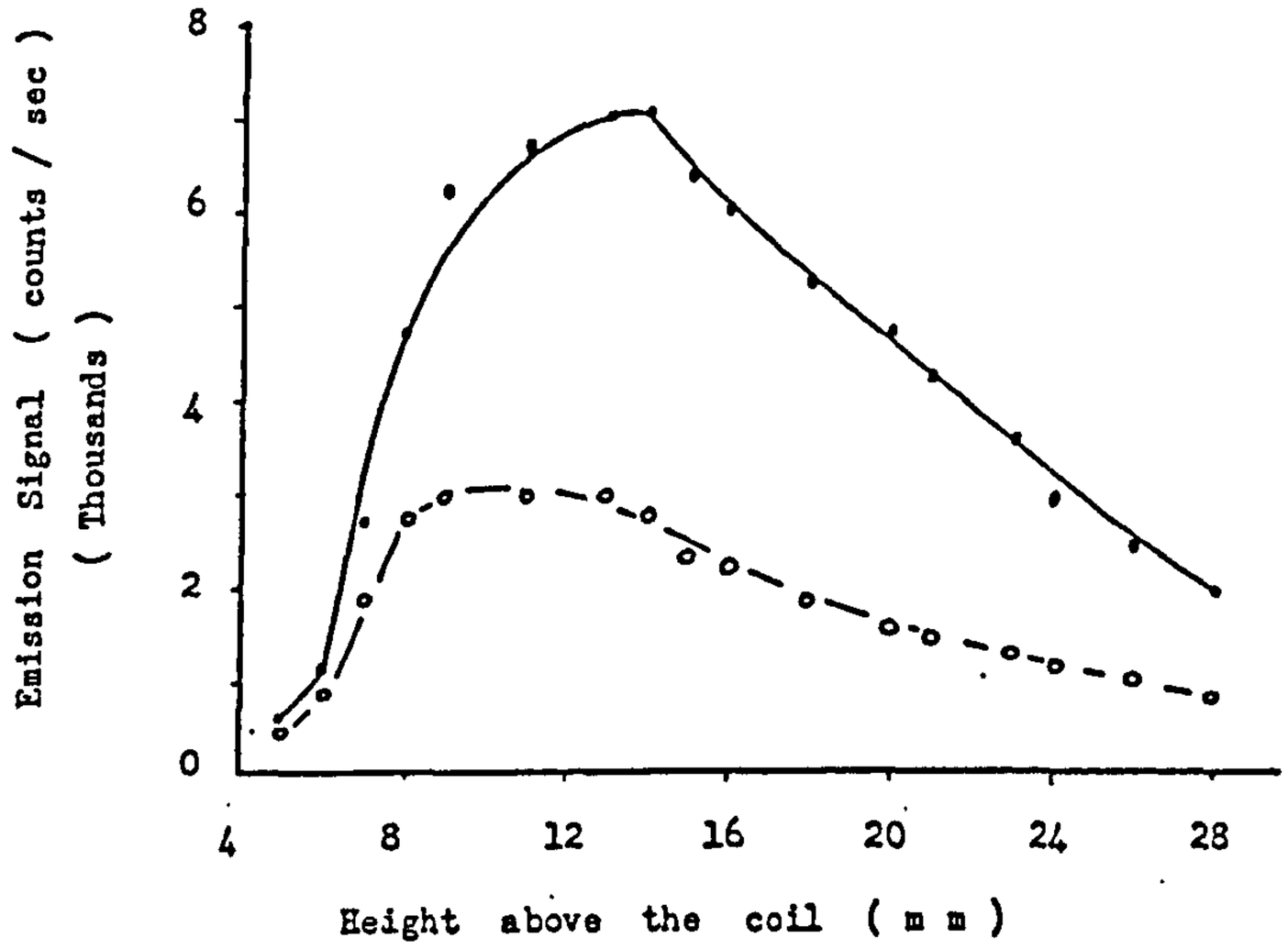

Figure (6.20)

The effect of changing measurement height above the coil on the signal to background ratio of an aqueous solution of lanthanum .

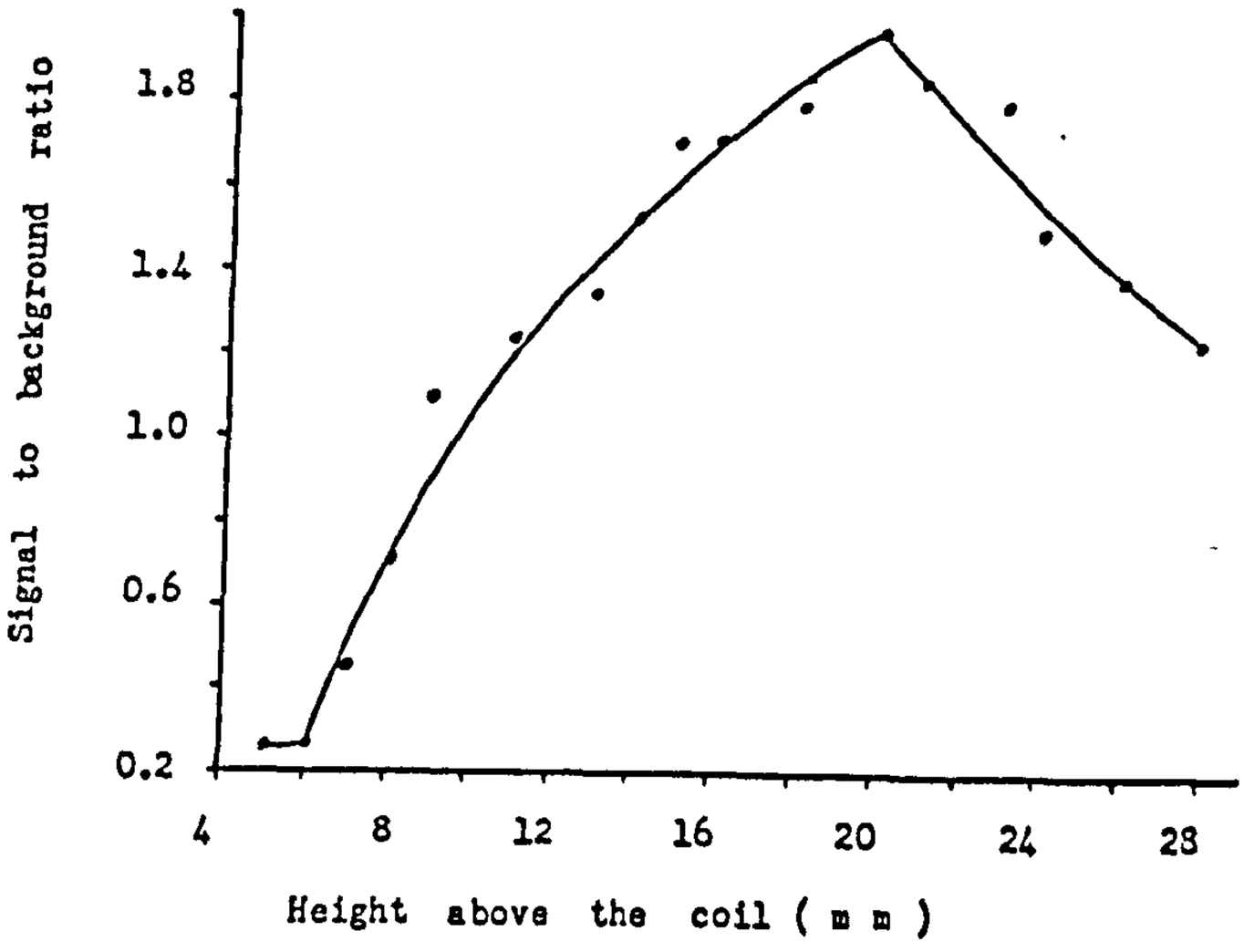

6.2.2 Interference Spectra.

The spectra were obtained using the wavelength modulation system, as described above for the analysis of the eluate from the anionic separation (section 6.1.2), except that no background correction was made and the signal was counted for 0.1 second at each one of 250 possible positions of the quartz plate. The computer processed these results automatically producing a spectra of the desired region. The wavelength was chosen to suit the analyte and then was unchanged while each of the other rare earth elements (the interferants) at a much higher concentration (10 mg dm^{-3}) were aspirated and the wavelength region scanned. All the rare earth elements were treated both as analytes and interferants. In addition, iron and calcium (100 mg dm^{-3} were included as interferants because it was believed possible that they could be incompletly washed from the cationic column and might contaminate the rare earth effluent; in the event, no such contamination was ever observed. The rare earth elements can interfere with the analysis in two ways by giving a signal at either the analyte wavelength or at a wavelength chosen to estimate the background. In the first case a positive interference results, in the second case a negative interference is caused (i.e. the estimated signal will be too low due to the subtraction of too large background). The results of this study are shown in the spectra (Figures 6.21 to 6.35) and are

discussed element by element below .

1) Yttrium.

Yttrium has a small positive interference from erbium and small partial positive interference from dysprosium,cerium, holmium and dysprosium will increase the measurements of the background and could give an effective negative interference. The other rare earth elements, calcium and iron will have no effect on the net signal, as can be seen in Figures 6.21.A to 6.21.D.

2) Lanthanum.

The interference of rare earth elements, calcium and iron on lanthanum are shown in Figures 6.22.A to 6.22.D. A direct line interference (positive) was obtained from praseodymium, while a partial line interference was observed for cerium and neodymium. The elements which affected the intensity of the background were praseodymium, cerium, samarium and dysprosium, each giving a negative interference. The rest of the elements had no effect on the net lanthanum signal.

3) Cerium.

The interference of rare earth elements, calcium and iron on cerium are shown in Figures 6.23.A to 6.23.D. From the Figures it can be seen that there were no direct line or partial line interferences, but praseodymium, gadolinium, neodymium and terbium affected the intensity of the background measurements. The rest

of the rare earth elements and iron had no emission in the measurement region. Calcium increases the continuum base line, but the net effect on the cerium intensity was zero.

4) Praseodymium.

The praseodymium interference spectra are shown in Figures 6.24.A to 6.24.D. Cerium and erbium gave a direct line interference, while cerium and neodymium had an affect on the background measurements. The rest of the rare earth elements and iron had no interference at all, while calcium increased the continuum base line but the net effect on the praseodymium intensity was zero.

5) Neodymium.

Interferences at the neodymium wavelength are shown in Figures 6.25.A to 6.25.D. From the figures it can be seen that there were no direct line interferences, although cerium and praseodymium have a partial line interference. The elements which will affect the measurements of the background are terbium, samarium, europium and erbium. The rest of the rare earths and iron have no interference, while calcium increased the continuum base line.

6) Samarium.

The interference at the samarium wavelength are shown in Figures 6.26.A to 6.26.D. From the figures it can be seen that neodymium gave a direct line interference (positive), but gadolynium had a partial

line interference (positive). Yttrium, holmium and terbium increased the measurement of the background (negative interference). The rest of the elements had no significant line intensity in the scanned region.

7) Europium.

The interferences at europium wavelength are shown in Figures 6.27.A to 6.27.D. Neodymium is the only element which had a direct line interference. The elements cerium, praseodymium and terbium increases the intensity of the background. The other rare earths had no lines in the scanned region, while iron had a strong line but it is far away from the position of even the background and can be neglected. Calcium increases the base line continuum.

8) Gadolinium.

The interference at the gadolinium wavelength are shown in Figures 6.28.A to 6.28.D. From the figures it can be seen that terbium and holmium had a direct line interference, while cerium, praseodymium and dysprosium had a partial line interference. Dysprosium, samarium and cerium affect the intensity of the background. The rest of the elements did not affect the net signal.

9) Terbium.

The interferences at the terbium wavelength are shown in Figures 6.29.A to 6.29.D. From the graphs it can be seen that samarium had a direct line interference, while holmium and dysprosium had partial

line interferences. Cerium, europium, holmium and dysprosium affect the intensity of the background. The rest of the elements had no line spectra in the measurement region.

10) Dysprosium.

The interferences at dysprosium wavelength are shown in Figures 6.30.A to 6.30.D. These graphs show that neodymium and terbium had a partial line interference, holmium increased the intensity of the background. The rest of the elements exhibited no spectral interference on dysprosium .

11) Holmium.

The interferences at holmium wavelength are shown in Figures 6.31.A to 6.31.D. Cerium and terbium had a direct line interference, while neodymium and samarium had a partial line interference. Terbium and dysprosmium increased the intensity of the background measurements. The rest of the elements had no interferences.

12) Erbium.

The interferences at the erbium wavelength are shown in Figures 6.32.A to 6.32.D. Terbium is the only element which had a partial line interference. Praseodymium, holmium and terbium increased the intensity of the background measurements. The rest of the elements had no interference effects.

13) Thulium.

The interferences at the thulium wavelength are

shown in Figures 6.33.A to 6.33.D. From the graphs it can be seen that terbium and erbium had partial line interferences. Cerium, gadolinium and holmium increased the background intensity. The rest of the elements have no effect.

14) Ytterbium.

The interferences at the ytterbium wavelength are shown in Figures 6.34.A to 6.34.D. From the graphs it can be seen that neodynium, dysprosium and thulium had partial line interferences. The rest of the elements had no effect on the net signal.

15) Lutetium.

The interferences at the lutetium wavelength are shown in Figures 6.35.A to 6.35.D. From the graphs, ytterbium is the only element which had a direct line interference. The rest of the elements had no effect on the net signal.

6.2.2.1 Conclusion.

The spectral interferences between the rare earth elements are very complex. The selection of wavelengths suitable for the measurement of the background is difficult because the selected position for one interfering element is not neccesary suitable for the other, also a suitable position for one analyte is not suitable for other analytes. Hence, a compromise position was used for each analyte to simplify the measurements. These compromise positions were at the

Figures (6.21 to 6.35)

Photoreduction of re-drawn high resolution scan spectra of inter-element interferences between the rare earth elements.

Spectral scan window has been calculated using the equation suggested by O'Haver et al. (147) .

$$\Delta\lambda = \frac{d\,l}{d\,x} * T * \emptyset * \frac{(n-1)}{n}$$

Where

$\emptyset$ = angle of rotation of quartz plate (V / deg.)

$\Delta\lambda$ = modulation interval in nm = window

T = thickness of quartz plate = 5 mm

n = refractive index of quartz plate at wavelength

$\frac{d\,l}{d\,x}$ = dispersion in nm mm^{-1} for the order of the wavelength of interest

Figures (6.21-A to 6.21-D)

Photoreduction of re-drawn high resolution scan spectra at yttrium wavelength (371.03 nm) - window = 0.117 nm , concentration of Y = 0.05 mg dm^{-3} , concentration of each REE = 10 mg dm^{-3} , concentration of Ca or Fe = 100 mg dm^{-3} .

(A)

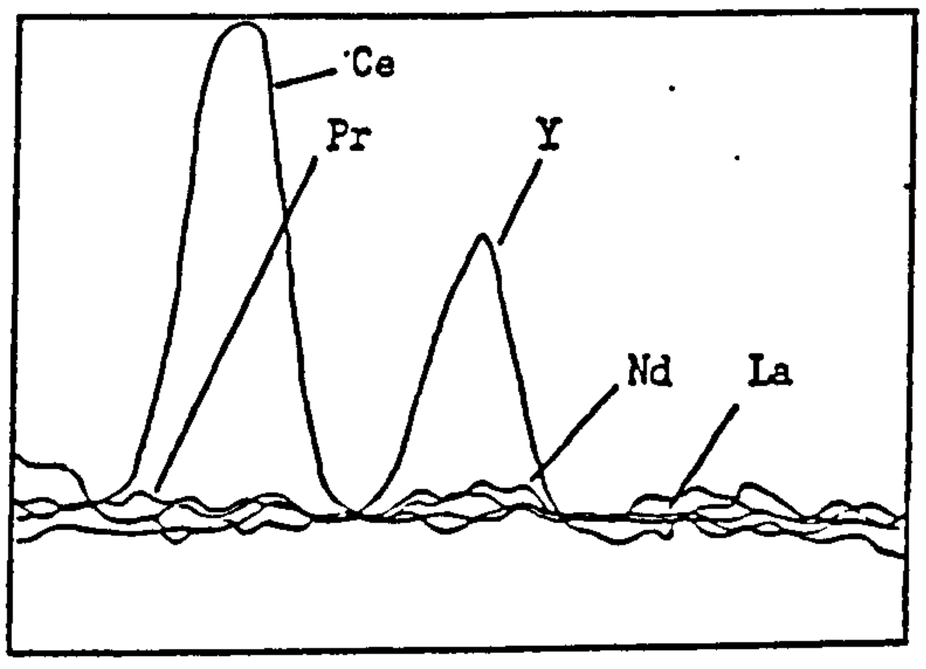

(B)

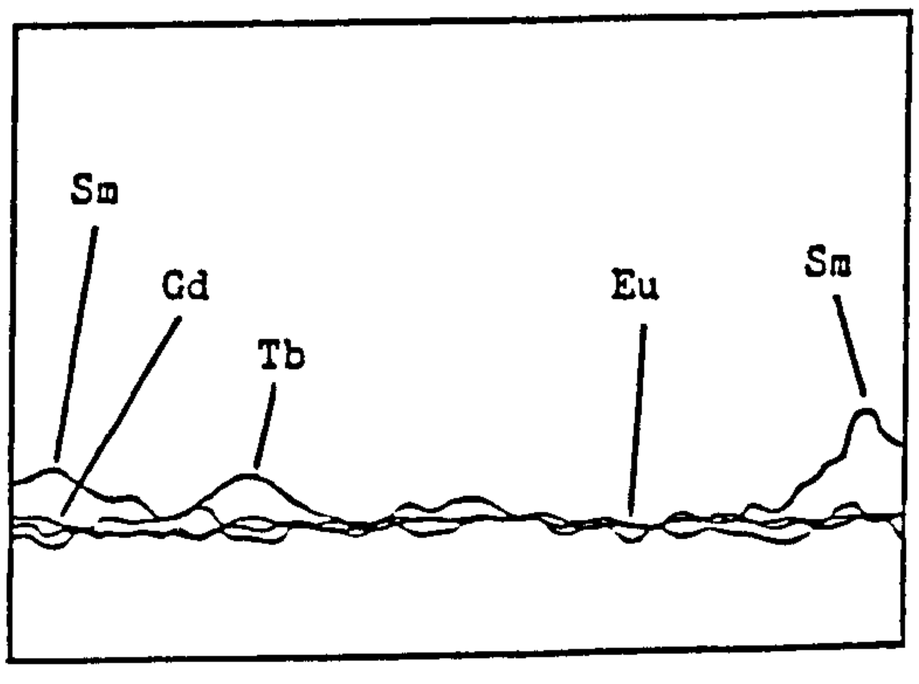

(C)

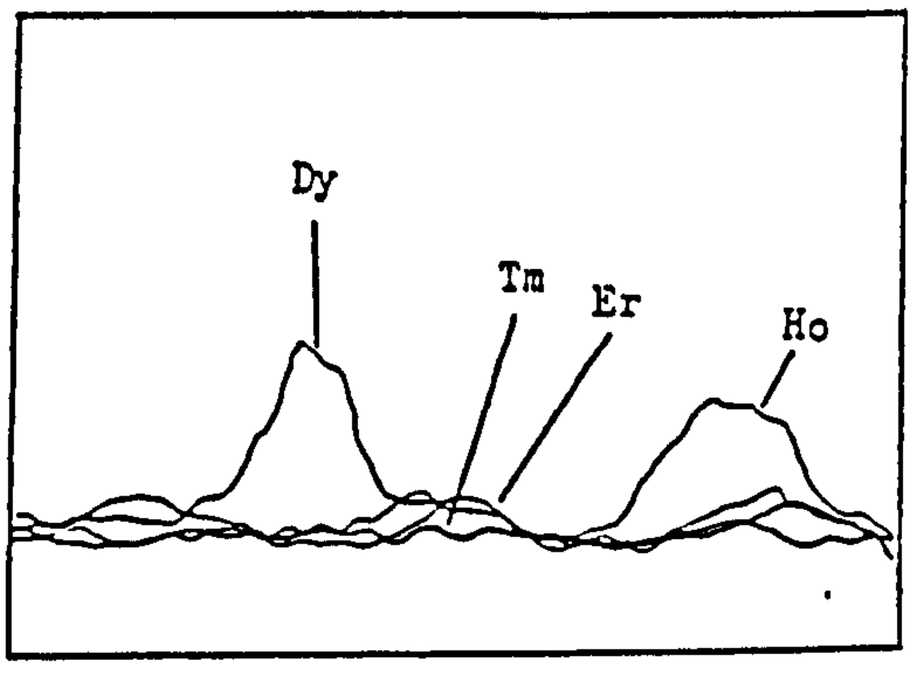

(D)

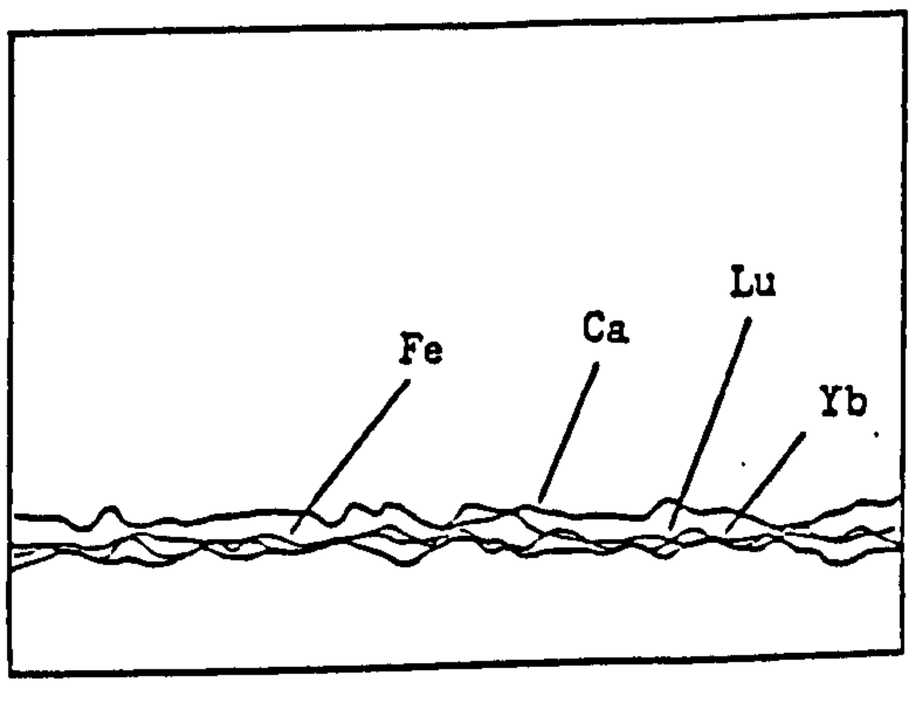

Figures (6.22-A to 6.22-D)

Photoreduction of re-drawn high resolution scan specra at lanthanum wavelength. (408.672 nm) - window = 0.123 nm , concentration of La = 0.1 mg dm^{-3} , concentration of each REE = 10 mg dm^{-3} , concentration of Ca or Fe = 100 mg dm^{-3} .

(A)

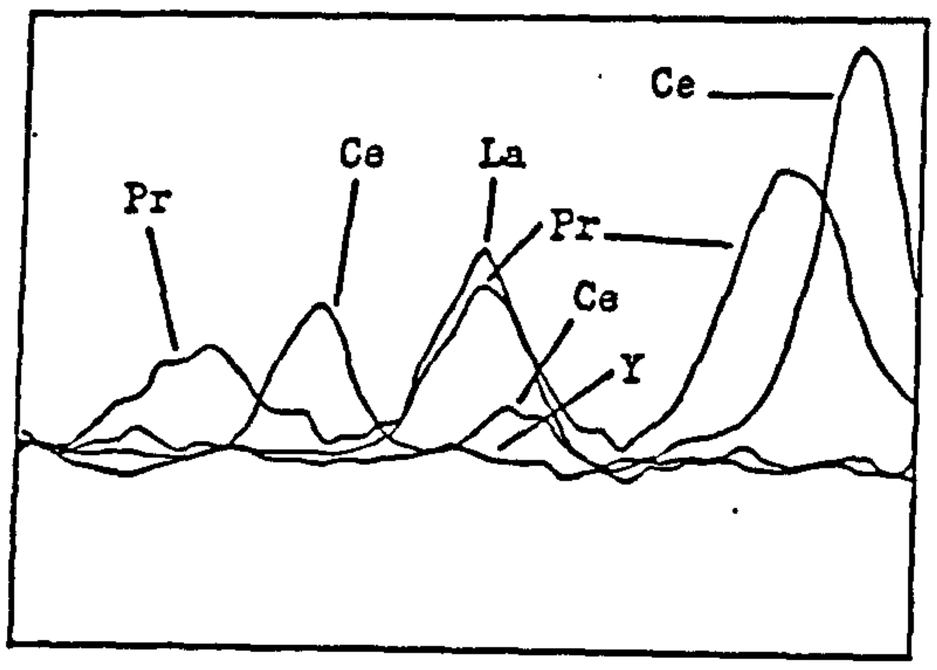

(B)

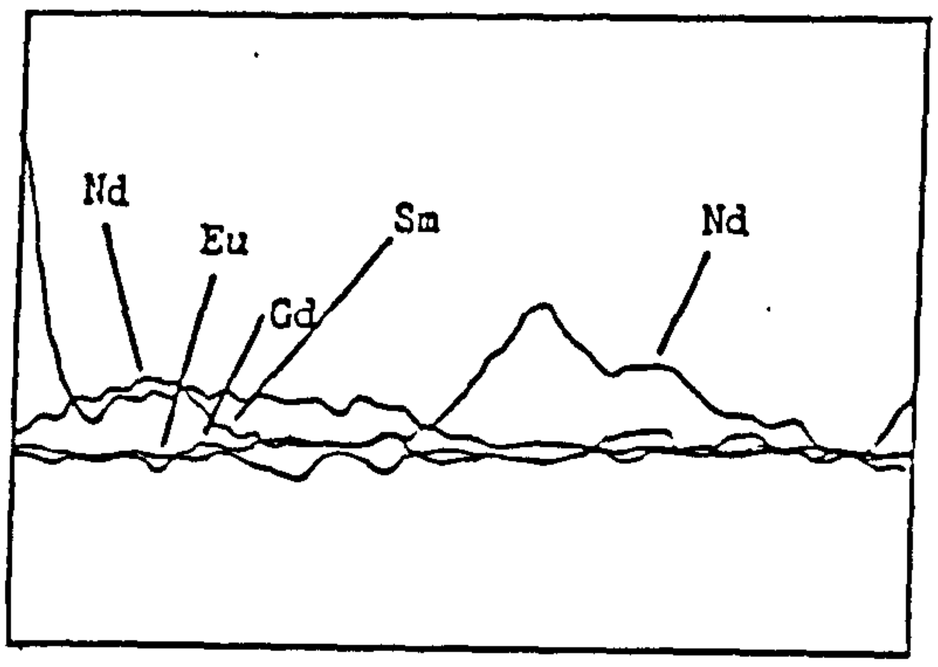

(C)

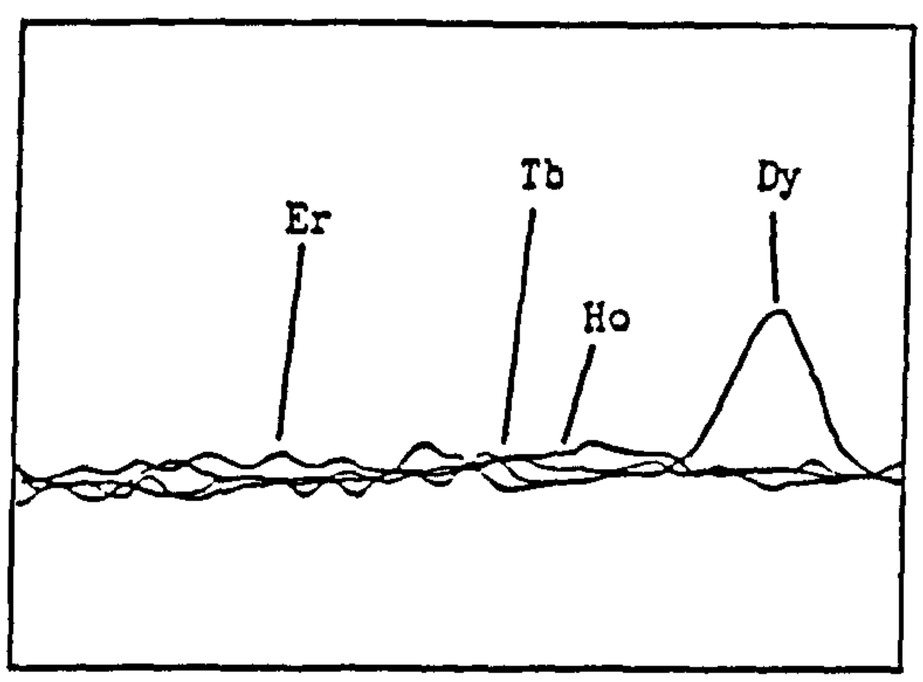

(D)

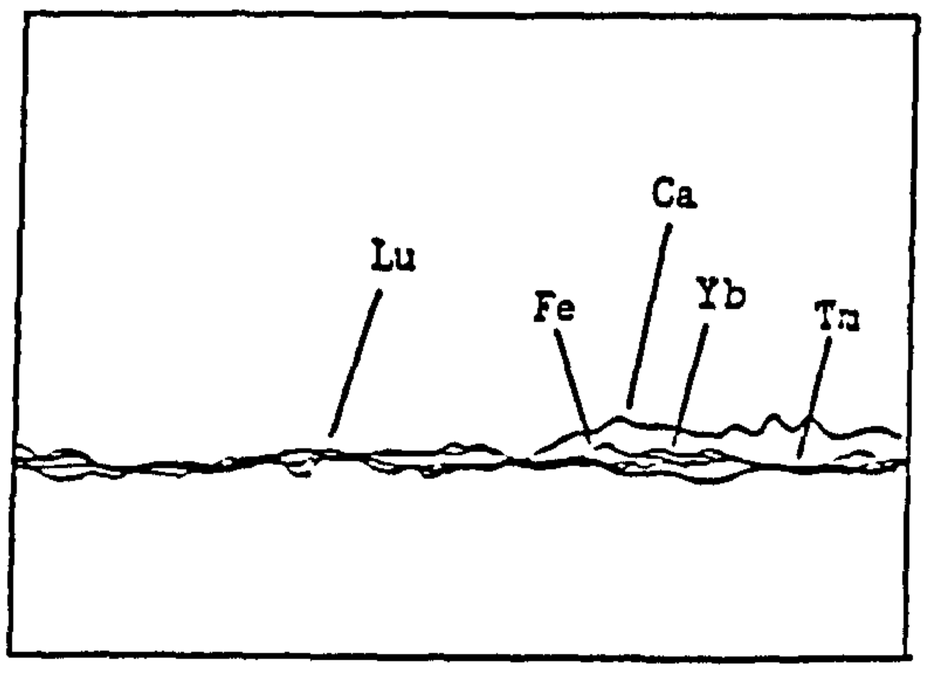

Figures (6.23-A to 6.23-D)

Photoreduction of re-drawn high resolution scan spectra at cerium wavelength (413.765 nm) - window = 0.129 nm , concentration of Ce = 0.4 mg dm^{-3} , concentration of each REE = 10 mg dm^{-3} , concentration of Ca or Fe = 100 mg dm^{-3} .

(A)

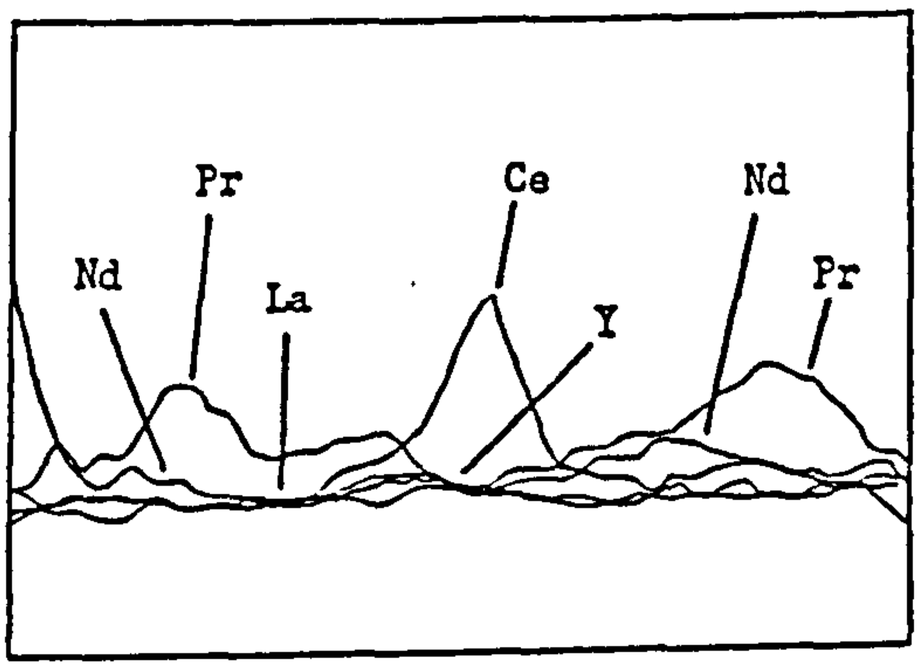

(B)

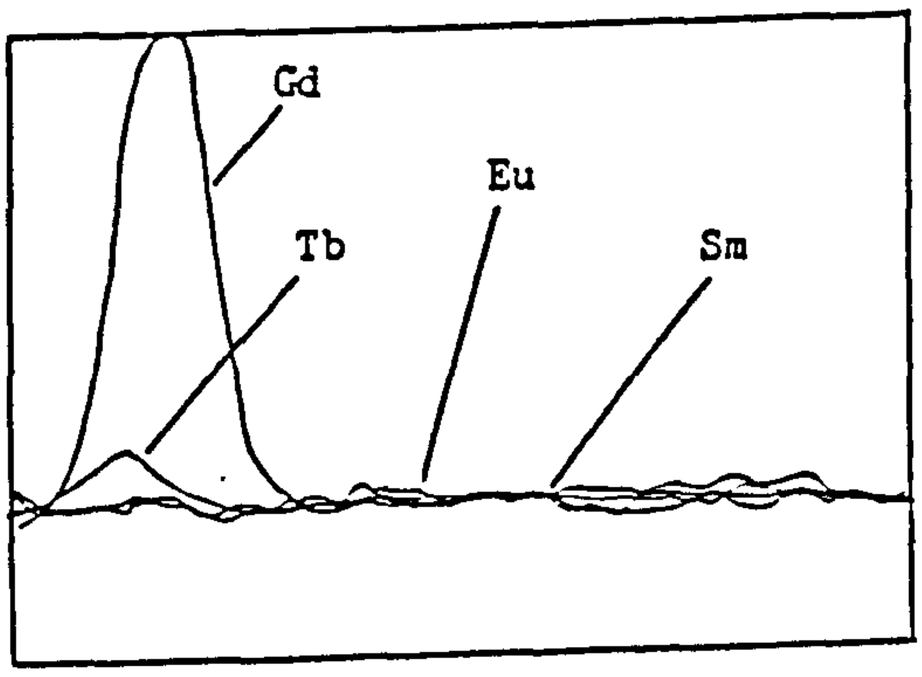

(C)

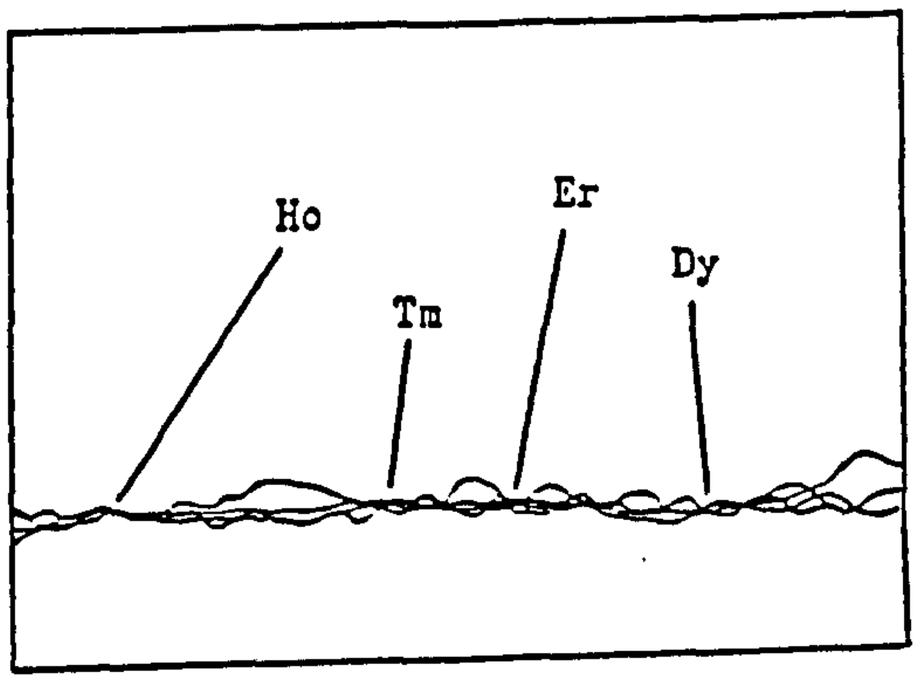

(D)

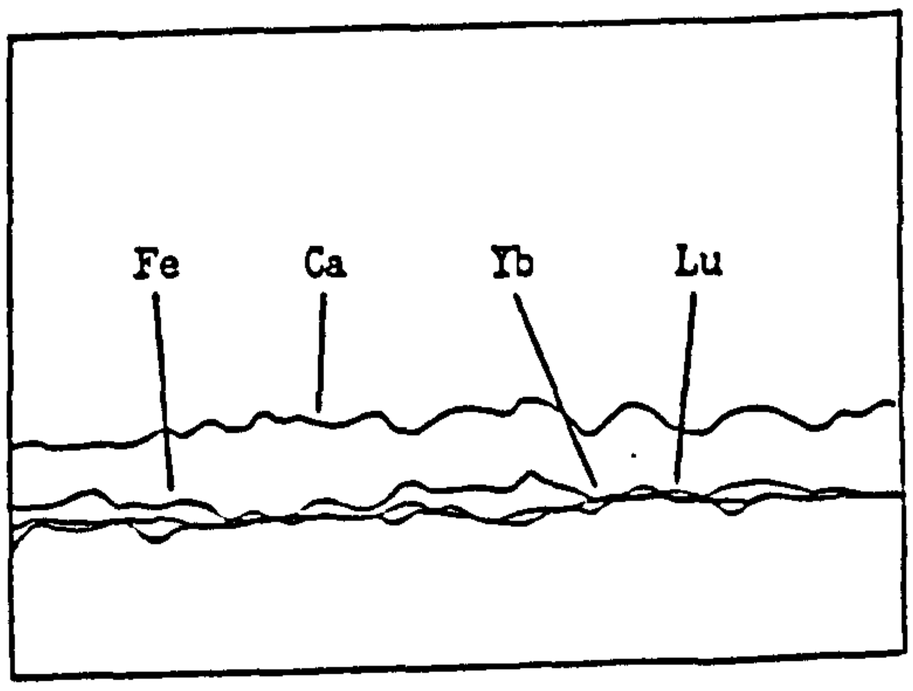

Figures (6.24-A to 6.24-D)

Photoreduction of re-drawn high resolution scan spectra at praseodymium wavelegth (390.844 nm) - window = 0.123 nm , concentration of Pr = 0.4 mg dm^{-3} , concentration of each REE = 10 mg dm^{-3} , concentration of Ca or Fe = 100 mg dm^{-3} .

(A)

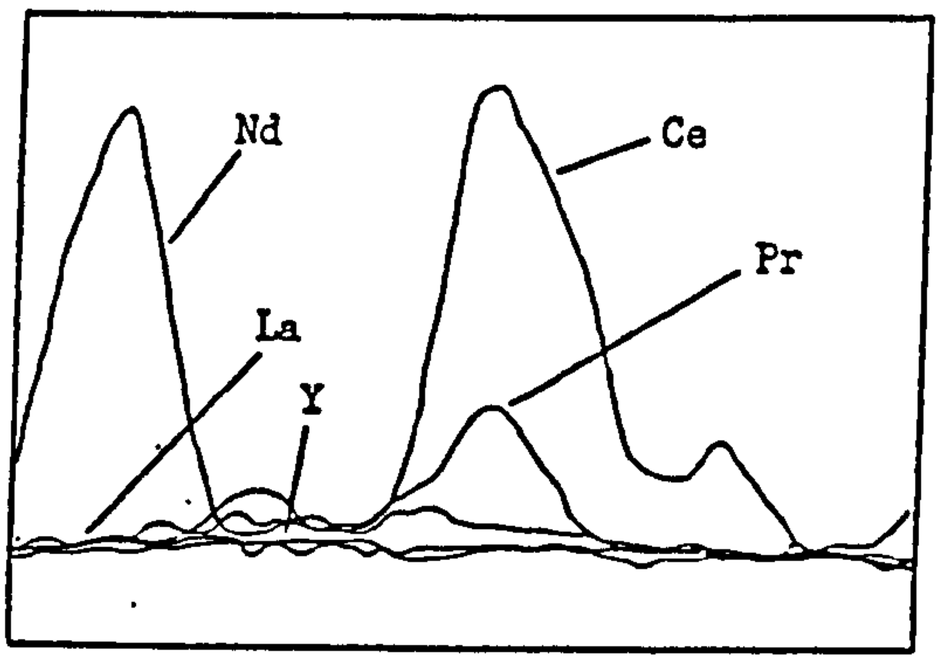

(B)

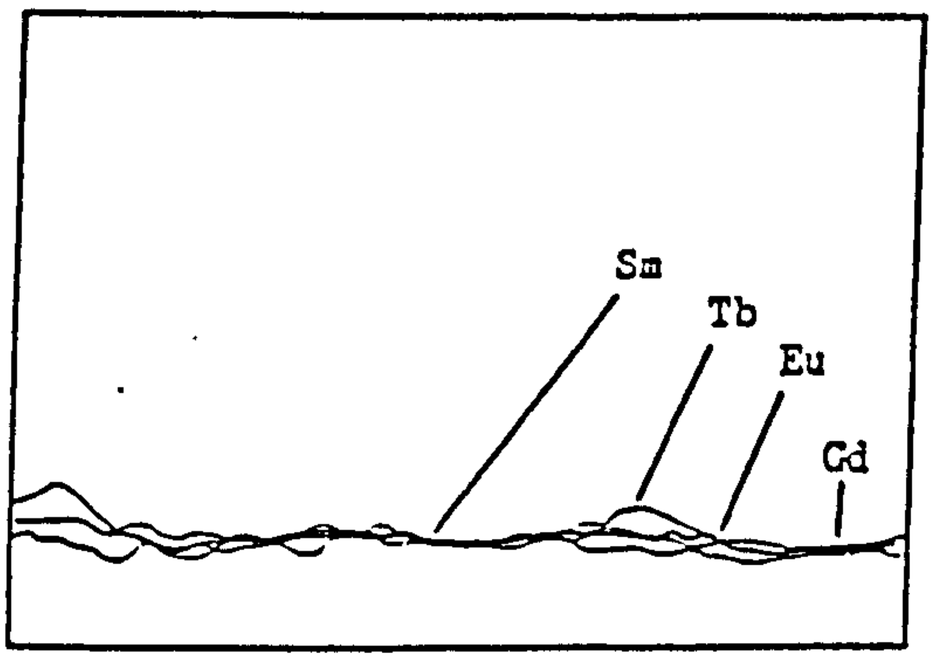

(C)

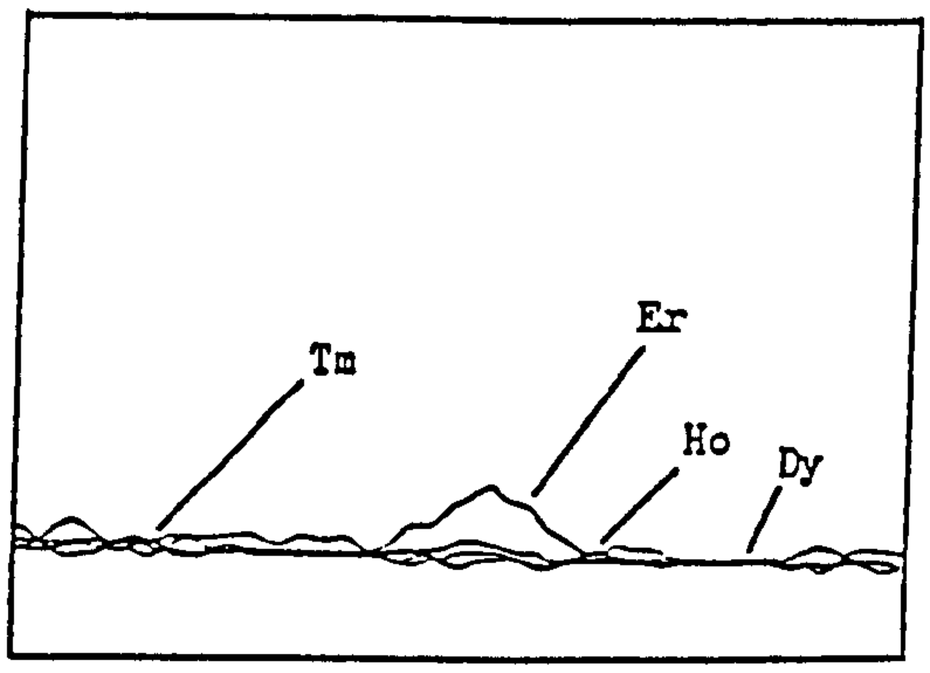

(D)

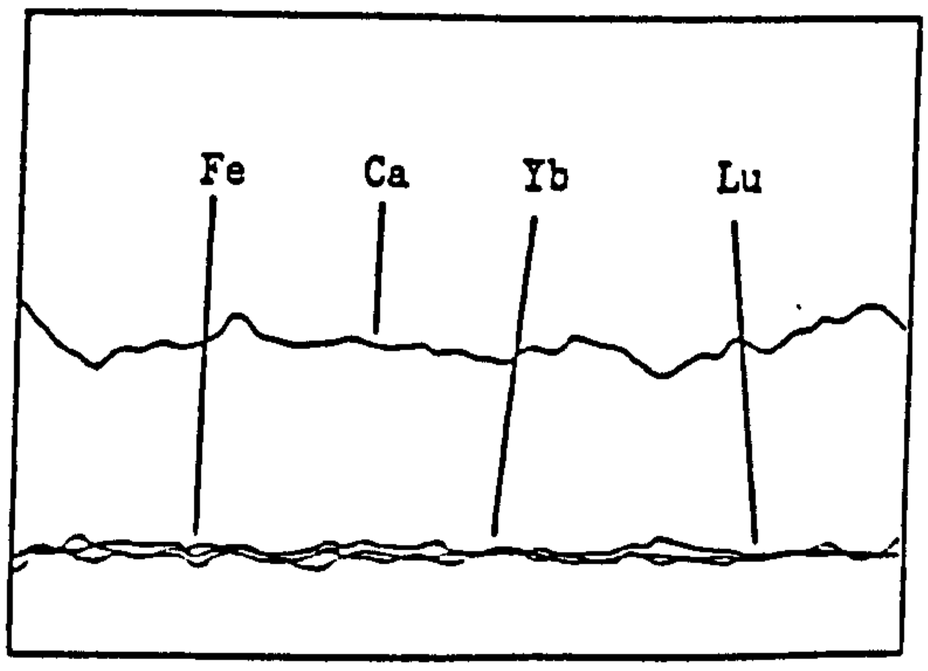

Figures (6.25-A to 6.25-D)

Photoreduction of re-drawn high resolution scan spectra at neodymium wavelength (401.225 nm) - window = 0.126 nm , concentration of Nd = 0.2 mg dm^{-3} , concentration of each REE = 10 mg dm^{-3} , concentration of Ca or Fe = 100 mg dm^{-3} .

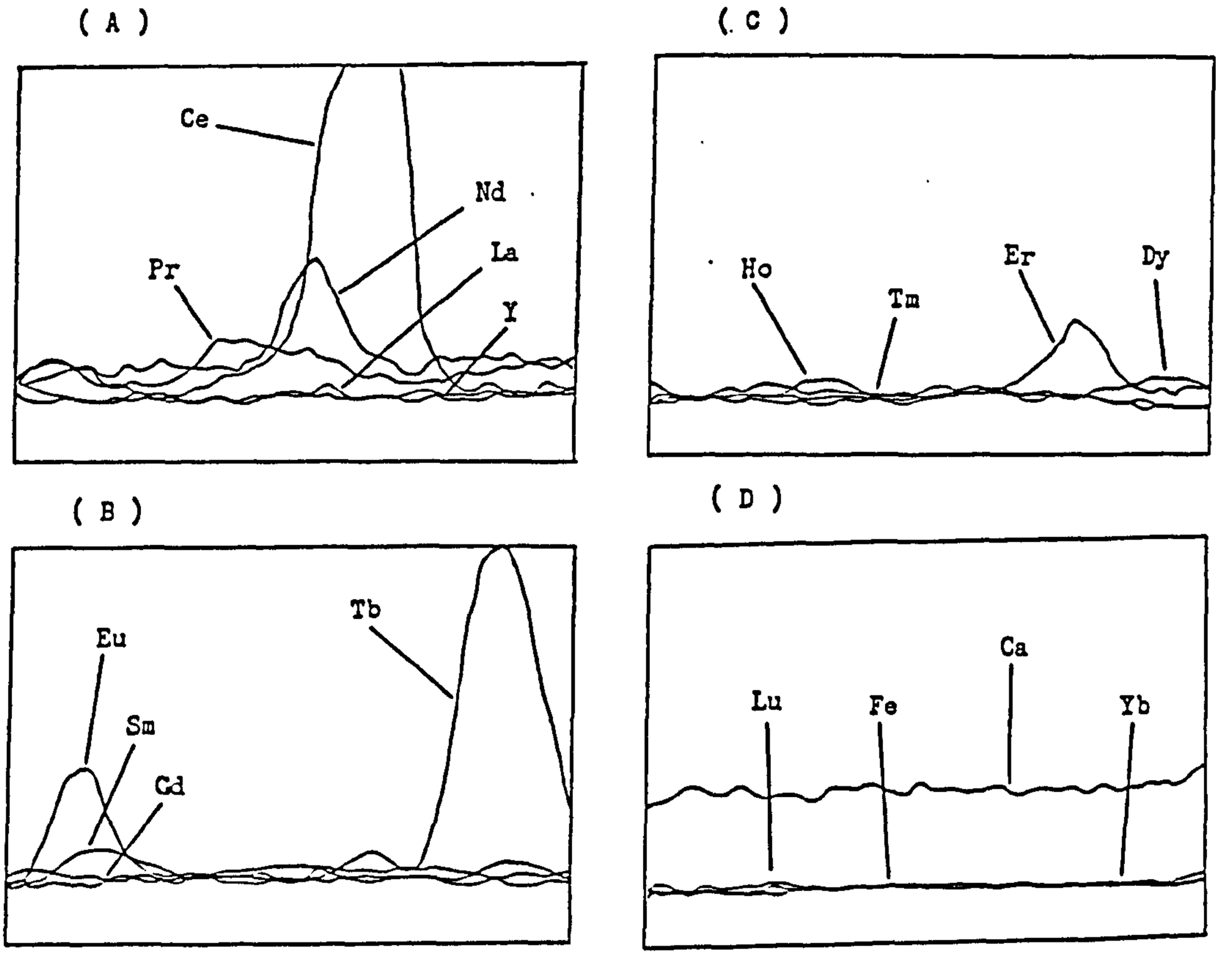

Figures (6.26-A to 6.26-D)

Photoreduction of re-drawn high resolution scan spectra at samarium wavelength (359.260 nm) - window = 0.114 nm , concentration of Sm = 0.4 mg dm^{-3} , concentration of each REE = 10 mg dm^{-3} , concentration of Ca or Fe = 100 mg dm^{-3} .

(A)

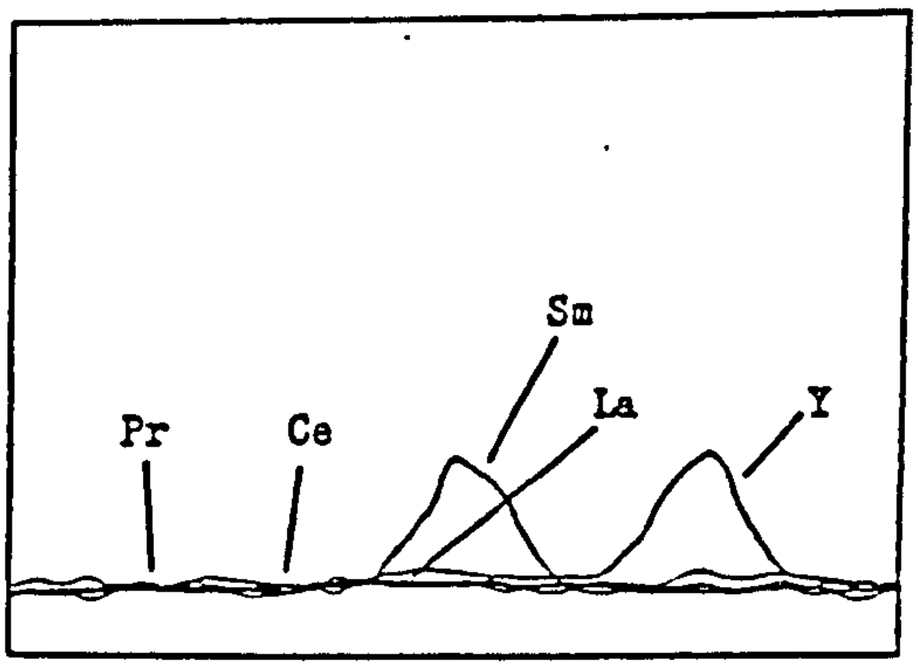

(B)

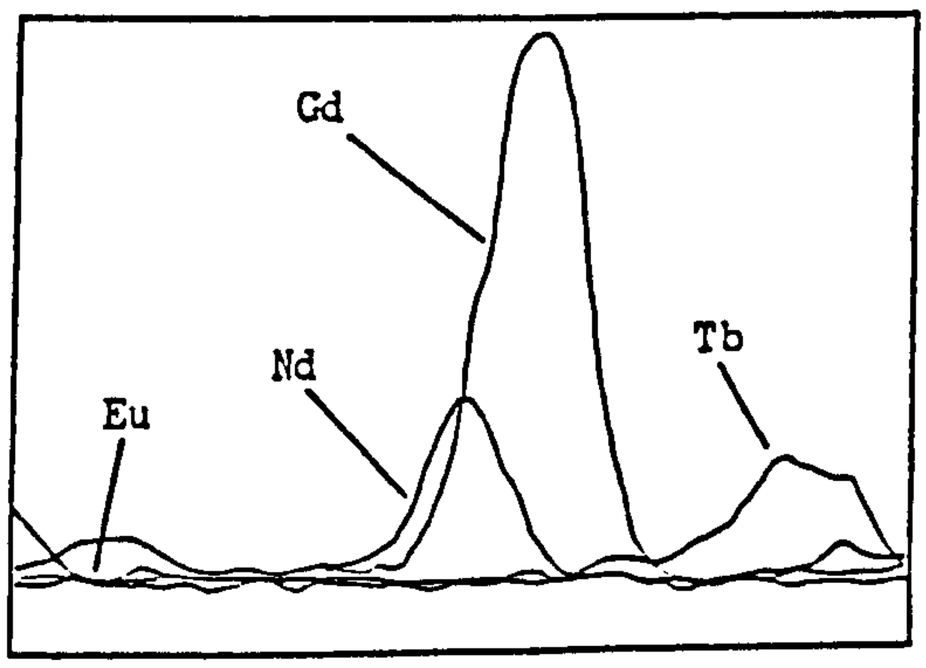

(C)

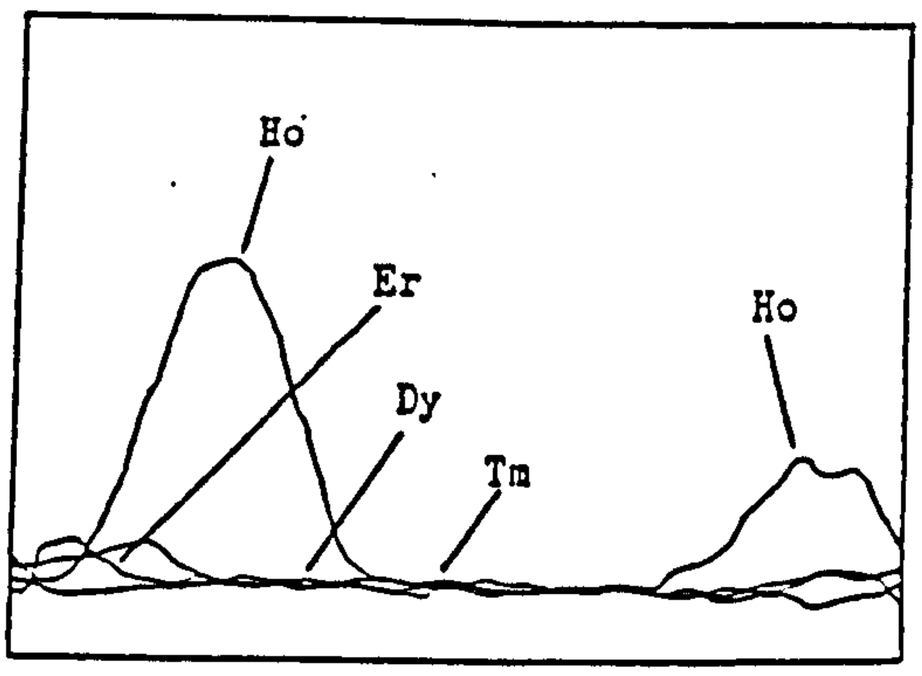

(D)

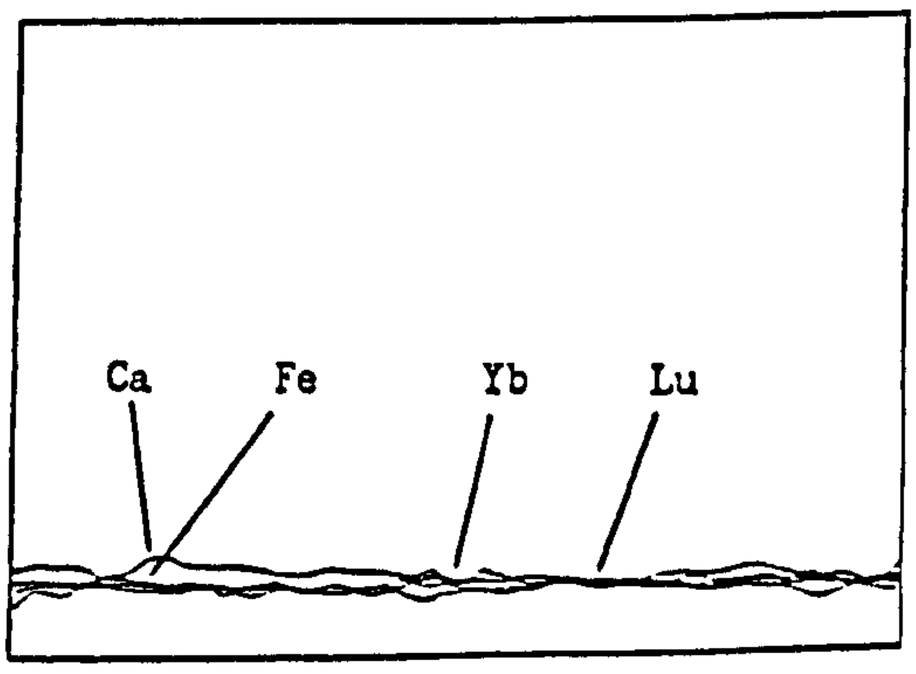

Figures (6.27-A to 6.27-D)

Photoreduction of re-drawn high resolution scan spectra at europium wavelength (381.967 nm) - window = 0.12 nm , concentration of Eu = 0.05 mg dm^{-3} , concentration of each REE = 10 mg dm^{-3} , concentration of Ca or Fe = 100 mg dm^{-3} .

(A)

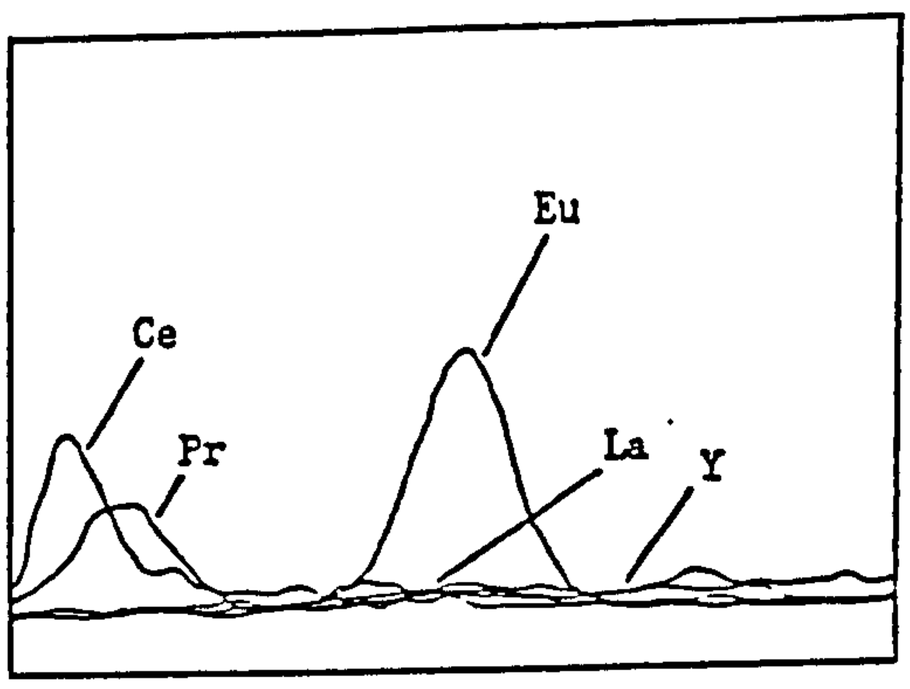

(B)

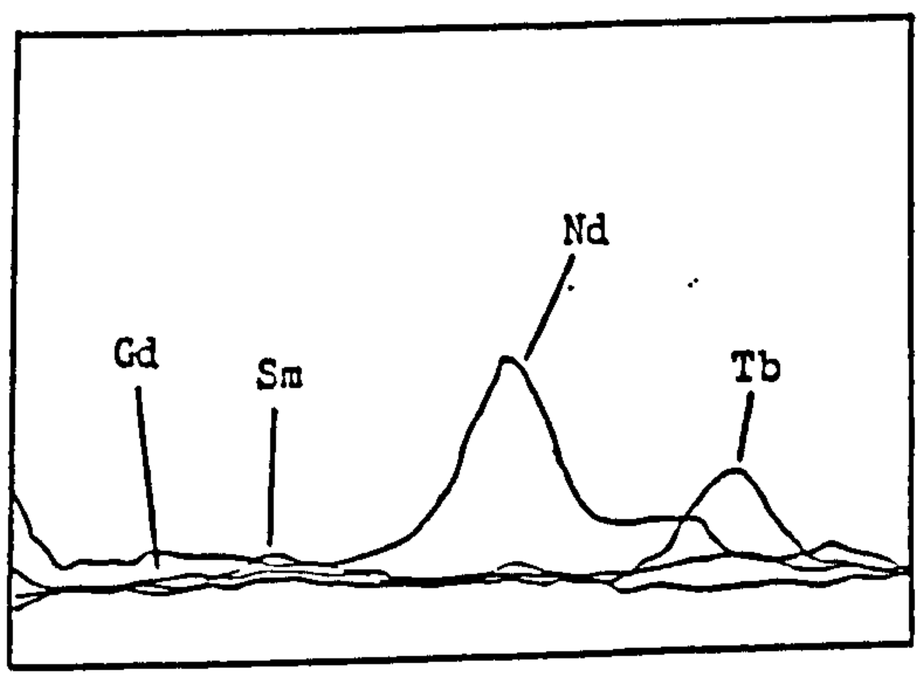

(C)

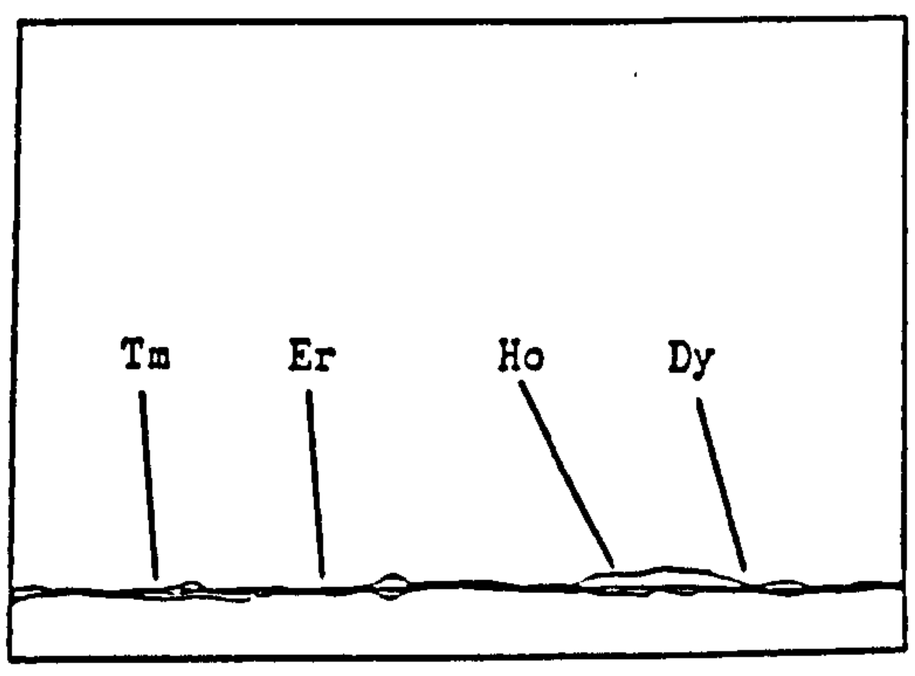

(D)

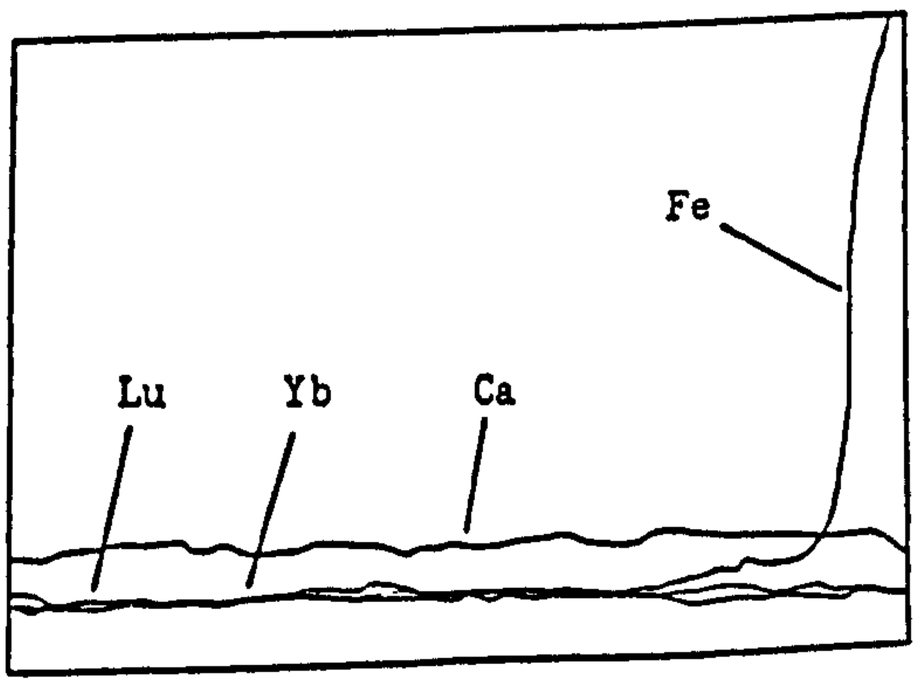

Figures (6.28-A to 6.28-D)

Photoreduction of re-drawn high resolution scan spectra at gadolinium wavelength (342.247 nm) - window = 0.109 nm , concentration of Gd = 0.25 mg dm^{-3} , concentration of each REE = 10 mg dm^{-3} , concentration of Ca or Fe = 100 mg dm^{-3} .

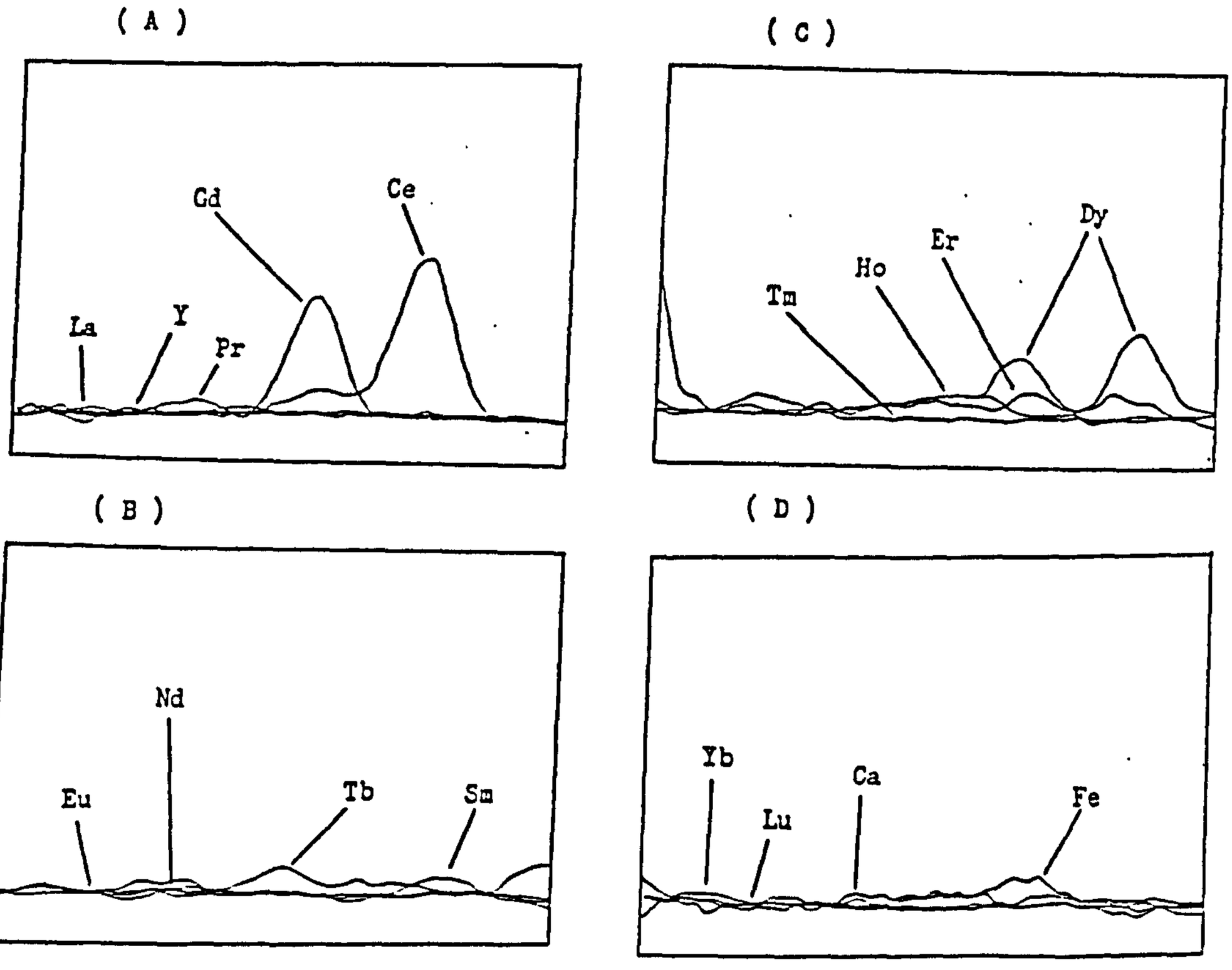

Figures (6.29-A to 6.29-D)

Photoreduction of re-drawn high resoltion scan spectra at terbium wavelength (350.917 nm) - window = 0.111 nm , concentration of Tb = 0.2 mg dm^{-3} , concentration of each REE = 10 mg dm^{-3} , concentration of Ca or Fe = 100 mg dm^{-3} .

(A)

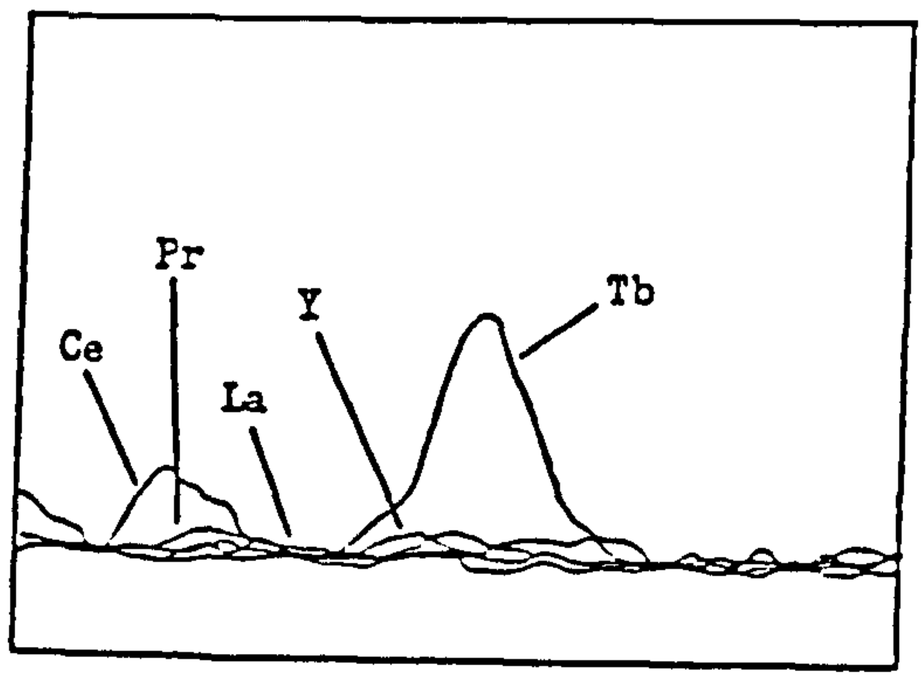

(B)

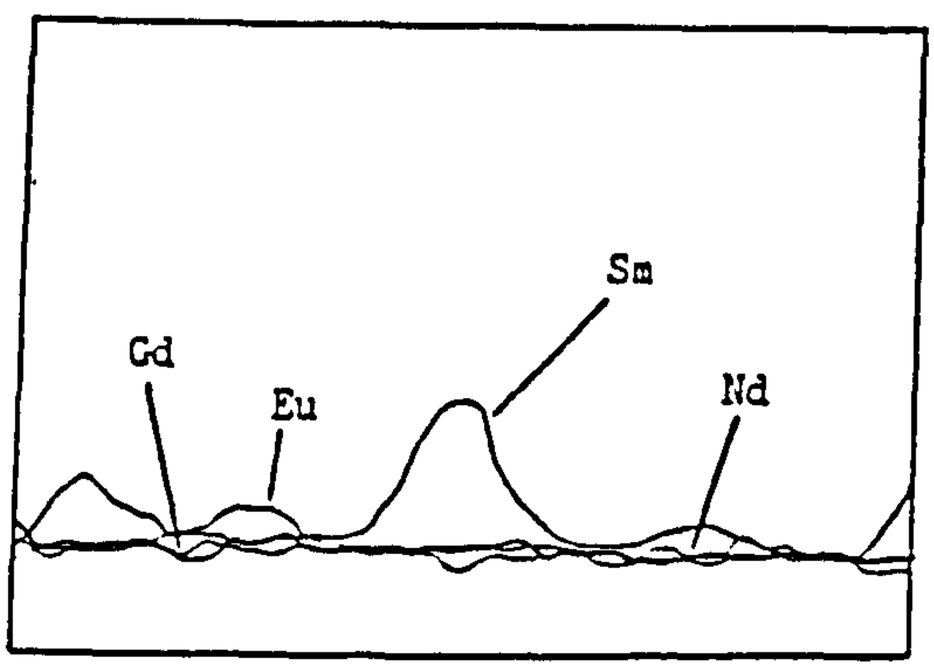

(C)

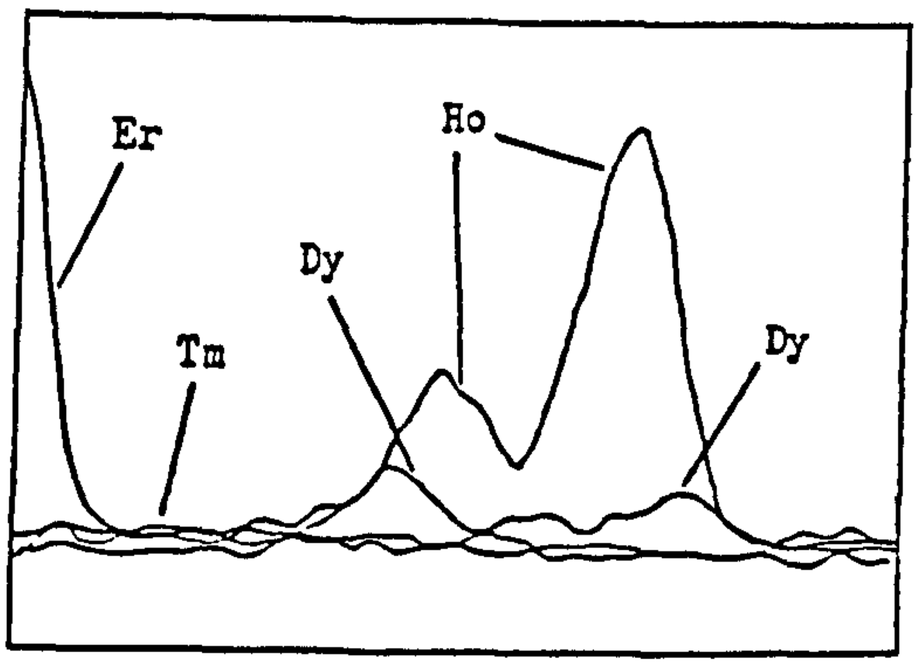

(D)

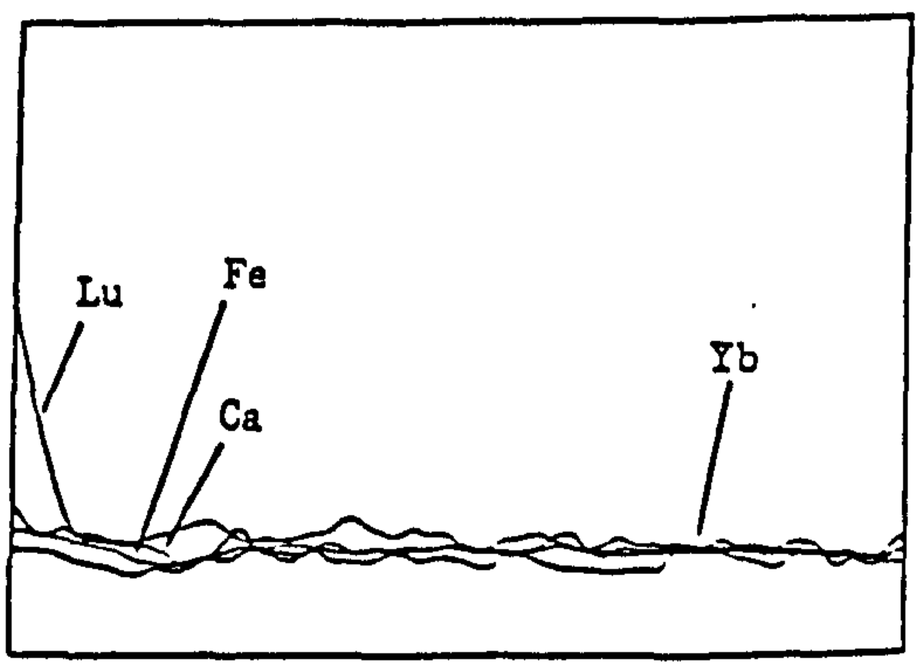

Figures (6.30-A to 6.30-D)

Photoreduction of re-drawn high resolution scan spectra at dysprosium wavelength (353.17 nm) - window = 0.112 nm , concentration of Dy = 0.2 mg dm^{-3} , concentration of each REE = 10 mg dm^{-3} , concentration of Ca or Fe = 100 mg dm^{-3} .

(A)

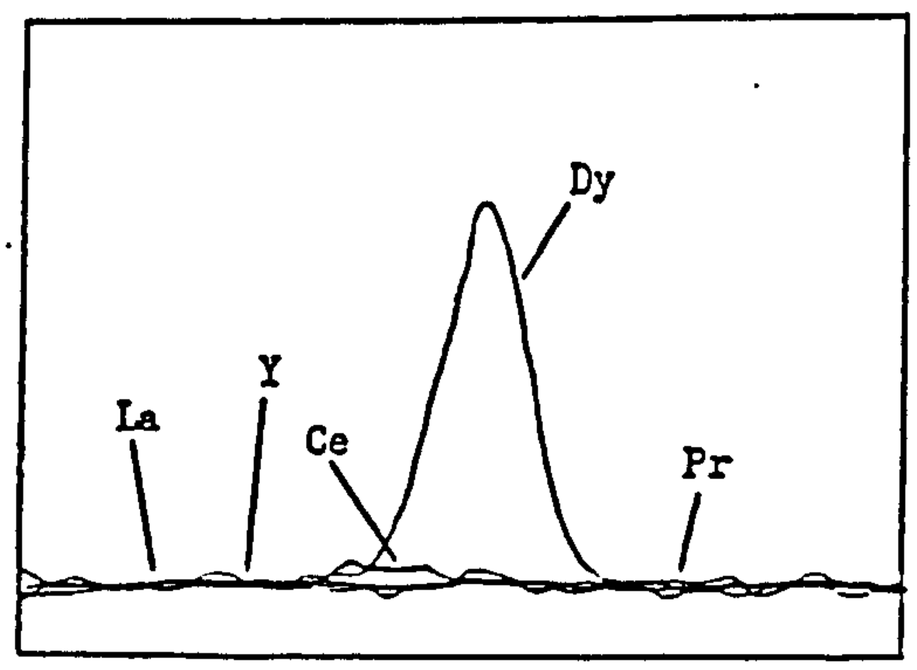

(B)

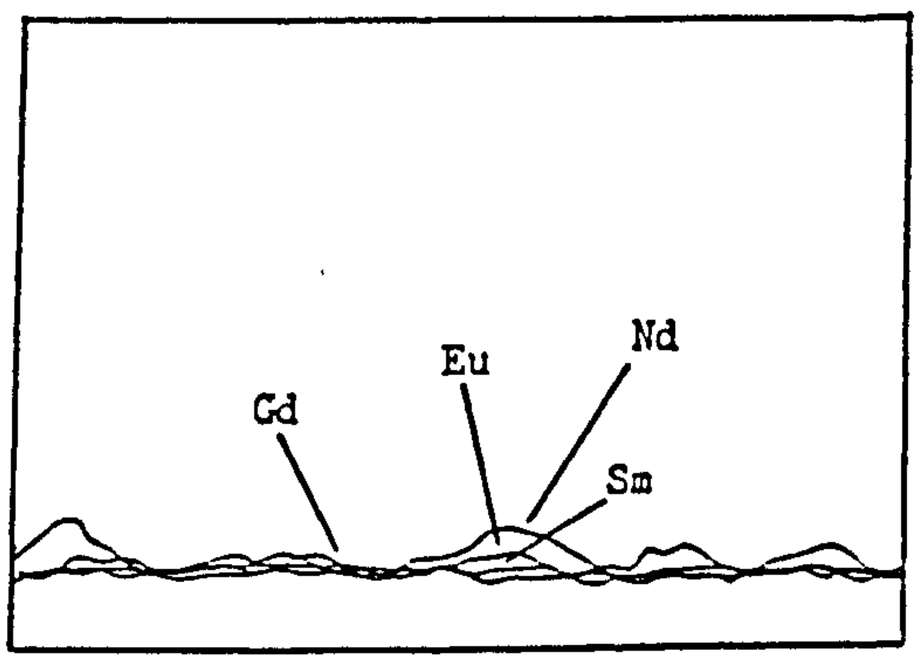

(C)

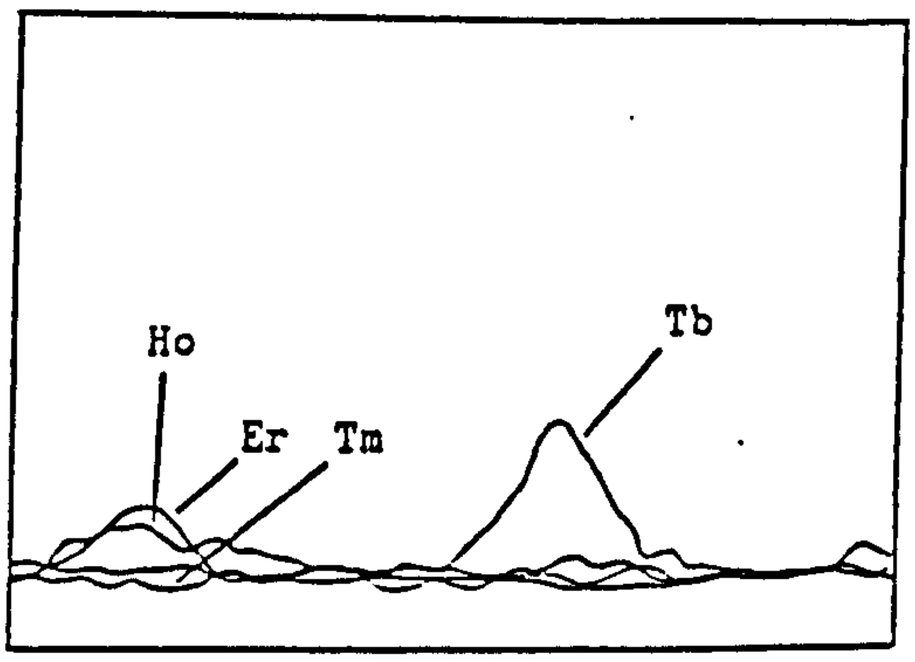

(D)

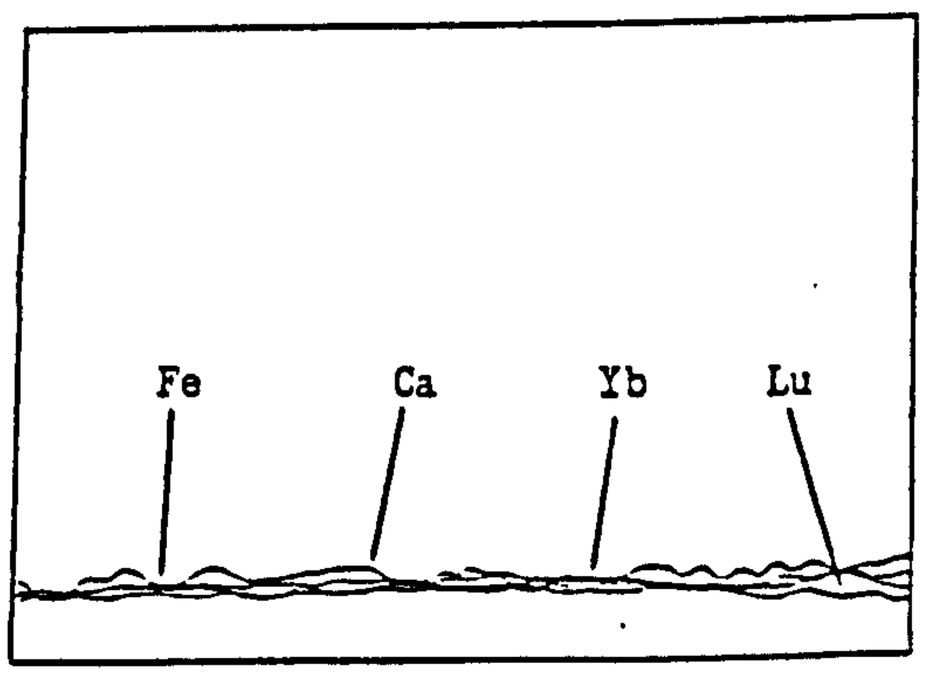

Figures (6.31-A to 6.31-D)

Photoreduction of re-drawn high resolution scan spectra at holmium wavelength (345.6 nm) - window = 0.11 nm , concentration of Ho = 0.1 mg dm^{-3} , concentration of each REE = 10 mg dm^{-3} , concentration of Ca or Fe = 100 mg dm^{-3} .

(A)

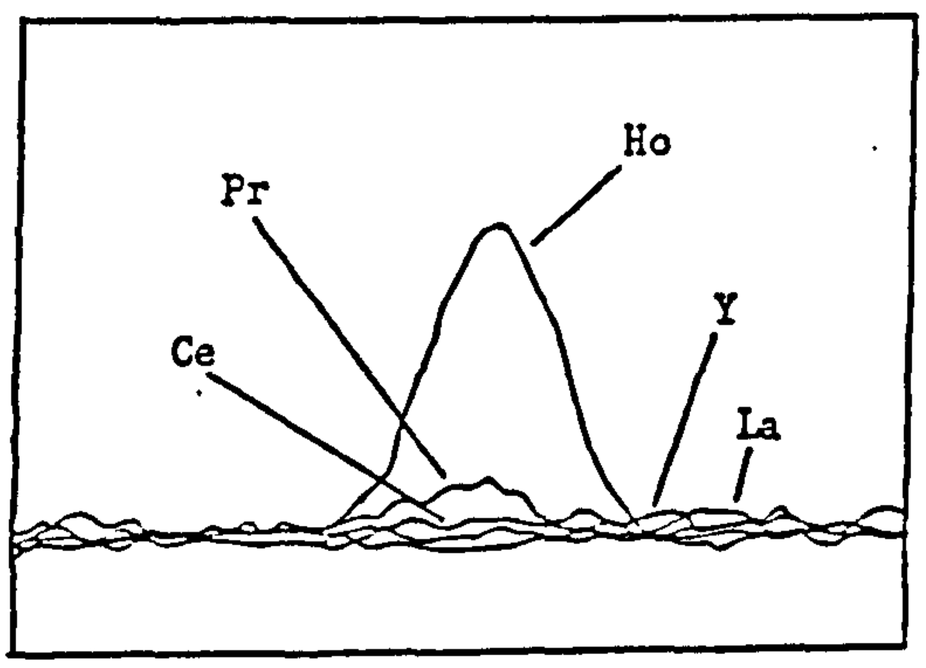

(B)

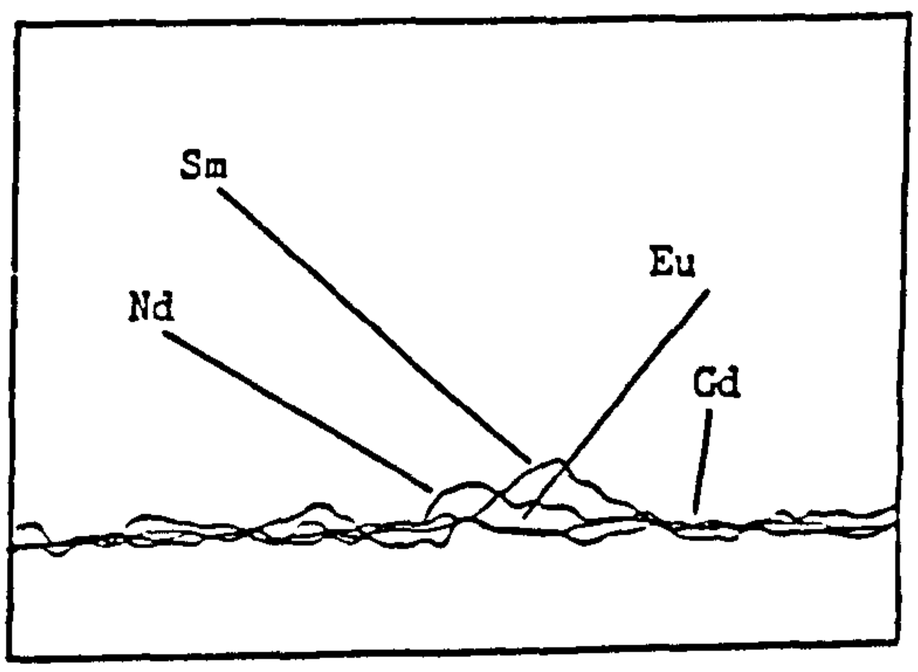

(C)

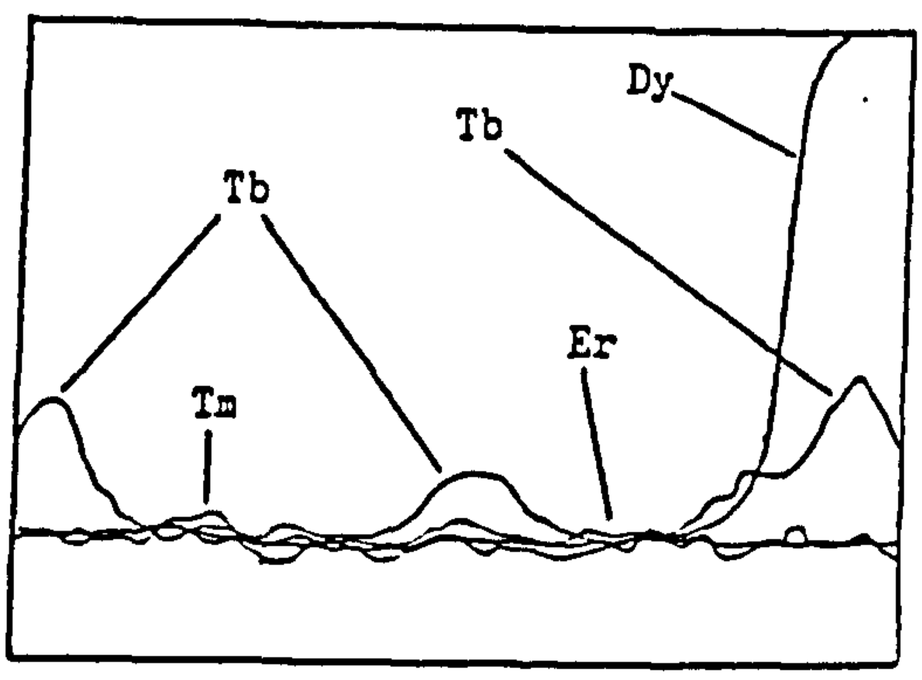

(D)

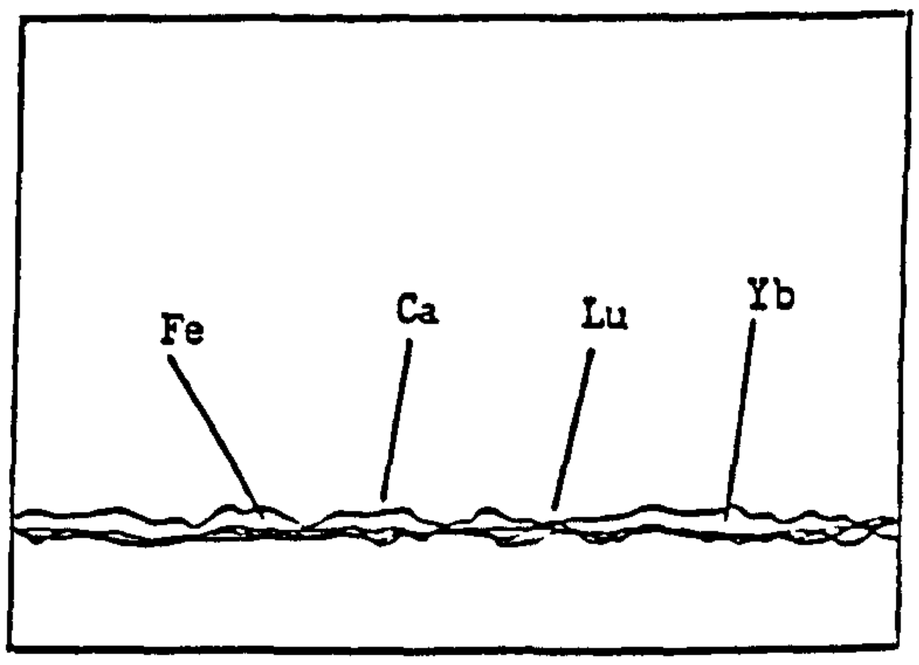

Figures (6.32-A to 6.32-D)

Photoreduction of re-drawn high resolution scan spectra at erbium wavelength (337.271 nm) - window = 0.107 nm , concentration of Er = 0.2 mg dm^{-3} , concentration of each REE = 10 mg dm^{-3} , concentration of Ca or Fe = 100 mg dm^{-3} .

(A)

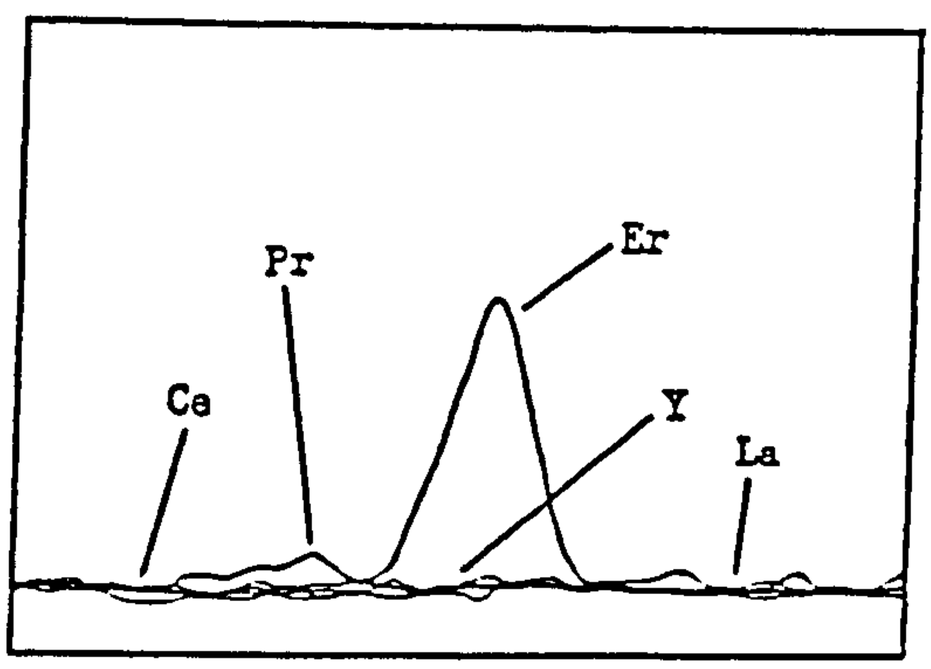

(B)

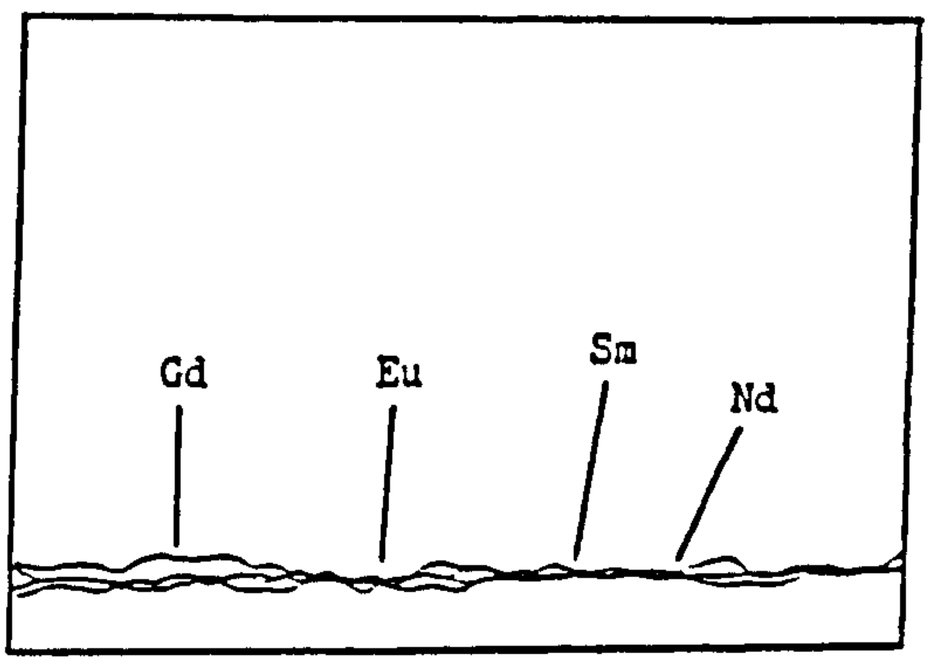

(C)

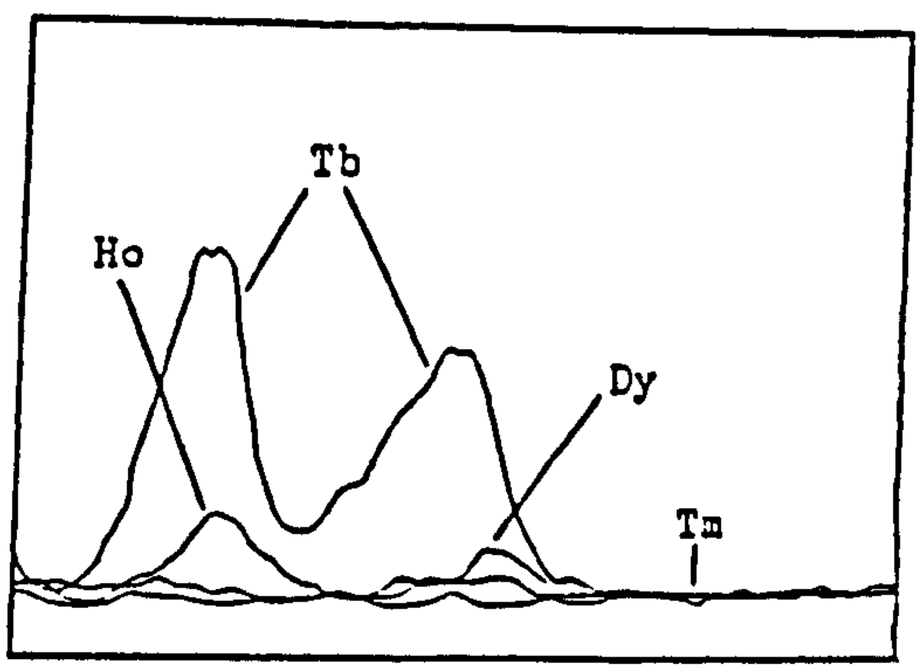

(D)

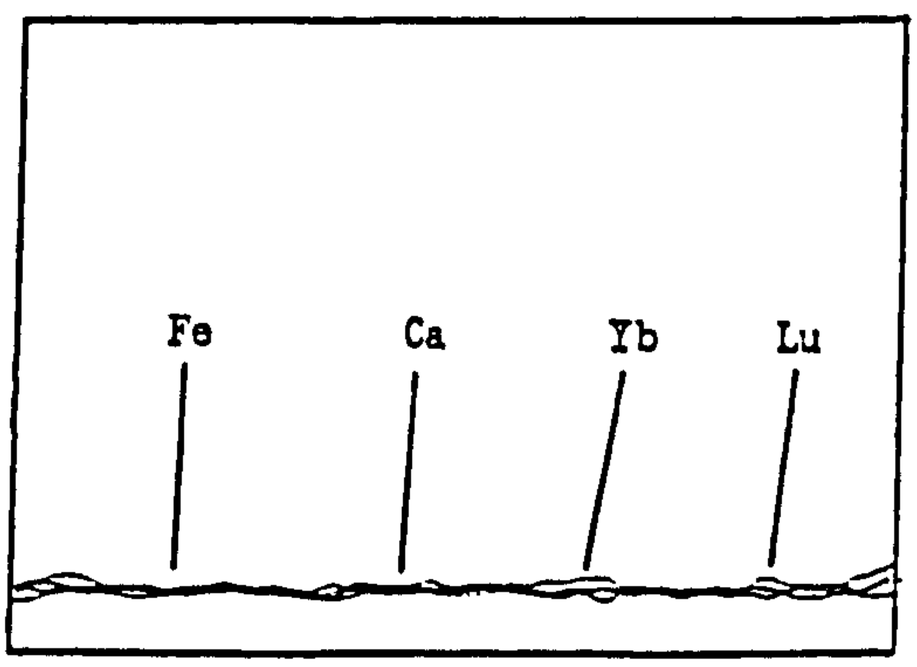

Figures (6.33-A to 6.33-D)

Photoreduction of re-drawn high resolution scan spectra at thulium wavelength (313.126 nm) - window = 0.1 nm , concentration of Tm = 0.2 mg dm^{-3} , concentration of each REE = 10 mg dm^{-3} , concentration of Ca or Fe = 100 mg dm^{-3} .

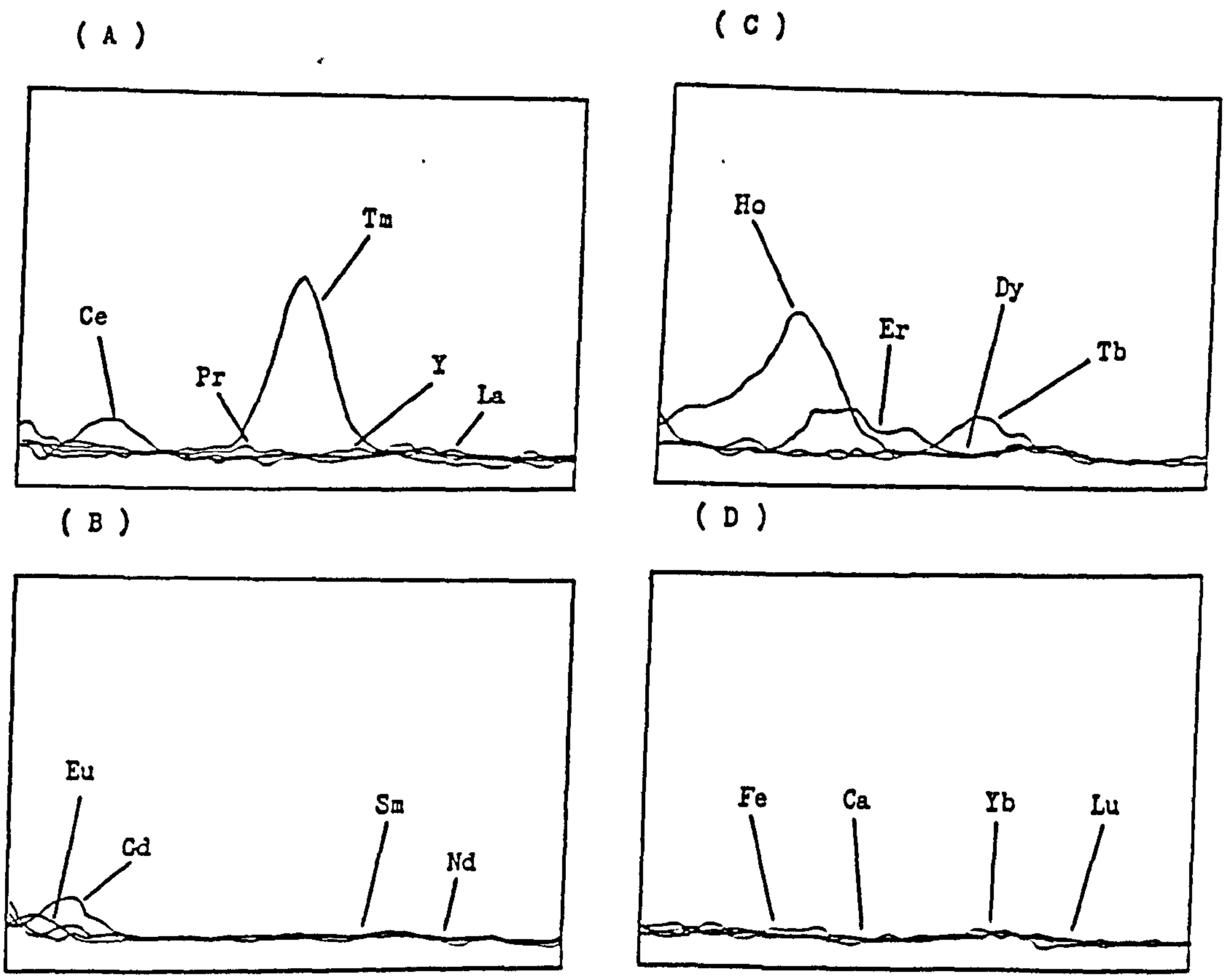

Figures (6.34-A to 6.34-D)

Photoreduction of re-drawn high resolution scan spectra at ytterbium wavelength (328.937 nm) - window = 0.105 nm , concentration of Yb = 0.02 mg dm^{-3} , concentration of each REE = 10 mg dm^{-3} , concentration of Ca or Fe = 100 mg dm^{-3} .

(A)

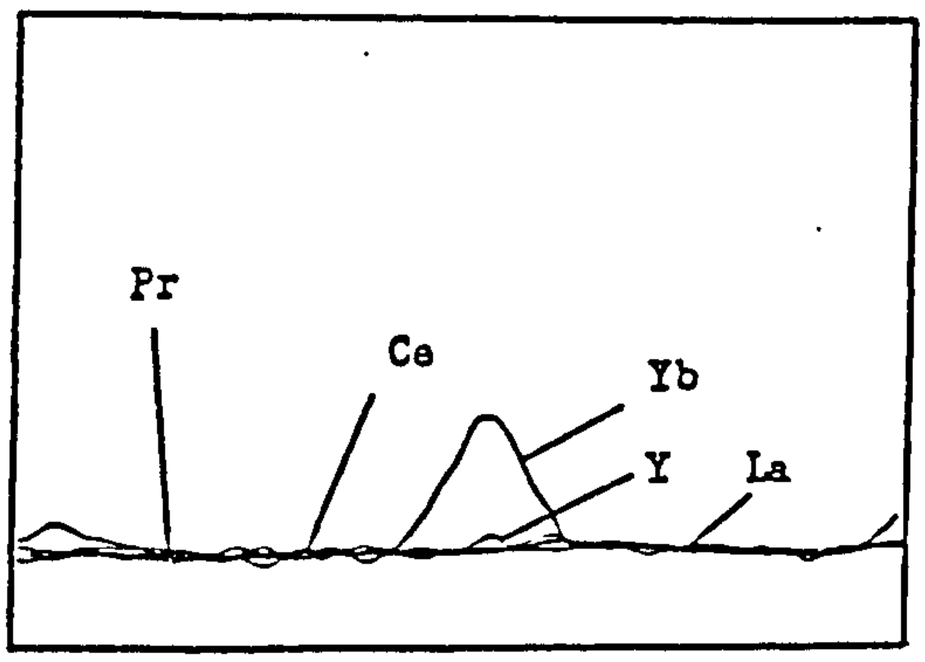

(B)

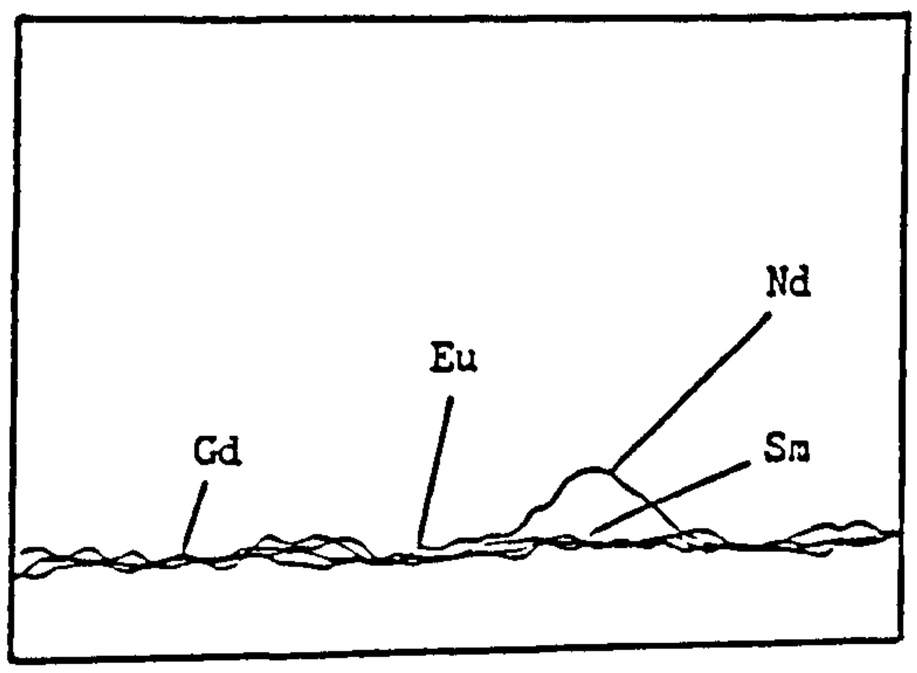

(C)

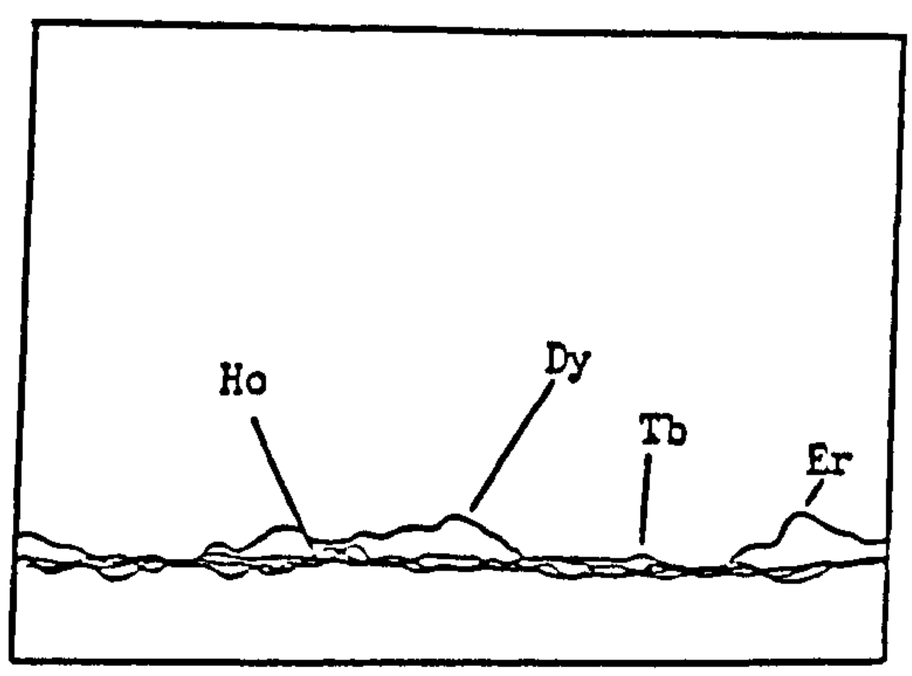

(D)

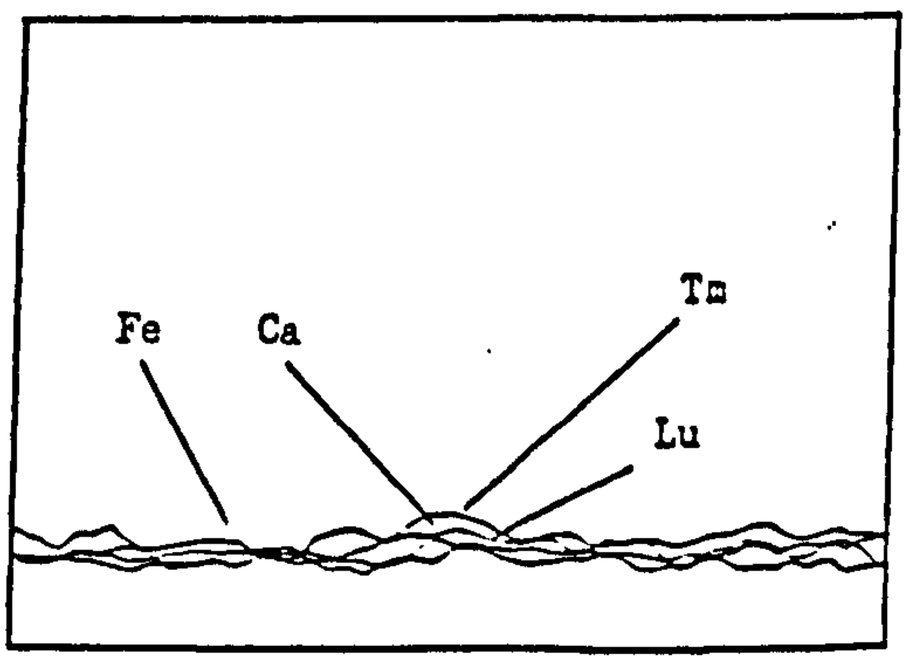

Figures (6.35-A to 6.35-D)

Photoreduction of re-drawn high resolution scan spectra at lutetium wavelength (261.542 nm) - window = 0.085 nm , concentration of Lu = 0.08 mg dm^{-3} , concentration of each REE = 10 mg dm^{-3} , concentration of Ca or Fe = 100 mg dm^{-3} .

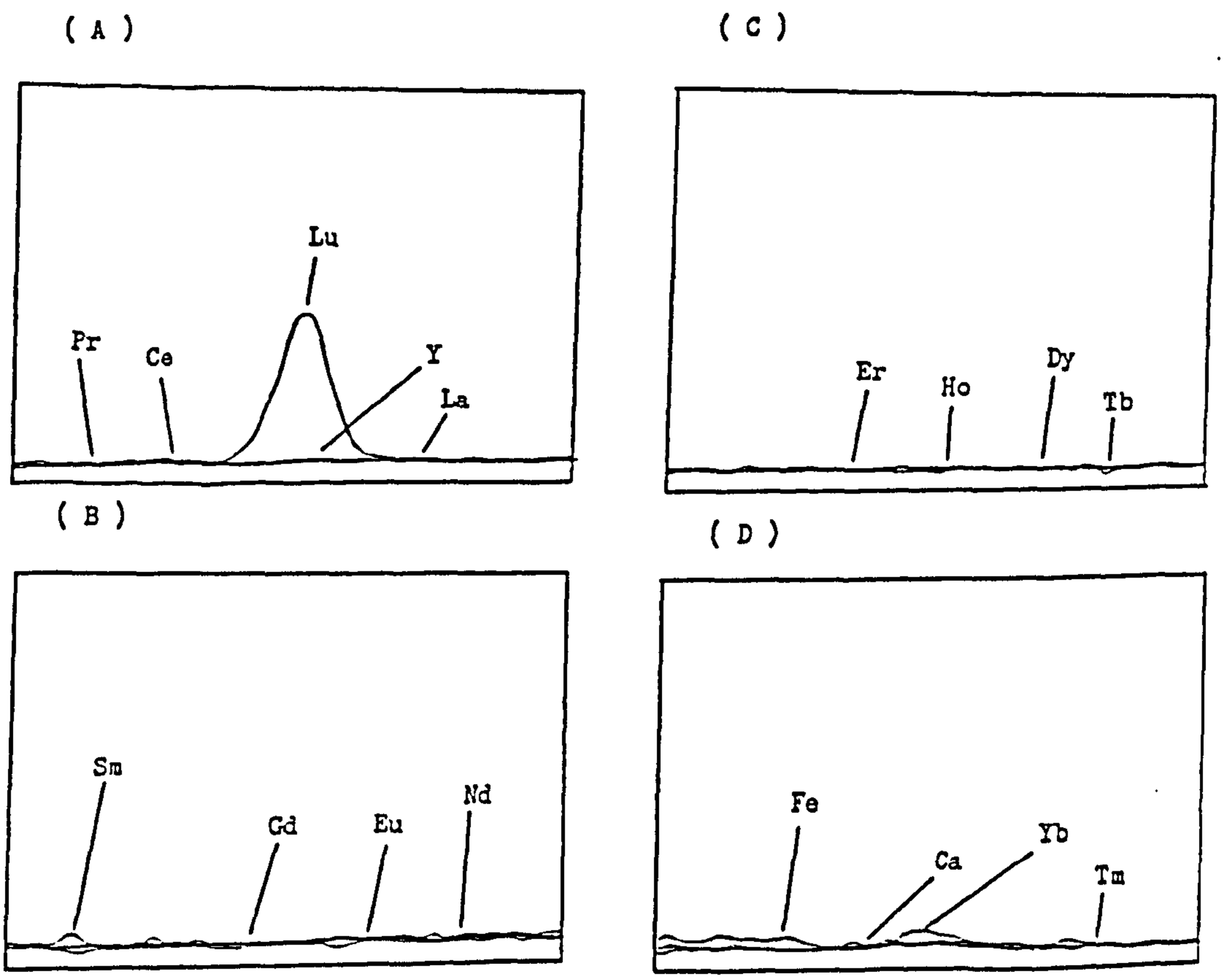

analyte most sensitive ionic wavelength (see table 2.6) for the measurements of analyte concentration in the sample, while the background intensity was measured at approximately equal spacing at about 0.025 nm from the analyte wavelength on both sides of the line. This meant that the background intensities were measured in the first and the last quarters of the modulation interval.

6.2.3 Equivalent Interferant Concentrations.

The equivalent interferant concentration calculated from signal given by the interferant at the analyte wavelength using the net signal is now considered. For the analysis of the cation exchange separation eluate the interferences are often smaller than estimated previously for the analysis of the anion exchange separation eluate (compare Table 6.2 [anion] with Table 6.4 [cation]). For parial line interferences the emission at the background wavelength may compensate for the emission at the analyte wavelength. Indeed, for these elements whose presence affect the background only, the interference will be negative. The interferences of all the rare earth elements are summarised in Table 6.4, where the equivalent interferent concentrations are recorded for the conditions chosen and the apparatus used for the analysis of the solution from the cation exchange separation .

TABLE 6.4

EQUIVELANT CONCENTRATION (mg dm^{-3}) CORRESPOND TO THE INTRODUCTION OF 10 mg dm^{-3} OF THE INTERFERRENT ELEMENT AT ANALYTE WAVELENGTH - WITH BACKGROUND CORRECTION.

ANALYTE	Y	La	Ce	Pr	Nd	Sm	Eu	Gd	Tb	Dy	Ho	Er	Tm	Yb	Lu
INTERFERENT															
Y	*	*	*	*	*	-0.01	*	*	*	*	*	*	*	*	*
La	*	*	*	*	*	*	*	*	*	*	*	*	*	*	*
Ce	-0.02	-0.02	*	1.0	0.94	*	*	-0.06	*	*	*	*	-0.01	*	*
Pr	*	0.07	-0.07	*	0.05	*	*	-0.01	*	*	0.02	*	*	*	*
Nd	*	0.01	-0.04	0.01	*	0.04	0.03	*	*	0.03	0.02	0.01	*	*	*
Sm	*	*	*	*	*	*	*	*	0.11	*	*	*	0.01	*	*
Eu	*	*	*	*	*	*	*	*	-0.02	0.01	*	*	*	*	*
Gd	*	*	*	*	*	0.37	*	*	*	*	*	*	*	*	*
Tb	*	*	*	-0.01	-0.01	*	*	0.04	*	0.01	0.03	0.11	0.01	*	*
Dy	-0.01	*	-0.02	*	*	*	*	-0.01	*	*	0.02	*	*	0.01	*
Ho	*	*	*	*	-0.02	-0.2	*	0.04	-0.05	*	*	*	-0.12	*	*
Er	0.01	*	*	0.23	-0.02	*	*	*	*	*	*	*	-0.02	*	*
Tm	*	*	*	*	*	*	*	*	*	*	*	*	*	0.01	*
Yb	0.01	*	*	*	*	*	*	*	*	*	*	*	*	*	*
Lu	*	*	*	*	*	*	*	*	*	*	*	*	*	*	*

N.B.:- * MEANS THAT THERE IS NO INTERFERENCE OR THE INTERFERENCE IS TOO SMALL (0.01 mg dm^{-3}), AND MAY BE TAKEN AS HAVING ZERO EQUIVELANT CONCENTRATION.

6.2.4 Correction for Interferences.

The calculation used to correct for the spectral interferences in the analysis of the solution from the anion exchange separation is suitable for the cation exchange conditions. However, the net signal (i.e. signal at the analyte wavelength minus the average signal at the selected background wavelength) must be used throughout for the cationic system instead of the signal at the analyte wavelength used previously in the anionic case.

Using the nett signals, (S_{TA}, and S_{TF}) values of H_{AA}, and A_{FA} were calculated and a modified computer programme similar to that used earlier was developed (see section 6.1.3). The only important changes were in the values of H_{FA} used and the omission of the element thorium. The elements calcium and iron were not included in the computer program since the H_{FA} values were zero. This program (appendix 2) was used later in the analysis of phosphate rock samples by the cation exchange separation method.

6.3 Comparison of the Optimum Conditions for Plasma Excitation with and without Methanol in the Sample.

In this section the optimisation of plasma parameters in the presence and the absence of methanol

are compared. The plasma parameters are carrier gas flow rate, auxiliary gas flow rate and the plasma gas flow rate. All tested elements (see section 6.1.1) in the methanolic solution show a similar response when the plasma parameters are changed and holmium was chosen to illustrate a typical behaviour, in methanolic solution, as had been stated before. Only lanthanum was used to optimise the plasma for aqueous solutions.

Over the common range of the carrier gas flow rates used for both sets, from 0.5 to 0.75 dm^3 min^{-1}, some similarities, between the methanolic and aqueous solutions observed in the trends were for analyte signal and background intensity. It was not possible to operate the plasma at a carrier gas flow rate lower than 0.5 dm^3 min^{-1} when methanol was present in the solution. In the operating range the main difference between the two optimisations is in the increase in anode current which occurs as the carrier gas flow rate increases for the methanolic solution. The decrease in the signal and background intensities at higher carrier gas flow rates was a direct consequence of the lower residence time of the aerosol in the coil region, and was also due to a possible increased cooling effect of the carrier gas stream on the plasma gases. This increase in anode current implied an increase in the applied power due to an increase of the coupling of RF energy into the plasma at a higher flow rate in the

presence of methanol. When aspirating aqueous solutions containing no organic species the anode current did not change with an increase in the carrier gas flow rate.

In the optimisation of the auxiliary gas flow rate with the two set of solutions, it was noticed that it was not possible to operate the plasma at an auxiliary gas flow rate higher than 1.125 dm^3 min^{-1} when methanol was present in the solution. A higher flow rate, up to 2.4 dm^3 min^{-1} was reached when an aqueous solution was used. There are no apparent differences between the trend of the signal intensity, background intensity and anode current as the auxiliary gas flow rate is increased, for the two sets of measurements (organic and aqueous). Under similar conditions the same anode current was observed in the two optimisations and if a higher flow rate could have been used with the organic solution, a similar anode current would have been observed.

The change in the signal and background intensities with an increase of the plasma gas flow rate is similar for the two sets of results and there is no peak in the signal plot. The main difference was in the change in anode current with change in the plasma gas flow rate. For the organic solution, the anode current increased with an increase in the gas flow rate, but no change was observed with the aqueous solution and

there are no clear reasons for this difference. Although the optimum conditions for the plasma gas flow rate are different for the two sets of solutions, the optimum anode current is the same in both cases (400 mA).

The anode current range applied to the plasma when optimising with the two sets of solutions were different. With the methanolic solution the minimum current which could be used was 400 mA while a lower current (340 mA) could be applied when optimising with aqueous solution. For both optimisation experiments the signal and the background intensities increased with an increase in the anode current, but the signal to background ratio decreased continuously from 360 mA upwards for aqueous solution and 400 mA for methanolic solution. These values therefore were the optimum current settings for the aqueous and methanolic solution, respectively.

On the basis of the signal to background ratios, the optimum observation heights were 20 mm for the aqueous solution and 9 mm for the methanolic solution. The net analyte intensity was at a maximum of 6 mm for the methanolic and 14 mm for the aqueous solutions. For the methanolic solution the background intensity decreased continuously from 4 mm to 10 mm, where as for the aqueous solution the background had a

maximum at 9 mm. The energy gradient in the plasma is lower when methanol is present probably because of the energy required to dissociate the methanol. Hence, the same effective ionising power is reached at a lower height for methanol (9 mm) than for aqueous solution (20 mm). The anode current is of course higher for methanol (400 mA) than for water (360 mA) because of the power needed to dissociate the methanol (under the same conditions of rare earth elements ionisation).

The final optimum conditions for the two sets of solutions (organic and aqueous), see Tables 6.1 and 6.3, were used to analyse a solution containing 0.25 mg dm^{-3} of each of the rare earth elements. Although the analyte and the background intensities obtained with the aqueous optimisation parameters was 2 to 5 times smaller than those obtained with the other set of optimisation, the signal to background ratios ((S-B)/B) are similar for most elements, as can be seen in Table 6.5.

Table 6.5 A comparison of the signals and background intensities and signal to background ratios for a solution contain 0.25 mg cm^{-3} of each of the rare earth elements

	CATION EXCHANGE			ANION EXCHANGE		
ANALYTE	S	B	SBR	S	B	SBR
Y	2818	220	11.81	10663	629	15.95
La	2587	480	4.39	10311	1750	4.89
Ce	1291	645	1.00	3611	1903	0.90
Pr	480	255	0.88	1563	719	1.17
Nd	1286	420	2.06	5175	1621	2.19
Sm	515	229	1.25	1212	470	1.58
Eu	5607	289	18.71	22245	957	22.25
Gd	737	208	2.54	2468	609	3.05
Tb	1088	306	2.56	4761	1019	3.67
Dy	1327	176	6.54	5278	577	8.15
Ho	2674	377	6.09	8883	1049	7.47
Er	1394	200	5.97	4481	624	6.18
Tm	949	190	4.00	4149	636	5.52
Yb	10042	265	36.89	32269	986	31.73
Lu	2348	121	18.41	8996	394	21.83

S Analyte signal intensity

B Background signal intensity

SBR Signal to background ratio ((S-B)/B)

Chapter Seven.

EVALUATION OF THE METHOD OF RARE EARTH ESTIMATION USED.

7.1 Neutron Activation Analysis.

The neutron activation analysis was used to analyse the six phosphate samples to test the validity of the anion exchange separation procedure. The results, see Tables 7.3 to 7.8, clearly demonstrate that the yield of the anion exchange was low. The high concentration of phosphate in the samples (ie. 20 to 30%), which produced a significant level of beta emitting 32_p, gave rise to Bremsstrahlung radiations. This gave a high background radiation over which the gamma peaks of the rare earths must be measured. For regular analysis of phosphate rocks by activation analysis, it is desirable that this activity should be eliminated by separation (either by pre- or post-irradiation). However, such a separation would take some time to optimise and develop and was not carried out. Another disadvantage of analysing these samples by activation was the low concentration of the rare earth elements which gave a large statistical counting error (more than 20%) for some of the rare earths: holmium, cerium, neodymium, yetterbium and lutetium. The short half life of some elements increased the statistical counting error.

The limited results obtained by neutron activation analysis were used primarily for guidance during the chemical development. However, they can be compared with the results of the finally established chemical method (cation exchange).

7.2 Comparison of Anion Exchange and Cation Exchange with Neutron Activation Analysis.

Six samples of phosphate rock (viz:- S-S-2, C-TH-SC-1A, SAND-TH-SC-1, CHALK-TH-SC-1, F-TH-SC-1 and S-G-1) have been analysed by all three procedures, anion exchange, cation exchange and neutron activation analysis.

Generally the anion exchange procedure gives lower results than those obtained by cation exchange, while neutron activation analysis always gave much higher results. This can be seen in Table 7.1. The results for the light rare earths by the two ion exchange methods agree generally better than the results for the heavy rare earths, but both give lower results than neutron activation analysis, as can be seen in Table 7.2. A full list of all the rare earths measured by the three procedures are shown in Tables 7.3 to 7.8. The analysis show that yttrium is poorly absorbed by the anion exchange resin. Light rare earth recoveries by anion exchange agree roughly, while the heavy rare

Table 7.1

A comparison of the total rare earths measured in the three procedures.

Sample	Rare Earth Concentration *		
	Anion Exchange	Cation Exchange	N.A.A.
SS-2	23	49	152
CTHSC-1A	107	83	174
SAND THSC-1	99	145	205
CHALK THSC-1	36	69	118
SG-1	199	168	203
FTHSC-1	71	75	87

* This is the sum of the concentration (mg kg^{-1}) of the 8 rare earths can be estimated by N.A.A. (ie. La, Ce, Nd, Sm, Eu, Ho, Yb and Lu).

Table 7.2

A comparison of the sum of the light and the sum of the heavy rare earths measured in the samples with different procedures.

Samples	∑ Light Rare Earths*			∑ Heavy Rare Earths**		
	Anion Exch.	Cation Exch.	N.A.A.	Anion Exch.	Cation Exch.	N.A.A.
SS-2	22	28	144	0.2	2.9	7.2
CTHSC-1A	107	79	164	0.3	4.5	10.6
SAND THSC-1	99	137	195	0.5	7.4	10.0
CHALK THSC-1	36	66	109	0.3	3.2	8.9
SG-1	197	155	185	2.4	12.5	17.3
FTHSC-1	70	72	78	0.5	3.5	9.5

* Light rare earths is the sum of La, Ce, Nd, Sm and Eu (mg kg^{-1}).

** Heavy rare earths is the sum of Ho, Yb and Lu (mg kg^{-1}).

Table 7.3

A comparison of the results (mg kg^{-1}) of the sample (SS-2).

Analyte	Anion Exchange	N.A.A.	Cat. Exch.
Y	7.26		32.6
La	5.93	20.8±2.3	15.2
Ce	12.2	57.3±12	15.5
Pr	1.91		0.73
Nd	8.33	7.8±2	13.5
Sm	1.04	10.7±0.2	1.13
Eu	0.39	0.6±0.1	0.25
Gd	0.64		2.02
Tb	0.51		0.50
Dy	0.66		2.50
Ho	0.18	3.5±1	0.94
Er	1.22		2.51
Tm	0.26		0.55
Yb	0.47	2±0.5	1.64
Lu	0.1	1.1±0.1	0.3
Th	1.51		

Table 7.4

A comparison of the results (mg kg^{-1}) of sample (CTHSC-1A).

Analyte	Anion Exchange	N.A.A.	Cat. Exch.
Y	5.37		55.9
La	43.9	40.8±4.3	29.8
Ce	53.3	79.4±14	18.1
Pr	2.27		6.46
Nd	36.4	15.0±4	26.8
Sm	4.44	38.6±0.2	3.57
Eu	0.67	1.2±0.3	0.67
Gd	1.77		4.63
Tb	1.07		0.75
Dy	1.18		5.13
Ho	0.18	3.5±1	1.11
Er	2.61		4.23
Tm	0.29		0.69
Yb	0.41	3.8±0.8	2.92
Lu	0.14	1.1±0.1	0.5
Th	2.92		

Table 7.5

A comparison of the results (mg kg^{-1}) of sample (SAND THSC-1).

Analyte	Anion Exchange	N.A.A.	Cat. Exch.
Y	10.08		96.8
La	33.3	44.3±3	46.0
Ce	46.0	107±15	58.3
Pr	2.29		11.3
Nd	25.6	18.9±4	24.3
Sm	5.71	18.2±0.2	7.19
Eu	1.31	1.65±0.5	1.59
Gd	2.71		7.92
Tb	0.73		1.14
Dy	1.92		8.28
Ho	0.33	3.5±1	1.81
Er	3.15		6.29
Tm	0.30		1.27
Yb	0.82	4.7±1	4.62
Lu	0.14	1.8±0.1	0.97
Th	1.87		

Table 7.6

A comparison of the results (mg kg^{-1}) of sample (CHALK-THSC-1).

Analyte	Anion Exchange	N.A.A.	Cat. Exch.
Y	5.24		39.0
La	8.48	28.5±3.2	24.3
Ce	20.4	57.2±11	30.9
Pr	1.44		3.42
Nd	16.3	7.4±3	7.91
Sm	1.82	17.6±0.2	2.43
Eu	0.77	0.9±0.2	0.54
Gd	1.04		3.26
Tb	0.82		0.43
Dy	0.76		3.27
Ho	0.14	3.5±1	0.60
Er	4.24		3.24
Tm	0.26		0.33
Yb	0.41	3±1	2.19
Lu	0.13	1.6±0.1	0.43
Th	2.84		

Table 7.7

A comparison of rare earths concentration ($mg\ kg^{-1}$) in sample (F-TH-SC-1).

Analyte	Anion Exchange	N.A.A.	Cat. Exch.
Y	6.28		48.9
La	23.5	33.8±3.4	24.1
Ce	27.7	N.D.	31.9
Pr	1.85		4.99
Nd	17.0	11.3±3	9.93
Sm	1.89	24.4±0.1	2.61
Eu	0.16	0.2±0.1	0.75
Gd	0.94		3.51
Tb	0.24		0.41
Dy	0.53		3.55
Ho	0.13	3.5±1	0.72
Er	0.73		3.11
Tm	0.13		0.33
Yb	0.31	3.7±1	2.62
Lu	0.04	2.3±0.1	0.44
Th	0.82		

N.D. not detected.

Table 7.8

A comparison of rare earths concentration ($mg\ kg^{-1}$) in sample (S-G-1).

Analyte	Anion Exchange	N.A.A.	Cat. Exch.
Y	199.3		146.9
La	87.4	102.8±9.7	74.8
Ce	42.7	N.D.	32.6
Pr	3.77		11.1
Nd	56.4	39.7±8	32.1
Sm	9.9	26.4±0.2	6.91
Eu	0.54	3.3±0.9	1.65
Gd	6.29		9.69
Tb	1.38		1.64
Dy	4.14		11.1
Ho	0.68	4.33±1	2.64
Er	2.62		9.72
Tm	0.39		1.34
Yb	1.48	9.8±3	7.44
Lu	0.22	3.2±0.1	1.71
Th	1.29		

N.D. not detected.

earths are more completely recovered by the cation exchange resin than the anion exchange resin, as previously noted (see Chapters 4 and 5). Cerium was not detected in two samples (S-G-1 and F-TH-SC-1) by neutron activation in spite of the high concentration revealed by the anion and cation exchange procedures. This is clearly an erroneous result and neutron activation analysis was dropped from further consideration.

7.3 Recoveries after Standard Addition for the Cation Exchange Procedure.

The cation exchange procedure was considered to give the best results and was tested for recovery and precision using nine samples, SAND-TH-SC-1, C-TH-SC-1A, S-S-2, S-G-1, F-TH-SC-1, CHALK-TH-SC-1, C-A-1, CONG-G-1 and S-A-12, which have a variety of major oxide composition (see Chapter 3) including calcareous, siliceous, conglomeratic and almost pure apatite.

In order to calculate the recovery, rare earths were added to the samples during the dissolution stage in a concentration about three times that present in the sample. The recovery of each element was calculated using the formula.

$$R\% = \frac{M_T - M_S}{M_A} * 100$$

Where $R\%$ = the recovery of the element.

M_T = the total concentration of the element measured after standard addition.

M_S = the concentration of the element measured in the sample without standard addition.

M_A = the concentration of the element added to the sample. ($M_A \simeq 3 * M_S$).

The calculated recoveries, see Table 7.9, for the nine samples show great variation both from one element to another and from one sample to another. The average recoveries are high, 81-93%, this is true for all the elements except for medium rare earths, samarium, europium and gadolinium, where the average recovery was lower (77%).

The three apatite samples (SAND-TH-SC-1, C-TH-SC-1A and F-TH-SC-1) gave a similar pattern of low recovery for the middle rare earths, see Figure 7.1, samarium, europium, gadolinium and terbium. Another sample, C-A-1, gave a low recovery for the light rare earths, yttrium, lanthanum, praseodymium and neodymium. The best recovery for all elements was observed with the sample CHALK-TH-SC-1. Two of the three siliceous samples show low recovery for praseodymium and while

Table 7.9

Calculated recoveries (%) of the rare earths from different samples.

	A	B	C	D	E	F	G	H	I	AVE
Y	94.8	94.8	81.0	99.0	99.6	67.7	62.0	86.1	89.5	85.4
La	84.9	92.2	84.2	96.0	101.6	80.3	74.9	76.7	89.5	86.7
Ce	93.0	102.3	87.0	95.0	102.6	66.3	78.0	76.1	97.6	88.6
Pr	88.5	75.6	83.9	80.9	100.3	68.4	68.2	74.2	85.1	80.6
Nd	80.7	93.3	89.1	75.5	88.4	81.3	70.8	98.0	63.1	82.2
Sm	70.2	72.5	68.2	70.7	91.6	78.6	75.0	75.6	98.8	77.9
Eu	76.0	54.4	67.0	78.0	79.0	74.0	80.0	85.0	96.0	76.6
Gd	77.2	73.3	70.4	95.5	91.8	50.8	82.0	76.2	96.1	78.8
Tb	73.0	82.0	72.0	77.5	96:0	79.0	80.0	106.0	88.0	83.7
Dy	86.2	90.7	83.8	85.9	98.6	50.9	81.1	73.6	93.1	82.6
Ho	82.4	81.2	83.2	96.6	89.2	66.0	77.2	96.0	94.4	85.0
Er	94.4	91.6	91.4	94.0	98.5	66.4	79.8	80.3	91.6	87.6
Tm	85.5	97.9	84.0	90.5	87.0	77.0	97.0	71.0	99.0	87.8
Yb	88.9	98.8	87.8	99.5	91.0	76.4	81.0	79.2	87.8	87.8
Lu	101.0	101.0	91.0	93.0	98.0	78.0	84.0	99.0	92.0	93.0

A - SAND THSC-1

B - CTHSC-1A

C - FTHSC-1

D - SG-1

E - CHALK THSC-1

F - SS-2

G - CA-1

H - CONG G-1

I - SA-12

AVE - AVERAGE.

Figure (7.1)

Recovery of rare earths from phosphate rock samples using cation exchange separation procedure .

Sample	Y.	La	Ce	Pr	Nd	Sm	Eu	Gd	Tb	Dy	Ho	Er	Tm	Yb	Lu
SAND-TH-SC-1															
C-TH-SC-1A															
F-TH-SC-1															
S-C - 1															
CHALK-TH-SC-1															
S-S-2															
C - A - 1															
CONG - C - 1															
S - A - 12															

recovery

> 75 %	
< 75 %	
< 60 %	

S-G-1 is low for samarium, but otherwise gave high recovery. The other silicous sample, S-S-2, produced the worst recovery (<75%) for eight elements from the light and the heavy rare earth elements.

7.4 Precision of the Cation Exchange Separation.

The precision of the analytical results is a measure of the variation between replicate analysis. The smaller the variation in these values and the greater the mean value, the greater the precision. The degree of precision expected is variable and depends upon the nature of the element, its concentration, the sample composition and the technique being used to determine it.

The precision for the cation exchange procedure was calculated from replicate analysis of the previous nine samples. These were analysed completely, that is dissolved, separate and measured several times. The mean and standard deviation was calculated for each element. The results show a great variation in the relative standard deviation for each element from sample to sample and element to element, as shown in Tables 7.10 to 7.12. From these tables it can be seen that praseodymium and lutetium give a very high relative standard deviation (about 17%) was obtained for terbium and thulium for all the samples. The rest of the

Table 7.10

Rare earths concentration (mg kg^{-1}) in three phosphate samples.

	SA-12			CA-1			CONG G-1		
	NUMBER OF DUPLICATES								
	2			3			2		
	A	B	C	A	B	C	A	B	C
Y	19.43	0.81	4.15	38.50	1.35	3.12	117.37	2.42	2.06
La	8.60	0.85	9.87	19.62	2.87	14.63	60.5	4.99	8.25
Ce	2.48	0.36	14.54	6.57	0.53	8.07	21.41	2.52	11.76
Pr	0.33	0.07	21.43	1.39	0.40	28.57	5.66	1.30	22.97
Nd	5.06	0.20	3.95	5.06	0.31	6.13	26.52	1.30	4.91
Sm	0.68	0.02	3.12	1.21	0.14	11.58	5.53	0.57	10.23
Eu	0.39	0.03	7.25	0.30	0.02	5.09	1.49	0.11	7.12
Gd	0.93	0.11	11.83	1.66	0.18	10.84	6.65	0.86	12.87
Tb	0.33	0.05	15.00	0.34	0.07	20.59	1.59	0.31	19.57
Dy	1.09	0.06	5.19	2.24	0.24	10.49	9.28	0.05	5.33
Ho	0.50	0.07	14.14	0.56	0.07	13.16	2.27	0.15	6.54
Er	0.68	0.05	7.28	3.78	0.32	8.40	6.78	0.61	8.97
Tm	0.36	0.07	19.44	0.33	0.03	9.74	1.66	0.26	15.76
Yb	1.01	0.07	6.93	1.89	0.25	13.11	5.86	0.67	11.32
Lu	0.34	0.07	20.59	0.50	0.13	26.56	1.69	0.29	17.16

A - mean B - standard deviation C - RSD%

Table 7.11

Rare earths concentration (mg kg^{-1}) in three phosphate samples.

	CTHSC-1A			SAND THSC-1			SS-2		
	NUMBER OF DUPLICATES								
	2			3			2		
	A	B	C	A	B	C	A	B	C
Y	55.13	1.11	2.01	95.09	1.47	1.54	35.72	2.3	6.43
La	31.24	2.09	6.70	45.11	2.26	5.02	16.41	0.86	5.21
Ce	19.41	1.90	9.76	62.18	3.77	6.06	16.22	1.73	10.65
Pr	5.66	1.13	19.99	9.37	1.63	17.40	0.65	0.11	16.23
Nd	24.60	3.15	12.82	27.48	2.78	10.13	14.33	1.07	7.46
Sm	3.37	0.29	8.60	6.11	0.95	15.47	1.00	0.09	9.43
Eu	0.70	0.43	6.06	1.30	0.29	21.95	0.36	0.03	8.33
Gd	4.52	0.32	7.08	7.58	0.31	4.12	1.80	0.24	13.32
Tb	0.64	0.16	24.31	0.96	0.16	16.37	0.49	0.07	14.47
Dy	4.66	0.67	14.42	8.54	0.39	4.55	2.17	0.27	12.27
Ho	0.99	0.18	17.86	1.39	0.12	8.63	0.75	0.17	22.54
Er	4.24	0.26	6.13	6.22	0.30	4.82	1.84	0.20	10.87
Tm	0.57	0.10	17.54	1.05	0.20	18.76	0.52	0.09	17.38
Yb	2.84	0.12	4.23	4.17	0.39	9.35	1.75	0.14	8.06
Lu	0.54	0.06	10.48	0.92	0.04	4.74	0.35	0.09	25.77

A - mean B - standard deviation C - RSD%

Table 7.12

Rare earths concentration (mg kg^{-1}) in three phosphate samples.

	SG-1			FTHSC-1			CHALK-THSC-1		
	NUMBER OF DUPLICATES								
	2			3			2		
	A	B	C	A	B	C	A	B	C
Y	145.76	3.72	2.55	48.45	2.03	4.19	39.66	1.09	2.75
La	74.96	6.10	8.14	23.81	4.17	17.49	22.26	2.93	13.15
Ce	32.60	5.23	16.14	32.34	1.13	3.50	29.42	2.11	7.19
Pr	10.47	2.05	19.55	4.29	1.01	23.54	4.81	0.55	11.32
Nd	32.00	3.45	10.77	9.93	0.69	6.98	7.33	0.82	11.19
Sm	6.91	0.63	9.14	2.58	0.19	7.40	2.38	0.17	2.97
Eu	1.65	0.26	15.60	0.80	0.12	15.03	0.57	0.04	7.44
Gd	9.66	0.65	6.70	3.52	0.28	7.96	3.05	0.30	9.84
Tb	1.46	0.28	19.18	0.47	0.09	19.15	0.42	0.04	9.52
Dy	11.36	0.23	10.78	3.54	0.22	6.22	3.21	0.20	6.23
Ho	2.46	0.20	8.00	0.81	0.10	12.22	0.69	0.12	17.42
Er	9.44	0.58	6.16	2.99	0.33	11.12	3.24	0.12	3.71
Tm	1.43	0.20	14.13	0.33	0.04	12.12	0.28	0.04	14.29
Yb	7.44	0.83	11.11	2.25	0.14	6.29	2.06	0.18	8.92
Lu	1.47	0.43	29.25	0.44	0.07	16.07	0.43	0.08	18.61

A - mean B - standard deviation C - RSD%

elements has a lower relative standard deviation and can be determined satisfactorily. This pattern is summarised in Figure 7.2.

In all nine phosphate rock samples, there is a straight line correlation between the concentration of the rare earths and the standard deviation when plotted on log/log scale, see Figures 7.3 to 7.6. The slope of the graphs divided these elements into three groups. In the first group, lanthanum, cerium, thulium, erbium, gadolinium, europium and holmium, the concentration of the element in the samples cover a wide range, and the slope is one showing that the relative standard deviation is constant, about 10% but varies from 7% for erbium to 16% for terbium. An example of this group (cerium) is illustrated in Figure 7.3. In another group, praseodymium and lutetium, the slope remains one but the relative standard deviation is higher, about 20%, as shown in Figure 7.4 for praseodymium. A third group, neodymium, samarium, dysprosium and ytterbium, gave higher slopes varying from 1.2 to 1.6. For this group the relative standard deviation is much smaller (about 5%) at low concentration than at high concentration (RSD about 11%), as illustrated in Figure 7.5 for dysprosium. Finally, yttrium give a poor correlation with a very high relative standard deviation, as shown in Figure 7.6.

Figure (7.2)

Relative standard deviation of the analysis of rare earths in the phosphate rock samples .

sample / element	Y	La	Ce	Pr	Nd	Sm	Eu	Gd	Tb	Dy	Ho	Er	Tm	Yb	Lu
SAND-TH-SC-1															
C-TH-SC-1A															
F-TH-SC-1															
S - G - 1															
CHALK-TH-SC-1															
S - S - 2															
C - A - 1															
CONG - G - 1															
S - A - 12															

Relative Standard Deviation

< 10 %	
10 - 20 %	
> 20 %	

Figure (7.3)

The effect of increasing cerium concentration on the standard deviation :- plot on Log-Log scale .

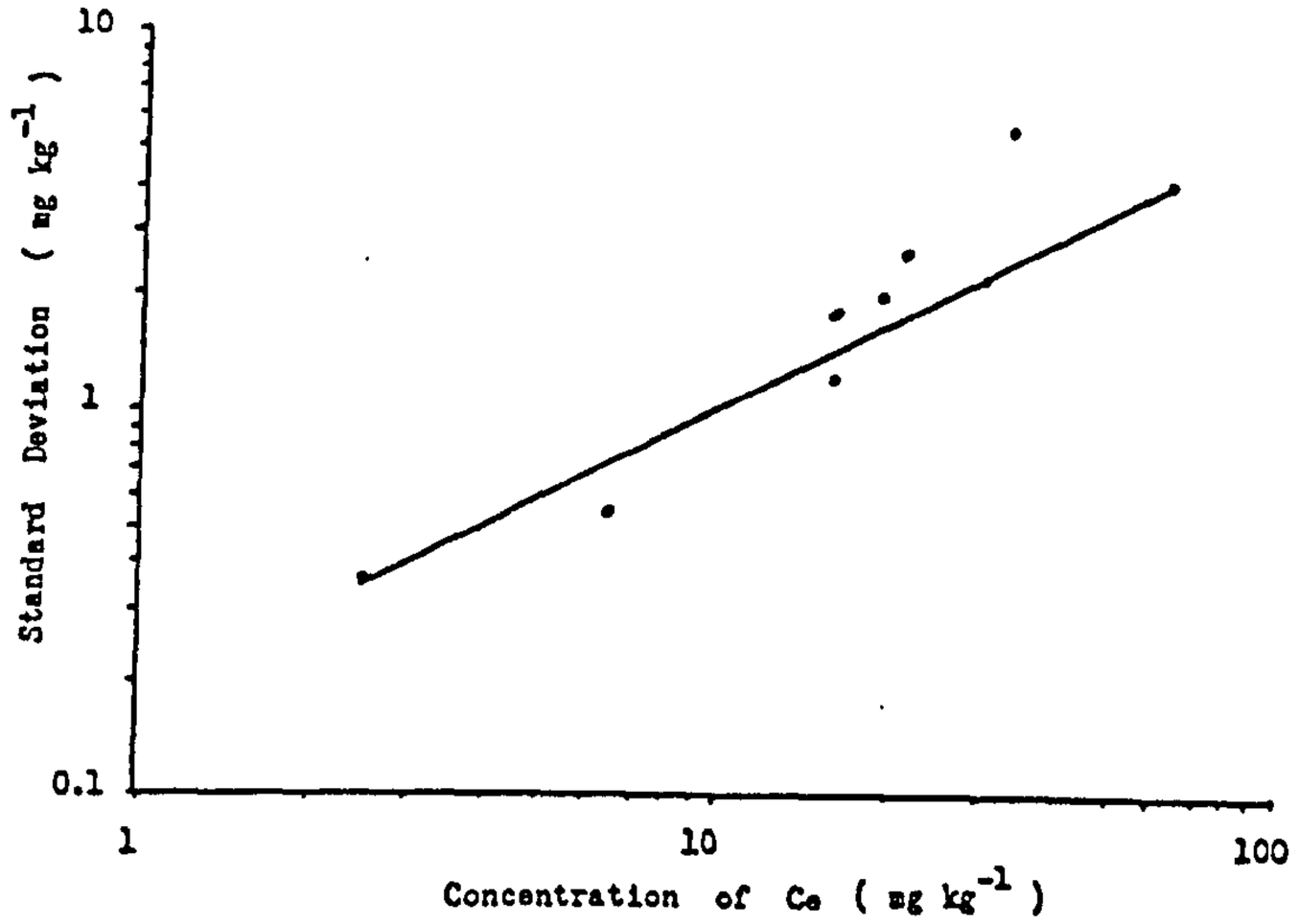

Figure (7.4)

The effect of increasing praseodymium concentration on the standard deviation :- plot on Log-Log scale .

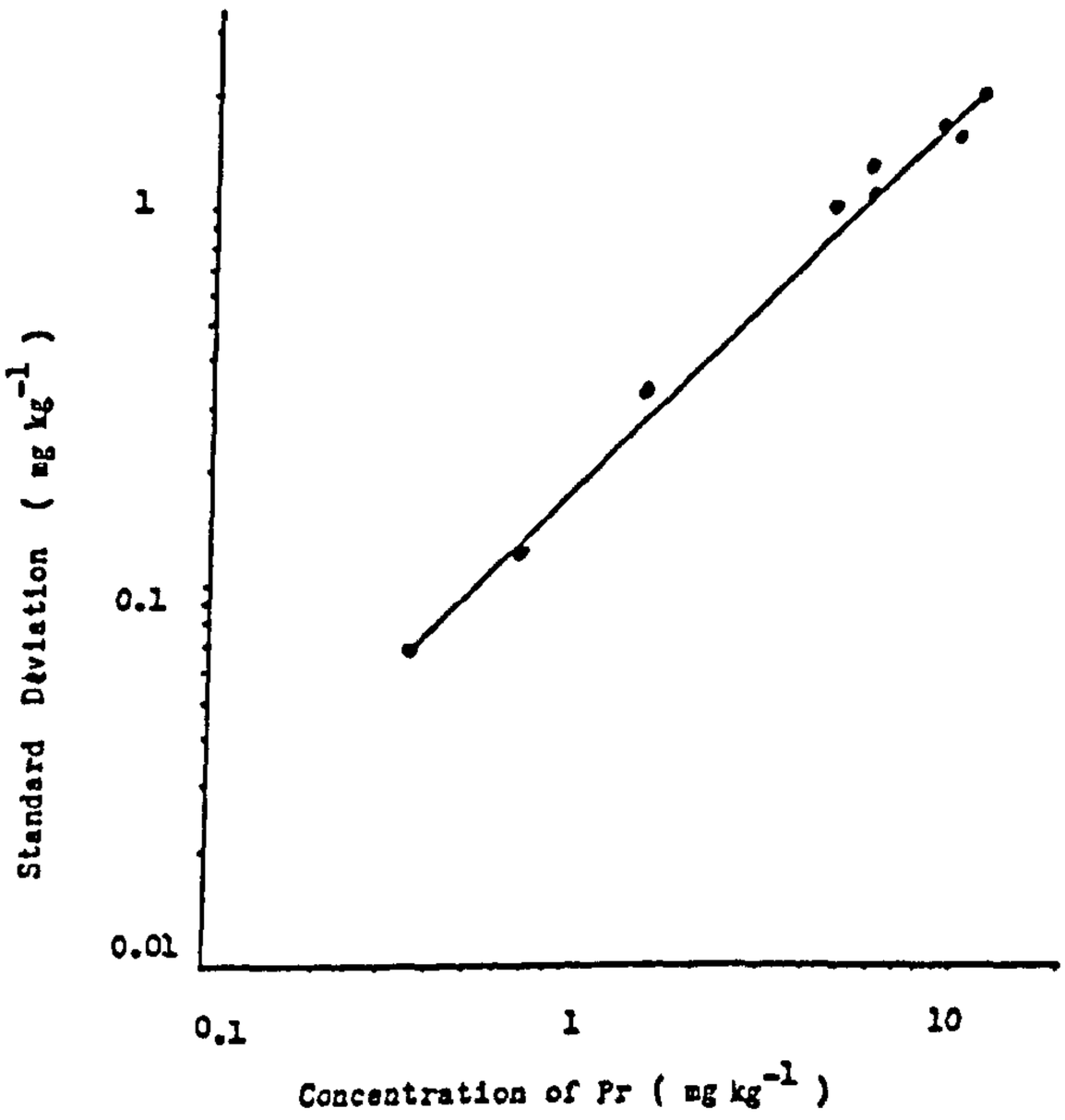

Figure (7.5)

The effect of increasing dysprosium concentration on the standard deviation :- plot on Log-Log scale .

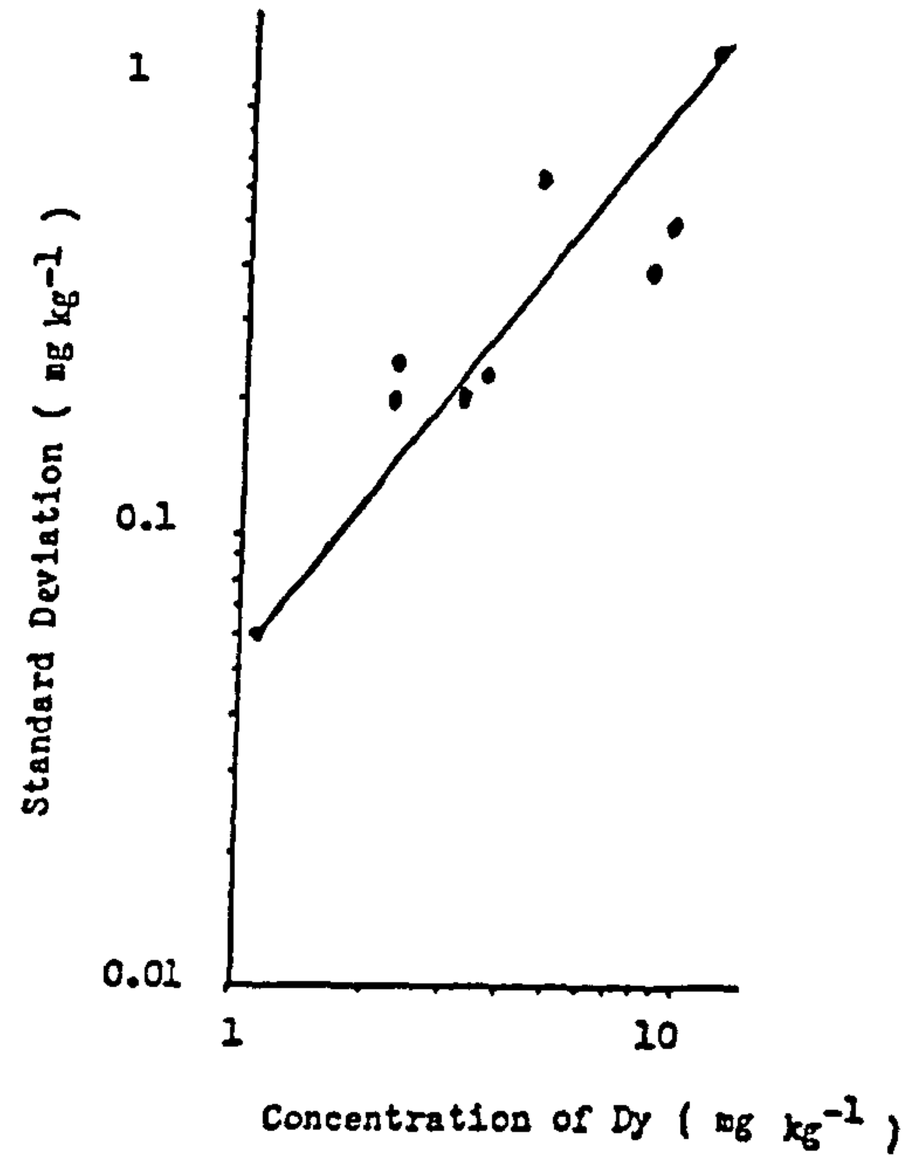

Figure (7.6)

The effect of increasing yttrium concentration on the standard deviation :- plot on Log-Log scale .

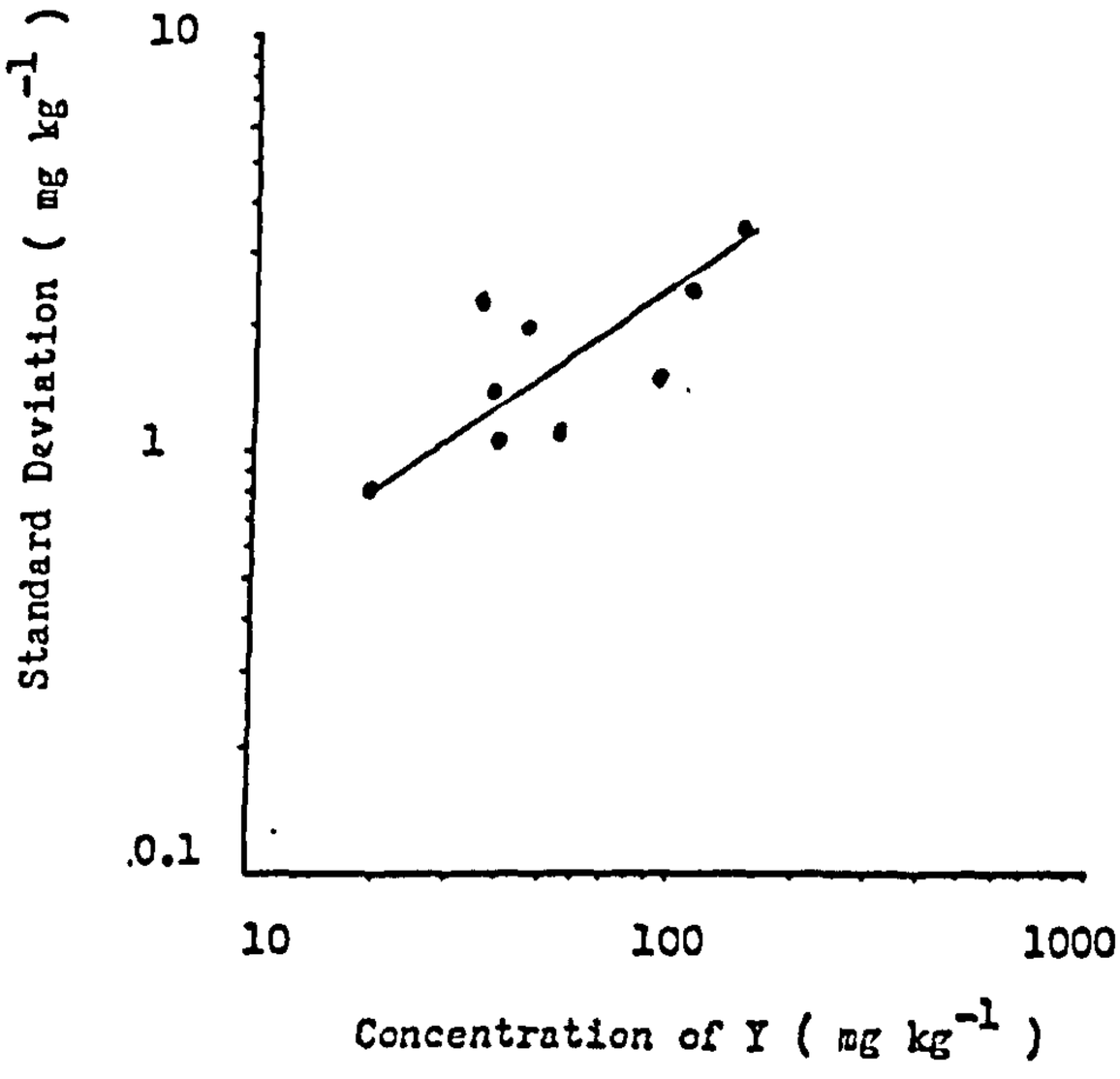

The relative standard deviation averaged over all samples varies from one element to another. It is about 20% for elements such as praseodymium and lutetium. For the elements, thulium, holmium and terbium, the relative standard deviation is about 15%. Finally for the rest of the elements it is less than 10%, as can be seen in Table 7.14. The overall relative standard deviation for all the elements is 13%, which is acceptable for this complex procedure.

7.5 Procedure Detection Limit.

The inductively coupled plasma technique is very sensitive for the detection of most elements. The detection limits of the rare earth elements in aqueous solution are in the range of sub-part per millions (33) as can be seen in Table 7.15. The concentration of the rare earths in the samples used is high and it was not possible to calculate the detection limits of the procedure. The detection limits correspond to a relative standard deviation of 50% and even the worst cases (Pr and Lu) did not approach this level, as illustrated in Table 7.14.

Table 7.14

Average relative standard deviation for each rare earths.

Analyte	Average RSD %
Y	6
La	9
Ce	11
Pr	20
Nd	9
Sm	10
Eu	12
Gd	10
Tb	18
Dy	10
Ho	15
Er	8
Tm	16
Yb	10
Lu	22

Table 7.15

Rare earths detection limits ($\mu g\ dm^{-3}$) in aqueous solution.

Element	Detection Limit
Y	2.3
La	6.7
Ce	32
Pr	25
Nd	33
Sm	29
Eu	1.8
Gd	9.3
Tb	15
Dy	6.7
Ho	3.8
Er	6.7
Tm	3.5
Yb	1.2
Lu	0.67

CHAPTER EIGHT: GEOCHEMICAL DISCUSSION OF THE ANALYTICAL RESULTS.

8.1 Collection of Samples.

Samples for this investigation were collected from five locations in the north of Saudi Arabia, see Figure 8.1. The samples were collected in a way which represented all the phosphate levels (see section 1.2) in due proportion. Only the phosphate horizons were sampled, the other horizons being neglected. The location and the description of samples are discussed below.

1 - Location 1, (31° 53′N, 39° 03′E).

Samples from this location, about 70 km east of Turayf town, represent the Arqah phosphate level. The area is relatively flat-lying with few outcrops. Samples were collected after a trench had been excavated to a depth of approximately 3 metres and the phosphate layers exposed. There are two layers of phosphate, an upper siliceous one (S-A-12) and a lower calcareous one (C-A-1).

2 - Location 2, (31° 41′N, 39° 03′E).

Samples from this location represent the Sib

Figure (8.1)

Map of the north of the Kingdom of Saudi Arabia showing the five localities sampled .

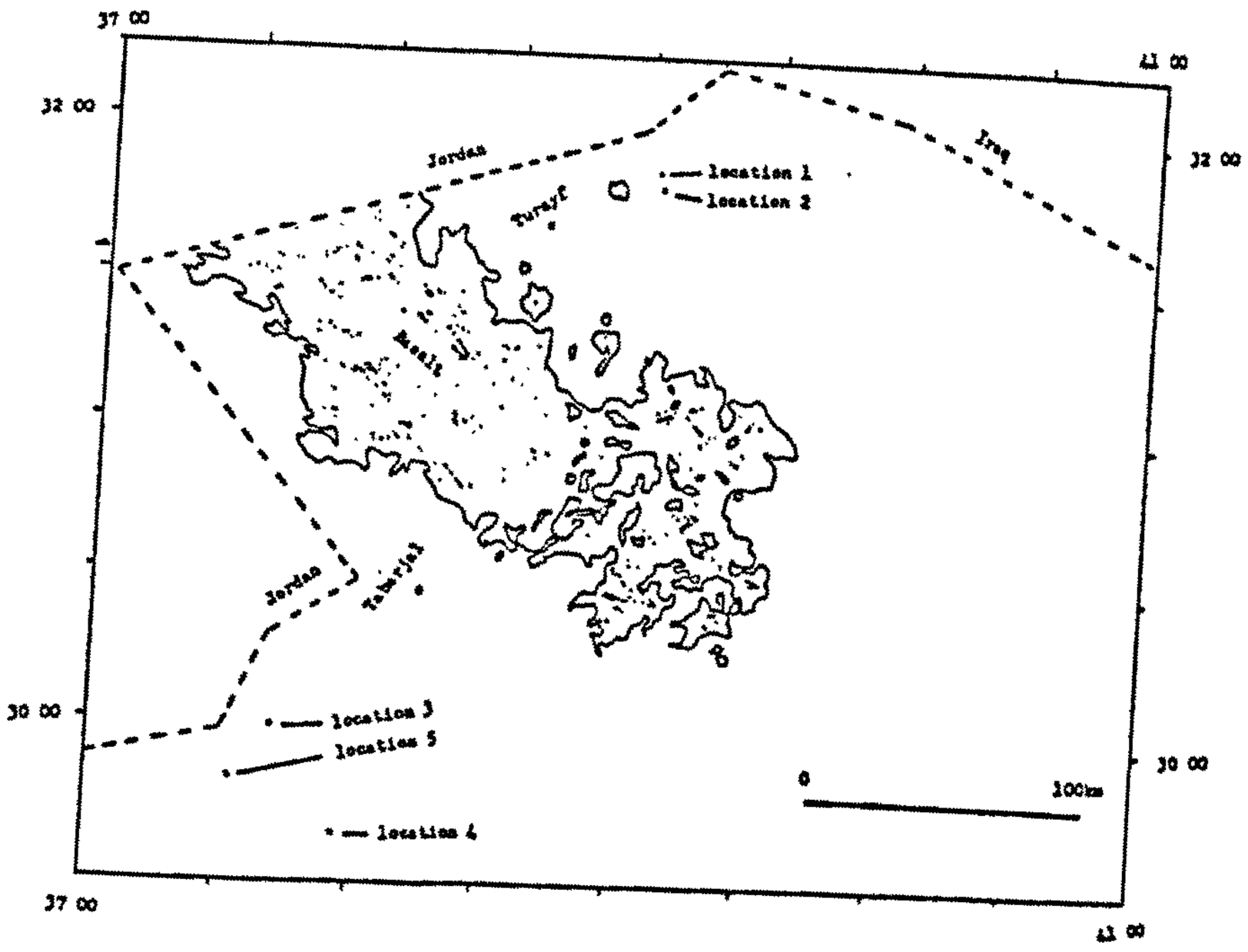

phosphate level. A small outcrop of this layer about 66 km east of Turayf town was sampled. The sample collected was given the number (S-S-2).

3 - Location 3, (30° 06′N, 37° 45′E)

Samples from this location (Wadi Al Ghinah - about 60 km south-west of Tabarjal town) represent the Ghinah phosphorite level. There is an outcrop along the side the wadi where samples were collected. There are two phosphate layers, an upper conglomeratic phosphate layer (CONG-G-1) and a lower siliceous one (S-G-1).

4 - Location 4, (29° 42′N, 38° 06′E)

This location is in the south-east of the area studied, about 90 km south-west of Tabarjal town, where a discontinuous escarpment consists of a series of cliff faces. The phosphate layers are found in the middle of these cliffs. Six samples were collected representing the west side of the Thaniyat phosphorite level. These samples from top to bottom are; friable layer (F-TH-SC-2) followed by a chalky layer (CHALK-TH-SC-1) followed by a second friable layer (F-TH-SC-1) followed by a calcareous layer (C-TH-SC-1A) followed by another calcareous layer (C-TH-SC-1) and finally a sandy layer (SAND-TH-SC-1).

5 - Location 5, (29° 30'N, 37° 35'E)

This location (about 85 km south-west of Tabarjal town) represents the east side of the Thaniyat phosphorite level (8), and is to the north of the Thaniyat escarpment. Four samples were collected from Wadi Al Kuwaykabah. These samples from the top to the bottom are; a friable layer (F-TH-1) followed by a siliceous layer (C-TH-2) followed by a semi-siliceous layer (SEMI-S-TH-1) and finally a cacareous layer (C-TH-1).

8.2 Rare Earth Elements in the Phosphate Rocks.

The cation exchange procedure showed a very high recovery of the rare earths in the tested samples, ranging from 73% to 93%, as previously discussed in detail in section 7.5. This procedure was applied in the separation of rare earths from all the phosphate samples collected from the five areas studied in the Kingdom of Saudi Arabia. The results are shown in Tables 8.1 to 8.5. These results show that the concentration of the rare earths varied from sample to sample. The samples which contain the highest rare earths are those collected from location 3 (S-G-1 and CONG-G-1). These samples have a total rare earths (plus yttrium) concentration of 350 and 274 mg kg^{-1}

Table 8.1.

Concentration (mg kg^{-1}) of rare earths and yttrium in the collected samples from area 1.

Analyte	CA-1	SA-12
Y	38.6	18.9
La	16.7	8.0
Ce	6.56	2.73
Pr	1.48	0.27
Nd	5.87	2.98
Sm	1.20	0.66
Eu	0.30	0.22
Gd	1.62	1.01
Tb	0.33	0.26
Dy	2.24	1.13
Ho	0.48	0.25
Er	7.23	1.33
Tm	0.31	0.14
Yb	1.93	1.03
Lu	0.64	0.25
Total	85.5	39.2

Table 8.2

Concentration (mg kg^{-1}) of rare earths and yttrium in the collected sample from area 2.

Analyte	SS-2
Y	37.2
La	17.3
Ce	16.9
Pr	0.75
Nd	13.5
Sm	0.9
Eu	0.31
Gd	1.82
Tb	0.19
Dy	2.27
Ho	0.53
Er	2.41
Tm	0.17
Yb	1.78
Lu	0.34
Total	96.4

Table 8.3.

Concentration (mg kg^{-1}) of rare earths and yttrium in the collected samples from area 3.

Analyte	SG-1	CONG-G-1
Y	138.2	115.7
La	79.3	60.5
Ce	38.6	23.2
Pr	8.56	5.61
Nd	29.6	24.6
Sm	6.26	5.93
Eu	1.58	1.56
Gd	9.6	7.25
Tb	1.43	1.41
Dy	10.8	9.63
Ho	2.43	2.37
Er	10.1	7.21
Tm	1.31	1.34
Yb	8.09	6.34
Lu	1.95	1.3
Total	347.8	274

Table 8.4.

Concentration (mg kg^{-1}) of rare earths and yttrium in the collected samples from area 4.

Analyte	A	B	C	D	E	F
Y	32.2	54.3	64.4	48.3	38.9	51.3
La	16.4	32.7	36.8	26.8	24.3	32.1
Ce	12.6	40.8	62.5	31.5	30.9	41.2
Pr	0.83	4.86	8.33	4.27	3.42	4.01
Nd	6.46	12.4	18.9	10.4	7.91	13.0
Sm	2.07	3.16	5.73	2.44	2.43	3.3
Eu	0.4	0.73	1.35	0.59	0.54	0.67
Gd	2.3	4.4	7.31	3.52	3.26	4.9
Tb	0.15	0.53	0.85	0.4	0.43	0.61
Dy	2.36	4.18	6.36	3.45	3.27	3.96
Ho	0.52	0.86	1.28	0.74	0.6	0.90
Er	2.31	4.25	5.1	3.22	3.24	4.01
Tm	0.15	0.45	0.8	0.34	0.33	0.39
Yb	1.56	2.75	3.93	2.36	2.19	2.55
Lu	0.13	0.58	0.89	0.49	0.43	0.53
Total	80.5	167	224.5	138.8	122.2	163.4

A - F-TH-SC-1

B - C-TH-SC-1A

C - SAND-TH-SC-1

D - F-TH-SC-2

E - CHALK-TH-SC-1

F - C-TH-SC-1

Table 8.5.

Concentration (mg kg^{-1}) of rare earths and yttrium in the collected samples from area 5.

Analyte	A	B	C	D
Y	33.1	20.1	29.6	26.4
La	19.7	11.1	14.3	10.1
Ce	25.9	7.5	11.6	13.1
Pr	5.22	1.76	2.2	2.2
Nd	9.81	2.21	5.5	5.64
Sm	2.66	0.74	1.37	1.53
Eu	0.61	0.41	0.34	0.43
Gd	2.74	0.85	1.59	1.94
Tb	0.48	0.37	0.36	0.34
Dy	3.02	0.99	1.95	1.68
Ho	0.51	0.4	0.4	0.47
Er	2.96	1.24	1.67	1.35
Tm	0.35	0.38	0.22	0.03
Yb	1.79	0.78	1.3	1.03
Lu	0.33	0.32	0.26	0.263
Total	109.2	49.2	72.7	66.5

A - C-TH-1
B - C-TH-2
C - F-TH-1
D - SEMI-S-TH-1

respectively. The other samples have total concentration varying from 39 to 225 mg kg^{-1}.

8.3 Geochemistry.

There are fourteen phosphate horizons in the area studied, duplicate samples were collected from each phosphate layer. The average major and trace element compositions of each layer are shown in Tables 3.2 to 3.16, while the rare earth elements contents are shown in Tables 8.1 to 8.5. The accuracy of the major analyses were checked by analysing an international phosphate rock standard (NBS-120b) alongside the sample. It was difficult to confirm the trace element results since there was no available published data for the trace elements in the standard used. Similarly recovery of rare earths was checked by means of the standard addition method alone because there was no published data on the concentration of rare earths in the standard.

From the available chemical and XRD data, it can be seen that the composition of the phosphate samples is variable. Silicon dioxide varies from 1 to 43%, occurring mainly as quartz. The calcium oxide concentration varies from 20 to 51%. Most calcium is combined with phosphate in apatite, but in some samples

calcite and/or gypsum can be found. Phosphate (P_2O_5) varied from 11 to 37% and is present as apatite. The fluorine content varies from 1 to 3.8% and it has been suggested (9, 138) that such concentration indicates a fluorapatite composition (francolite). The carbon dioxide content varied from 1 to 21%, but most samples (about 75%) contain less than 2%. The XRD analysis of the samples which contain high concentrations of carbon dioxide show the presence of calcite and carbonate-apatite (dahilite). The rest of the oxides form less than 4% of the total of the rock.

From the composition tables, it is noticeable that some elements exhibit strong correlations with each other, in spite of their different age, location and classification. The sample ages range from Palaeocene to Eocene. The samples were collected from phosphate horizons which represent the four phosphate levels and calcareous, siliceous, friable and conglomeratic types.

Calcium has a strong negative, curvilinear correlation with silicon: as calcium increases silicon decreases, as can be seen in Figure 8.2. A similar effect was observed between phosphate and silicon. Fluorine increases with the increase in phosphate, suggesting it is in the apatite, as can be seen in Figure 8.3, whilst a poor correlation was observed with calcium since it can be present in the apatite or the

Figure (8.2)

Correlation between the concentration of calcium oxide (%) and silicon oxide (%) :- Log / Log scale

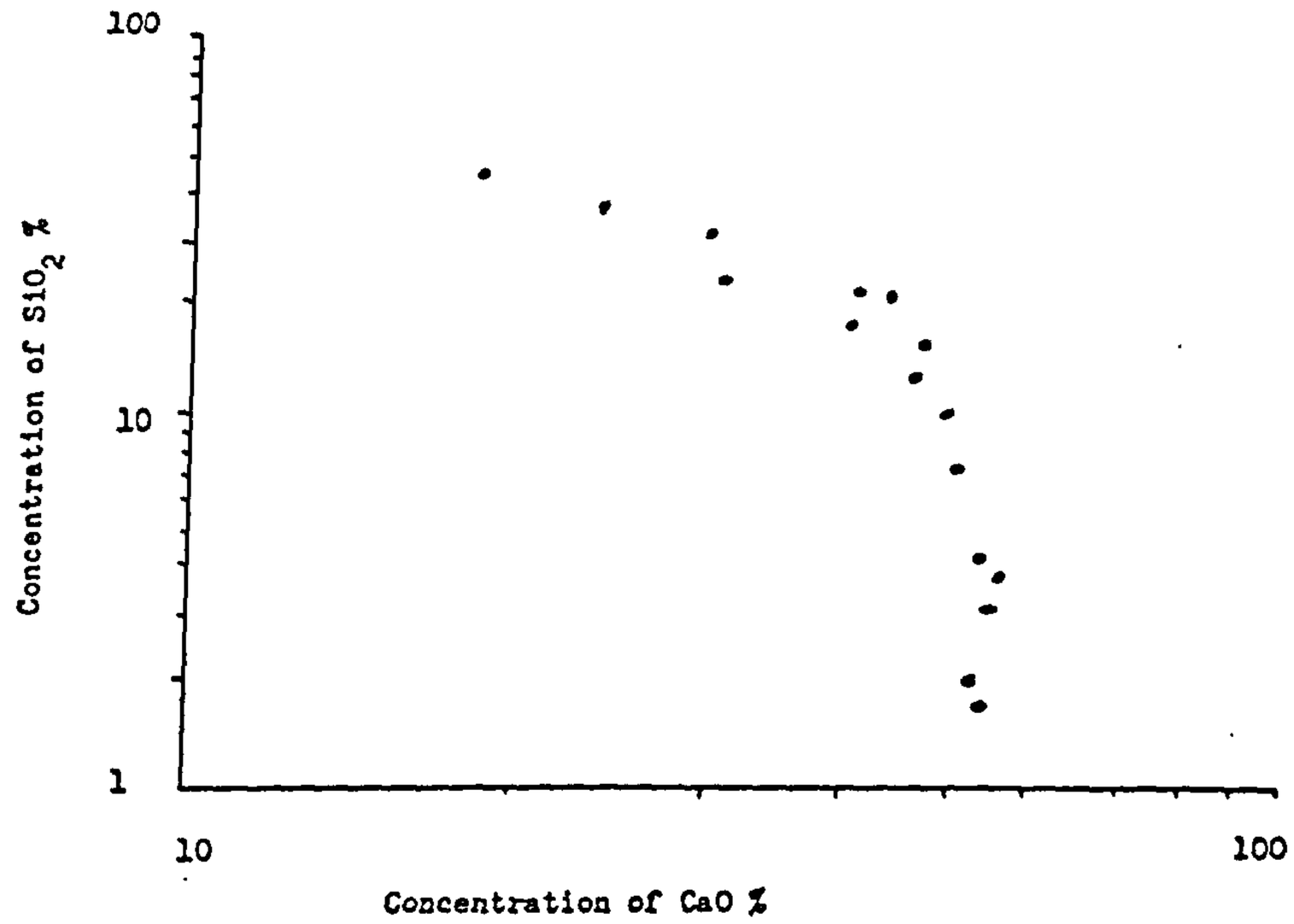

Figure (8.3)

Correlation between the concentration of phosphate (%) and fluorine (%) :- Log / Log scale

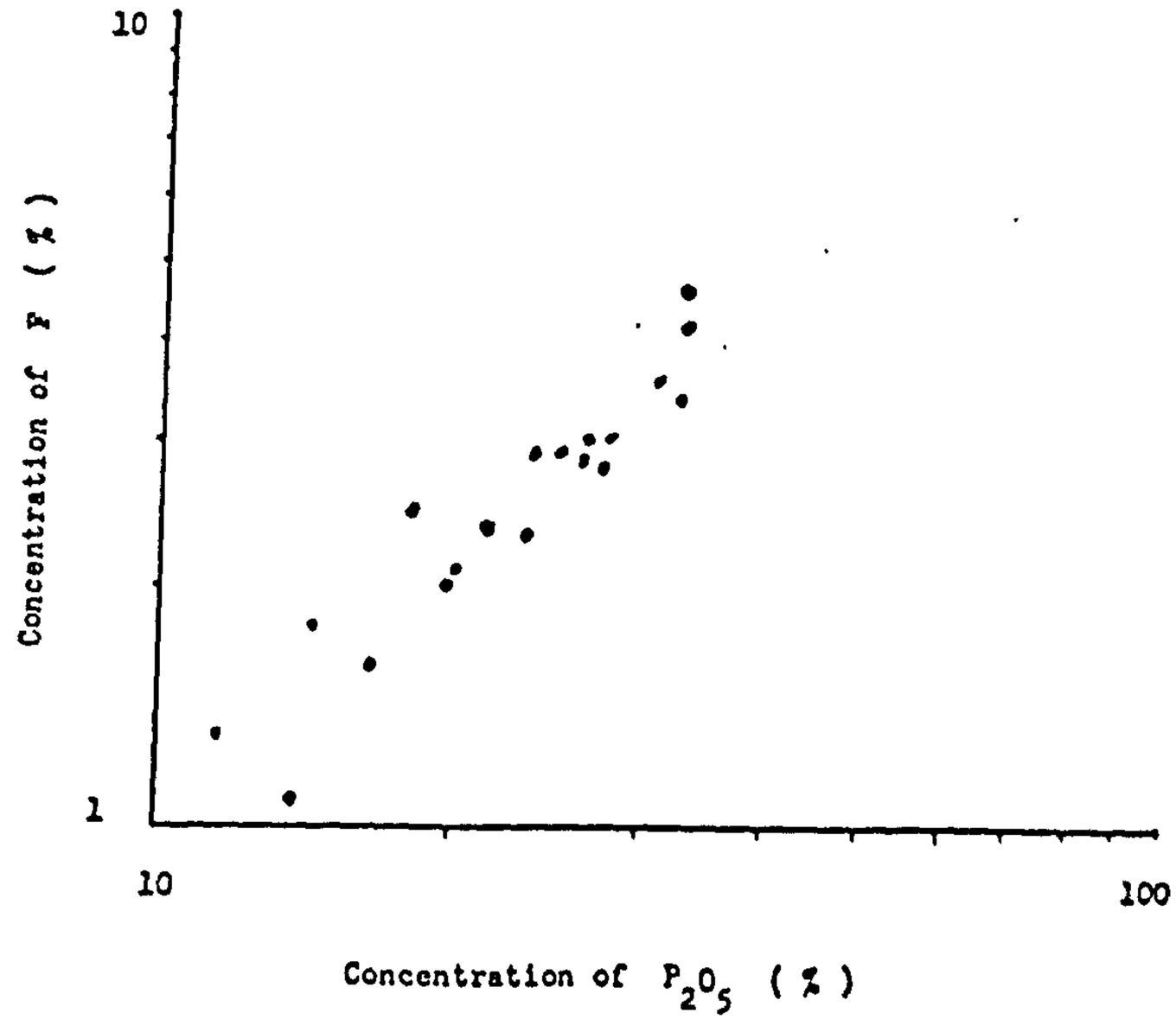

calcite. There is an increasing trend of zirconium concentration with an increase in calcium, as can be seen in Figure 8.3, but some samples were encriched in zirconium which is usual in sedimentary rocks. A poor correlation was observable between zirconium and phosphate, zironium and total rare earths and zirconium and yttrium. The light rare earths are correlated positively with the heavy rare earths, as shown in Figure 8.5., and the total rare earths are also correlated with yttrium, see Figure 8.6., and phosphate as shown in Figure 8.7., in the case of phosphate the samples S-G-1, CONG-G-1 and SAND-TH-SC-1 do not fit this correlation. The correlations reflect the geochemical similarities between rare earths and yttrium. Thus, it is possible to state that rare earths and yttrium accumulate within the same phosphate mineral - apatite, otherwise a different correlation would have been obtained.

A graph of rare earth elements concentration against atomic number (Figure 8.8) exhibits a typical alteration in concentration of even and odd rare earth elements, even elements are about 5 times the concentration of the odd elements. Normalisation against the average C1 chondrites (125) (Figure 8.9) eliminates this alteration and reveals an inhancement in the concentration of the light rare earth elements (La - Sm).

Figure (8.4)

Correlation between the concentration of calcium oxide (%) and zirconium (mg kg^{-1}) :- Log / Log scale

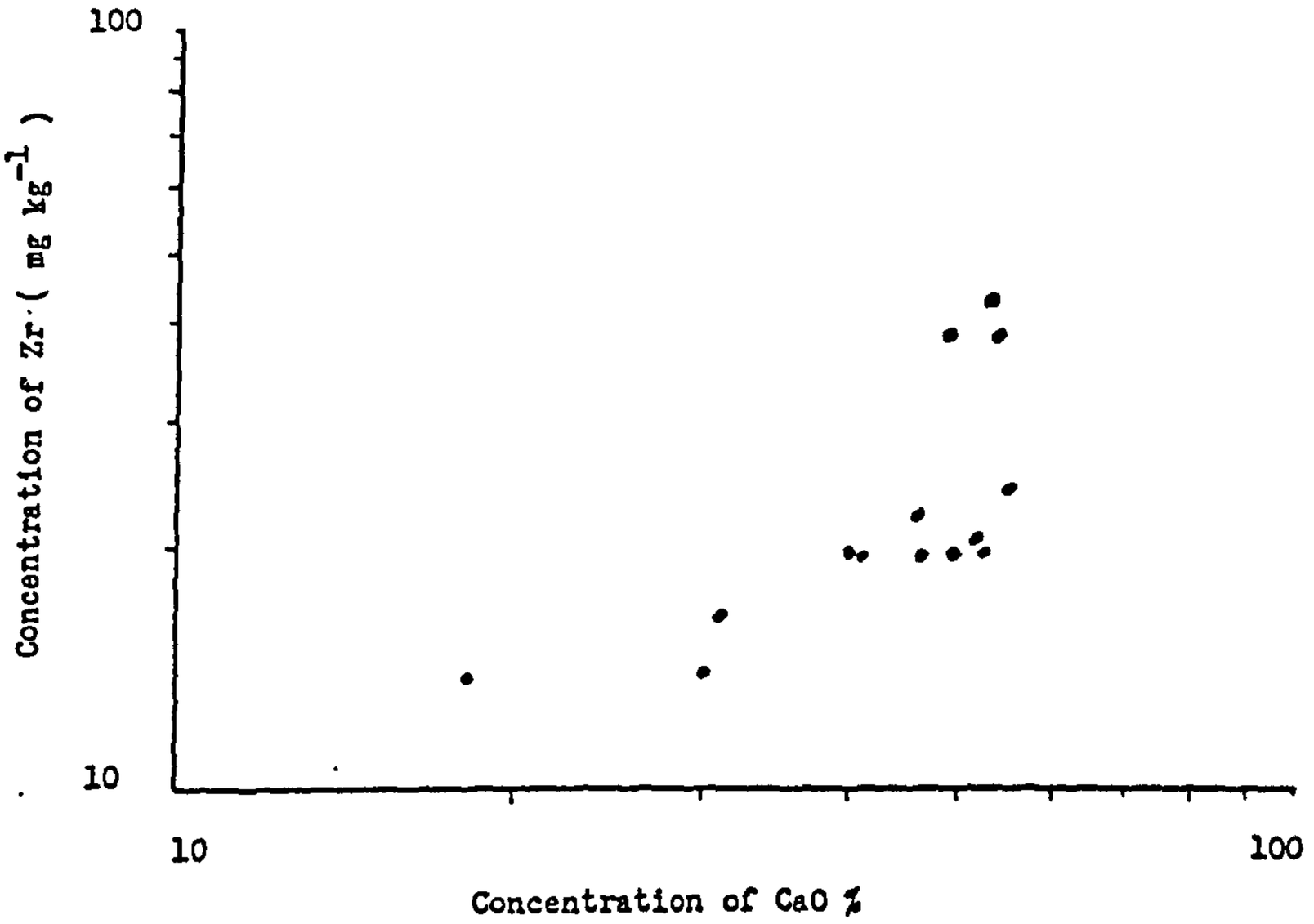

Figure (8.5)

Correlation between the concentration (mg kg^{-1}) of light and heavy rare earth elements :- Log / Log scale

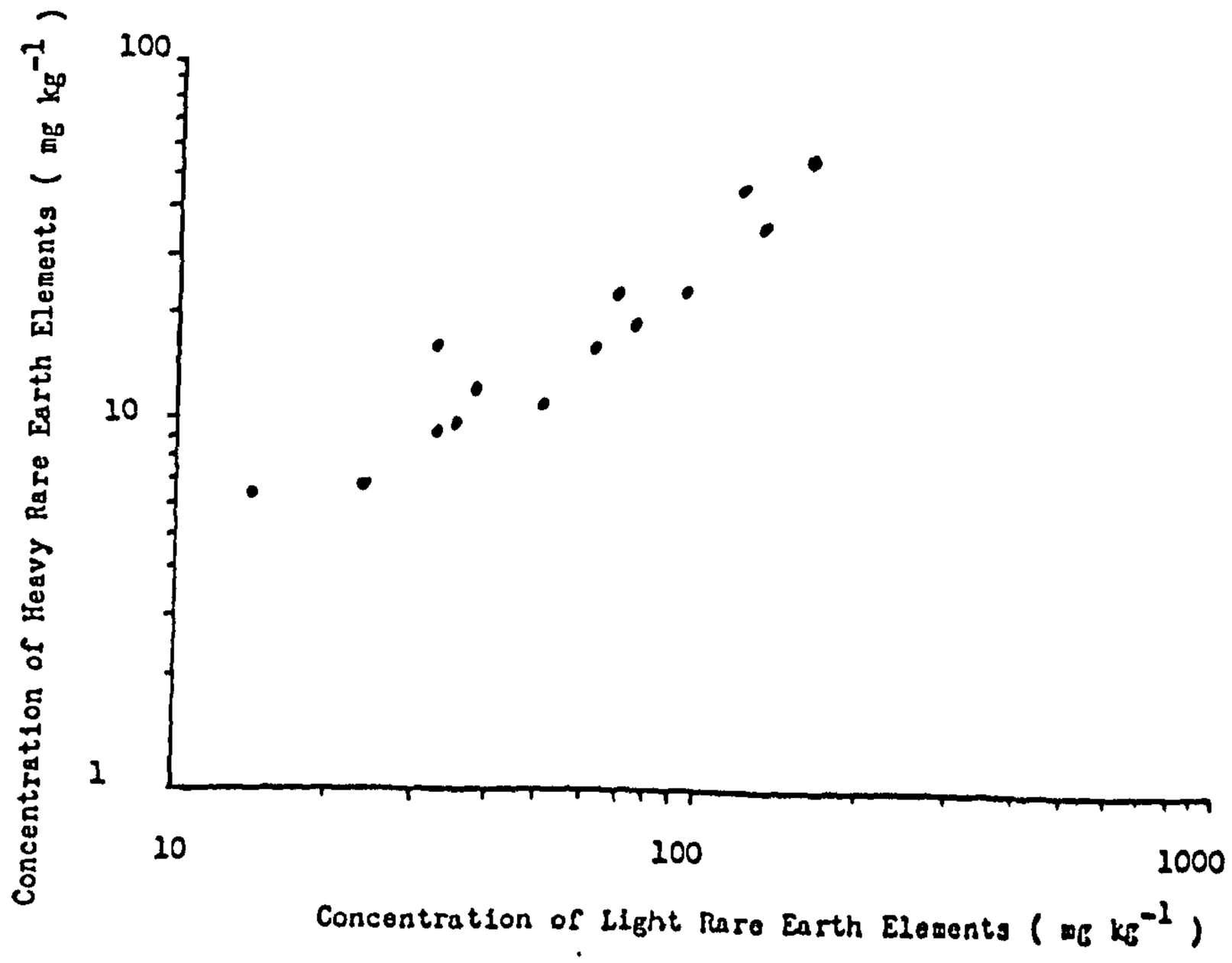

Figure (8.6)

Correlation between the concentration (mg kg^{-1}) of the total rare earth elements and yttrium :- Log / Log scale

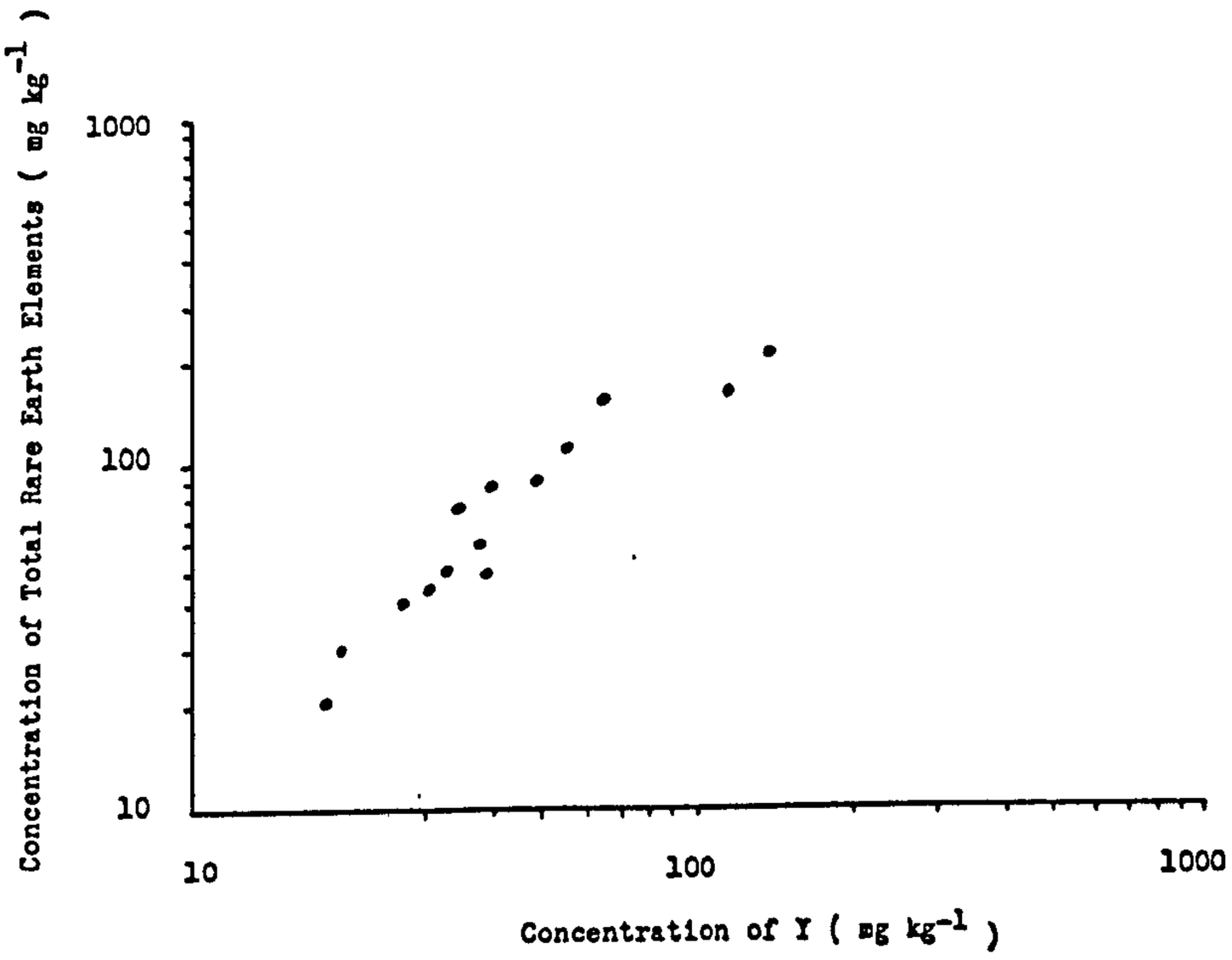

Figure (8.7)

Correlation between the concentration of phosphate (%) and total rare earth elements (mg kg^{-1}) :- Log / Log scale

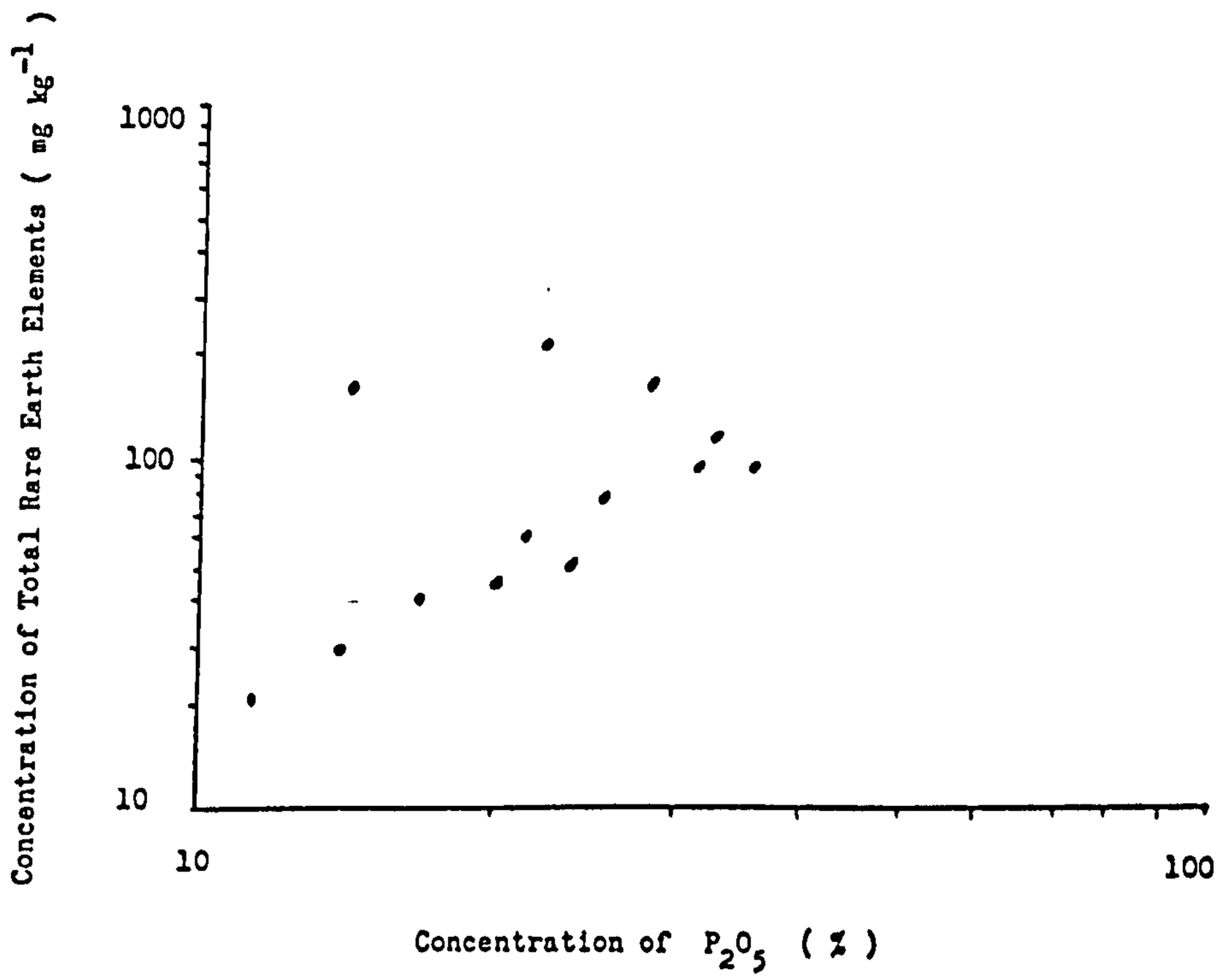

Figure (8.8)

Plot of the concentration of rare earth elements (mg kg^{-1}) in the two extreme samples againest an increase atomic number - from 57 (La) to 71 (Lu) .

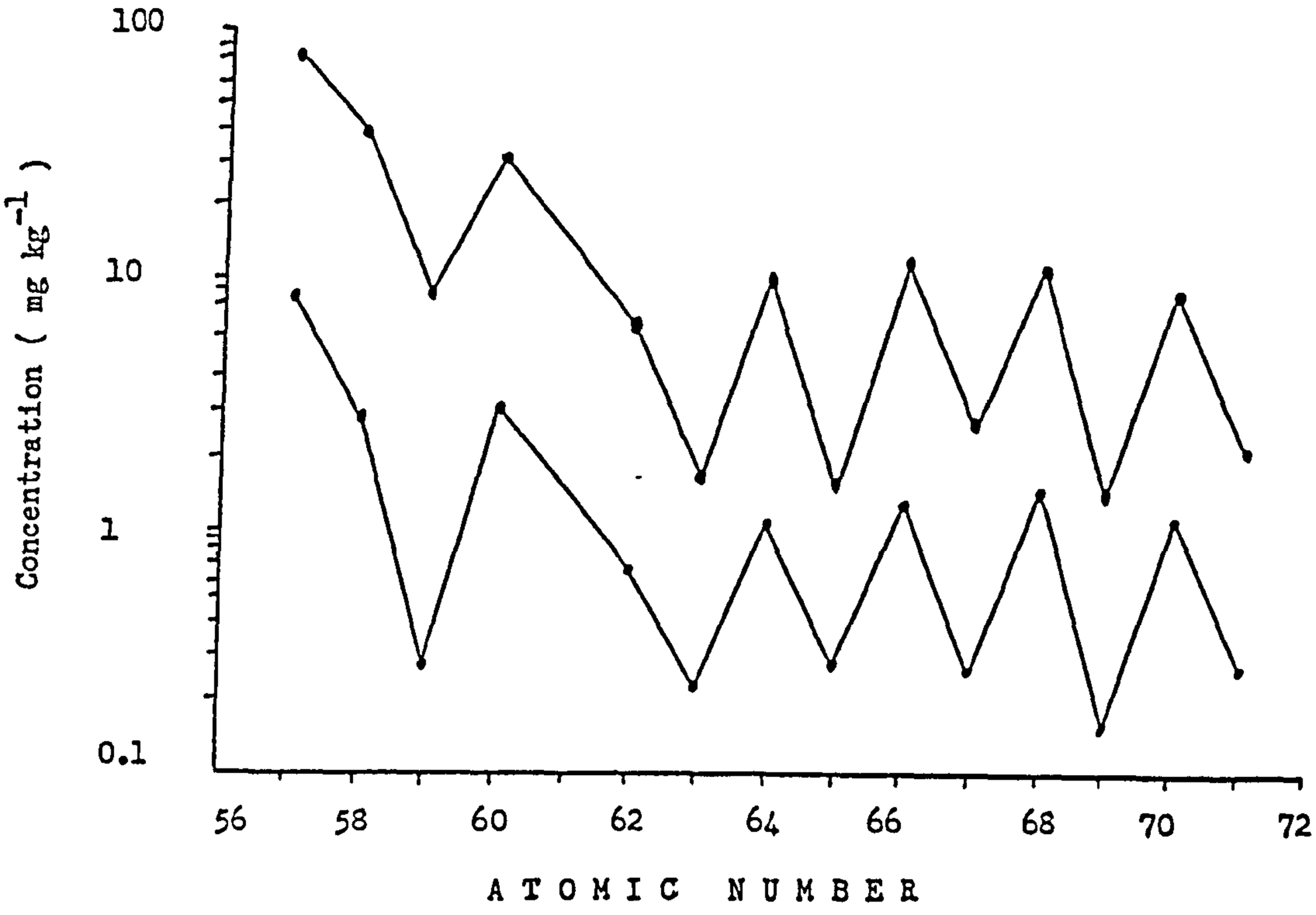

Figure (8.9)

Rare earth elements abundances in the two extremes samples compared to a composite of Cl Chondrites .

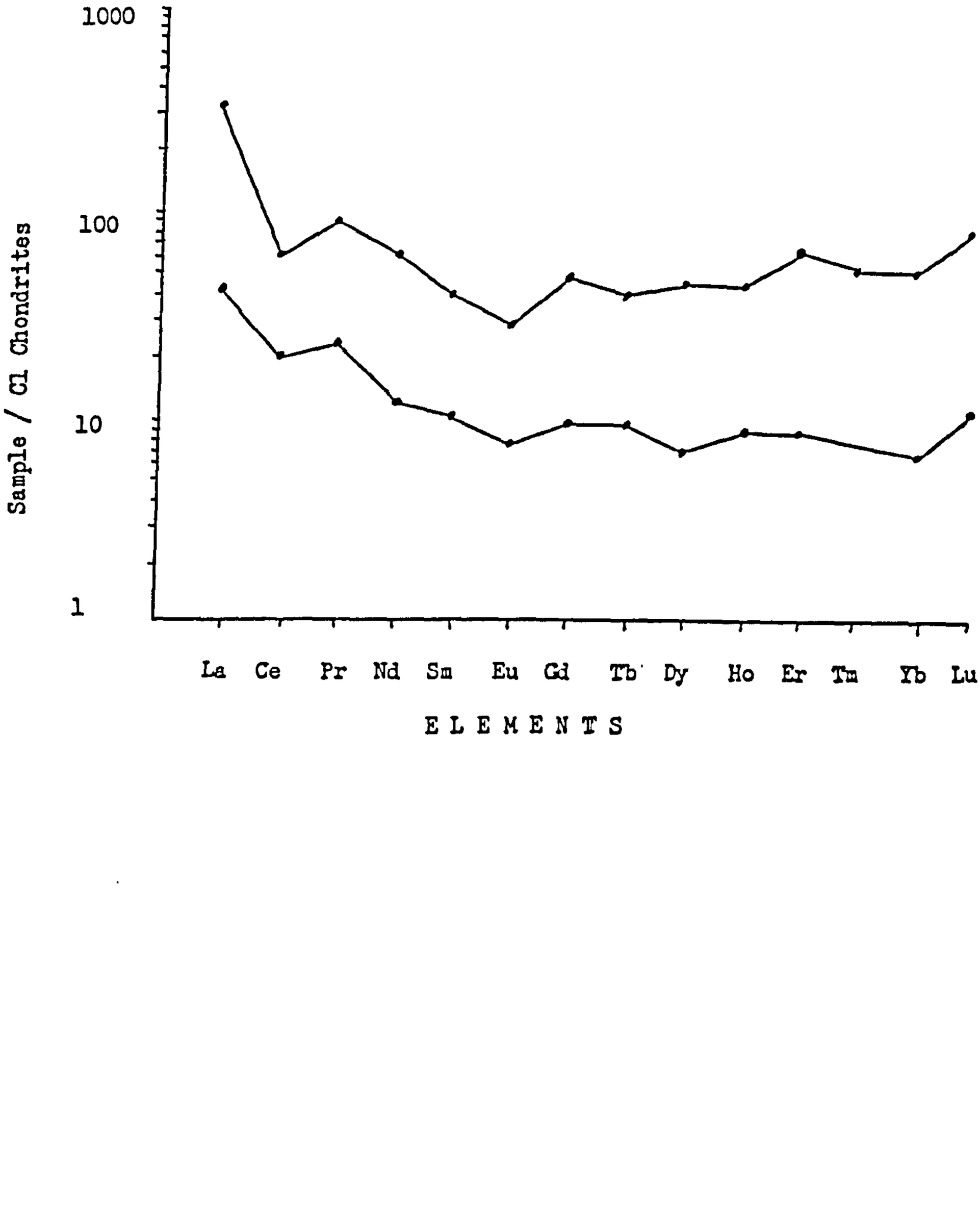

The concentration of the rare earths in the samples were normalised to the concentration in North American Shale (139). The two extremes are illustrated in Figure 8.10. The other samples produce graphs which are parallel to those illustrated and lie between them. The graphs show negative cerium anomalies, heavy rare earth enrichment and a convex-upward shape. Cerium is known to fractionate from other rare earths only under oxidising conditions (140, 141), thus these rocks were deposited under oxidising conditions. These plots exactly parallel those of North Atlantic deep water (144) normalised to the shale as shown in Figure 8.8. This suggests that the samples were deposited in marine conditions (108, 142). Martin et al (143) have shown that there is no cerium anomaly in sediments from the Gironde estuary and Hogdahl et al (144) have shown that there is no cerium anomaly in the sediments from the Barent sea - a shelf sea, similarily there is no cerium anomaly in the atlantic shelf sediments off the U.S.A. (145). On the other hand it has been shown (142) that the cerium anomaly can be found in deep water sediments from the open oceans. Thus the sediments found in Saudi Arabia were probably deposited from open ocean.

Rare earth elements in phosphate rocks may be derived either directly or indirectly from sea water. The concentration of rare earths in oceanic water is extremely low (146). The samples were normalised to the

Figure (8.10)

Comparison of rare earth elements abundances in the two extreme samples and North Atlantic Deep water to a composite of North American Shale :- (●——) phosphate rock sample , (o - -) North Atlantic Deep water

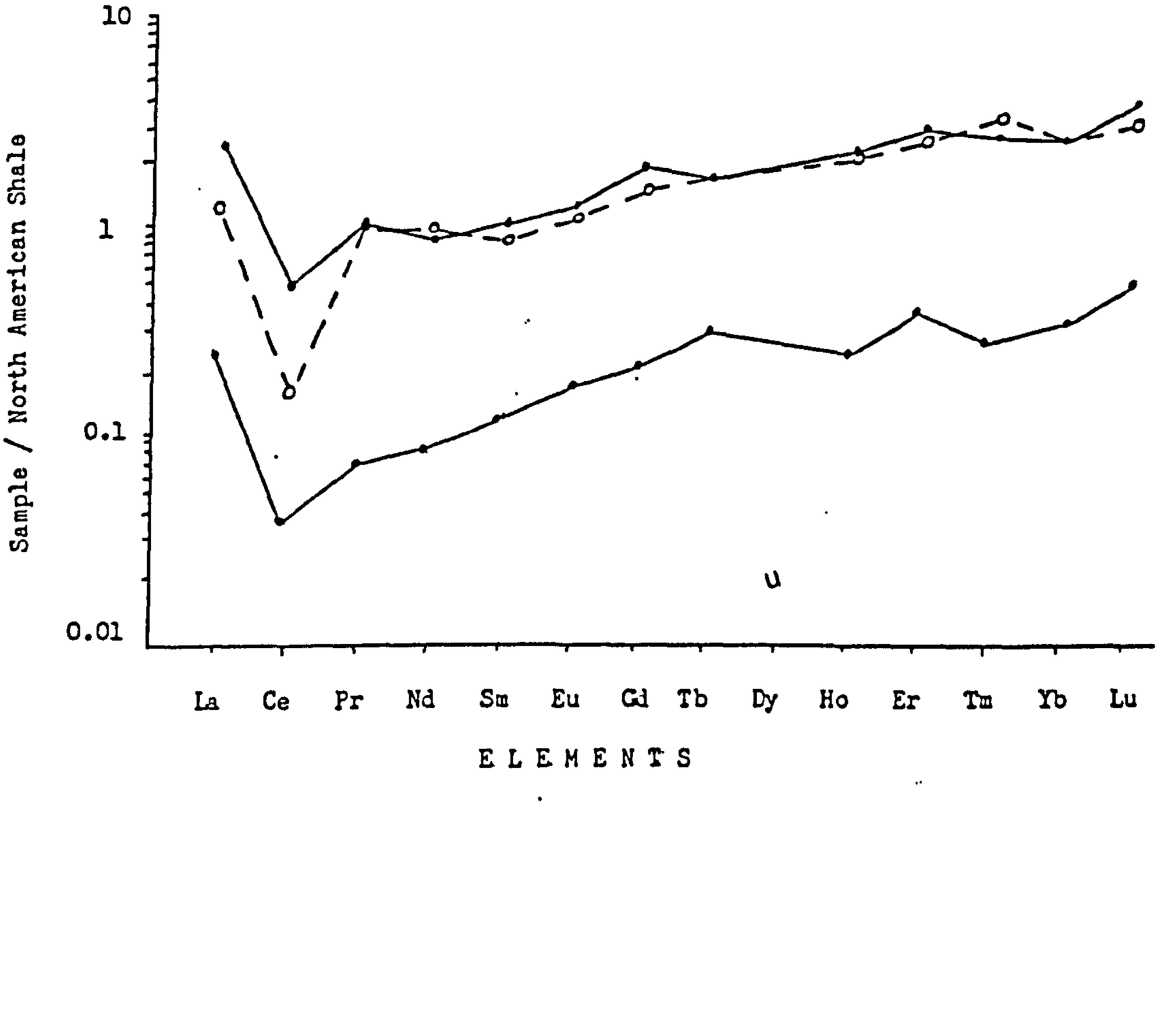

concentration in north atlantic ocean water at a depth of 2500 metres. The two extremes are illustrated in Figure 8.11. The other samples produce graphs which are parallel to those illustrated and lie between them. Similar graphs were obtained when normalization was performed for other depths (ie. 100, 600 and 4500 metres). The graphs show negative europium anomalies, a constant heavy rare earths enrichments and a decreasing enrichments for the light rare earths. This suggests that europium had been removed from the sea water by substitution for calcium in the carbonate deposites in the area.

Figure (8.11)

Rare earth elements abundance in the two extreme samples compared to a composite of North Atlantic Ocean water at a depth of 2500 metres .

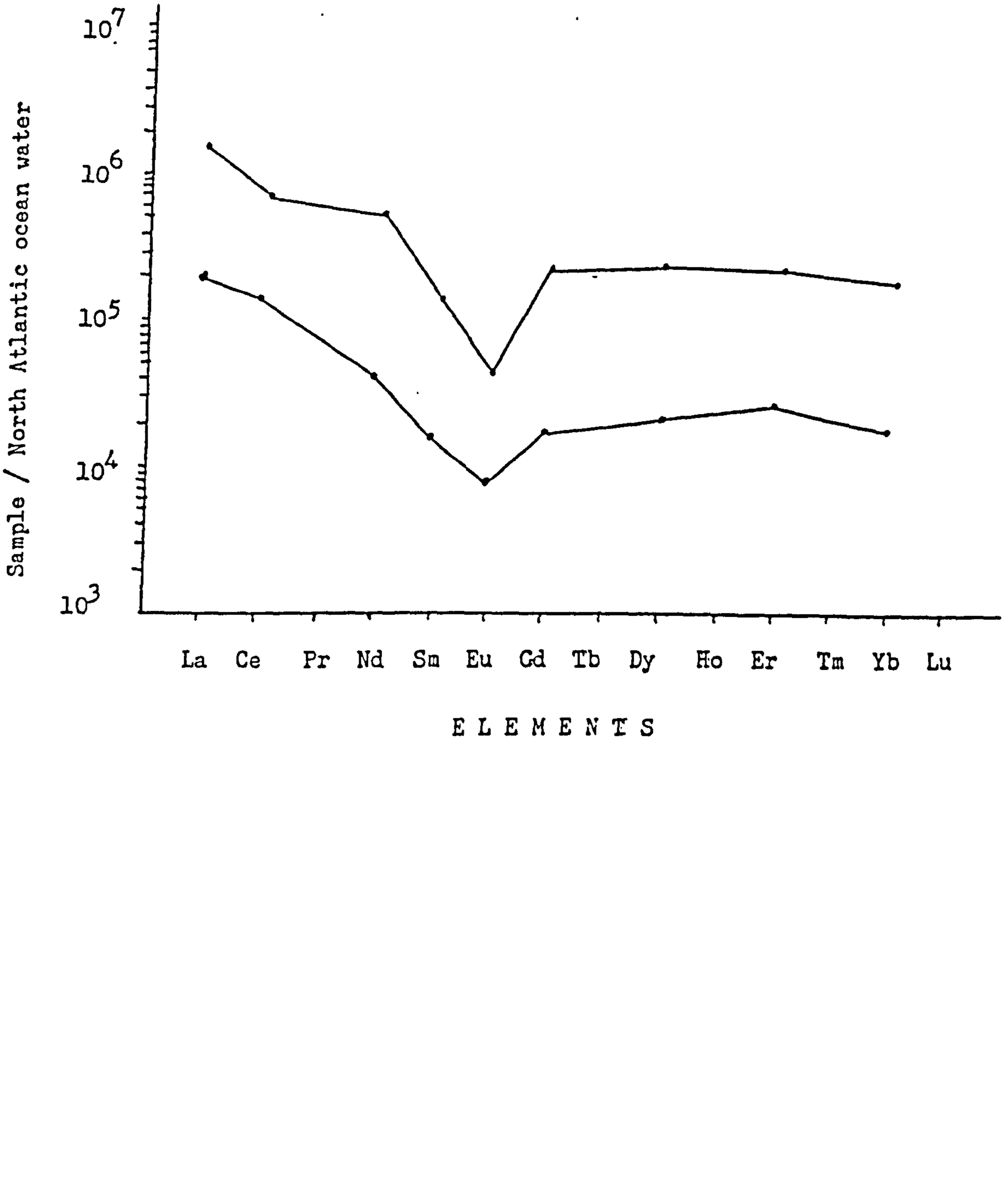

CONCLUSION.

Rare earth elements, yttrium, thorium and uranium are known to be enriched in phosphate deposits. This research was carried out to investigate the separation of these elements from a calcium phosphate matrix using an anion exchange or a cation exchange separation procedure. The eluted elements from the separation column were determined using inductively coupled plasma emission spectrometry. The procedure which showed complete recoveries of the elements from an artificial sample was selected and used in the separation of the rare earths from phosphate rock samples collected from the north of the Kingdom of Saudi Arabia. Neutron activation analysis was used to justify the results obtained by the two separation procedures.

The anion exchange separation procedure which used a strongly basic resin and an organic solvent/nitric acid mixture as eluant showed complete recovery of each individual element from the matrix if it was present alone. In the absence of calcium phosphate light rare earths were completely recovered from a mixture of rare earths. Heavy rare earths, yttrium and thorium recoveries were poor when a mixture of rare earths was used. The addition of calcium phosphate to a mixture of all the elements reduced the recoveries and the

reduction in recoveries increased with an increase in the concentration of calcium phosphate added. The analysis of six selected samples by the anion exchange procedure using two columns for each sample revealed that rare earths escaped from the first column to the second column. Investigation showed that calcium reduced the recovery but that phosphate did not. An attempt was made to remove calcium as sulphate but most of the rare earths were co-precipitate with calcium. The anion exchange procedure was abandoned because of poor recoveries from a mixture of rare earths, made worse by calcium interference.

Next the cation exchange procedure using a strong acid resin was investigated. A nitric acid media was selected because it was most suitable for the phosphate samples from Saudi Arabia. Preliminary studies showed that rare earths and yttrium were retained but that thorium and uranium were not. hence these two elements were abandoned and not investigated further. The resin AMBERLIT IR-120 was chosen after comparison with two other resins. The rare earths were recovered completely when an aqueous solution, or a solution containing only phosphate was used. The presence of either calcium phosphate or calcium alone in the solution reduced the recoveries. Recoveries from a rare earth mixture were almost constant whenever the concentration was kept constant. In the large column

(100cm x 2cm), the recoveries were very high and not affected by an increase in the concentration of calcium phosphate until it exceeded 5% (w/v). This limit allowed the analysis of 10 g of the real sample dissolved in 100 cm^3 since the sample only contains 50% calcium phosphate. The analysis of an artificial phosphate rock sample gave high recoveries ranging from 81 to 100%.

In order to analyse the rare earths after the ion exchange separation plasma parameters were optimised in the presence and the absence of methanol. The optimisation showed that higher gas flows and a higher power were essential when the eluant contained methanol. While lower gas flows and lower power were sufficient for aqueous solutions. Spectral interferences in the ICP are serious for the rare earths since the high temperature of the plasma excited each element to produce a complex spectra. The ICP instrument has a single channel PMT, and the most sensitive lines were chosen for greater sensitivity. As all the rare earths were eluted together from the resin (anion or cation), a correction programme was used with and without background correction. The background correction was applied by means of an oscillating quartz plate enabling measurements of the background on both sides of the analytical wavelength.

Having optimised both the separation and estimation, finally the recoveries of the rare earths from nine samples were measured using the standard addition method applied to the cation procedure and using full background correction with the ICP. The results show that the recovery varies from element to element and from sample to sample. The average recovery from the nine samples was found to vary for different elements from 81% (Pr) to 93% (Lu). These values are acceptable for such a complex sample preparation and analysis. This cation exchange procedure was next applied for the analysis of all the samples collected in the Kingdom of Saudi Arabia. The pattern of rare earth elements in these phosphate rocks suggested that they were deposited from an open ocean, marine, oxidizing environment.

APPENDIX 1.

Computer program designed to correct for spectral interferences of rare earths separated with anion exchange procedure and calculate the final concentration of rare earths in the sample.

```
1     REM ------- REE CORREC.- ANION EXCHANGE -------
2     REM CA(1) = CONCENTRATION OF ANALYTE IN
      SOLUTION SPREAD IN PLASMA - mg dm^-3
3     REM CM(1) = CONCENTRATION OF SAMPLE IN SOLUTION
      SPREAD IN PLASMA - g dm^-3
4     REM S = CONCENTRATION OF ANALYTE AFTER
      CORRECTION IN THE CURRENT ITERATION
5     REM S1 = CONCENTRATION OF ANALYTE BEFORE
      CORRECTION IN THE CURRENT ITERATION
6     REM ST = TOTAL CORRECTED CONCENTRATION OF
      ANALYTE IN THE SAMPLE - mg dm^-3
7     REM F = SLOPE OF CALIBRATION GRAPH FOR THE
      INTERFERENT AT ANALYTE WAVELENGTH * 1E-4
8     REM Z = CORRECTION
9     REM H(I,J) = RELATION CHANGE OF SIGNAL OF
      ANALYTE (I) CAUSED BY A CHANGE IN THE SIGNAL OF
      THE INTERFERENT
10    REM I = ANALYTE
11    REM J = INTERFERENT
```

```
12    REM E = THE RELATIVE CHANGE IN THE ANALYTE
      CONCENTRATION PRODUCED BY THE CURRENT ITERATION
13    REM NE$ = NAME OF ELEMENT
14    REM ------------------------------------------
15    DIM CA(20), CM(20), F(20), H(20,20), S(20),
      S1(20), ST(20), Z(20), NE$(20)
20    DATA "Y", "La", "Ce", "Pr", "Nd", "Sm", "Eu",
      "Gd"
30    DATA "Tb", "Dy", "Ho", "Er", "Tm", "Yb", "Lu",
      "Th"
40    FOR I = 1 TO 16: READ NE$(1): NEXT 1
50    DATA 0,0,0,0,0,0,0,0,0,0,0,40.7,0,18.8,0,0
60    DATA 0,0,64,188.8,37.4,0,0,0,0,0,0,0,0,0,0,2.3
70    DATA 0,0,0,58.7,0,0,0,12.5,0,0,0,0,0,0,0,0
80    DATA 0,0,270.9,0,22.4,0,0,0,0,0,0,36.1,0,0,0,0
90    DATA 0,0,1192.5,131.7,0,0,0,0,0,0,0,0,0,0,0,0
100   DATA 0,0,0,0,119,0,0,106.8,0,0,0,0,0,0,0,0
110   DATA 0,0,0,0,261.6,0,0,0,0,0,0,0,0,0,0,0
120   DATA 0,0,35.1,0,0,0,0,0,18.8,20.4,15.4,0,0,0,0,
            0
130   DATA 0,0,0,0,0,89.2,0,0,0,0,84,0,0,0,0,0
140   DATA 0,0,0,0,56.5,0,0,0,75.7,0,0,6.2,0,0,0,0
150   DATA 0,0,0,32,32.2,0,0,0,54,0,0,12.2,0,0,0,0
160   DATA 0,0,0,0,4.7,0,0,0,136.5,0,0,0,0,0,0,0
170   DATA 0,0,0,0,0,9,0,0,19,0,0,25.9,0,0,0,0
180   DATA 0,0,0,0,0,0,0,0,0,56.6,0,0,79.2,0,0,0
190   DATA 0,0,0,0,0,0,0,0,0,0,0,0,0,8,0,0
```

```
200   DATA 0,0,0,0,29.4,0,0,0,3.9,3.2,0,4.9,0,0,0,0
300   FOR I = 1 TO 16: FOR J = 1 TO 16: READ H(I,J):
      NEXT J: NEXT I
350   DATA 20.23,116.39,96.98,1488.48,1010.84,830.76,
      69.18,229.42
360   DATA 236.97,97.89,77.38,180.45,40.48,12.08,
      5.00,572.61
370   FOR I = 1 TO 16: READ F(1): NEXT
390   SP$ = "                                                    "
499   REM ---------------- MAIN PROGRAM ----------------
500   GOSUB 1000 : REM INPUT
600   GOSUB 2000 : REM CALC. OF CORRECTED
      CONCENTRATIO
800   GOSUB 4000 : REM OUTPUT
850   RUN
900   END
995   REM ------------------------------------------
997   REM ----------------INPUT ---------------------
999   REM ------------------------------------------
1000 HOME : INPUT "NAME OF SAMPLE?"; NS$
1010 FOR I = 1 TO 16
1020 FOR J = 5 TO 18
1030 VTAB(J) : PRINT SP$
1040 NEXT
1050 VTAB(5) : PRINT "ANALYTE ="; NE$(1)
1060 VTAB(10) : PRINT "What is the concentration of
      ANALYTE in"
```

```
1070 VTAB(11) : PRINT "the solution sprayed into the
     plasma"
1080 VTAB(12) : INPUT "in mg dm^-3?" ; CA(I)
1090 VTAB(14) : PRINT "What is the concentration of
     SAMPLE in"
1100 VTAB(15) : PRINT "the solution sprayed into the
     plasma"
1110 VTAB(16) : INPUT "in g dm^-3?" : CM(1)
1120 ST(1) = CA(1)* 1000 / CM(1) / (1 + F(1) / 1000)
1150 NEXT
1200 HOME : PRINT "DO YOU WISH TO CHANGE ANY OF
     THESE VALUES?"
1210 INPUT "Y" or "N ?"; A$
1220 IF A$ = "N" THEN 1900
1300 INPUT "Which element?"; NE$
1310 I = 1
1320 IF NE$ = NE$(1) THEN 1340
1330 I = 1 + 1: IF I > 16 THEN 1300
1335 GOTO 1320
1340 HOME: VTAB(10): PRINT "What is the
     concentration of ANALYTE in"
1350 PRINT "the solution sprayed into the plasma"
1360 INPUT "in mg dm^-3?" ; CA(I)
1390 VTAB(14) : PRINT "What is the concentration of
     SAMPLE in"
1400 PRINT "the solution sprayed into the plasma"
1410 INPUT "in mg dm^-3"; CA(I)
1420 ST(I) = CA(I) * 1000 /CM(I) / (1 + F(I) /1000)
```

```
1430 GOTO 1200
1900 RETURN
1995 REM ------------------------------------------
1997 REM ------- CALCULATION OF CORRECTION --------
1999 REM ------------------------------------------
2000 FOR I = 1 TO 16
2010 S(I) = ST(I) : S1(I) = S(I) : Z(I) = 0
2020 NEXT I
2100 FOR I = 1 TO 16
2110 FOR J = 1 TO 16
2120 Z(I) = (H(I,J) * S(J) * 1E-4) + Z(I)
2130 NEXT J
2131 REM ------------------------------------------
2132 REM --- CALCULATION OF SIZE OF CORRECTION-----
2133 REM ------------------------------------------
2140 S(I) = ST(I) - Z(I)
2150 Z(I) = 0
2160 NEXT I
2175 REM ------------------------------------------
2180 REM --CALCULATION OF CORRECTED CONCENTRATION--
2185 REM ------------------------------------------
2190 E = 0
2200 FOR I = 1 TO 16
2210 E = E + ABS ( (S(I) - S1(I) ) / S(I) )
2220 S1(I) = S(I)
2230 NEXT I
2240 PRINT E: IF E < 0.001 THEN GOTO 2300
2245 REM ------------------------------------------
```

```
2246 REM ---- TERMINATE INTERATION IF CHANGE IN ---
2247 REM ---- CONCENTRATION DUE TO THIS ITERATION--
2248 REM ------------ IS VERY SMALL -------------
2249 REM ----------------------------------------
2250 GOTO 2100
2300 RETURN
2995 REM ----------------------------------------
2997 REM ----------OUTPUT----------
4000 PRE 1
4010 PRINT "SAMPLE = " ; NS$: PRINT : PRINT
4020 FOR I = 1 TO 16
4030 PRINT NEE(I), S(I), "mg dm^-3"
4040 NEXT I
4050 PRINT : PRINT: PRINT
4060 PRINT "CORRECTION RATIOS"
4070 FOR I = 1 TO 16
4080 PRINT NE$(I), S(I) / ST(I)
4090 NEXT I
4100 PRINT : PRINT
4110 PRINT "----------"
4120 PRINT : PRINT : PRINT
4130 PRE 0
4900 RETURN
4999 REM ----------
```

APPENDIX 2.

Computer program designed to correct for spectral interferences of rare earths separated with cation exchange procedure and calculate the final concentration of rare earths in the sample.

```
1     REM ----- REE CORRECT. - CATION EXCHANGE -----
2     REM CA(I) = CONCENTRATION OF ANALYTE IN
      SOLUTION SPREAD IN PLASMA - mg dm^-3
3     REM CM(I) = CONCENTRATION OF SAMPLE IN SOLUTION
      SPREAD IN PLASMA -g dm^-3
4     REM S = CONCENTRATION OF ANALYTE AFTER
      CORRECTION IN THE CURRENT ITERATION
5     REM S1 = CONCENTRATION OF ANALYTE BEFORE
      CORRECTION IN THE CURRENT ITERATION
6     REM ST = TOTAL CORRECTED CONCENTRATION OF
      ANALYTE IN THE SAMPLE - mg dm^-3
7     REM F = SLOPE OF CALIBRATION GRAPH FOR THE
      INTERFERENT AT ANALYTE WAVELENGTH * 1E-4
8     REM Z = CORRECTION
9     REM H(I,J) = RELATION CHANGE OF SIGNAL OF
      ANALYTE (I) CAUSED BY A CHANGE IN THE SIGNAL OF
      THE INTERFERENT
10    REM I = ANALYTE
11    REM J = INTERFERENT
```

```
12    REM E = THE RELATIVE CHANGE IN THE ANALYTE
      CONCENTRATION PRODUCED BY THE CURRENT ITERATION
13    REM NE$ = NAME OF ELEMENT
14    REM ------------------------------------
15    DIM CA(20),CM(20),F(20),H(20,20),S(20),S1(20),
      ST(20),Z(20,NE$(20)
20    DATA "Y","La","Ca","Pr","Nd","Sm","Eu","Gd"
30    DATA "Tb","Dy","Ho","Er","Tm","Yb","Lu"
40    FOR I = 1 TO 15: READ NE$(I): NEXT I
50    DATA 0,0,-76.5,0,0,0,0,0,0,-34.8,0,26,0,25.5,0
60    DATA 0,0,-39.3,191,35.1,0,0,0,0,0,0,0,0,0,0
70    DATA 0,0,0,-45.4,-24.5,0,0,0,0,0,0,0,0,0,0
80    DATA 0,0,174.3,0,1.6,0,0,0,-9.4,0,0,39.5,0,0,0
90    DATA 0,0,1180.9,58.9,0,0,0,0,-15,0,-21.3,
      -26.9,0,0,0
100   DATA -4.5,0,0,0,138.2,0,0,126,0,0,-68.8,0,0,
      0,0
110   DATA 0,0,0,0,234.2,0,0,0,0,0,0,0,0,0,0
120   DATA 0,0,-35.8,-5.5,0,0,0,0,21.7,-4.2,21.9,0,0,
      0,0
130   DATA 0,0,0,0,0,103.9,-16.7,0,0,-17,-48.1,0,0,
      0,0
140   DATA 0,0,0,0,39.9,0,12,0,8.6,0,0,0,0,0,0
150   DATA 0,0,0,37.3,37.8,0,0,0,68.9,0,0,0,0,0,0
160   DATA 0,0,0,0,7.5,0,0,0,135,25,0,0,0,0,0
170   DATA 0,0,-14.9,0,0,11.1,0,0,20.1,0,-177.6,-24.1
      0,0,0
```

```
180   DATA 0,0,0,0,0,0,0,0,0,28,0,0,28.7,0,0
190   DATA 0,0,0,0,0,0,0,0,0,0,0,0,0,12.4,0
300   FOR I = 1 TO 15 : J = 1 TO 15 : READ H(I,J)
330   NEXT J : NEXT I
350   DATA -14.23,70.76,-123.46,1181.56,934.91
355   DATA 552.53,31.21,-3.12,24.27,44.71
360   DATA 62.31,134.27,-129.18,10.23,5.12
370   FOR I = 1 TO 15 : READ F(I) : NEXT
390   SP$ = "                                                    "
499   REM ------------MAIN PROGRAM---------------------
500   GOSUB 1000 : REM INPUT
600   GOSUB 2000 : REM CALC. OF CORRECTED
      CONCENTRATIO
800   GOSUB 4000 : REM OUTPUT
850   RUN
900   END
995   REM ----------------------------------------
997   REM -----------INPUT----------------------------
999   REM ----------------------------------------
1000 HOME : INPUT "NAME OF SAMPLE?"; NS$
1010 FOR I = 1 TO 15
1020 FOR J = 5 TO 18
1030 VTAB(J) : PRINT SP$
1040 NEXT
1050 VTAB(5) : PRINT "ANALYTE = " ; NE$(I)
1060 VTAB(10) : PRINT "What is the concentration of
      ANALYTE in"
```

```
1070 VTAB(11) : PRINT "the solution sprayed into the
     plasma"
1080 VTAB(12) : INPUT "in mg dm^-3?  " ; CA(I)
1090 VTAB(14) : PRINT "What is the concentration of
     SAMPLE in "
1100 VTAB(15) : PRINT "the solution sprayed into the
     plasma"
1110 VTAB(16) : INPUT " in g dm^-3 ? " ; CM(I)
1120 ST(I) = CA(I) * 1000 / CM(I) / (1 + F(I) /
     10000)
1150 NEXT
1200 HOME : PRINT "DO YOU WISH TO CHANGE ANY OF
     THESE VALUES?"
1210 INPUT "Y or N?" ; A$
1220 IF A$ = "N" THEN 1900
1300 IF NE$ = NE$(I) THEN 1340
1320 I = I + 1 : IF 1 > 15 THEN 1300
1335 GOTO 1320
1340 HOME : VTAB(10) : PRINT "What is the
     concentration of ANALYTE in"
1350 PRINT "the solution sprayed into the plasma"
1360 INPUT " in mg dm^-3 ?" ; CA(I)
1390 VTAB(14) : PRINT "What is the concentration of
     SAMPLE in"
1400 PRINT "the solution sprayed into the plasma"
1410 PRINT "in mg dm^-3 " ; CA(I)
1420 ST(I) = CA(I) * 1000 / CM(I) / (1 + F(I) /
     10000)
```

```
1430 GOTO 1200
1900 RETURN
1995 REM ------------------------------------------
1997 REM --------CALCULATION OF CORRECTION----------
1999 REM ------------------------------------------
2000 FOR I = 1 TO 15
2010 S(I) = ST(I) : S1(I) = S(I) : Z(I) = 0
2020 NEXT I
2100 FOR I = 1 TO 15
2110 FOR J = 1 TO 15
2120 Z(I) = (H(I,J) * S(J) * 1E-4) + Z(I)
2130 NEXT J
2131 REM ------------------------------------------
2132 REM --- CALCULATION OF SIZE OF CORRECTION------
2133 REM ------------------------------------------
2140 S(I) = ST(I) - Z(I)
2150 Z(I) = 0
2160 NEXT I
2175 REM ------------------------------------------
2180 REM ----CALCULATION OF CORRECTED CONCENTRATION-
2185 REM ------------------------------------------
2190 E = 0
2200 FOR I = 1 TO 15
2210 E = E + ABS ( ( S(I) - S1(I) ) / S(I) )
2220 S1(I) = S(I)
2230 NEXT I
2240 PRINT E : IF E < 0.001 THEN GOTO 2300
2245 ------------------------------------------
```

```
2246 REM ----TERMINATE INTERATION IF CHANGE IN -----
2247 REM --- CONCENTRATION DUE TO THIS ITERATION----
2248 REM ------------IS VERY SMALL-------------------
2249 REM ------------------------------------------
2250 GOTO 2100
2300 RETURN
2995 REM ------------------------------------------
2997 REM --------------OUTPUT----------------------
2999 REM ------------------------------------------
4000 PRE 1
4010 PRINT "SAMPLE = " ; NS$ : PRINT : PRINT
4020 FOR I = 1 TO 15
4030 PRINT NE$(I) , S(I), "mg dm^-3"
4040 NEXT I
4050 PRINT : PRINT : PRINT
4060 PRINT " CORRECTION RATIOS"
4070 FOR I = 1 TO 15
4080 PRINT NE$(I), S(I) / ST(I)
4090 NEXT I
4100 PRINT : PRINT
4110 PRINT "------------------------------------
4120 PRINT : PRINT : PRINT
4130 PRE 0
4900 RETURN
4999 REM ------------------------------------------
```

REFERENCES.

1. Sheldon, R.P.
U.S. Geol. Surv. Prof. Paper, 501-c, C106-C113 (1964).

2. Motton, J.W.
U.S. Geol. Surv. Open File Report, Part 2, P.20 (1967).

3. Meissner, C.R., Jr.
U.S. Geol. Surv. Open File Report, P.8 (1967).

4. Kluyver, H.M., Bege, V.B., Smith, G.H., Ryder, J.M. and Van Eck, M.

5. Riofinex Geological Mission.
Kingdom of Saudi Arabia, Ministry of Petroleum and Mineral Resources, Open File Report RF-1979-13(1979).

6. Meissner, C.R. and Ankary, A.
Kingdom of Saudi Arabia, Ministry of Petroleum and Mineral Resources, Mineral Resources report of Investigations 2 (1972).

7. Riddler, G.P., Khallaf, H.M. and Farasani, A.M.
Kingdom of Saudi Arabia, Ministry of Petroleum and Mineral Resources, Open File Report RF-OF-03-22 (1983).

8. Berge, J.W. and Jack, J.
Economic Geology, 77, 1912 (1982)

9. McConnell, D.
"Apatite, its crystal chemistry, minerology, utilization, geology and biological occurrences"., Applied minerology, Vol.5, Springer-Verlag, N.Y., 1973.

10. Slansky, M.
"Geology of Sedimentary Phosphates", translated by Cooper, P., North Oxford Academic, Revised 1986.

11. Notholt, A.J.K. and Hartley, K.
"Phosphate rock", Mining Journal Book Ltd., Instit. of Geol. Scien., London, 1983.

12. Nriagu, J.O. and Moore, P.B.
"Phosphate minerals", Springer-Verlag, Berlin, 1984.

13. Lehr, J.R., McClellan, G.H., Smith, J.P. and Frazier, A.W.
Characterization of apatites in commercial phosphate rocks: in: Coll. Int. Phos. Miner. Solides, 2, 29, (16-20 May 1967).

14. Krauskopf, K.B.
Economic Geology, 50, 411 (1955).

15. Tooms, J.S., Summehayes, C.P. and Cronan, D.S.
Oceanorg. Mar. Biol. Ann. Rev., 49, 49 (1969).

16. Pre-vot, L., Lucas, J., Nathan, Y. and Shiloni, Y.
"Original and distribution of the elements"., Ed. Ahrens, L.H., p. 293-304, Pergamon, Oxford, 1979.

17. Altschuler, Z.S., Clarke, R.S., Jr. and Young, E.J.
U.S. Geol. Surv. Prof. Paper, 314-D, 45-90 (1958).

18. Marhol, M.
"Ion exchangers in analytical chemistry, their properties and use in inorganic chemistry"., Vol. XIV, Elsevier Scien. Pub. Comp., Oxford, 1982.

19. Minczewski, J., Chwastowska, J. and Dybczynski, R.
"Separation and preconcentration methods in inorganic trace analysis"., Trans. by Masson, Mary Y., Ellis Horwood Ltd. Pub., Chichester, 1982.

20. Ritchie, A.S.
"Chromatography in Geology", Elsevier Pub. Comp., Amsterdam, 1964.

21. Mizuike, A.
"Enrichment techniques for inorganic trace analysis"., Spring-Verlag, Berlin, 1983.

22. Martin, A.J.P. and Synge, R.L.M.
Biochem. J., 35, 1358 (1941).

23. Mayer, S.W. and Tompkins, E.R.
J. Am. Chem. Soc., 69, 2866 (1947).

24. Greenfield, S., Jones, I.L. and Berry, C.T.
Analyst, 89, 713 (1964).

25. Wendt, R.H. and Fassel, V. A.
Anal. Chem., 37, 920 (1965).

26. Boumans, P.W.J.M.
Spectrochim. Acta, 37B, 75 (1982).

27. Boumans, P.W.J.M., McKenna, R.J. and Bosveld, M.
Spectrochim. Acta, 36B, 1031 (1981)

28. Boumans, P.W.J.M. and Vrakking, J.J.A.
Spectrochim. Acta, 40B , 1085 (1985)

29. Boumans, P.W.J.M. and Vrakking, J.J.A.
Spectrochim. Acta, 40B , 1446 (1985)

30. Boumans, P.W.J.M. and Vrakking, J.J.A.
Spectrochim. Acta, 42B , 553 (1987)

31. McLaren, J.W. and Berman, S.S.
Spectrochim. Acta, 40B, 217 (1985).

32. Boumans, P.W.J.M.
Spectrochim. Acta, 38B, 747 (1983).

33. Boumans, P.W.J.M.
Spectrochim. Acta, 36B, 169 (1981).

34.Winge, R.K., Peterson, V.J. and Fassel, V.A.
Appl. Spectrose., 33, 206 (1979).

35. Kalnicky, D.J., Kniseley, R.N. and Fassel, V.A.
Spectrochim. Acta, 30B, 511 (1975).

36. Kornblum, G.R. and De Galan, L.
Spectrochim. Acta, 32B, 71 (1980).

37. Alder, J.F., Bombelka, R.M. and Kirkbright, G.F.
Spectrochim. Acta, 35B, 163 (1980).

38. Lovett, R.J.
Spectrochim. Acta, 37B, 969 (1982).

39. Thompson, M. and Walsh, J.N.
"A handbook of inductively coupled plasma spectrometry"., Blackie, Glasgow, 1983.

40. Bamin, R.M.
"Developments in atomic plasma spectrochemical analysis"., John Wiley and Sons, N.Y., 1983.

41. Fassel, V.A. and Kniseley, R.N.
Anal. Chem., 46, 1110A (1974).

43. Greenfield, S., McGeachin, H. McD. and Smith, P.B.
Talanta, 23, 1 (1976).

44. Mermet, J.M. and Trassy, C.
Spectrochim. Acta, 36B, 269 (1982).

45. Harrison, G.R.
"Massachusetts Institute of Technology, wavelength tables"., M.I.T. Press, Cambridge, M.A. U.S.A., reprent 1969.

46. Boumans, P.W.J.M.
Spectrochim. Acta, 31B, 147 (1976).

47. Fassel, V.A., Katzenberger, J.M. and Winge, R.K.
Appl. Spectrosc., 33, 1 (1979).

48. Hall, D.H.
"Background correction procedures and developments in spectrometer design for ICP-AES"., PhD thesis, University of Strathclyde, 1980.

49. Kano, T. and Yanagida, H.
"Rare earths: properties and applications"., Gihodo, Tokyo, 1980.

50. Henderson, P.
"Rare earth elements geochemistry, developments in geochemistry - 2"., Elsevier, Amsterdam,. 1984.

51. Spedding, F.H. and Daane, A.H.
"The rare earths"., Robert E. Kreiger Pub. Comp. Inc., N.Y., 1961.

52. Ryabchikov, D.I. and Ryabukhin, V.A.
"Analytical chemistry of yttrium and the lanthanide elements"., Translated by Aladjem, A., Ed. Vinogradov, A.P., Ann Arbor - Humphrey Science Pub., London, 1970.

53. Schoeller, W.R. and Powell, A.R.
"Analysis of Minerals and ores of the Rarer Elements"., Charles Griffin and Co., Ltd., London, reprent 1955.

54. Brunfelt, A.O. and Steinnes, E.
Analyst, 94, 979 (1969).

55. Potts, P.J., Thorpe, O.W., Isaacs, M.C. and Wright, D.W.
Chem. Geol., 48, 145 (1985).

56. Desai, H.B., Iyer, K. and Sanker Das, M.
Talanta, 11, 1249 (1964).

57. Brunfelt, A.O., Roelandts, I. and Steinnes, E.
Analyst, 99, 277 (1974).

58. Murugaiyan, P., Verbeek, A.A., Hughes, T.C. and Webster, R.K.
Talanta, 15, 1119 (1968).

59. Masuda, A., Nakamura, N. and Tanaka, T.
Geochim. Cosmochim. Acta, 57, 239 (1973).

60. Eby, G.N.
Anal. Chem., 44, 2137 (1972).

61. Roelandts, I.
Anal. Chem., 53, 676 (1981).

62. Rose, H.J., Jr. and Cuttitta, F.
Appl. Spectro., 122, 426 (1968).

63. Robinson, P., Higgins, N.C. and Jenner, G.A.
Chem. Geol. 55, 121 (1986).

64. Qing-Lie, H., Hughes, T.C., Haukka, M. and Hannaker, P.
Talanta, 32, 495 (1985).

65. Ooghe, W. and Verbeek, F.
Anal. Chim. Acta, 73, 87 (1974).

66. Sen Gupta, J.G.
Talanta, 31, 1045 (1984).

67. Sen Gupta, J.G.
Talanta, 23, 343 (1976).

68. Sen Gupta, J.G.
Anal. Chim. Acta, 138, 295 (1982).

69. Sen Gupta, J.G.
Talanta, 28, 31 (1981).

70. Sen Gupta, J.G.
Talanta, 32, 1 (1985).

71. Horsky, S.J. and Fletcher, W.K.
Chem. Geol., 32, 335 (1981).

72. Grobenski, Z.
Fresenius Z. Anal. Chem., 289, 337 (1978).

73. Boumans, P.W.J.M. and DeBoer, F.J.
Spectrochim. Acta, 27B, 391 (1972).

74. Feigenson, M.D. and Carr, M.J.
Chem. Geol., 51, 19 (1985).

75. Johanson, G.W. and Sisneros, T.E.
Rare Earth in Modern Scien. and Tech., 3, 525 (1982).

76. Edge, R.A. and Ahrens, L.H.
Anal. Chim. Acta, 26, 355 (1962).

77. Broekaert, J.
Spectrochim. Acta, 35B, 225 (1980).

78. Yashida, K. and Haraguchi, H.
Anal. Chem., 56, 2580 (1984).

79. Larson, G.F., Fassel, V.A., Scott, R.H. and Kniseley, R.N.
Anal. Chem., 47, 238 (1975).

80. Broekaert, J.A.C., Leis, F. and Laqua, K.
Spectrochim. Acta, 34B, 167 (1979).

81. Brenner, I.B., Watson, A. E., Russell, G.M. and Goncalves, M.
Chem. Geol., 28, 321 (1980).

82. Broekaert, J.A.C., Leis, F. and Laqua, K.
Spectrochim. Acta, 34B, 73 (1979).

83. Crock, J.G. and Lichte, F.E.
Anal. Chem., 54, 1329 (1982).

84. Buchanan, S.J. and Dale, L.S.
Spectrochim. Acta, 41B, 236 (1986).

85. Fischer, P.T. and Ellgren, A.J.
Spectrochim. Acta, 38B, 309 (1983).

86. Bolton, a., Hwang, J. and Voet, A.V.
Spectrochim Acta, 38B, 165 (1983).

87. Walsh, J.N., Buckley, F. and Barker, J.
Chem. Geol., 33, 141 (1981).

88. Broekaert, J.A.C., Leis, F. and Laqua, K.
Spectrochim. Acta, 34B, 73 (1979).

89. Brenner, I.B., Watson, A.E., Steele, T.W., Jones, E.A. and Goncalves, M.
Spectrochim. Acta, 36B, 785 (1981).

90. Strelow, F.W.E. and Jackson, P.F.S.
Chem. Geol., 46, 1481 (1974).

91. Strelow, F.W.E. and Jackson, P.F.S.
Chem. Geol., 62, 351 (1972).

92. Crock, J.G. Lichte, F.E. and Wildeman, T.R.
Chem. Geol., 45, 149 (1984).

93. Huffman, E.H. and Oswalt, R.L.
J. Am. Chem. Soc., 72, 3323 (1950).

94. Nervik, W.E.
J. Phys. Chem., 59, 690 (1955).

95. Minczewski, J. and Dybczynski, R.
J. Chromatog., 7, 98 (1962).

96. Bunnwy, L.R., Ballou, N.E., Pascual, J. and Foti, S.
ANAL. Chem., 31, 324 (1959).

97. Danon, J.
J. Inorg. Nucl. Chem., 5, 237 (1958).

98. Korkisch, J., Hazan, I. and Arrhenius, G.
Talanta, 10, 865 (1963).

99. Edge, R.A.
Anal. Chim. Acta, 29, 321 (1963).

100 Roelandts, I., Duyckaerts, G. and Brunfelt, A.O.
Anal. Chim. Acta, 73, 141 (1974).

101 Brunfelt, A.O., Roelandts, I and Steinnes, E.
Analyst, 99, 277 (1974).

102 Roelandts, I. and Duyckaerts, G.
Anal. Chim. Acta, 68, 131 (1974).

103 SenGupta, J.G.
Geostds. Newsl., 1, 149 (1977).

104 Hwang, J., Shih, J., Yeh, Y. and Wu, S.
Analyst, 106, 869 (1981).

105 Burgett, C.A. and Fritz, J.S.
Anal. Chem., 44, 1738 (1972).

106 Jangida, B.L., Krishnamachari, N., Varde, M.S. and Venkatasubramanian, V.
Anal. Chim. Acta, 32, 91 (1965).

107 El-Kammar, A.M., Zayed, M.A. and Amer, S.A.
Chem. Geol., 24, 69 (1979).

108 McArthur, J.M. and Walsh, J.N.
Chem. Geol., 47, 191 (1984/1985).

109 Altschuler, Z.S., Cuttitta, F. and Berman, S.
U.S. Geol. Surv. Prof. Pap., 575-B, B-1 (1967).

110 Altschuler, Z.S.
"The weathering of phosphate deposites. Geochemical and environmental aspects in Environmental phosphorous handbook"., Wiley, N.Y., 1973.

111 Kadam, B.V., Maiti, B. and Sathe, R.M.
Analyst, 106, 724 (1981).

112 Bock, R.
"Handbook of decomposition methods in analytical chemistry"., Translated by Marr, I.L., International Textbook Comp., Glasgow 1979.

113 Fletcher, W.K.
"Handbook of exploration geochemistry, analytical methods in geochemical prospecting"., Vol.1, Ed. Govett, G.J.S., Elsevier Science Pub., Amsterdam, 1981.

114 Monk, R.G.
Analyst, 88, 476 (1963).

115 Ficklin, W.H.
U.S. Geol. Surv. Prof. Pap., 700-C, 186 (1970).

116 Crenshaw, G.L. and Ward, F.N.
U.S. Geol. Surv. Bull., 1408, 77 (1975).

117 Kitson, R.E. and Mellon, M.G.
Indus. and Eng. Chem., Anal. Ed., 16, 379 (1944).

118 Shapiro, L.
U.S. Geol. Surv. Bull., 1401, 38 (1978).

119 Ure, A.M., Bacon, J.R., Berron, M.L. and Watt, J.J.
Geoderma, 22, 1 (1979).

120 Upor, E., Mohal, M. and Novak, G.Y.
"Photometric methods in inorganic trace analysis, comprehensive analytical chemistry"., Vol. XX, Ed. Svehla, G., Elsevier, Amsterdam, 1985.

121 Serdyuk, L.S. and Smirnaya, V.S.
J. of Anal. Chem. of the U.S.S.R., 19, 413 (1964).

122 Ingram, B.L.
Anal. Chem., 42, 1825 (1970).

123 Huffman, E.W.D., Jr.
Microchemical Journal, 22, 567 (1977).

124 West, A.C., Fassel, V.A. and Kniseley, R.N.
Anal. Chem., 45, 242 (1973).

125 Evensen, N.W., Hamilton, P.J. and O'Nions, R.L.
Geochim. Cosmochim. Acta, 42, 1199 (1978).

126 Crock, J.G., Lichte, F.E. and Wildeman, T.R.
Chem. Geol., 45, 149 (1984).

127 Washington, H.S.
Amm. J. Sci., 4th Ser., 10, 59 (1900).

128 Washington, H.S.
"The chemical analysis of rocks"., 2nd Ed., Wiley, N.Y., 1910.

129 Hillebrand, W.F., Lundell, G.E.F., Bright, H.A. and Hoffman, J.I.
"Applied inorganic analysis"., 2nd Ed., Wiley, N.Y., 1953.

130 Groves, A.W.
"Silicate Analysis"., 2nd Ed., George Allen and Unwin, London, 1951.

131 Johnson, W.M. and Maxwell, J.A.
"Rock and mineral analysis.", 2nd Ed., John Wiley and Sons, N.Y., 1981.

132 Wainerd, R.E. and Uken, E.A.
"Modern methods of geochemical analysis"., Plenum Press, N.Y. 1971.

133 Reeves, R.D. and Brooks, R.R.
"Trace elements analysis of geological materials"., John Wiley and Sons, N.Y., 1978.

134 Zussman, J.
"Physical methods in determinative minerology, 2nd Ed., Academic Press, London, 1977

135 Hutchison, C.S.
"Laboratory handbook of petrographic techniques"., John Wiley and Sons, N.Y., 1974.

136 Fletcher, W.K.
"Analytical methods in geochemical prospecting"., Vol. 1, Elsevier Science Pub., Amsterdam, 1981.

137 Giddings, J.C.
"Dynamics of chromatography"., Part 1, Dekker, N.Y., 1965.

138 Deer, W.A., Howie, R.A. and Zussman, J.
"An introduction to the rock forming minerals"., Logman, 1983.

139 Turner, D.R. and Whitfield, M.J.
Nature, 296, 214 (1982).

140 Elderfield, H. and Greaves, M.J.
Nature, 281, 468 (1979).

141 Piper, D.Z.
Chem. Geol., 14, 285 (1974).

142 Shimizu, H. and Masuda, A.
Nature, 266, 346 (1977).

143 Martin, J.M., Hogdahl, O. and Philipott, S.C.
J. Geophys. Res., 81, 3119 (1976).

144 Hogdahl, O.T., Melsom, S. and Bowen, V.T.
Adv. Chem. Ser., 73, 308 (1968).

145 Carpenter, J.H. and Grant, V.E.
J. Mar. Res., 25, 228 (1967).

146 Elderfield, H and Greaves, M.J.
Nature, 296, 214 (1982).

147 Miller, N.J., O'Haver, T.C. and Harnly, J.M.
Anal. Chem., 54, 799 (1982).

148 Ure, A.M. and Bacon, J.R.
Analyst 103, 807 (1978).

149 Bacon, J.R. and Ure, A.M.
Anal. Chim. Acta, 105, 163 (1979)